Alma Mater Studiorum – Università di Bologna

DOTTORATO DI RICERCA IN

TECNOLOGIE INNOVATIVE E USO SOSTENIBILE DELLE RISORSE DI PESCA E BIOLOGICHE DEL MEDITERRANEO (FISHMED-PHD)

Ciclo 35

Settore Concorsuale: 05/C1 - ECOLOGIA

Settore Scientifico Disciplinare: BIO/07 - ECOLOGIA

EVALUATION AND MANAGEMENT OF DEMERSAL STOCKS IN THE ADRIATIC: THE CASE OF COMMON SOLE (*SOLEA SOLEA*, L.) IN THE NORTHERN AND CENTRAL ADRIATIC SEA

Presentata da: Francesco Masnadi

Coordinatore Dottorato

Stefano Goffredo

Supervisore

Giuseppe Scarcella

Co-supervisore

Stefano Goffredo

Esame finale anno 2023

Abstract

The main objective of the Common Fisheries Policy (CFP) is to match sustainable exploitation of the fish stocks within socio-economic sustainability. However, in the recent past, most of the stocks in the Mediterranean Sea have been exploited at rates well above the CFP's objective. To address this, international working groups have recommended reducing fishing mortality and developing management plans to achieve this reduction over time. In this context, this PhD thesis aimed to assess the status of common sole, one of the main commercial stocks in the northern and central Adriatic Sea, using a mix of conventional and innovative techniques and methodologies to provide more reliable estimates of stock status compared to past advice. First, a focus on the *rapido* trawl fishery was provided, which accounts for about half of the common sole landings in the Adriatic Sea. Due to lack of data and biological information for most of the species caught by this gear, stock status was only available for a few of them, while other species remain unassessed. To address this, a meta-analysis was carried out using data-poor assessment model (CMSY software) to analyze the whole catch assemblage. Although among the species analyzed no one was sustainably exploited, some of the stocks showed trajectory toward the recovery status. The outcomes of CMSY model were then used to estimate rebuilding time and forecast expected catches under different harvest control rule scenarios, with a reduction of 20% of fishing effort being suggested as a way to allow most of the target and accessory species to recover to sustainable levels within 15 years. Secondly, an ensemble of data-rich assessment models (Stock Synthesis) was developed specifically for common sole. This was the first time an ensemble of models has been used in the Mediterranean to provide management advice. Specifically, the ensemble approach permitted to better incorporate uncertainty by using alternative hypotheses of selectivity, natural mortality and steepness (18 runs). Moreover, new quantitative criterion based on diagnostic scores was adopted to combine the outcomes of the ensemble grid. Consistent with the result obtained in the data-poor analysis, the ensemble outcomes indicated that the common sole stock was showing a positive recovering trend, with fishing mortality below to reference point and spawning biomass around 70 % of the reference point. Recovering status was probably due to the effective management actions underway in the area (spatial-temporal closures) rather than the moderate effort reduction according to the actual management plan. Additionally, a exceptional event such as the COVID-19 pandemic has had a positive effect on the recovery process that was already underway. As convention, the growth pattern in the data-rich approach was described as constant throughout life. Nevertheless, a change in the growth due to a re-allocation of energy during individual lifespan seemed plausible. To test this, back-calculation measurements obtained from SoleMon survey data were used to fit and compare monophasic and biphasic growth curves through the use of non-linear mixed effects models. The analyses revealed that the fitting of the biphasic curve was superior, confirming the theory that growth in size would decrease as a consequence of reproductive effort. To test the implication on scientific advice a stock assessment simulation showed how the use of the monophasic pattern would result in a critical overestimation of biomass that could lead to a greater risk of overfishing. As a final step, a simulation-testing procedure (short-cut MSE) was applied to determine the best performing reference points for common sole using stock-specific characteristic. The study found that a mortality rate that results in SSB (spawning stock biomass) of 35% of virgin biomass was a good alternative to the officially adopted reference point, as it was more in line with the objectives of the CFP. Additionally, the procedure could be routinely adopted during benchmark sessions to increase transparency in the calculation of reference points enhancing the credibility and legitimacy of scientific advice.

Index

1. Introduction

1.1. Common sole in central and northern Adriatic Sea: stock identification and biological information

The common sole (*Solea solea*, Linnaeus, 1758; Figure 1.1.1) is a demersal species, particularly abundant on relatively low depth (< 150 meters) sandy and muddy bottoms in the Mediterranean Sea and north-eastern Atlantic (Quéro et al., 1986). Sole feed primarily during night period, remaining buried in the seabed during the day. Juveniles feed preferably on small polychaetes, amphipods, and bivalves, while adult large on bigger polychaetes and holoturians (Beyst et al., 1999; Grati et al., 2013).

Figure 1.1.1. Solea solea (Linneo, 1978)

Tagging experiments using the traditional mark-and-recapture procedure showed that all of the soles caught inside the northern Adriatic Sea were recaptured in the sub-basin (Pagotto et al., 1979). However, based on the mitochondrial DNA variation, Guarniero et al. (2002) and Sabatini et al. (2018) concluded that in the Adriatic Sea two near-panmictic populations of common sole exist. The first inhabits the northern-central Adriatic Sea and the western part of the southern Adriatic sea, while the second population is located along the Albanian coasts (eastern part of the southern Adriatic sea). The hydro-geographical features of this semi-enclosed basin might support the overall pattern of differentiation of the Adriatic common soles. The northern Adriatic Sea has a high geographical homogeneity, with a wide continental shelf and eutrophic shallow-waters. The southern Adriatic in contrast, is characterized by narrow continental shelves and a marked, steep continental slope (1200 m deep). Significant geographical barrier such as local currents, eddies and canyons (Artegiani et al., 1997), may prevent a high rate of exchange of adult spawners and the mixing of planktonic larval

stages from nursery areas of adjacent basins (Magoulas et al., 1996). Reproduction period in the central and northern Adriatic Sea takes place in coastal areas between November and March (Piccinetti and Giovanardi, 1984) when the species reaches a size of 25 cm (L50%= 25.8 cm; MEDISEH, 2013). Hatching occurs after eight days and the larva measures 3 to 4 mm TL (Tortonese, 1975; Wagemans and Vandewalle, 2001). Eye migration starts at 7 mm TL and ends at 10-11 mm TL. Benthic life begins after seven or eight weeks (15 mm) in coastal areas, estuaries, lagoon systems and brackish waters along the Italian coast of the central and northern Adriatic Sea. The entire life cycle of sole seems to follow the general Adriatic circulation and the cyclonic gyres which in autumn, in correspondence to the spawning season of this species, occur in the northern and central Adriatic (Russo and Artegiani, 1996). In confirmation of this, data on the spatial distribution reveals distribution is a function of age with a progressive spawners migration from coastal waters, which is a shallow water area characterized by a high concentration of nutrients, to deeper ones outside the western coast of Istria (Figure 1.1.2.; Scarcella et al., 2014).

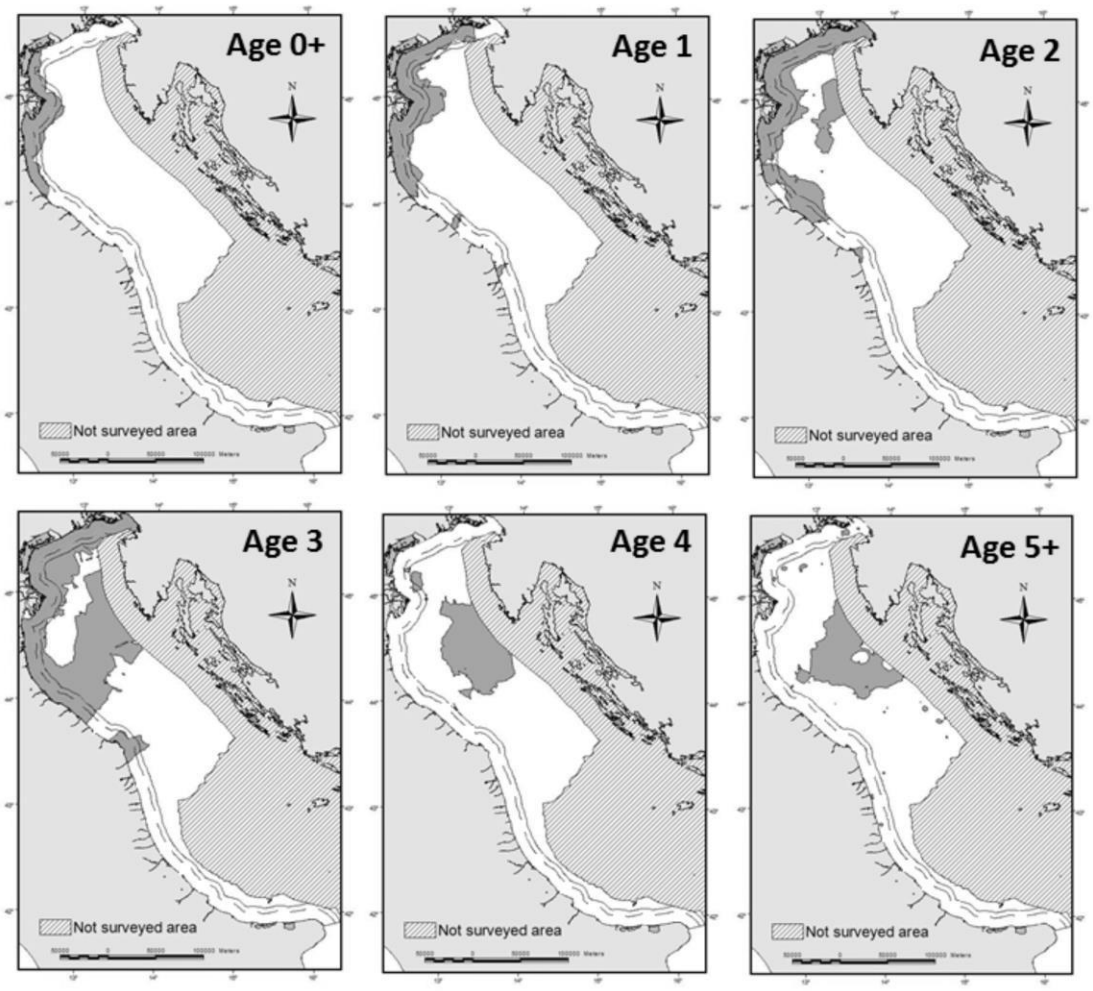

Figure 1.1.2. Maps of hotspots calculated for the age classes of soles. The 6 and 9 nautical miles from the Italian coast are shown respectively by broken and continuous black lines. Source: Scarcella et al., 2014.

1.2. Study area: central and northern Adriatic Sea

The investigated area of this thesis is the central and northern part of Adriatic Sea, management unit defined by FAO-GFCM as Geographical Sub-Area 17 (GSA 17; northern Adriatic Sea). The Adriatic Sea is the largest continental shelf area in the Mediterranean Sea. It is an elongated basin located in the northern Mediterranean, between the Italian peninsula and the Balkans, with its major axis aligned in the northwest–southeast direction, located in the central Mediterranean (Figure 1.2.1). The eastern coast is generally steep and rocky, whereas the western coast is flat and mostly sandy. The central and northern Adriatic Sea has an extended continental shelf and eutrophic shallow waters (depth generally does not exceed 100 m), whereas the southern Adriatic is characterized by a narrow continental shelve and a marked, steep continental slope. Moreover, the central sub-basin is separated from the southern one by the Pomo Pit, where depth decreases down to around 300 m. Due to the pronounced seasonal fluctuations in environmental forcing, coastal waters show a high seasonal variation in bottom temperature, ranging from 7 °C (winter) to 27 °C (summer). The thermal variability of deeper areas is very much reduced with values ranging between 10 °C (winter) and 18 °C (summer) at 50 m depth (Russo et al., 2012). A large number of rivers discharge into the basin with significant influence on the overall water circulation. Particularly relevant are the Po River in the northern basin and the ensemble of the Albanian rivers in the south-eastern basin. The rivers flowing down along the western coast of the central and northern Adriatic Sea contribute to around 20% of the whole Mediterranean river runoff (Hopkins, 1992) and introduce large fluxes of nutrients (Zavatarelli et al., 1998) that make the northern Adriatic Sea one of the most productive areas of the Mediterranean Sea (Campanelli et al., 2011). In particular, the Po River discharge forms a nutrient-rich buoyant coastal layer that flows southwards along the Italian coast (Marini et al., 2008). The general cyclonic circulation of the Adriatic Sea is composed of two branches, one flowing northwards along the Albanian–Croatian coast and the other flowing southwards along the Italian coast. In addition, the circulation in the three sub-basins (northern, central, and southern Adriatic) is often dominated by their own cyclonic gyres that vary in intensity according to the season (Artegiani et al., 1997). Northern and central Adriatic Sea sediments and associated benthic fauna show a complex spatial pattern that reflects the geological history of the area (Santelli et al., 2017). On the western side of the basin, benthic communities associated with the biocoenosis of fine well-sorted sand (FWSS) occur in the most inshore, dynamic areas and are alternated with terrigenous sediments and muddy detritic bottoms in proximity of river mouths located in particular, in front and southward from the Po river. By contrast, the eastern basin is characterized by the present of relict sands and detritic bottoms (Gamulin-Brida, 1967; Ott, 1992). These features provide ideal trawling conditions

almost throughout the basin (especially in the western side), which is one of the most intensely exploited fishing grounds in the Mediterranean Sea (Eigaard et al., 2017; Ferra` et al., 2018).

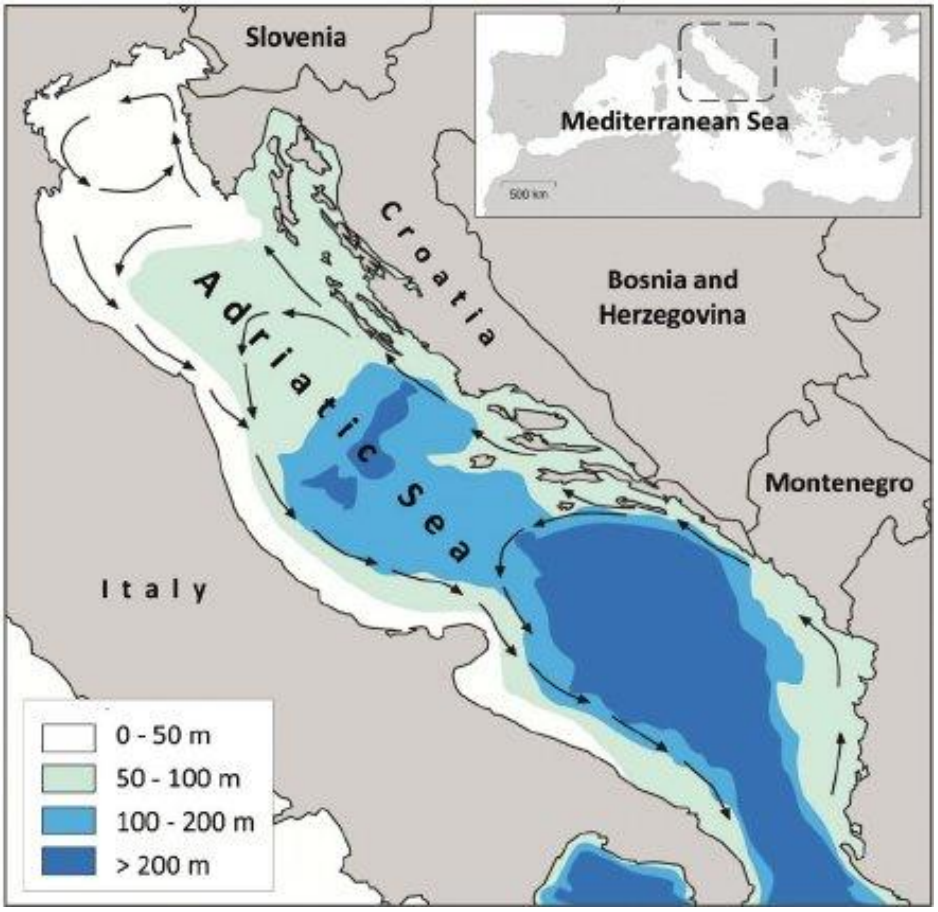

Figure 1.2.1. Map of the Adriatic Sea, with bathymetry and direction of major sea currents. Source: Gračan et al., 2014.

1.3. Focus on "rapido" trawls

Common sole is unevenly distributed in the Mediterranean Sea, with more than half of the overall fishery production attributable to Adriatic Sea catches (52%), followed by Aegean Sea (14%) and Levant Sea catches (11.5%). In this thesis particular attention is paid to *rapido* trawl fishery, a unique reality in the Mediterranean panorama that accounts for about half of *S. solea* landings in the Adriatic Sea (FAO-GFCM, 2021). The *rapido* trawl fishery has been in place for more than 50 years in the western side of the north-central Adriatic Sea, where it is carried out all year round on the soft bottoms outside three nautical miles offshore. Analysis of Automatic Identification System (AIS) data according to the method described by Galdelli et al. (2019) has demonstrated that *rapido* trawls are usually deployed in fishing grounds characterized by sandy or muddy bottoms and a depth < 50 m. Its catch therefore consists mainly of organisms living in close contact with the bottom or buried in sediment, such as flatfish and shellfish. As already observed in previous studies (Scarcella et al.,

2014), fishing effort is distributed in accordance with the distribution of the main target species *Solea solea* (Figure 1.3.1), recording the maximum effort intensity in the northern sector of the GSA. About 90% of the *rapido* trawlers can be found in the maritime compartments located between Ancona and Venice, while some are located in the compartments of Trieste and Pescara. The main port are: Chioggia (VE), Ancona, Rimini. The first zone of effort concentration is inshore between 3 and 9 nautical miles from the Italian coast, between 43° and 44° latitude, and is mainly exploited by vessels belonging to Ancona and Rimini harbors. The second zone is between Po river mouth and Venice lagoon and is concentrated at the same distance from the coast as the first region. This region is mainly exploited by the Chioggia *rapido* trawl fleet. The third area of effort concentration is offshore, near Istria peninsula and is exploited by both Chioggia and Rimini *rapido* trawl fleets. The area southward of this last region is not exploited by rapido trawlers mainly due to the high concentrations of debris and benthic communities that are dominated by holothurians (Despalatović et al., 2009; Santelli et al., 2017). *Rapido* trawlers usually tow four gears simultaneously at a speed of 5-7 knots for 12–24 hours a day, depending on local customs, 3-4 days a week according to seasonal regulations. More technical details on *rapido* gear will be provided in the dedicated section in the chapter 3.3.1

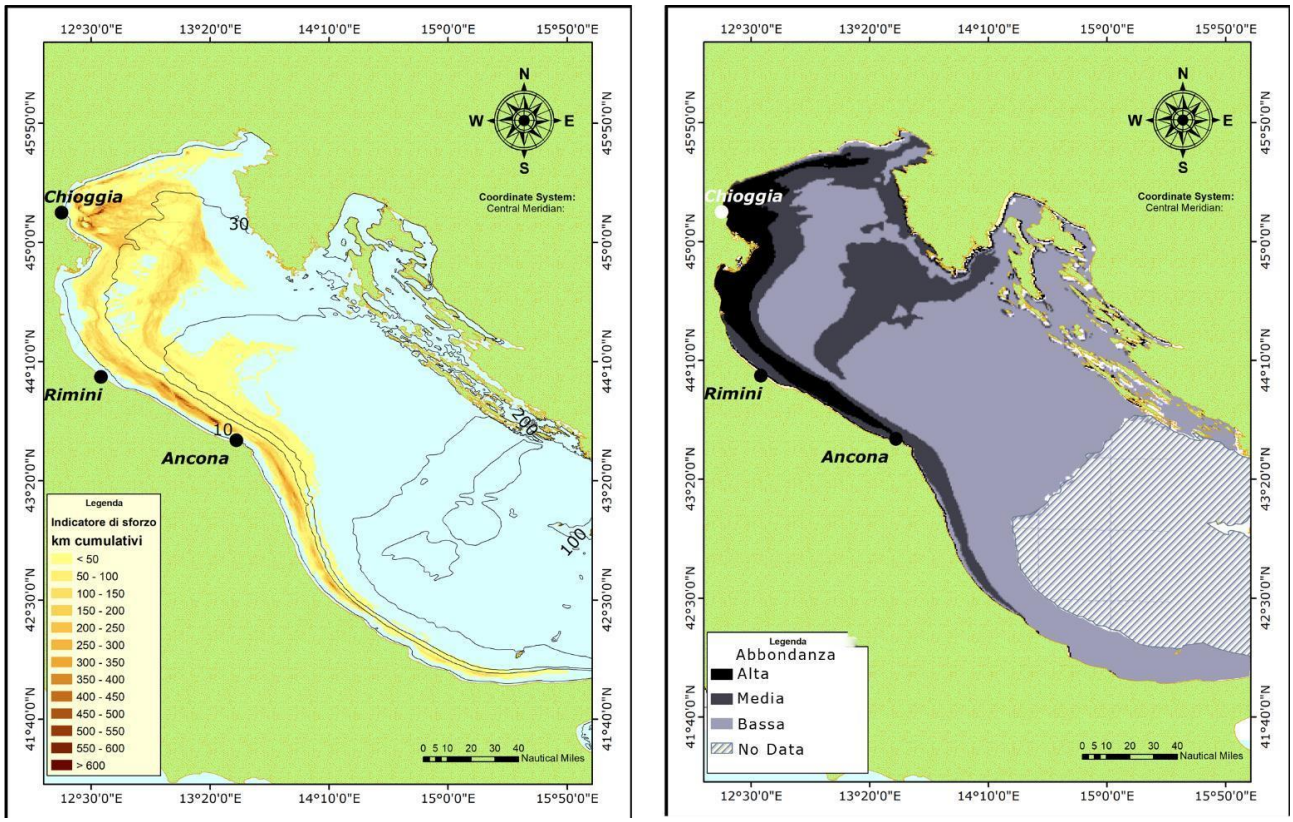

Figure 1.3.1. Rapido trawl fishery effort distribution in GSA 17 North Adriatic sea: a) Intensity of fishing effort exercised by vessel > 15 m obtained with AIS data analysis, métier "rapido", referred to the year 2017; b) Abundance (n individuals/km2) of Solea solea predicted with Solemon survey data (2009-2017). Source: Masnadi et al., 2021.

1.4. Overview: Management and stocks status in Mediterranean Sea.

The Common Fisheries Policy (hereafter CFP) fixes the rules and directions for a sustainable exploitation of marine resources exploited by European fishing fleets (Regulation EU No 1380/2013). Reflecting the specificities of different fisheries, management objectives shall be adopted as a priority in consultation with operators in the fishing industry, scientists and other stakeholders having an interest in fisheries (STECF 2016). In recent years European fisheries managers have witnessed the success of CFP in the north (i.e., North East Atlantic, Cardinale et al. 2012; Fernandes and Cook 2013) and at the same time, its failure in the south (i.e., Mediterranean Sea, Colloca et al. 2013; Vasilakopoulos et al. 2014, Cardinale and Scarcella 2017). A striking difference in the management of marine fish stocks between North East Atlantic and the Mediterranean Sea is that Mediterranean Sea is primarily managed by effort control (input control) while North East Atlantic stocks management has been based primarily on output controls such as TACs (Total Available Catches). The scientific advice on TAC is regularly provided by ICES (International Council for the Exploration of the Sea) to the European Commission. The Mediterranean stocks have largely declined in the last 15 years and their exploitation level has raised or remained above the FMSY (Fishing mortality at Maximum Sustainable Yield) level during the same period of time (Vasilakopoulos et al. 2014; Cardinale and Scarcella 2017, STECF 2019). In 2019 STECF report for Mediterranean and Black Sea stocks, out of 47 stocks, only around 13% (6 stocks) are considered not overfished and the value F/FMSY, which varies around 2.3, indicates that these stocks are being exploited on average at rates well above the FMSY CFP objective (Figure 1.4.1, STECF 2019).

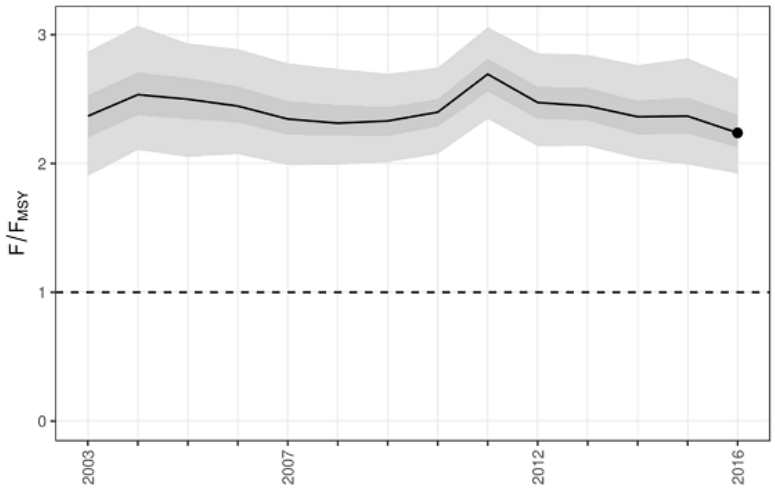

Figure 1.4.1. Trend in F/FMSY (based on 47 Mediterranean and Black Sea stocks). Dark grey zone shows the 50% confidence interval; the light grey zone shows the 95% confidence interval. Source STECF 2019.

In this context, international working groups in the framework of European Commission (Scientific, Technical and Economic Committee for Fisheries; EC-STECF) and Food and Agriculture

Organization-General Fisheries Council for the Mediterranean (Scientific Advisory Council; FAO-GFCM-SAC), have recommended reducing fishing mortality by 80% as well as the development of a management plan to achieve this reduction over time. Moreover, the "Mediterranean Regulation" (EU, 2006) foreseen that management plans within Mediterranean countries territorial waters are adopted for trawling and other fishing activities. According to GFCM/43/2019/5, a five-year fishing effort regime shall be established for 2022–2026: each year, on the basis of SAC advice, the GFCM shall establish yearly effort quotas, thus contributing to reaching Fmsy and staying within safe biological limits. In 2020 and 2021, a transitional fishing effort regime has been established: at least 12% reduction for otter trawlers and 16 % for *rapido* trawlers with respect to the annual effort exerted in 2015 or to the three-year average within the 2015–2018 period. Despite this, Cardinale and Scarcella 2017 study showed that major reasons for the alarming situation of Mediterranean Sea stocks can be found precisely in the ineffectiveness of the current effort-based system to control fishing mortality which is sensitive to the problem of "hyperstability" (effort reduction is not accompanied by a concomitant reduction in fishing mortality). On the other hand, output control system relies more on stock assessment which may be a problem considering the instability of many of the Mediterranean stock assessments due to short time series and data limitations (STECF 2016).

1.5. What is Stock Assessment?

A stock assessment is the process of collecting, analyzing, and reporting demographic information to determine changes in the abundance of fishery stocks in response to fishing with the aim to give managers advice about the status of a fishery and the possible outcomes of management actions. The mathematical and statistical techniques used to complete a stock assessment are referred to as assessment models. Fisheries stock assessment models are therefore one of the most valuable tools for providing scientific advice regarding stock status, historical productivity, and changes in stock composition (Gulland 1983; Hilborn and Walters 1992). For this reason, improving the reliability of the assessment results is mandatory and of primary interest to guide decisions regarding future regulation of harvest (Hilborn and Walters, 1992, Lorenzen, 2016) and to preserve the status of Mediterranean stocks in accordance with the objectives of the CFP.

In general, stock assessments models require three primary categories of information:

1. *Fishery dependent information* - the amount of fish removed from a stock by fishing; usually timeseries of market landing data coming from official national fishery monitoring programs. This category is discussed in details in sub-chapter 4.2 for common sole in GSA 17.
2. *Fishery independent information* – a measure, or relative index, of the number or weight of fish in the stock; usually data come from a statistically-designed, fishery-independent survey

(systematic sampling carried out by research or contracted commercial fishing vessels separately from commercial fishing operations) that samples fish throughout the stock's range the same way each year, providing a relative index of abundance over time. This category is discussed in details in sub-chapter 4.3 for common sole in GSA 17.

3. *Biology data* – all information on stock life histories parameters such as growth rates and natural mortality. This category is discussed in details in sub-chapter 4.4 for common sole in GSA 17.

1.6. State of the art: Models used, previous advice and identified issues for common sole in GSA17

In the context of FAO-GFCM Working Group on Stock Assessment of Demersal species (hereafter WGSAD), the official assessment of common sole has historically been carried out using only the GSA17 (Northern Adriatic Sea) as management unit since the landings of common sole in the western part of the southern Adriatic (GSA18) are negligible (Sabatini et al., 2018).

The assessments methods and the outcomes in terms of fishing mortality (F), relative to reference point (F_{target}) obtained before the start of this PhD program are summarized in Table 1.6.1. Of these models, Extended Survival Analysis (XSA; Shepherd 1999) is an *ad hoc* technique for tuning a Virtual Population Analysis model (VPA; Darby and Flatman, 1994) that uses information on individual cohort sizes to estimate population numbers and fishing mortalities at age by back-calculating values down each cohort. Stock Synthesis (SS3; Methot and Wetzel, 2013) is one of the most widely-used, modelling frameworks that implements statistical age-structured population modelling (forward projection of population in the Statistical catch-at-age approach) using a wide range of minimally processed fishery and survey data (Maunder and Punt 2013). The model "integrates" these multiple sources of information to internally estimate a wide range of biological and fisheries parameters (as well as management quantities and target reference points) and their associated uncertainty. Despite changes in assessment methodology from 2012 on, the stock has always been considered to be in overexploitation with relatively low biomass. However, the ratio of fishing mortality (F/F_{target}) seems to follow a decreasing trend over the years starting from very high levels of overexploitation (> 5 in 2010 and 2011 reference years) to settle on values below 2 in the last years (2015-2016 reference years). Since the common sole has been included in the European DCF, fish aging analysis based on otoliths were conducted in the Adriatic Sea both on commercial and survey data, and catch-at-age (CAA) data series were officially provided to the experts of the working group to be used as input data in stock assessment analyses. However, in 2018 (2017 assessment reference year), age data were no longer considered reliable by the EWG 18-16 (STECF 2018) due to internal inconsistencies and reports from Italian and Croatian experts that the otolith

readings were being recalibrated. Due to these problems, stock assessment of common sole in GSA 17 was not performed during the 2018 FAO-GFCM WGSAD. To overcome the problems in the age data, the stock assessment experts planned the move toward a length-based input data approach (using length frequency distribution data instead of CAA). This approach needed a good estimation of the von Bertalanffy parameters in general and overall a good estimation of the L_{∞}.

Table 1.6.1 Summary of FAO-GFCM assessments and scientific advice for common sole in GSA 17 from 2010 to 2017.

Reference year	Method used for advice	F_{curr}	F_{target}	Ratio	Status	WGSAD Comments
2010	XSA	1.34	0.26	5.15	In overexploitation with relatively low biomass	The group highlights the use of data from the eastern side of the basin. Moreover, the group underlines the need to extend the *rapido* trawl survey inside the 12 nm from the Croatian coast, as was performed in 2005 and 2006.
2011	XSA	1.43	0.26	5.5	In overexploitation with relatively low biomass	The group considered the use of the SS3 method as a good initiative. Comparisons of outputs with classical approaches should be made.
2012	SS3	0.93	0.31	3.00	In overexploitation with relatively low biomass	The group appreciated the comparison between the two models provided, as requested by last year's working group.
2013	SS3			1.50	In overexploitation with relatively low biomass	
2014	SS3	0.62	0.26	2.40	In overexploitation with relatively low biomass	
2015	SS3	0.35	0.26	1.35	In overexploitation with relatively low biomass	The group advised exploring alternative selectivity patterns.

2016	SS3	0.41	0.26	1.58	In overexploitation with relatively low biomass	
2017	None	-	-	-	No advice	Ageing issues were identified and they will be tackled in a future benchmark.

1.7. References

Artegiani, A., Bregant, D., Paschini, E., Pinardi, N., Raicich, F., Russo, A., 1997. The Adriatic Sea general circulation. Part II: baroclinic circulation structure. Journal of Physical Oceanography 27, 1515–1532.

Beyst, B., Cattrijsse, A., Mees, J., 1999. Feeding ecology of juvenile flatfishes of the surf zone of a sandy beach. Journal of Fish Biology 55, 1171–1186.

Campanelli, A., Grilli, F., Paschini, E., Marini, M., 2011. The influence of an exceptional Po River flood on the physical and chemical oceanographic properties of the Adriatic Sea. Dynamics of Atmospheres and Oceans 52, 284–297.

Cardinale, M. and Scarcella, G. 2017. Mediterranean Sea: A Failure of the European Fisheries Management System. Front. Mar. Sci. 4:72 doi: 10.3389/fmars.2017.00072.

Cardinale, M., Doerner H., Abella A., Andersen J. L., Casey J., Döring R., et al. 2012. Rebuilding EU fish stocks and fisheries, a process under way? Marine Policy 39, 43–52. doi: 10.1016/j.marpol.2012.10.002.

Colloca, F., Cardinale M., Maynou F., Giannoulaki M., Scarcella G., Jenko K., et al. 2013. Rebuilding Mediterranean fisheries: a new paradigm for ecological sustainability. Fish Fish. 14, 89–109. doi:10.1111/j.1467-2979.2011. 00453.

Darby C.D., Flatman S. 1994. Virtual Population Analysis: Version 3.1 (Windows/Dos) user guide. Info. Tech. Ser., MAFF Direct. Fish. Res., Lowestoft, (1): 85 pp.

Despalatović, M., Grubelić, I., Piccinetti, C., Cvitković, I., Antolić, B., Žuljević, A., Nikolić, V., 2009. Distribution of echinoderms on continental shelf in open waters of the northern and middle Adriatic Sea. J. Mar. Biol. Assoc. U. K. 89, 585–591.

Eigaard, O. R., Bastardie, F., Hintzen, N. T., Buhl-Mortensen, L., Buhl-Mortensen, P., Catarino, R., Dinesen, G. E., et al. 2017. The footprint of bottom trawling in European waters: distribution, intensity, and seabed integrity. ICES Journal of Marine Science, 74: 847–865.

EU (2006). Council Regulation (EC) No 1967/2006 of 21 December 2006 Concerning Management Measures for the Sustainable Exploitation of Fishery Resources in the Mediterranean Sea, Amending Regulation (EEC) No 2847/93 and Repealing Regulation (EC) No 1626/94, EU.

EU (2013). Regulation (EU) No 1380/2013 of the European Parliament and of the Council of 11 December 2013 on the Common Fisheries Policy, Amending Council Regulations (EC) No 1954/2003 and (EC) No 1224/2009 and Repealing Council Regulations (EC) No 2371/2002 and (EC) No 639/2004 and Council Decision 2004/585/EC Official Journal of the European Union. Brussels: EU.

FAO-GFCM. 2021. Report of the Working Group on Stock Assessment of Demersal Species (WGSAD) – Benchmark session for the assessment of common sole in GSA 17, Scientific Advisory Committee on Fisheries (SAC). Online via Microsoft Teams, 12–16 April 2021.

Fernandes, P. G., and Cook, R. M. 2013. Reversal of fish stock decline in the Northeast Atlantic. Curr. Biol. 23, 1432–1437. doi: 10.1016/j.cub.2013.06.016.

Ferra`, C., Tassetti, A. N., Grati, F., Pellini, G., Polidori, P., Scarcella, G., and Fabi, G. 2018. Mapping change in bottom trawling activity in the Mediterranean Sea through AIS data. Marine Policy, 94: 275–281.

Fortibuoni, T. et al. 2017. Fish and fishery historical data since the 19th century in the Adriatic Sea, Mediterranean. Sci. Data 4:170104 doi: 10.1038/sdata.2017.104.

Galdelli, A., Mancini, A., Tassetti, A. N., Ferrà Vega, C., Armelloni, E., Scarcella, G., et al. 2019. A Cloud Computing Architecture to Map Trawling Activities Using Positioning Data. Vol. 9 15th IEEE/ASME Int. Conf. Mechatron. Embed. Syst. Appl. doi:10.1115/DETC2019-97779.

Gamulin-Brida, H., 1967. The benthic fauna of the Adriatic Sea. Oceanography and Marine Biology. Annual Review 5, 535–568.

Giovanardi, O., Pranovi, F., and Franceschini, G. (1998). “Rapido” trawl-fishing in the Northern Adriatic: preliminary observations on effects on microbenthic communities. Acta Adriat. 39, 37–52.

Gračan, R., Mladineo, I. & Lazar, B. 2014. Insight into the diet composition and gastrointestinal parasite community of the common smooth-hound, *Mustelus mustelus* (Carcharhiniformes: Triakidae), in the northern Adriatic Sea. Nat. Croat., Vol. 23, No. 1, 35–44, 2014, Zagreb.

Grati, F., Scarcella G., Polidori P., Domenichetti F., Bolognini L., Gramolini R., Vasapollo C., Giovanardi O., Raicevich S., Celić I., Vrgoč N., Isajlovic I., Jenič A., Marčeta B., Fabi G. 2013. Multi-annual investigation of the spatial distributions of juvenile and adult sole (*Solea solea*, L.) in the Adriatic Sea (Northern Mediterranean). J. Sea Res. http://dx.doi.org/10.1016/j.seares.2013.05.001.

Guarniero, I., Franzelletti S., Ungaro N., Tommasini S., Piccinetti C., Tinti F. 2002. Control region haplotype variation in the central 1 Mediterranean common sole indicates geographical isolation and population structuring in Italian stocks. J. Fish Biol. 60, 1459–1474.

Gulland, J.A. 1983. Fish Stock Assessment: A Manual of Basic Methods. New York: Wiley. 223 p.

Hall-Spencer, J., Froglia, C., Atkinson, R. J. A., and Moore, P. G. (1999). The impact of Rapido trawling for scallops,*Pecten jacobaeus* (L.), on the benthos of the Gulf of Venice. ICES J. Mar. Sci. 56, 111–124. doi: 10.1006/jmsc.1998.0424.

Hilborn, R.W. and Walters C. 1992. Quantitative Fisheries Stock Assessment: Choice, Dynamics, and Uncertainty. New York: Chapman and Hall. 570 p.

Hopkins, T.S., 1992. The structure of Ionian and Levantine Seas. Reports in Meteorology and Oceanography 41 (II), 35–56.

Lorenzen, K. 2016. Toward a new paradigm for growth modeling in fisheries stock assessments: Embracing plasticity and its consequences. Fisheries Research, 180, 4–22. https://doi.org/10.1016/j.fishres.2016.01.006.

Magoulas, A., Tsimenides, N., Zouros, E., 1996. Mitochondrial DNA phylogeny and the reconstruction of the population history of a species: the case of the European anchovy (*Engraulis encrasicolus*). Mol. Biol. Evol. 13, 178–190.

Marini, M., Jones, B.H., Campanelli, A., Grilli, F., Lee, C.M., 2008. Seasonal variability and Po River plume influence on biochemical properties along western Adriatic coast. Journal of Geophysical Research 113, C05S90. http://dx.doi.org/10.1029/2007JC004370.

Maunder, M. N., and Punt, A. E. (2013). A review of integrated analysis in fisheries stock assessment. Fish. Res. 142, 61–74. doi:10.1016/j.fishres.2012.07.025.

McClenachan, L., Ferretti, F. & Baum, J. K. From archives to conservation: Why historical data are needed to set baselines for marine animals and ecosystems. Conserv. Lett 5, 349–359 (2012).

Mediterranean Sensitive Habitats, 2013. Edited by Giannoulaki M., A. Belluscio, F. Colloca, S. Fraschetti, M. Scardi, C. Smith, P. Panayotidis, V. Valavanis M.T. Spedicato. DG MARE Specific Contract SI2.600741, Final Report, 557 p.

Methot, R. D., and Wetzel C. R. 2013. Stock synthesis: a biological and statistical framework for fish stock assessment and fishery management. Fisheries Research, 142: 86–99.

Ott, J.A., 1992. The Adriatic Benthos: problems and perspectives. In: Colombo, G., Ferrari, I., Ceccherelli, V.U., Rossi, R. (Eds.), Marine Eutrophication and Population Dynamics, pp. 367–378.

Pagotto, G., Piccinetti, C., Specchi, M., 1979. Premières résultats des campagnes de marquage des soles en Adriatique: déplacements. Rapp. Comm. Int. Explor. Sci. Mer Médit. 25/26 (10), 111–112.

Petovic, S., Markoviæ, O., Ikica, Z., Đuroviæ, M., and Joksimoviæ, A. (2016). ´ Effects of bottom trawling on the benthic assemblages in the south Adriatic Sea (Montenegro). Acta Adriat. 57, 81–92.

Piccinetti, C., Giovanardi, O., 1984. Données biologique sur Solea vulgaris en Adriatique. FAO Fisheries Report 290, 117–118.

Pranovi, F., Raicevich, S., Franceschini, G., Farrace, M. G., and Giovanardi, O. (2000). Rapido trawling in the northern Adriatic Sea: effects on benthic communities in an experimental area. ICES J. Mar. Sci. 57, 517–524. doi: 10.1006/jmsc.2000.0708.

Quéro, J.-C., M. Desoutter and F. Lagardère, 1986. Soleidae. p. 1308-1324. In P.J.P. Whitehead, M.-L. Bauchot, J.-C. Hureau, J. Nielsen and E. Tortonese (eds.) Fishes of the North-eastern Atlantic and the Mediterranean. UNESCO, Paris. Vol. 3.

Rosenberg, A. A. et al. The history of ocean resources: modelling cod biomass using historical records. Front.Ecol.Environ. 3, 84–90 (2005).

Russo, A., Artegiani, A., 1996. Adriatic Sea hydrography. Scientia Marina 60, 33–43.

Russo, A., Carniel, S., Sclavo, M., Krzelj, M., 2012. Climatology of the Northern– Central Adriatic Sea. Modern Climatology. Book 8. http://digitalcommons.usu.edu/modern_climatology/8.

Sabatini, L., Bullo, M., Cariani, A., Celić, I., Ferrari, A., Guarniero, I., et al. 2018. Good practices for common sole assessment in the Adriatic Sea: Genetic and morphological differentiation of *Solea solea* (Linnaeus, 1758) from *S. aegyptiaca* (Chabanaud, 1927) and stock identification. J. Sea Res. 137, 57–64. doi:10.1016/j.seares.2018.04.004.

Santelli A, Cvitković I, Despalatović M, Fabi G and others (2017) Spatial persistence of megazoobenthic assemblages in the Adriatic Sea. Mar Ecol Prog Ser 566:31-48. https://doi.org/10.3354/meps12002.

Scarcella, G., Grati F., Raicevich S., Russo T., Gramolini R., Scott R. D., Polidori P., Domenichetti F., Bolognini L., Giovanardi G., Celić I., Sabatini L., Vrgoč N., Isajlović I., Marčeta B., Fabi G., 2014. Common sole in the northern and central Adriatic Sea: Spatial management scenarios to rebuild the stock. J. Sea Res. http://dx.doi.org/10.1016/j.seares.2014.02.002.

Schückel, S., Sell, A. F., Kihara, T. C., Koeppen, A., Kröncke, I., and Reiss, H. (2013). Meiofauna as food source for small-sized demersal fish in the southern North Sea. Helgol. Mar. Res. 67, 203–218. doi: 10.1007/s10152-012-0316-1.

Scientific, Technical and Economic Committee for Fisheries (STECF). 2016 – Multiannual plan for demersal fisheries in the Western Mediterranean (STECF-16-21); Publications Office of the European Union, Luxembourg; EUR 27758 EN; doi:10.2788/103428.

Shepherd J. G. 1999. Extended survivors analysis: An improved method for the analysis of catch-at-age data and abundance indices. ICES Journal of Marine Science, 56: 584-591.

Smedbol, R.K., Stephenson, R.L., 2001. The importance of managing within-species diversity in cod and herring fisheries of the North-Western Atlantic. J. Fish Biol. 59 (A), 109–128.

STECF 2018. Scientific, Technical and Economic Committee for Fisheries (STECF) Stock Assessments - Part 2 (STECF-18-16). Publications Office of the European Union, Luxembourg, 2018, ISBN 978-92-79-79399-8, doi:10.2760/598716, JRC114787.

STECF 2019. Scientific, Technical and Economic Committee for Fisheries (STECF). Monitoring the performance of the Common Fisheries Policy (STECF-Adhoc-19-01). Publications Office of the European Union, Luxembourg, ISBN 978-92-76-02913-7, doi:10.2760/22641, JRC116446.

Tortonese, E. 1975. Osteichthyes - Fauna d'Italia vol. XI, Calderini, Bologna.

Vallisneri, M., Piccinetti, C., Stagni, A.M., Colombari, A., Tinti, F., 2000. Dinamica di popolazione, accrescimento, riproduzione di *Solea vulgaris* (Quensel 1806) nell'alto Adriatico. Biologia Marina Mediterranea 7 (1), 65–70.

Vasilakopoulos, P., Maravelias C.D., Tserpes G. 2014. The alarming decline of Mediterranean fish stocks. Curr. Biol. 24, 1643–1648. doi: 10.1016/j.cub.2014.05.070.

Wagemans, F. and Vandewalle, P. 2001. Development of the bony skull in common sole: brief survey of morpho-functional aspects of ossification sequence. Journal of Fish Biology, 59: 1350 1369. https://doi.org/10.1111/j.1095-8649.2001.tb00197.x.

Zavatarelli, M., Raicich, F., Bregant, D., Russo, A., Artegiani, A., 1998. Climatological biogeochemical characteristics of the Adriatic Sea. Journal of Marine Systems 18, 227–263.

2. Aim of the study and objectives

The main objective of this PhD thesis is to assess the state of the stock of *Solea solea* in the northern and central Adriatic combining the use of conventional and innovative techniques and methodologies, such as the use of SS3 modelling platform in an ensemble approach, to provides a more robust quantification of uncertainty and more reliable predictions of stock status compared to past advice. In this context, it is of primary importance to assess, deepen and improve scientific knowledge on the subject to date through a holistic view starting from the revision of fundamental biological information (such as life history traits recalibrated based on new available data and biological assumptions), passing through the updating, improvement and application of new techniques and approaches related to population modeling, up to the topic of prioritize and maximize scientific advice quality and reliability in managerial context. Particular attention is paid to *rapido* fishery, a unique reality in the Mediterranean panorama. Moreover, all the topics are contextualized in the overall framework of the current (e.i. Rec. GFCM/43/2019/54) and alternative (e.i. TACs) management strategies to be adopted in the Adriatic Sea area with a special regard to the main CFP objectives, such as the restoring and maintaining of the stocks above levels which can produce the Maximum Sustainable Yield (MSY). The various topics will be dealt within the following four chapters (from Chapter 3 to 6) which constitute the scientific apparatus of this thesis and are briefly summarized below. The studies and analyses reported in these chapters are entirely taken or adapted from scientific papers and reports published during the 3-year doctoral period.

Chapter 3 – In this chapter, a study on the use of data poor models to analyze and to project in the medium-term future the state of exploitation of the catch assemblage caught by *rapido* fishery in the Adriatic Sea is presented. Firstly, species that are caught almost exclusively by this gear, are evaluated through a Bayesian state-space implementation of the Schaefer production Model (BSM) of the CMSY software. Then, the outcomes are used to run a CMSY model extension to estimate rebuilding time and to forecast expected catches under four different harvest control rule (HCR) scenarios based on plausible levels of effort reduction, through 15-years forecasts. This chapter is taken from the paper "*Data poor approach for the assessment of the main target species of rapido trawl fishery in Adriatic Sea*" written in collaboration with colleagues of CNR-IRBIM of Ancona, and published in Frontiers in Marine Science.

Chapter 4 – In this chapter, all implementation stages of data-rich stock assessment model developed for common sole in GSA 17 is presented. Among the improvements made, a new set of von Bertalanffy growth parameters are estimated based on new otolith reading from commercial and survey sampling based on the more accurate thin section methodology. The biggest novelty introduce in the modeling part is the use of an ensemble of Stock Synthesis (SS3) models developed to

incorporate uncertainty. The uncertainly is based on alternative hypotheses of selectivity, natural mortality and steepness three parameters (18 runs) which claim to represent as faithfully as possible the true state of nature of the stock under analysis. In this context, a new quantitative criterion based on diagnostic scores for weighting the runs is used to join posterior distribution of the key estimates via delta-MVLN estimator. Moreover, short-term projections are presented using the same approach. Most of the data and analyses shown in this chapter are taken or adapted from the scientific report "*Stock Assessment Form Demersal species - Stock assessment of common sole in GSA 17*" presented in the context of the Working Group on Stock Assessment of Demersal Species.

Chapter 5 – In this chapter, a study on the exploration and application of different growth dynamics for common sole in GSA17 is presented. More precisely, back-calculation measurements obtained from SoleMon survey data are used to fit and compared monophasic and biphasic growth curves to test if a change in the growth due to a re-allocation of energy during individual lifespan occur in Adriatic sole stock. The outcomes are used to test and compare the two growth pattern within the stock assessment model used for providing scientific advice in the FAO-GFCM context. This chapter is taken from the paper "*Biphasic versus monophasic growth curve equation, an application to common sole (Solea solea, L.) in the northern and central Adriatic Sea: effects on stock assessment and advice*" written in collaboration with colleagues of CNR-IRBIM of Ancona, COISPA of Bari and Swedish University of Agricultural Sciences of Lysekil and published in Fisheries Research.

Chapter 6 - In this chapter, an application of a simulation-testing procedure to determine best performing reference points depending on stock-specific characteristics is presented for common sole in GSA 17. In particular, the procedure is adapted from the "short-cut" management strategy evaluation (MSE) approach developed and discussed during the ICES Workshops WKREF1 & 2 and is run on the ensemble assessment grid presented in chapter 4. The aim of the study is to test a range of fishing mortalities and biomass thresholds in relation to virgin stock size (B0) and to rank them on the basis of performance evaluation criteria in accordance with the precautionary objectives of CFP framework. The outputs of this simulation are discussed in order to provide recommendations to tailor stock-specific reference point for common sole stock in GSA17. This chapter is partially taken and adapted from the ICES scientific reports *"Workshop on ICES reference points (WKREF1)"* and *"Workshop on ICES reference points (WKREF2)"* in which the candidate actively participated during the second year of the PhD and of which he is co-author.

Finally, Chapter 7 provides a general discussion and draw conclusions based on the different analyses presented in the previous chapters of the thesis.

3. Data-poor approach for the assessment of the main target species of *rapido* trawl fishery in Adriatic Sea

From the paper: *Armelloni E.N., Scanu M., **Masnadi F**., Coro G., Angelini S. and Scarcella G. 2021. Data Poor Approach for the Assessment of the Main Target Species of Rapido Trawl Fishery in Adriatic Sea. Front. Mar. Sci. 8:552076. doi:10.3389/fmars.2021.552076.*

3.1. Abstract

Information on stock status is available only for a few of the species forming the catch assemblage of *rapido* fishery of the North-central Adriatic Sea (Mediterranean Sea). Species that are caught almost exclusively by this gear, either as target (such as Pectinidae) or accessory catches (such as flatfishes apart from the common sole), remain unassessed mainly due to the lack of data and biological information. Based on cluster analysis, the catch assemblage of this fishery was identified and assessed using CMSY model. The results of this data-poor methodology showed that, among the species analyzed, no one is sustainably exploited. The single-species CMSY results were used as input to an extension of the same model, to test the effect of four different harvest control rule (HCR) scenarios on the entire catch assemblage, through 15-years forecasts. The analysis showed that the percentage of the stocks that will reach Bmsy at the end of the projections will depend on the HCR applied. Forecasts showed that a reduction of 20% of fishing effort may permit to most of the target and accessory species of the *rapido* trawl fishery in the Adriatic Sea to recover to Bmsy levels within 15 years, also providing a slight increase in the expected catches.

3.2. Introduction

Single Species Fishery Management (SSFM) has many limitations since it does not consider the effects of fishing on non-target species and the effect of species interaction on the fisheries (Link, 2010). Typically, in an SSFM context, advice given for a few species is the unique information used to control the whole fishery (Moffitt et al., 2016), and this might lead to over-pressured bycatch species (Browman et al., 2004). Nevertheless, when applying management measures specifically developed for one species (e.g., introduction of quotas), they will affect the entire catch assemblage ("technical interaction"; Punt et al., 2002). Although few practical experiments are available, intergovernmental marine science organizations strongly advise about the limited view given by single-stock management on multiple stocks caught in mixed fisheries (ICES., 2017). To avoid this situation, and under the government's recommendation, in recent years fishery science has been focused on developing a multi-species approach (Link, 2010; Hilborn, 2011; Froese et al., 2018; Howell and Subbey, 2019). However, to date management advices for the Mediterranean Sea mostly rely on single-species stock assessment methodologies (FAO-GFCM, 2019). Above all, considering

the intrinsic multi-specific nature of the fishery, there is a strong need to move forward to more comprehensive management of stocks in the Mediterranean Sea (Colloca et al., 2013; Cardinale et al., 2017). Sophisticated assessment models able to give insights into ecosystem complexity have been proposed, though they are limited by the large amount of data required (Maunder and Punt, 2013). As such, these models are not easy to fit data-poor environments such as the Mediterranean Sea (Maravelias and Tsitsika, 2008). To find an alternative solution, we tested an advanced surplus production model implementation that assess the status of multiple species at once in data-poor scenarios (Froese et al., 2018). Surplus production models calculate fisheries parameters at Maximum Sustainable Yield (MSY) (e.g., biomass, exploitation, catch) based on the estimates of the intrinsic rate of growth (r) and the carrying capacity (*k*) parameters that are specific and tailored to the stock, rather than referring to the species in general.

This paper presents the first attempt to analyze and to project in the medium-term future the state of exploitation of the catch assemblage caught by *rapido* trawlers in the North Adriatic Sea (General Fisheries Commission for the Mediterranean – GFCM, Geographical Sub-Area – GSA 17), one of the most impacting fisheries in the Mediterranean Sea (Colloca et al., 2017). Based on the Annual Economic Report of the Scientific, Technical and Economic Committee for Fisheries (STECF), 64 vessels belonging to this segment were active in 2018, accounting for about 270 engaged crew and a gross value of landing estimated around 20 million € (STECF, 2019). This fishery represents an interesting case study, because—thanks to the gear conformation— *rapido* trawlers are able to catch some species that are difficult to get with other gears. Many species that are almost exclusively caught by this gear—either as target (such as *Pectinidae*) or accessory catches (such as flatfishes other than sole), remain unassessed mainly due to lack of data and biological information. Therefore, it could be difficult to implement an ecosystem approach to fishery management and there is a high risk of underestimating the impact of this fishery. The catch assemblages of the most important demersal gears in GSA 17 were first reconstructed and clustered through multivariate analysis, to detect leading species for *rapido* fishery. At a second stage, the status of these stocks was evaluated through a Bayesian statespace implementation of the Schaefer production Model (BSM) of the CMSY software (Froese et al., 2017). Finally, the BSM estimates were used to run a CMSY extension on the entire *rapido* trawl catch assemblage (Froese et al., 2018), to estimate rebuilding time and to forecast expected catches. This extension considers fisheries' inter-dependencies to predict the overall status of the stocks under four different harvest control rule (HCR; Berger et al., 2012) scenarios up to 15 years in the future (2033). The main novelty of this study is the application of data-poor methodologies to jointly assess the status of the entire catch assemblage, while also assessing how rebuilding time depends on the level of future exploitation.

3.3. Materials and methods

3.3.1. Rapido Fishery

The *rapido* trawl fishery has been in place for more than 50 years in the western side of the north-central Adriatic Sea (Figure 3.3.1.1), where it is carried out all year round on the soft bottoms outside three nautical miles offshore (Scarcella et al., 2007). This gear is constituted by a cone-shaped net with a rigid metallic mouth opening up to 4 m wide, which slides on the seafloor aided by sleds. The mouth is equipped with a wooden plank on the top, acting as a depressor that allows the iron teeth in the lower edge to penetrate the sediment (Hall-Spencer et al., 1999). The gear shape enables trawlers to target flatfishes and species that live buried in the sediments, which are usually difficult to catch with otter trawling. As a result, catch composition forms a specific assemblage, mainly constituted by Pectinidae, in the sandy offshore areas of the North-East Adriatic (Giovanardi et al., 1998), and by flatfishes in the muddy inshore areas of central Adriatic (Pranovi et al., 2000). The penetration of the iron teeth in the sediment makes this gear particularly invasive to the sea-bottom, especially affecting the macro and meiobenthic communities (Pranovi et al., 2000; Petovic´ et al., 2016; Santelli et al., 2017). Indeed, since many fish species, such as flatfish and gobies, feed on meiofaunal species (Schückel et al., 2013) this fishing gear acts not only as direct pressure on demersal fish stocks but also as an indirect pressure interfering with the distribution of stocks' preys.

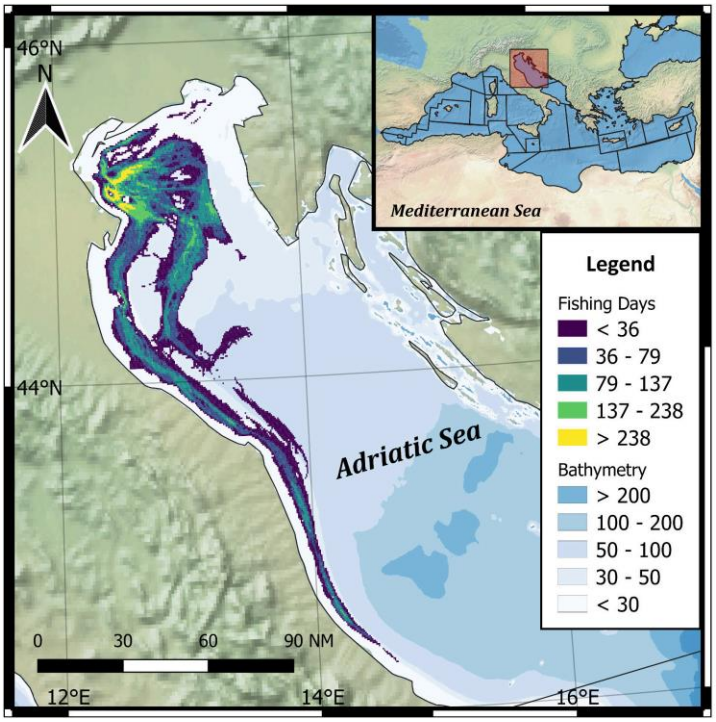

Figure 3.3.1.1. Rapido trawl fishery effort distribution in GSA 17 North Adriatic sea, obtained with AIS data analysis based on Galdelli et al. (2019).

3.3.2. Multivariate Analyses to Define Catch Assemblages

Data used to reconstruct the catch assemblages for main demersal gears in the GSA 17 were gathered from the STECF Annual Economic Report (STECF, 2019), which contains catch amount by species at gear and nation levels. The dataset was manually filtered to exclude pelagic species and taxonomic categories higher than the family level. Fishing gears representing small- scale fishery were grouped under the polyvalent passive gears (PGP) category. The yearly time frame considered was 2012–2017, due to data gaps in STECF (2019), namely Croatian data before 2012 and Italian data for 2018. The species list was sorted by magnitude of total catches and those falling within the 99% of the cumulative distribution were retained for the successive analysis. Then, for each selected species a vector was constructed, with each element representing mean catch by gear and by country. The obtained data were normalized by applying the *chord* transformation—i.e., scaling each vector to norm 1 (Legendre and Gallagher, 2001). The vectors obtained were assembled into a matrix (MC, Supplementary Table 1), where rows represented species, columns represented gears, and cells included normalized values of catches. Then, a multivariate analysis was applied to verify, firstly, if there were differences between catch assemblages of gears considered and if there were species strictly affected by *rapido* trawl fishery rather than by other gears. Differences between catch assemblages of gears were assessed through a one-way permutational multivariate analysis of variance (PERMANOVA) with 9,999 permutations (Oksanen et al., 2016) applied to a matrix of Euclidean distances computed over the MC columns. A pairwise analysis (Arbizu, 2017) was used to explore the gear contribution to the difference. Then, to identify species strictly affected by specific gears, the species list was partitioned through a hierarchical cluster analysis—based on the Ward method (Ward, 1963)—applied to the matrix of Euclidean distance computed over the MC rows. As a result, this process identified a group of species that were mostly correlated (i.e., targeted) with *rapido* trawling on which a joint HCR test would be more meaningful. Multiscale bootstrap resampling (Borcart et al., 2018)—from the "pvclust" R package (Suzuki and Shimodaira, 2015)—was used to verify the statistical robustness of the identification of these species. To understand the contribution of each gear and nation to the cluster definition, MC rows were aggregated on the clusters identified, then mean values by MC column were computed for each group and represented through radar plots (Bion, 2021).

3.3.3. Stock Assessment

The stock assessments of the species identified through cluster analysis were performed using the CMSY software. CMSY includes a BSM, which fits catch and—optionally—biomass (or catch-per-unit-of-effort) data through a Markov Chain Monte Carlo method based on the Schaefer function for biomass dynamics. The model estimates fisheries reference points (MSY, Fmsy, Bmsy) as well as relative stock size (B/Bmsy) and exploitation (F/Fmsy) from catch data and broad priors for "resilience" (approximated by r) and stock's relative biomass (B/k) at the beginning and the end of the catch time series. For the scopes of this paper, BSM was executed on landing data and biomass indices. The biomass indices were obtained from the SoleMon project (Grati et al., 2013), a trawl survey carried out from 2005 up to the present with *rapido* trawl in a 36,742-km2 area of the Northern and Central Adriatic Sea (Scarcella et al., 2014). To improve the indices estimates, data were smoothed through the "BCrumb" routine, a state-space model for trend analysis of ecological time series that is part of the JABBA (Winker et al., 2018) and JARA (Winker and Sherley, 2019) models. This tool treats relative biomass as an unobservable state variable that follows a log-linear Markovian process to reduce the influence of observation error on the CMSY estimates (Winker et al., 2018). As input for the catch data, the longest series of landings in GSA17 available for each species were used (see Table 3.3.3.1 and Supplementary Table 2; Fortibuoni et al., 2018; STECF, 2019; DCF-ITA). Missing data of Croatian and Slovenian landings were reconstructed through a mean proportion, derived from the years in which they were available for all GSA17 bordering countries. Priors for r were either taken from previous specific studies in this area (Froese et al., 2018) or inferred from their averages in FishBase and SeaLifeBase (Palomares and Pauly, 2018; Froese and Pauly, 2019). The choice of an increasing pattern from the initial to the final depletion prior in the reference models was supported by an overall increase in the fishing pressure in the Adriatic Sea (Colloca et al., 2017) followed by a reduction of the productivity of the commercial fishery over the study period (Marini et al., 2017). A sensitivity analysis was conducted to test the effect of different sets of viable depletion priors (Bstart/k and Bend/k) on the final B/Bmsy value. A Feed-Forward Artificial Neural Network was used to estimate these viable prior ranges of relative biomass for each studied species, based on characteristics of the catch time series such as minimum and maximum catch, length, slope in the final years, and shape (Froese et al., 2021 submitted). The network was trained with the data of 400 stock to detect interplay patterns of catch and abundance and predict relative biomass priors directly from the catch time series. Following the procedure described in Falsone et al. (2021), the accuracy of the final result was calculated through the percent difference between the reference model's values and the Artificial Neural Network model's values.

Table 3.3.3.1: Input data of the CMSY analysis. Stocks are presented by FAO 3-Alpha code, scientific and common name of the species, Start year= first year of the analisys, End year= last year of the analisys, r.hi/r.low= range specified for resilience, stb.low/stb.hi= prior biomass range relative to the unexploited biomass (B/k) at the beginning of the time series, Endb.low/Endb.hi= prior relative biomass (B/k) range at the end of the catch time series, Smoothed index= smooth to the biomass index.

FAO 3-Alpha Code	Scientific name	Common name	Start year	End year	r. low	r. high	stb.low	stb.hi	Endb.low	Endb.hi	Smoothed index
BLL	*Scophtalmus rhombus*	Brill	1972	2018	0.31	0.71	0.4	0.8	0.01	0.2	Y
BOY	*Bolinus brandaris*	Purple dye murex	1972	2018	0.64	1.46	0.7	1	0.4	0.8	N
SJA	*Pecten jacobaeus*	Mediterranean scallop	1972	2018	0.25	0.74	0.4	0.8	0.1	0.3	Y
SOL	*Solea solea*	Common sole	1972	2018	0.33	0.76	0.4	0.8	0.1	0.5	N
SCX -> QSC	*Aequopecten opercularis*	Queen scallop	2004	2008	0.37	0.84	0.2	0.6	0.01	0.4	Y

3.3.4. Stock Projections

The outputs of single-species stock assessments were used to run an advanced implementation of CMSY (Froese et al., 2018). This model uses a rewrite of the Schaefer function to predict next year's status of the biomass, based on the parameters estimated by the CMSY model:

$$\frac{B_{t+1}}{B_{msy}} = \frac{B_t}{B_{msy}} + 2\,F_{msy}\,\frac{B_t}{B_{msy}}\left(1 - \frac{B_t}{2\,B_{msy}}\right) - \frac{B_t}{B_{msy}}\,F_t$$

In the equation, B_t and F_t respectively represent the biomass and the fishing effort in a certain year (t), while B_{t+1} is the biomass in the following year. The model assumes that the estimated r and k CMSY parameters remain constant over the projection time. The catch assemblage analysis iteratively uses the above formula under different relative effort scenarios, i.e. as different ratios of fishing mortality (F) over the fishing mortality in the last estimation year (F_{last_year}). In particular, for

the stocks identified in the cluster analysis, the following HCR scenarios, based on the F of every single stock, were used:

- Scenario (1): 0.5 F_{2018} simulating a reduction of 50%,
- Scenario (2): 0.6 F_{2018} simulating a reduction of 40%,
- Scenario (3): 0.8 F_{2018} simulating a reduction of 20%,
- Scenario (4): 0.95 F_{2018} simulating a reduction of 5%,

where F_{2018} is the F value of the last year of each stock time series. The advanced implementation of CMSY is a non-Bayesian statistical algorithm that builds on the Bayesian estimates of CMSY. Based on the F scenarios, the algorithm cycles through the following steps for each scenario:

1. For each stock, produce 1000 iterations of the biomass in time, starting from values in the neighborhoods of B/B_{msy};
2. Average all the generated B/B_{msy} time series of each stock;
3. Average the averaged B/B_{msy} time series of all stocks;
4. Estimate confidence intervals and plot the forecasts.

Step 1 of the algorithm is necessary to account for uncertainty around the estimate of B/B_{msy}, also due to a random error term used in the Schaefer function in CMSY.

Since CMSY accounts for stock depletion at very low biomass levels, the effort scenarios consider also different effects of the exploitation level on low-biomass stocks. In particular, during the projections, the following rules are applied:

1. In Scenario (1), the fishing mortality of a stock is set equal to zero when $B < 0.5\ B_{msy}$;
2. In the other scenarios, when $B < 0.5\ B_{msy}$, F is linearly decreased with biomass, according to the relation $F = \frac{(2\ Bt)}{Bmsy}\ Fmsy$.

Rule number 2 comes from a $\frac{2B_t}{B_{msy}}$ linearly decreasing multiplier of F_{msy} used in CMSY to account for repopulation hysteresis for low relative biomasses (Froese et al., 2018, 2020). Projecting biomass after fixing relative fishing mortality to the one in the last year for each stock, allows accounting for the real and different effects of the fisheries on each stock. Indeed, this assumption proportionally reduces the effort on each stock, assuming that the fishing strategies and gears do not change. Thus, in this way, a uniform reduction of the fishing hours in a certain year will affect each stock differently.

3.4. Results

The taxonomic list analysed with the multivariate analysis was composed of 87 species (Supplementary Table 3). The PERMANOVA test highlighted a significant difference between the

catch assemblages of the nation-gear combination (Table 3.4.1). Further, pairwise contrast indicated that *rapido* (ITA_TBB) column was statistically different from the majority of the gears (Table 3.4.2), except for Italian polyvalent passive gears (ITA_PGP) and Croatian bottom trawlers (HRV_DTS).

Table 3.4.1. Results of One-Way PERMANOVA analysis. (Df = degrees of freedom, SS = sum of square, MS = mean of square, F = Fisher value, R^2 = R square, Pr = significance).

Source	Df	SS	MS	F	R^2	Pr (>F)
Gear	8	19.46	4.11	16.34	0.22	0.001 ***
Residuals	464	62.27	0.25		0.78	
Total	472	81.72				

Table 3.4.2. Results of pairwise PERMANOVA analysis, p-values corrected with the Bonferroni method. The gears code is composed, by a first group three letters representing the nation (HRV= Croatia, ITA=Italy and SVN=Slovenia) and a second referring to the fleet segment (DTS= bottom trawl, PGP= polyvalent passive gears, RMP= rampon, DRB= towed dredge, TBB = rapido beam trawl). Significant contrasts are reported in bold.

	HRV_DTS	HRV_PGP	HRV_RMP	ITA_DRB	ITA_DTS	ITA_PGP	ITA_TBB	SVN_DTS
HRV_PGP	**0.036**							
HRV_RMP	**0.036**	1						
ITA_DRB	**0.036**	**0.036**	**0.036**					
ITA_DTS	**0.036**	**0.036**	**0.036**	**0.036**				
ITA_PGP	1	**0.036**	**0.036**	**0.036**	**0.036**			
ITA_TBB	1	0.18	**0.036**	**0.036**	**0.036**	1		
SVN_DTS	**0.036**	1	1	**0.036**	**0.036**	**0.036**	0.108	
SVN_PGP	**0.036**	0.072	0.864	1	**0.036**	**0.036**	**0.036**	0.72

The cluster analysis partitioned the species list into 11 groups, nine of which statistically confirmed (Figure 3.4.1). DTS was the main driver for three clusters (1, 2, and 3), which contrast was due to different contributions of ITA and HRV catches. ITA_PGP was the major driver of three clusters (4, 5, and 6) that were differentiated for the degree of contribution of ITA_DTS. Group 7 was driven by ITA_PGP, while it accounted for large contributions of ITA_DTS and ITA_TBB. One group (8) was entirely driven by ITA_DRB. The last group (9) was almost exclusively driven by ITA_TBB, which therefore was our target group. This latter assemblage of species was composed of *Pecten jacobaeus, Scophtalmus rhombus, Solea solea, Bolinus brandaris, Aequopecten opercularis* (SJA, BLL, SOL, BOY, SCX; Tab. 8.4.1). Even if the SCX FAO 3-Alpha Code stands for the *Pectinidae* family, the species selected for the stock assessment was *Aequopecten opercularis*, since this species constitutes the majority of the *Pectinidae* catches in the north Adriatic basin.

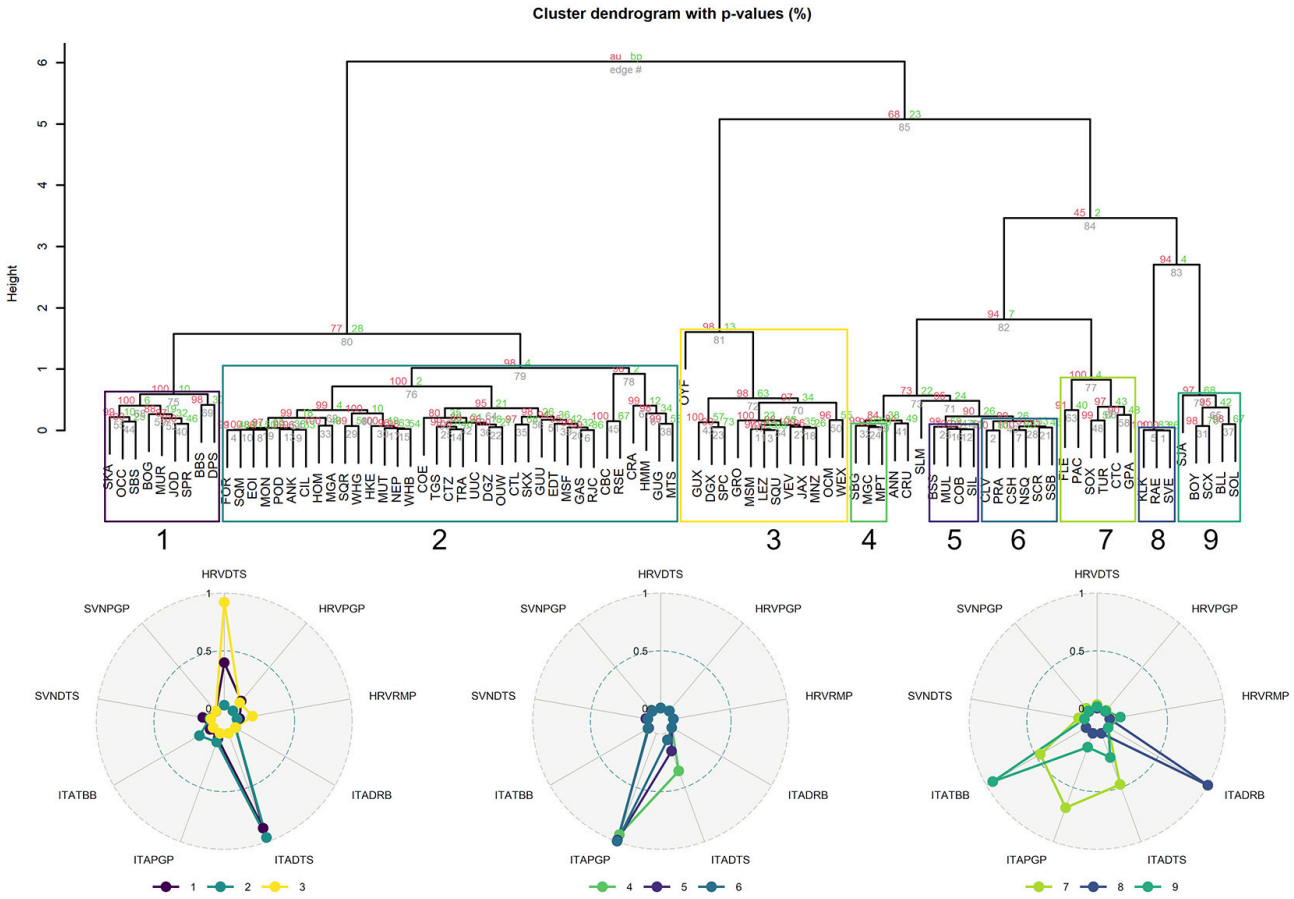

Figure 3.4.1. Hierarchical cluster analysis with the Ward method (Ward, 1963) applied to the gear-by country table. AU p-value (printed in red color in default) is the abbreviation of "approximately unbiased" p-value, which is calculated by multiscale bootstrap resampling. BP value (printed # in green color by default) is "bootstrap probability" value, which is less accurate than AU value as p value. Clusters with high AU values (e.g., 95%) are indicated with blue edges and are strongly supported by data.

Based on the data series and priors in Table 3.3.3.1, the results of the single species assessments are reported in Figure 3.4.2. The majority of the stocks assessed in the present study were considered to be in a data-limited situation due to the lack of information, except for common sole (SOL) for which stock assessment was also available from age-based approaches (GFCM, 2018).

The BSM analysis highlighted several observations: for what regards biomass, the analyzed stocks showed a value lower than B_{msy} from the year 2000 onward, whereas common sole (Figure 3.4.2.d) and purple dye murex (Figure 3.4.2.b) were over the reference point in last years. As for the common sole, in the last twenty years, biomass was estimated to range between B_{msy} and B_{lim} (50% B_{msy}). Purple dye murex was the only species for which values of biomass never went under B_{msy}. For what regards fishing mortality, F was estimated to go under F_{msy} in the last years for three stocks. On the contrary, brill (Figure 3.4.2.a) was in a strong overexploitation status due to a continuous increase of fishing mortality (F/F_{msy} in 2018 was ~ 2). As for the common sole, fishing mortality cycled around F_{msy} during the time series, and F showed an increasing trend that reached a F/F_{msy} ratio of about 1 in

2018, consistently to the age-based assessment (FAO-GFCM, 2019). The F pace of purple dye murex was a counter-trend: it remained below the reference point until recent times and reached it only in the last year. To sum up, the stock trajectories of the Mediterranean scallop (Figure 3.4.2.c) and queen scallop (Figure 3.4.2.e) reported in the Kobe plot (Maunder and Aires-da-Silva, 2009) passed from red to yellow area, *i.e.* there was a slight decrease in fishing mortality while the state of biomass was still below the reference point. As for brill, the stock trajectory remained in the red quadrant, with low biomass and a high level of F. The trajectory of the purple dye murex stock indicated sustainable exploitation during the majority of the time series, however, it went into an overfishing status in the last years. Common sole trajectory oscillated around the reference point during the last years and finally stabilized around MSY.

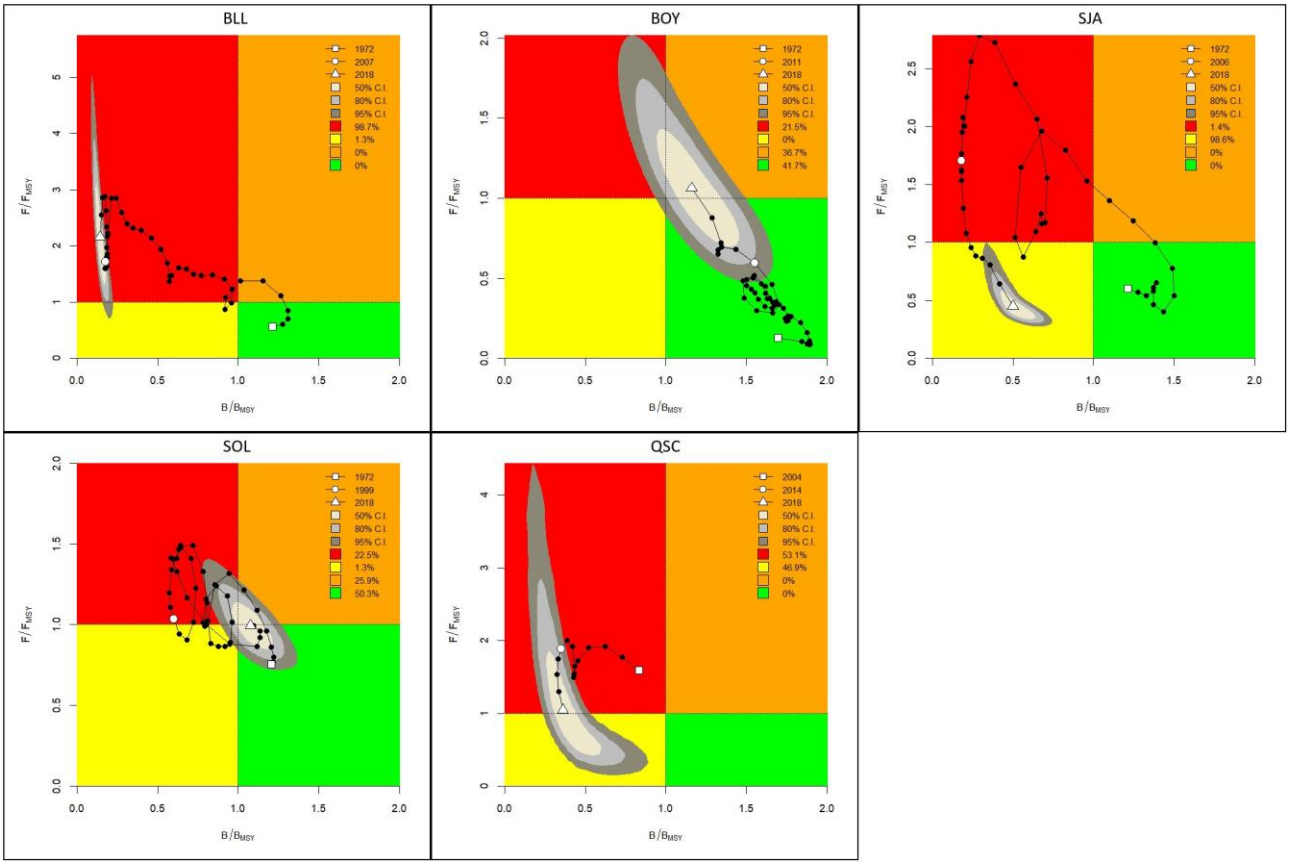

Figure 3.4.2. Kobe plots resulting from the single species stock assessment: (A) Brill, (B) Purple dye murex, (C) Mediterranean scallop, (D) Common sole, and (E) Queen scallop.

The Artificial Neural Network-based sensitivity analysis showed that a moderate alteration of the relative biomass priors did not affect the final B/B_{msy} estimation substantially. The difference between our results and those obtained through the Artificial Neural Network was always under 20% for all studied species, ranging from a 6% minimum for the Mediterranean scallop to a 19% maximum for common sole (Table 3.4.3).

Table 3.4.3. Summary table of the sensitivity analysis over the B/BMSY estimation that compares the results obtained using our priors against those estimated by an Artificial Neural Network.

Species	Prior *Bstart/k* ref	Prior *Bend/k* ref	Prior *Bstart/k* s.a.	Prior *Bend/k* s.a.	*B/BMSY* ref	*B/BMSY* s.a.	Δ %
QSC	0.2 - 0.6	0.01 - 0.4	0.25 - 0.72	0.07 - 0.33	0.36	0.40	-11.5
BOY	0.7 - 1	0.4 - 0.8	0.73 - 0.98	0.17 - 0.55	1.15	1.01	12.77
SJA	0.4 - 0.8	0.1 - 0.3	0.13 - 0.46	0.04 - 0.26	0.50	0.47	5.82
BLL	0.4 - 0.8	0.01 - 0.2	0.17 - 0.54	0.02 - 0.23	0.14	0.13	6.71
SOL	0.4 - 0.8	0.1 - 0.5	0.35 - 0.77	0.23 - 0.67	1.07	1.28	-19.02

Based on these assessments, the CMSY extended analysis, performed on the entire catch assemblage, produced different projections depending on the applied HCR (Figure 3.4.3). In Scenarios (1) and (2), 80% of the stocks reached B_{msy} in 2030, whereas in Scenario (3) a few more years were required to reach B_{msy}. On the contrary, in Scenario (4), under a more permissive HCR, only 60% of the stocks were observed to reach B_{msy} in 2033. Catch projections showed an opposite pattern to biomass, with an initial decrease whose steepness depended on the HCR (Figure 3.4.4). Overall, all four scenarios showed an initial drop of the catches followed by a recovery and stabilization. In the long-term, Scenario (3) and (4) stabilized at a higher level than the initial estimates.

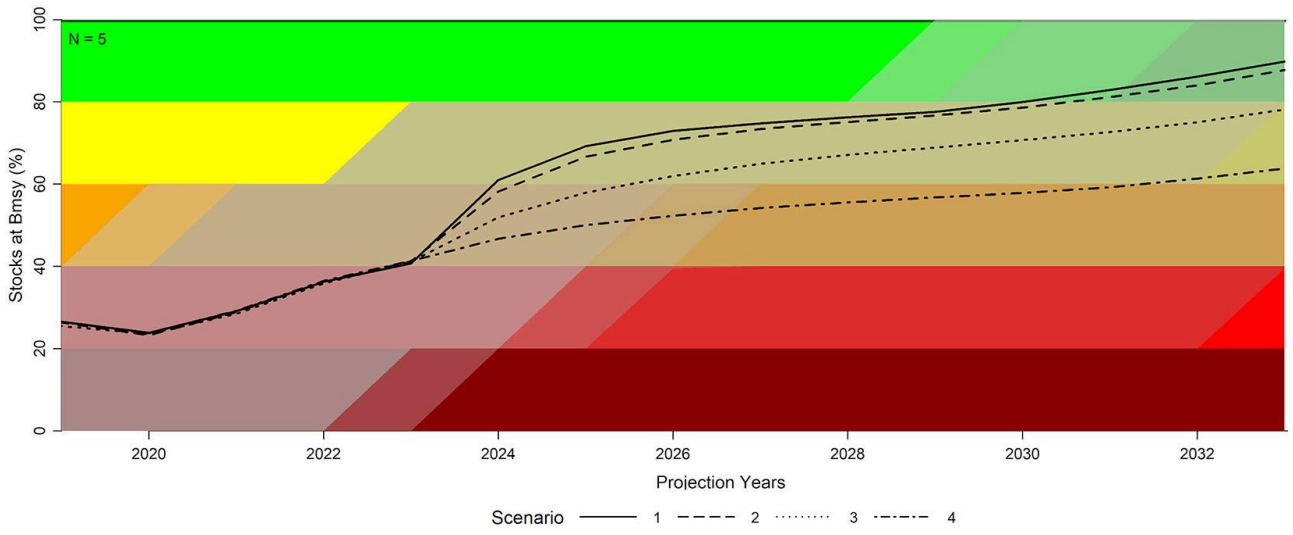

Figure 3.4.3. Forecast of alternative HCRs from the CMSY extended analysis on the catch assemblage: percentage of stocks at Bmsy. Stronger the effort reduction, shorter the range of time in which 80% of the stocks will reach the Bmsy. Scen. (1): 50% of effort reduction; Scen. (2): 40% of effort reduction; Scen (3): 20% of effort reduction; Scen. (4): 5% of effort reduction.

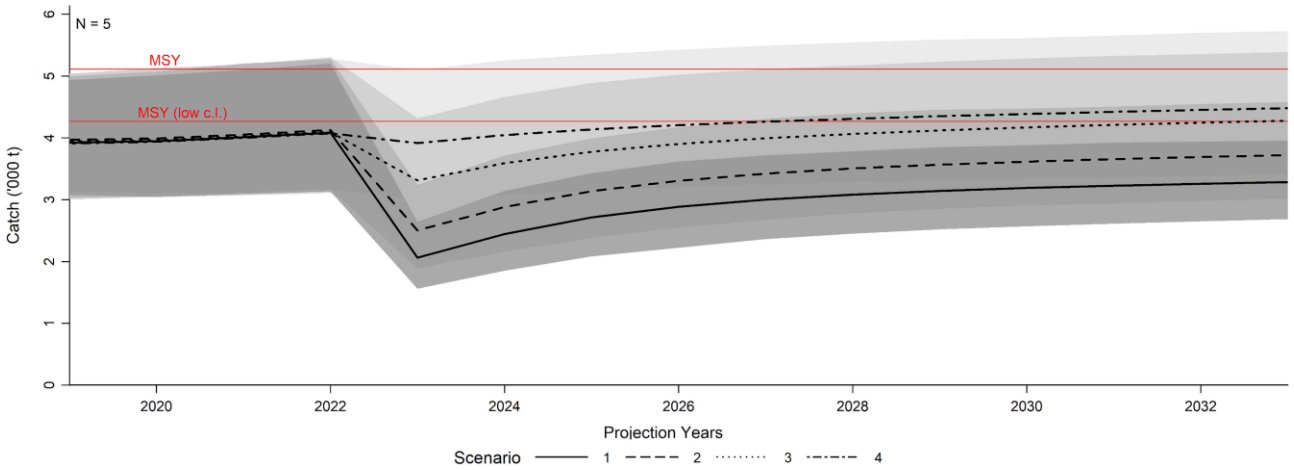

Figure 3.4.4. Forecast of alternative HCRs from the CMSY extended analysis on the catch assemblage: projections of catch time series. After a first decrease, all the scenarios, independently from the strength of the control rule, will figure a stabilization in catches.

3.5. Discussion

This was the first extensive assessment-based meta-analysis of the main target and accessories species of *rapido* trawl fishery in the Adriatic Sea. In the case of mixed fisheries, formulating policies for management and conservation requires the use of models capable of predicting how catch assemblages change in response to fishing effort (Welcomme, 1999). However, when management objectives point toward fishing at reference points of the main target species, the overpressure of accessory species of the same catch assemblage is very plausible (Punt et al., 2002). These considerations fit well the Mediterranean context where demersal fisheries are commonly multispecific (Colloca et al., 2003). Within this context, identifying clusters of commercially important species might help to define conservation units in management plans (Rogers and Pikitch, 1992). In the case of the demersal fishery in the Adriatic Sea, the cluster analysis highlights that a few resources were characterizing the catch assemblages of each gear, except for ITA_PGP and ITA/HRV_DTS, which resulted to be the more generalists. The fact that these fleets showed the most diversified assemblage compared with the other gears reflected the *modus operandi* of these fisheries: ITA_PGP seasonally switches gears and grounds following resource availability (Grati et al., 2018), while the DTS footprint is by far the larger in the area (Russo et al., 2020), spreading across the spatial range of many different species. In contrast, some of the most landed resources were mainly targeted by one specific gear, such as the group formed by clams (SVE: *Chamelea gallina*, KLK: *Callista chione*, RAE: *Solen marginatus*) targeted by Italian DRB, and the cluster made by Pectinidae (SJA, SCX) and flatfishes (SOL: *Solea solea*, BLL: *Scophtalmus rhombus*, TUR: *Scophthalmus maximus*) targeted by Italian TBB. These findings allowed us to consider the assemblage of species analyzed as representative of the exploitation exerted by the *rapido* fishery. Although the Adriatic sea is one of the most intensively trawled area of the Mediterranean sea

(Eigaard et al., 2017; Ferrà et al., 2018) and in the entire world (Amoroso et al., 2018), some of the stocks analyzed showed an increase in biomass at the end of the analysis time-scale (evident in the single-species Kobe plot trajectory toward the recovery area). A possible explanation may be found in the management measures adopted in the last decades: current regulation includes a summer ban to the trawling activity—total closure for 1 month (EC, 2006), extending temporary spatial restrictions up to 4 or 6 nm depending on vessel length since 2012. These measures might have had relevant consequences for recruitment success in coastal areas (Scarcella et al., 2014) leading to a general improvement in the overall status of stocks exploited by *rapido* fishery. However, species respond in different manners to effort reduction due to different resilience, competition, and recruitment impairment (Gamble and Link, 2009), and those species for which biomass levels have fallen below 0.5 B/Bmsy, a threshold that characterizes impaired stocks (Froese et al., 2016), remained in alarming status. Nevertheless, literature reports that flatfishes recruitment success does not strictly depend on stock size (Iles, 1994; Maunder, 2012; Van der Hammen et al., 2013), therefore additional work is required to explain the alarming status of brill. Environmental characteristics of the study area may have a large effect on the resources: organic matter input from rivers and the resulting nutrient enrichment can lead to a high rate of primary productivity, particularly in the Northern and the Central Adriatic (Cognetti et al., 2000), which helps to maintain recruitment capacity in marine fish stocks (Britten et al., 2016), mainly for species with high resilience such as common sole. On the other hand, North Adriatic is a recognized key area for seasonal low oxygen depletion, whether it be eutrophication or climate change-related (Kollmann and Stachowitsch, 2001), and has been repeatedly affected over the last three decades by bottom anoxia and benthic mortalities (e.g., Pectinidae family; Mattei and Pellizzato, 1996). This facilitates detritus-feeding group establishment, such as purple-dye murex, that can make a stand to the recovery of the suspension feeders, i.e., Pectinidae, by consuming and smothering the potential recruits (Riedel et al., 2010). These dynamics, together with continuous trawling, might have led scallops to such low biomass. Nevertheless, it is important to underline that the biomass of the Mediterranean scallop was estimated to have recently increased over 0.5 Bmsy.

The aggregated forecast analysis showed that the percentage of the stocks that will reach Bmsy at the end of the projections will depend on the HCR applied. Scenario (1) and (2) were the fastest in reaching Bmsy (80% of the stocks by 2030), however, they required the biggest drop in catches in the short period; this sudden reduction would be probably economically and socially unsustainable for the Adriatic fishing sector. On the opposite, Scenario (4) could be preferable from an economic point ofview due to higher catches in the long term, but it would allow fewer stocks to reach B_{msy} by 2033 (only 60%), breaching the sustainability principles of the EU Common Fisheries Policy (European Parliament, 2013). Scenario (3) foreseen that 80% of the stocks will reach B_{msy}

in 15 years if the *F* will be reducedby 20% providing a possible compromise between long-term environmental and social sustainability (relatively high expected catch and reasonably fast and good rebuilding in stock biomass). Scenario (3) was therefore more sustainable and compatible with the fundamental principles of CFP, which is to match sustainable exploitation of the fish stocks with socio-economic sustainability (Reg EU No. 1380/2013). Despite simulation of HCRs showed a biomass recovery for the majority of the stocks regardless of the scenario (>60% of the stocks reach for all the rebuilding strategies B_{msy}), it may be less reliable for brill and Mediterranean scallop, which were classified in critical status. In fact, in forecast analyses, an increase in the total biomass of the considered species might have been driven by those stocks that were already in a recovering phase.

Therefore, other management measures should be combined with a reduction of fishing effort to allow for stocks' recovering (Demirel et al., 2020), especially in the most depleted cases. Considering that the areas of persistency of these species are well known (AdriaMed, 2011), specific adaptive measures for *rapido* trawl fishery should be implemented, such as spatio-temporal closures to protect the stocks (Hall-Spencer et al., 1999): guaranteeing protected areas might allow stocks to be more resilient to local depletions (Kritzer and Liu, 2014). Furthermore, effort reduction by itself does not imply a concomitant overall reduction of the fishing mortality for all stocks (Cardinale et al., 2017). Thus, even if the actual management plan (Recommendation GFCM/43/2019/5) already envisages a fishing effort reduction comparable to scenario (3), other management measures may be necessary to avoid the depletion of the most pressured commercial and accessory species.

The presented approach and the used models implicate strong assumptions on the stocks' life-history traits as well as in exploitation status that should be carefully considered. In addition, the CMSY model does not account for the size and age structure of the stock and therefore tends to overestimate sustainable productivity in stocks where excessive fishing pressure has truncated the population structure (Froese et al., 2018). Moreover, the forecasting algorithm assumes that fishing strategies and gears do not change in time. Thus, the estimates coming from the present study should not be taken as a detailed reproduction of reality. Nevertheless, they were sufficient to produce an overall sound snapshot of the performance of different future inter-correlated fisheries scenarios, which would have required many years of data preparation and data gap-filling if data-rich approaches had been used.

3.6. Supplementary material

The Supplementary Material for this paper can be also found online at: https://www.frontiersin.org/articles/10.3389/fmars.2021.552076/full#supplementary-material.

Supplementary Figures

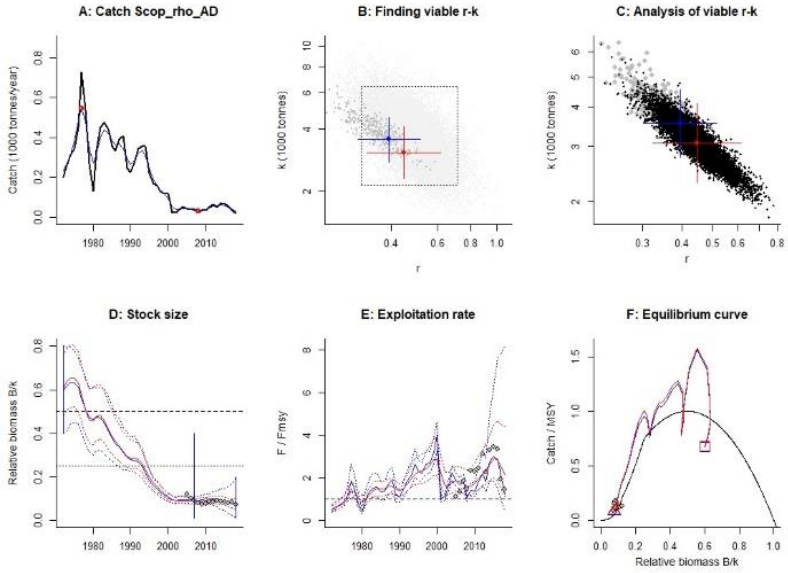

Supplementary Figure 1. Results of CMSY and BSM analyses for brill (BLL).

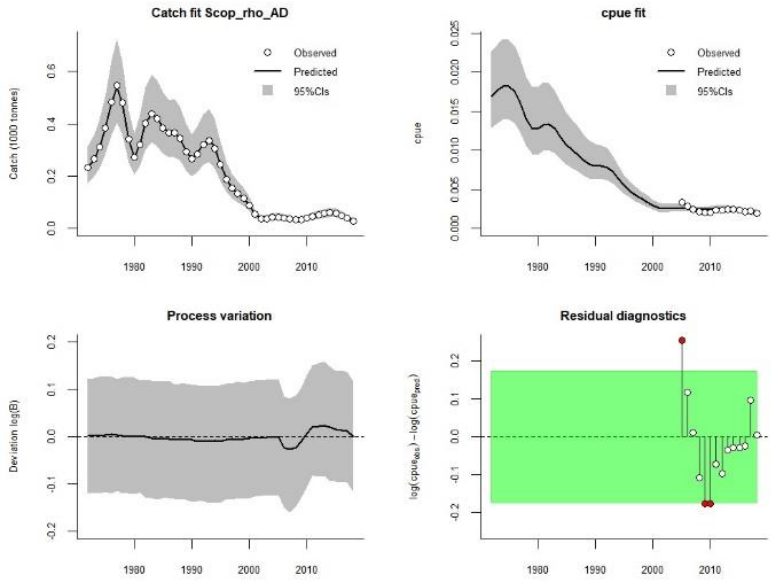

Supplementary Figure 2. Analytical graph for BSM analysis of brill (BLL), showing the fit of the predicted to the observed catch (top left) and CPUE (top right), the deviation from observed to

predicted biomass (bottom left), and an analysis of the log-CPUE residuals (bottom right) with a green background meaning a negligible autocorrelation of residuals.

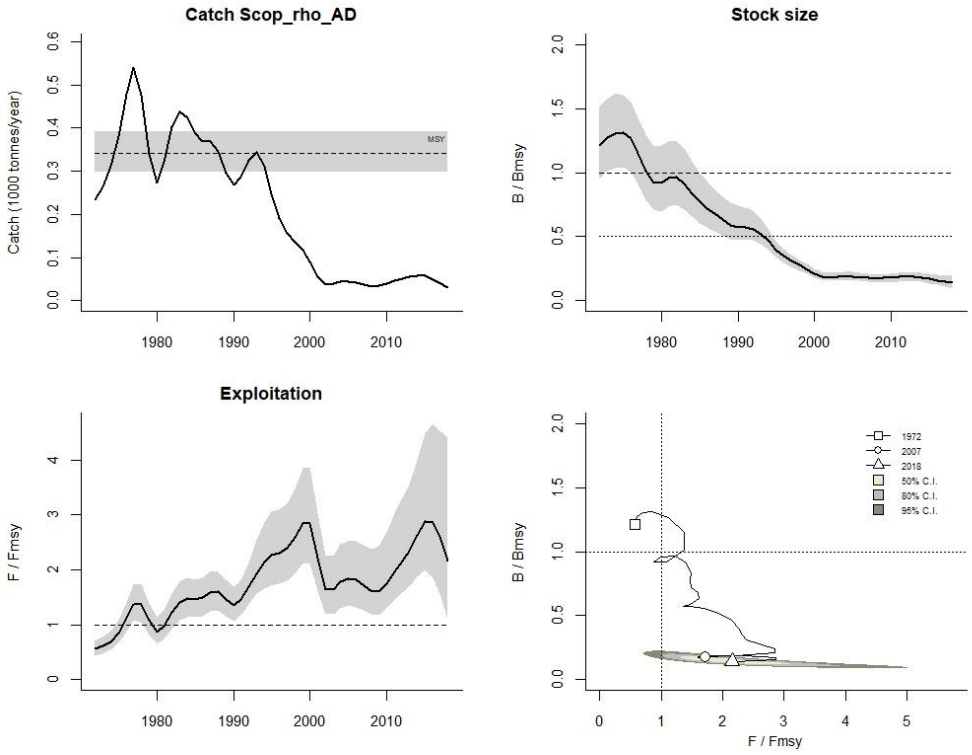

Supplementary Figure 3. Final results of analyses for brill (BLL).

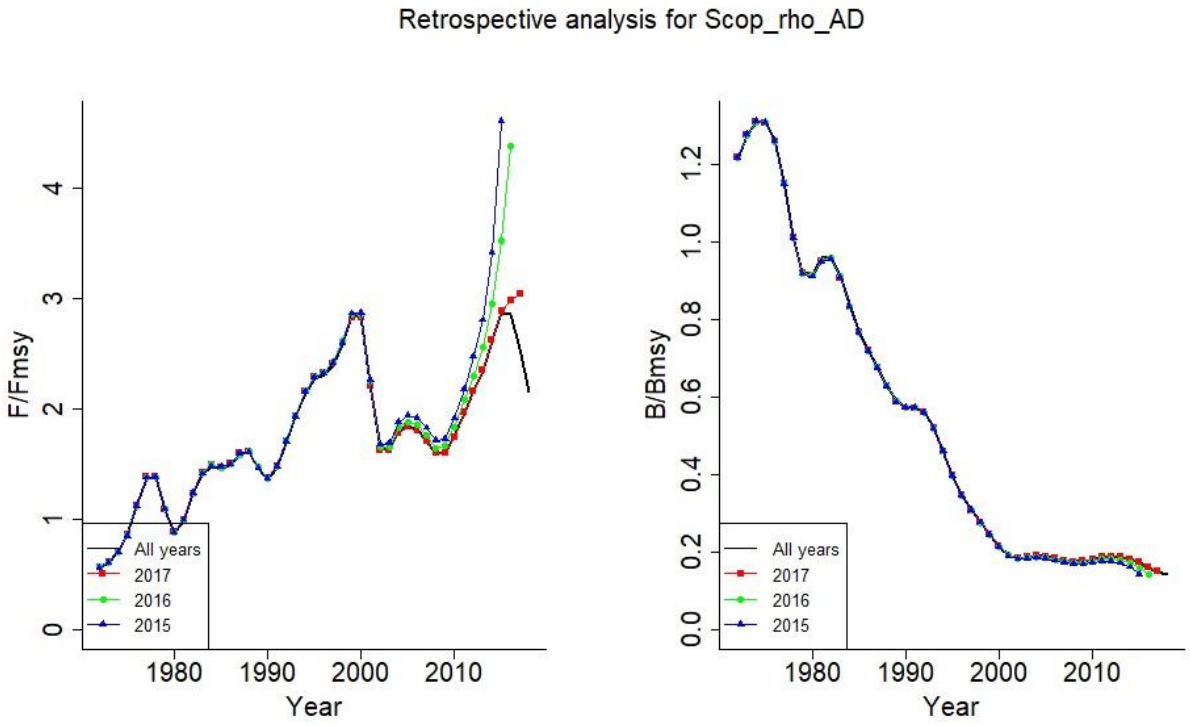

Supplementary Figure 4. CMSY retrospective analysis of brill (BLL). The results show the exploitation F/F_{msy}; left) and the relative stock size (B/B_{msy}; right) when removing the last 3 years of the time series. The figure shows higher consistency in biomass estimation than in fishing mortality.

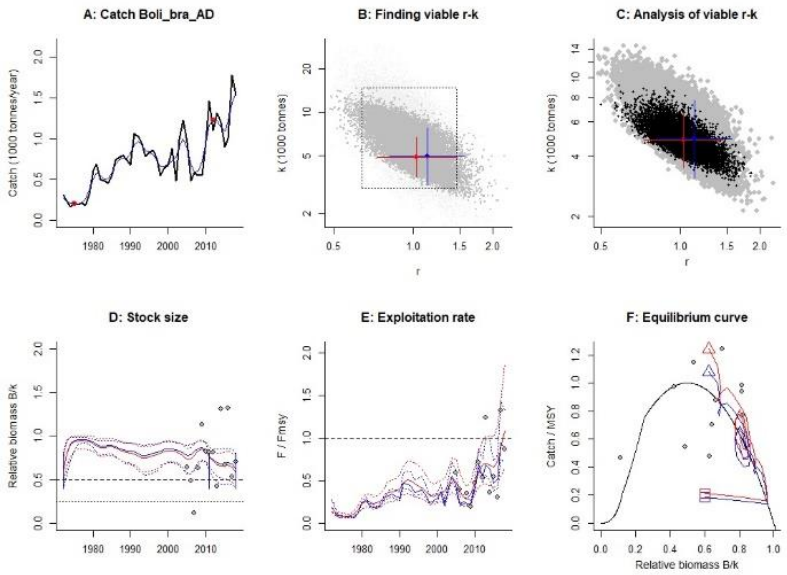

Supplementary Figure 5. Results of CMSY and BSM analyses for purple dye murex (BOY).

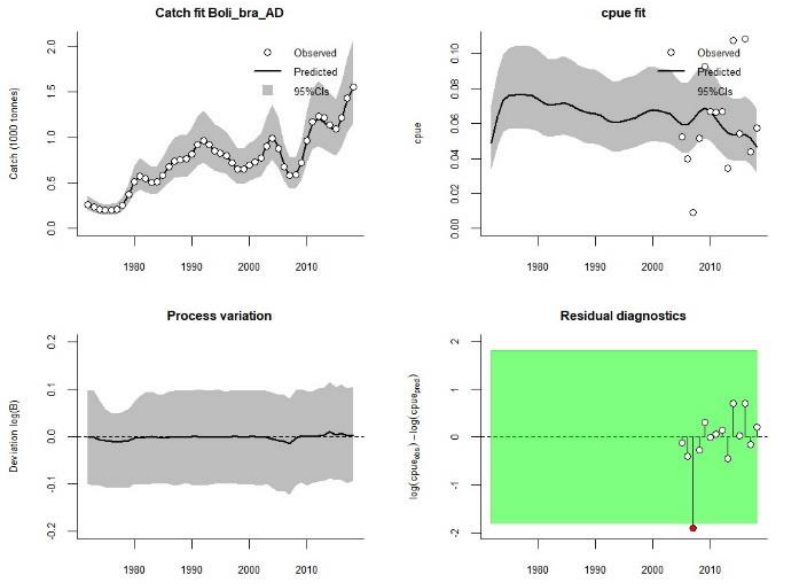

Supplementary Figure 6. Analytical graph for BSM analysis of purple dye murex (BOY), showing the fit of the predicted to the observed catch (top left) and CPUE (top right), the deviation from

observed to predicted biomass (bottom left), and an analysis of the log-CPUE residuals (bottom right) with a green background meaning a negligible autocorrelation of residuals.

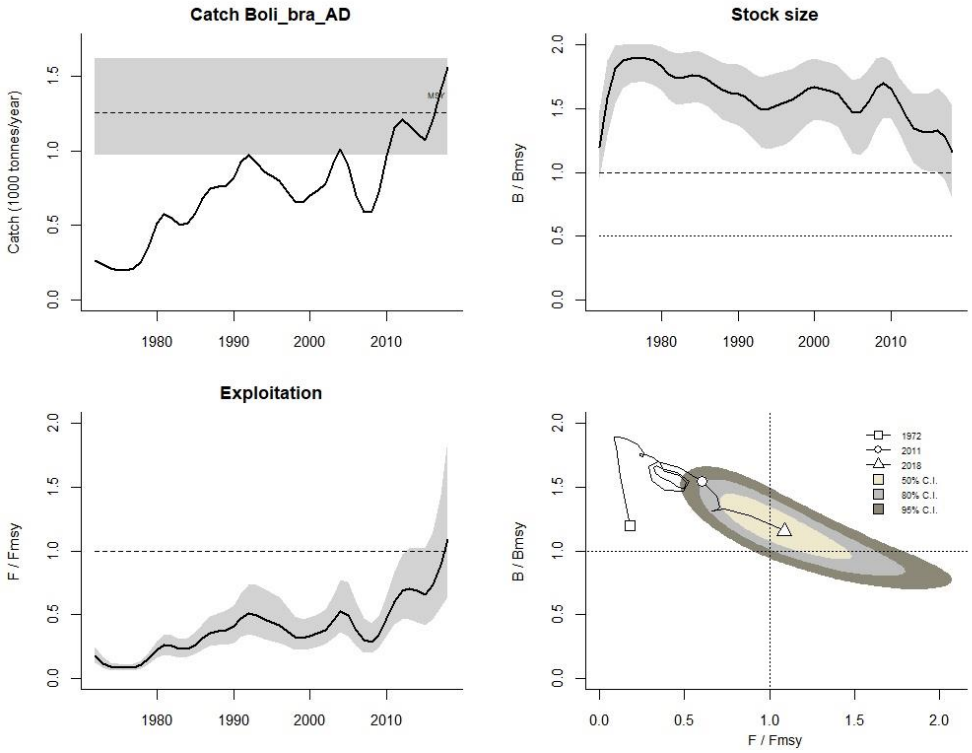

Supplementary Figure 7. Final results of analyses for purple dye murex (BOY).

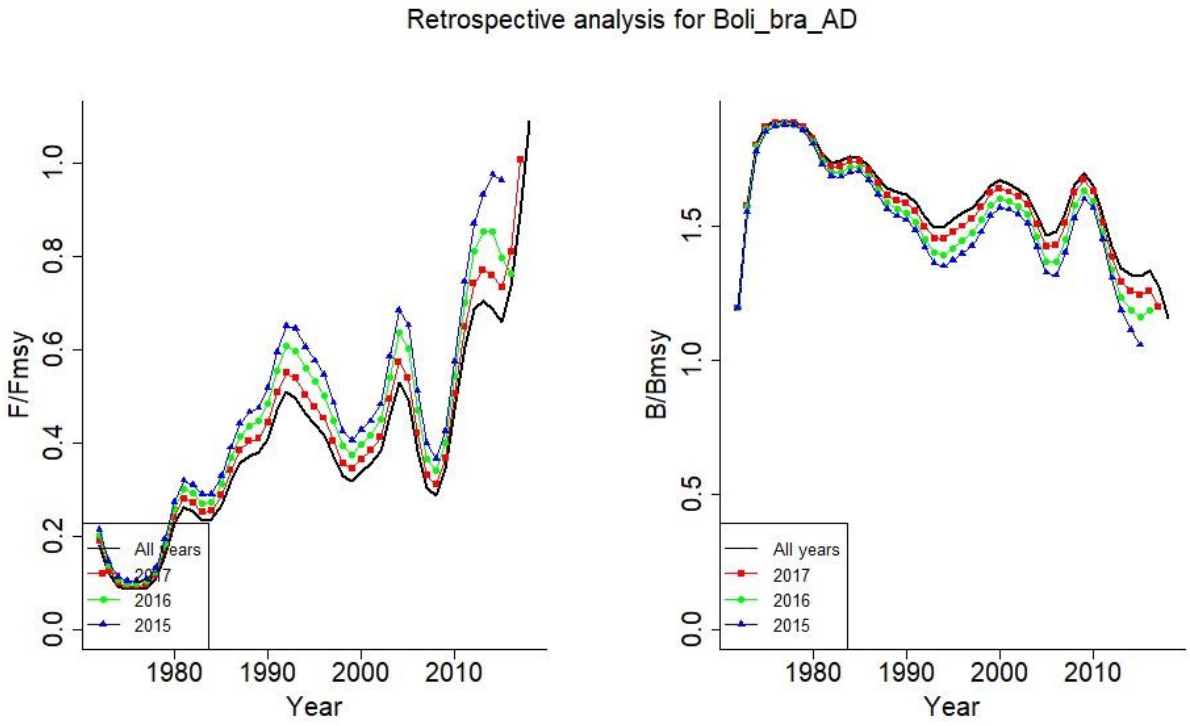

Supplementary Figure 8. CMSY retrospective analysis of purple dye murex (BOY). The results show the exploitation F/F_{msy}; left) and the relative stock size (B/B_{msy}; right) when removing the last 3 years of the time series. The figure shows quite good consistency between models.

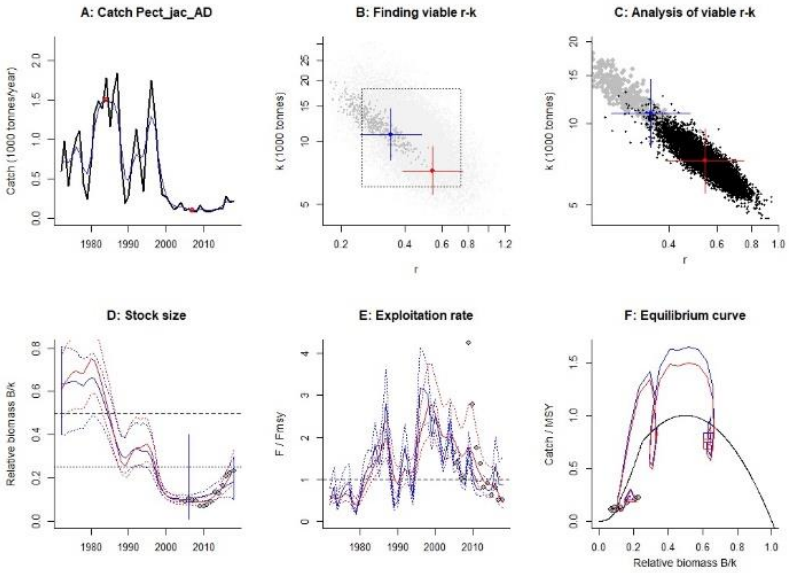

Supplementary Figure 9. Results of CMSY and BSM analyses for Mediterranean scallop (SJA).

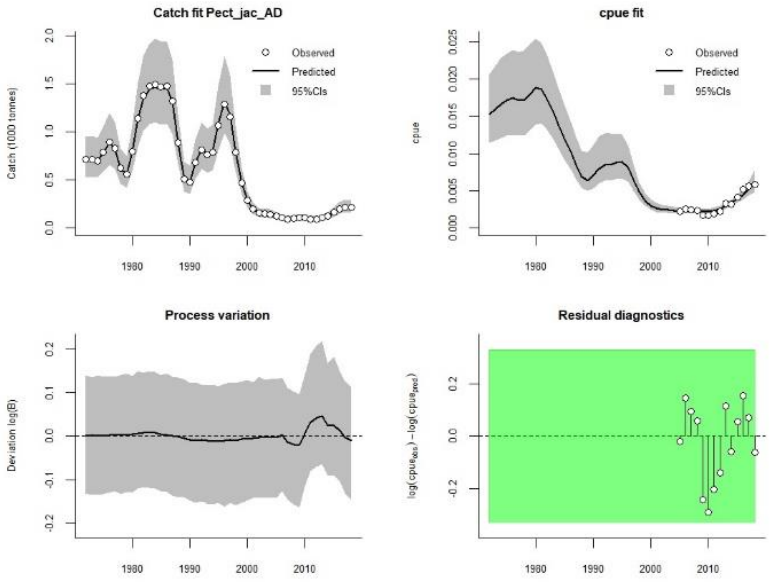

Supplementary Figure 10. Analytical graph for BSM analysis of Mediterranean scallop (SJA), showing the fit of the predicted to the observed catch (top left) and CPUE (top right), the deviation from observed to predicted biomass (bottom left), and an analysis of the log-CPUE residuals (top right) with a green background meaning a negligible autocorrelation of residuals.

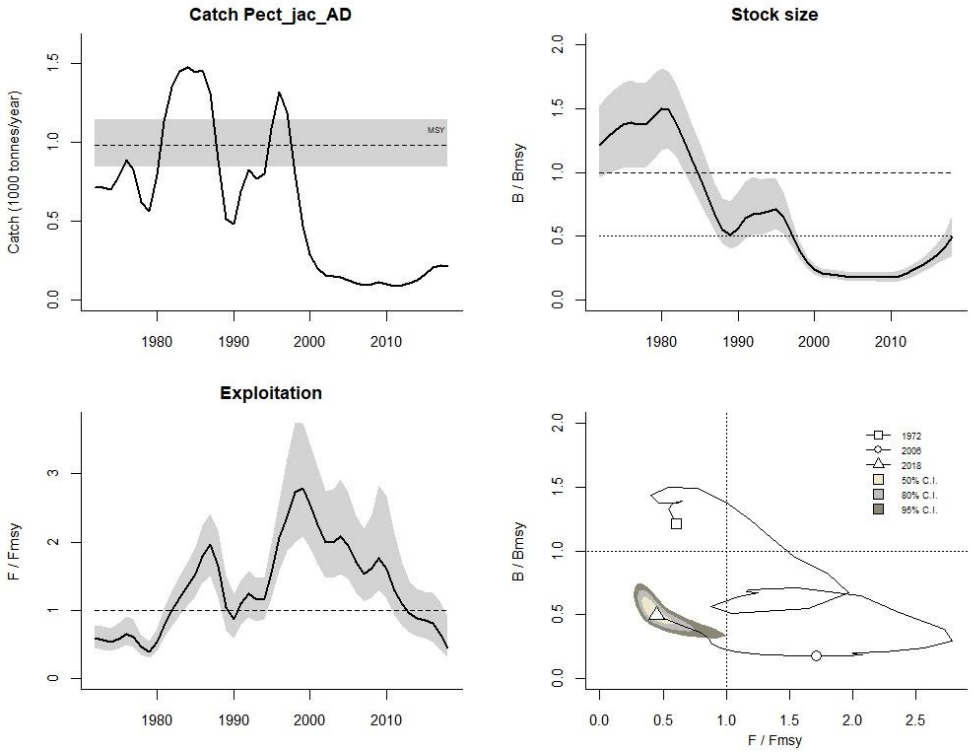

Supplementary Figure 11. Final results of analyses for Mediterranean scallop (SJA).

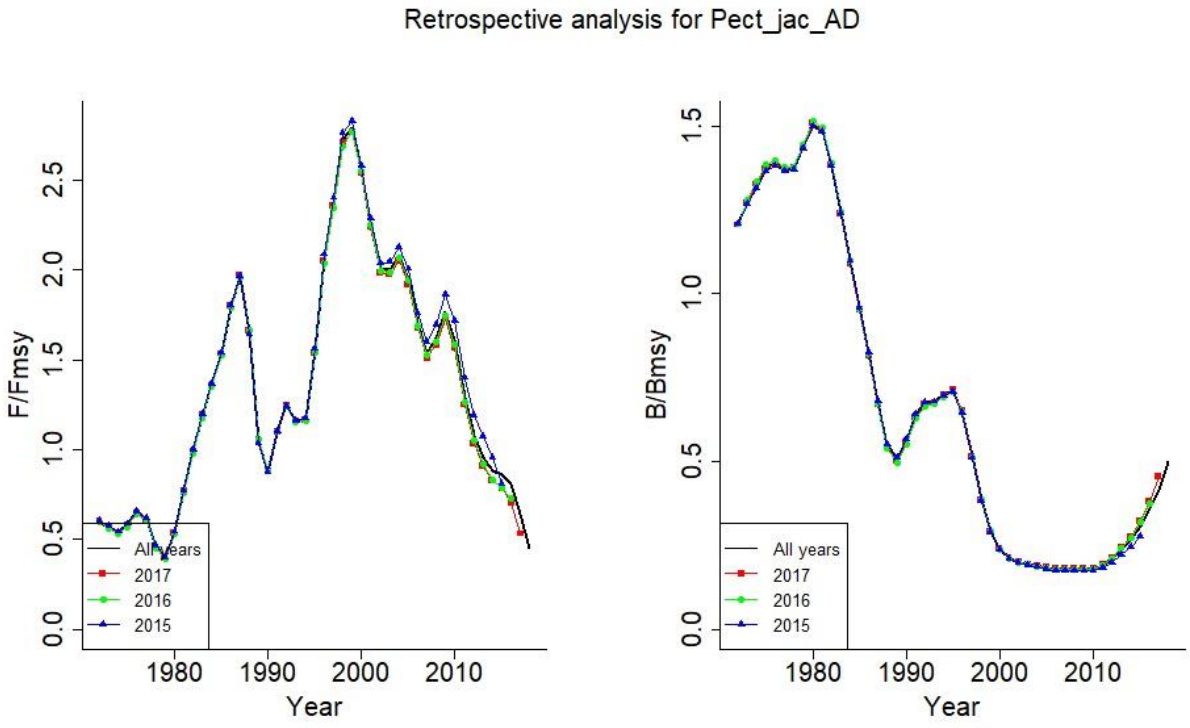

Supplementary Figure 12. CMSY retrospective analysis of Mediterranean scallop (SJA). The results show the exploitation F/F_{msy}; left) and the relative stock size (B/B_{msy}; right) when removing the last 3 years of the time series. The figure shows good consistency between models.

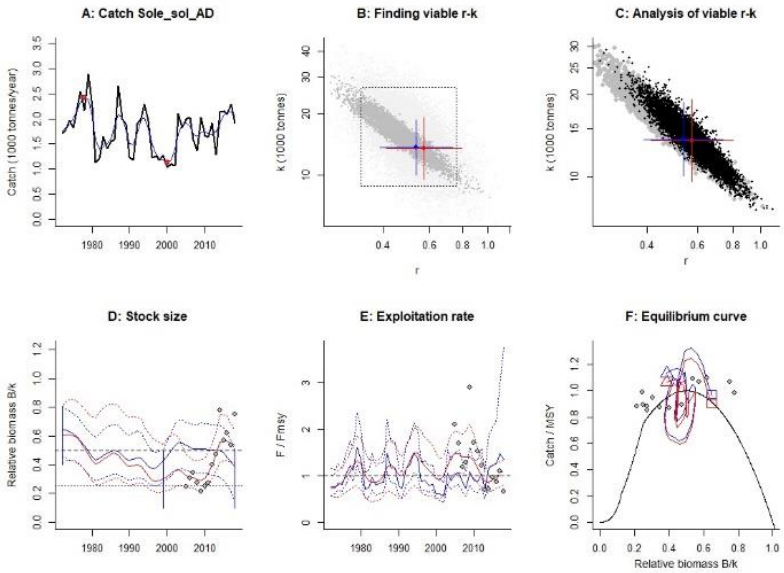

Supplementary Figure 13. Results of CMSY and BSM analyses for common sole (SOL).

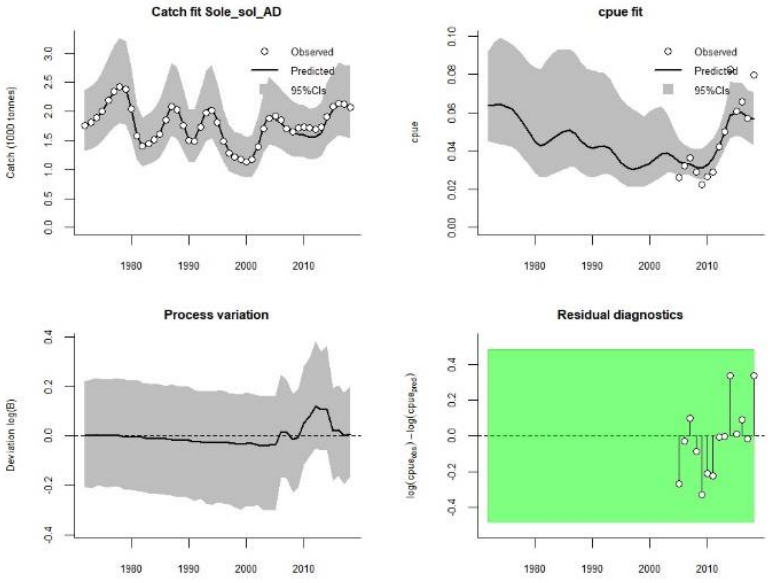

Supplementary Figure 14. Analytical graph for BSM analysis of common sole (SOL), showing the fit of the predicted to the observed catch (top left) and CPUE (top right), the deviation from observed

to predicted biomass (bottom left), and an analysis of the log-CPUE residuals (bottom right) with a green background meaning a negligible autocorrelation of residuals.

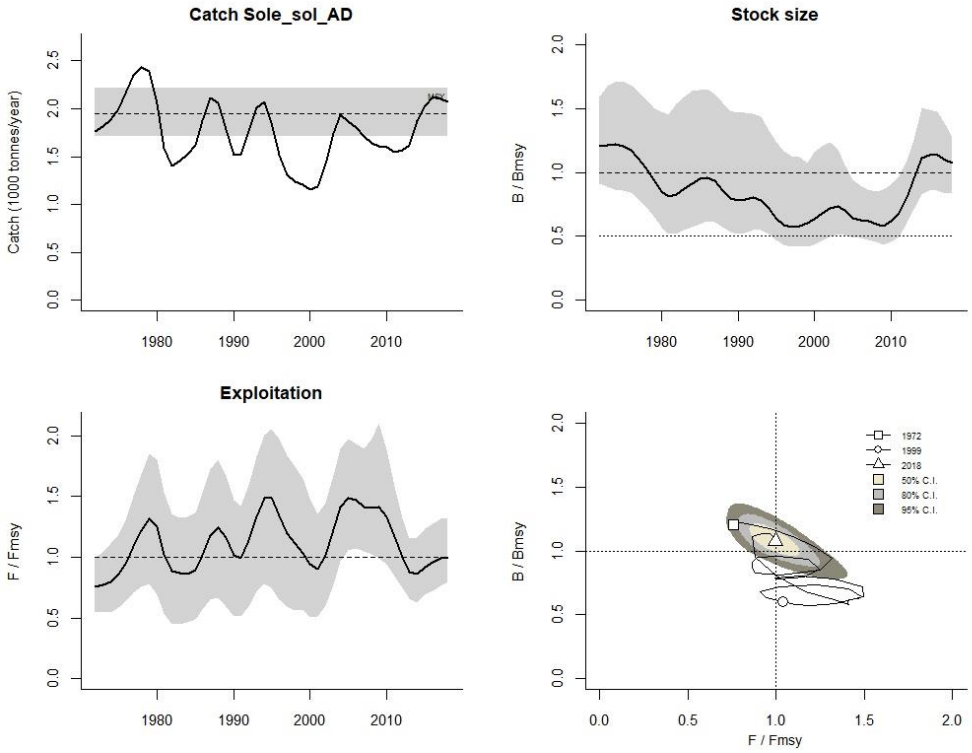

Supplementary Figure 15. Final results of analyses for common sole (SOL).

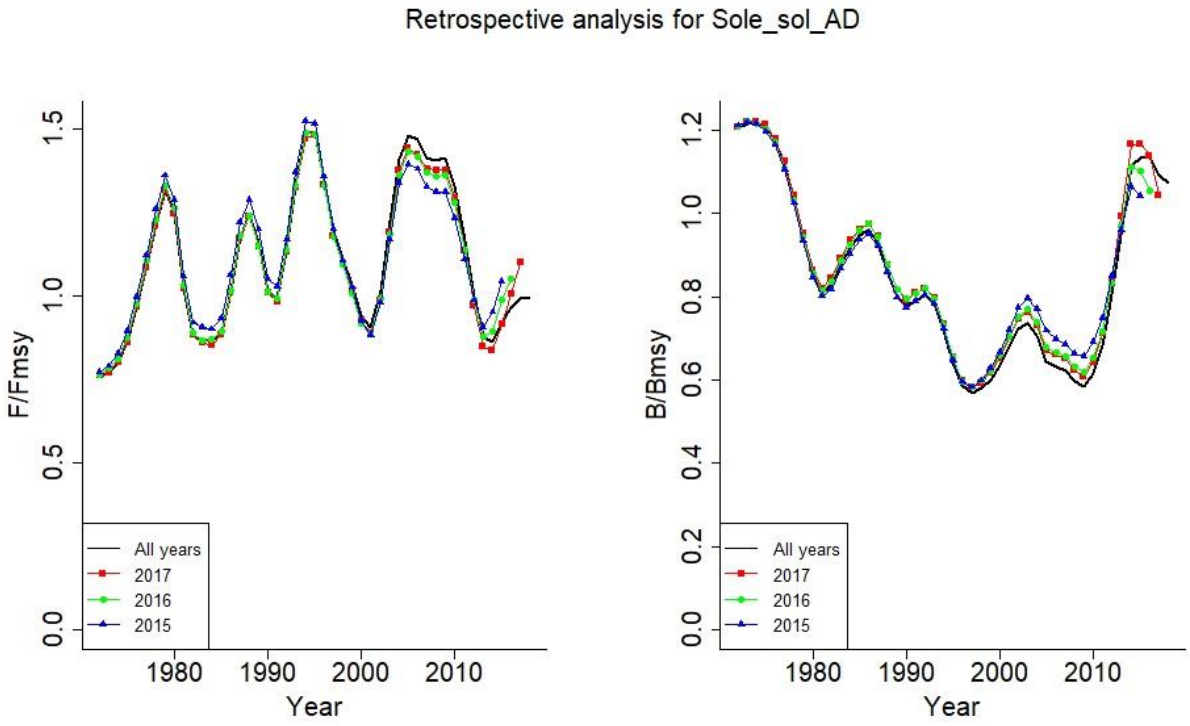

Supplementary Figure 16. CMSY retrospective analysis of common sole (SOL). The results show the exploitation F/F_{msy}; left) and the relative stock size (B/B_{msy}; right) when removing the last 3 years of the time series. The figure shows good consistency between models.

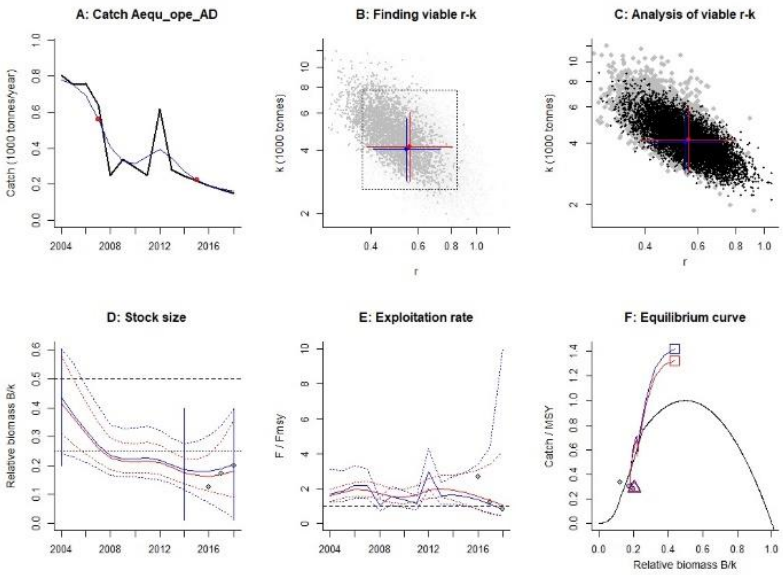

Supplementary Figure 17. Results of CMSY and BSM analyses for queen scallop (QSC).

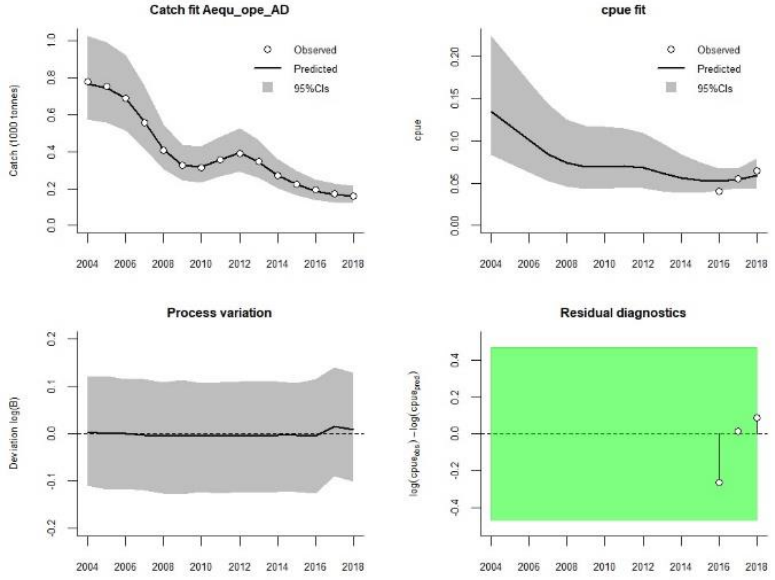

Supplementary Figure 18. Analytical graph for BSM analysis of queen scallop (QSC), showing the fit of the predicted to the observed catch (top left) and CPUE (top right), the deviation from observed to predicted biomass (bottom left), and an analysis of the log-CPUE residuals (bottom right) with a green background meaning a negligible autocorrelation of residuals. Retrospective analysis for this species is missing due to the short data series of the index.

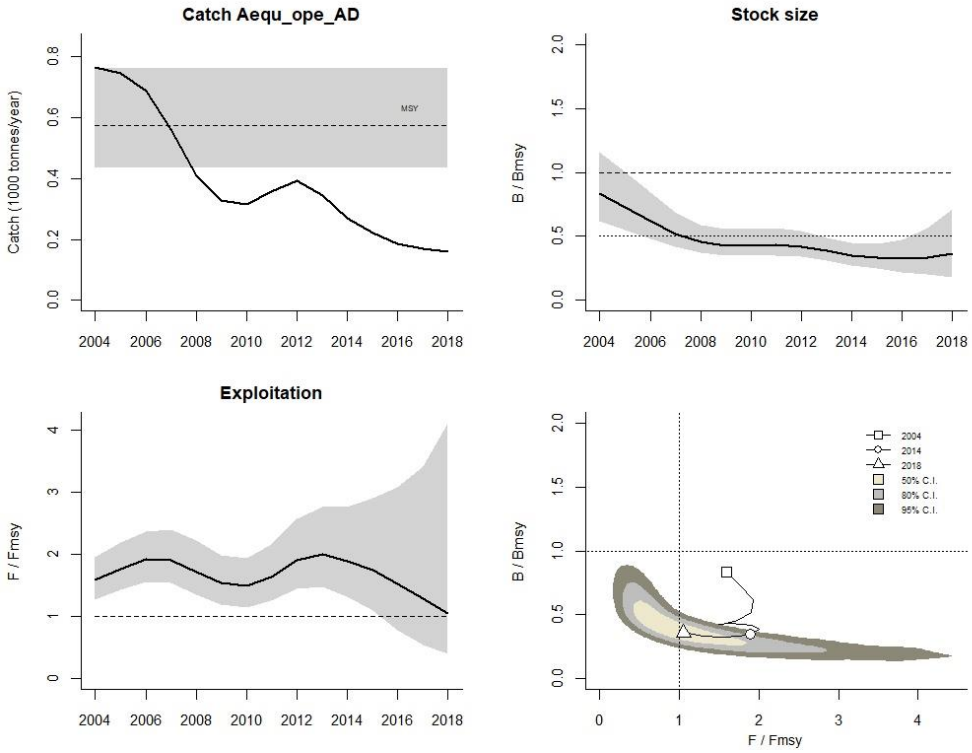

Supplementary Figure 19. Results of CMSY and BSM analyses for queen scallop (QSC).

Supplementary Tables

Supplementary Table 1. Matrix of normalized catch contribution by gear-country for each species. The gears code in columns is composed by a first group three letters representing the nation (HRV= Croatia, ITA=Italy and SVN=Slovenia) and a second referring to the fleet segment (DTS= bottom trawl, PGP= polyvalent passive gears, RMP= rampon, DRB= towed dredge, TBB = rapido beam trawl). The species are reported through the FAO 3-alpha identifier.

	HRV_DTS	HRV_PGP	HRV_RMP	ITA_DRB	ITA_DTS	ITA_PGP	ITA_TBB	SVN_DTS	SVN_PGP
ANK	0.000	0.000	0.000	0.001	0.999	0.002	0.036	0.000	0.000
ANN	0.012	0.029	0.003	0.000	0.243	0.965	0.010	0.096	0.014
BBS	0.511	0.346	0.101	0.000	0.772	0.000	0.111	0.009	0.019
BLL	0.000	0.000	0.000	0.000	0.284	0.278	0.917	0.001	0.021
BOG	0.497	0.168	0.022	0.000	0.815	0.069	0.009	0.235	0.003
BOY	0.000	0.000	0.000	0.000	0.172	0.063	0.983	0.000	0.000
BSS	0.011	0.010	0.001	0.001	0.160	0.985	0.015	0.053	0.022
CBC	0.000	0.000	0.000	0.000	0.807	0.002	0.590	0.019	0.000
CIL	0.000	0.000	0.000	0.000	1.000	0.000	0.027	0.000	0.000
CLV	0.000	0.000	0.000	0.000	0.000	1.000	0.000	0.000	0.000
COB	0.002	0.002	0.000	0.000	0.161	0.987	0.013	0.008	0.009
COE	0.118	0.085	0.008	0.000	0.972	0.114	0.142	0.043	0.008
CRA	0.000	0.000	0.000	0.009	0.791	0.611	0.032	0.000	0.000
CRU	0.021	0.003	0.002	0.000	0.266	0.962	0.054	0.000	0.000
CSH	0.000	0.000	0.000	0.000	0.078	0.997	0.002	0.000	0.000
CTC	0.010	0.003	0.024	0.001	0.557	0.505	0.659	0.008	0.001
CTL	0.069	0.001	0.006	0.000	0.944	0.032	0.321	0.000	0.000
CTZ	0.000	0.000	0.000	0.004	0.992	0.000	0.127	0.000	0.000
DGX	0.967	0.248	0.062	0.000	0.000	0.000	0.000	0.000	0.000
DGZ	0.000	0.000	0.000	0.000	0.985	0.110	0.134	0.000	0.000
DPS	0.684	0.001	0.000	0.001	0.730	0.000	0.002	0.000	0.000
EDT	0.000	0.000	0.000	0.000	0.965	0.017	0.246	0.086	0.000
EOI	0.000	0.000	0.000	0.001	1.000	0.000	0.011	0.000	0.000
FLE	0.000	0.000	0.000	0.000	0.595	0.721	0.268	0.188	0.141
FOR	0.000	0.000	0.000	0.000	1.000	0.000	0.000	0.000	0.002
GAS	0.003	0.001	0.001	0.000	0.968	0.055	0.246	0.000	0.000
GPA	0.000	0.000	0.000	0.000	0.561	0.677	0.476	0.000	0.000
GRO	0.988	0.126	0.090	0.000	0.000	0.000	0.000	0.000	0.000
GUG	0.000	0.000	0.000	0.020	0.880	0.404	0.250	0.000	0.000
GUU	0.000	0.000	0.000	0.006	0.958	0.171	0.232	0.003	0.007
GUX	0.934	0.351	0.040	0.000	0.000	0.000	0.000	0.042	0.027
HKE	0.090	0.007	0.000	0.003	0.995	0.004	0.029	0.001	0.000
HMM	0.000	0.000	0.000	0.009	0.957	0.290	0.007	0.000	0.000
HOM	0.000	0.000	0.000	0.001	0.996	0.080	0.017	0.031	0.001
JAX	0.996	0.088	0.007	0.000	0.000	0.000	0.000	0.002	0.009
JOD	0.350	0.060	0.015	0.000	0.911	0.074	0.038	0.192	0.003
KLK	0.006	0.000	0.000	1.000	0.000	0.000	0.000	0.000	0.000
LEZ	1.000	0.005	0.001	0.000	0.000	0.000	0.000	0.000	0.000
MGA	0.000	0.000	0.000	0.000	0.988	0.153	0.002	0.019	0.006
MGC	0.000	0.000	0.000	0.000	0.330	0.944	0.000	0.000	0.000
MNZ	0.999	0.049	0.007	0.000	0.000	0.000	0.000	0.000	0.000

MON	0.000	0.000	0.000	0.000	1.000	0.009	0.011	0.000	0.000
MPT	0.000	0.000	0.000	0.000	0.376	0.926	0.022	0.000	0.000
MSF	0.000	0.000	0.000	0.000	0.974	0.021	0.225	0.000	0.000
MSM	1.000	0.016	0.007	0.000	0.000	0.000	0.000	0.000	0.000
MTS	0.003	0.000	0.000	0.002	0.924	0.315	0.215	0.001	0.000
MUL	0.002	0.010	0.003	0.001	0.177	0.984	0.006	0.017	0.006
MUR	0.321	0.079	0.040	0.000	0.911	0.185	0.088	0.134	0.001
MUT	0.146	0.001	0.005	0.005	0.988	0.014	0.034	0.010	0.000
NEP	0.160	0.009	0.000	0.000	0.987	0.001	0.007	0.000	0.000
NSQ	0.000	0.000	0.000	0.000	0.086	0.996	0.000	0.000	0.000
OCC	0.265	0.093	0.010	0.000	0.953	0.116	0.017	0.000	0.000
OCM	0.979	0.011	0.202	0.000	0.000	0.000	0.000	0.000	0.000
OUW	0.000	0.000	0.000	0.000	0.992	0.065	0.109	0.000	0.000
OYF	0.223	0.020	0.975	0.000	0.000	0.000	0.000	0.000	0.001
PAC	0.175	0.019	0.014	0.000	0.492	0.841	0.071	0.112	0.048
POD	0.000	0.000	0.000	0.004	0.999	0.017	0.027	0.001	0.000
PRA	0.000	0.000	0.000	0.000	0.001	1.000	0.000	0.000	0.000
RAE	0.000	0.000	0.000	1.000	0.000	0.000	0.000	0.000	0.000
RJC	0.000	0.000	0.000	0.000	0.968	0.057	0.244	0.006	0.002
RSE	0.043	0.076	0.008	0.000	0.831	0.111	0.537	0.000	0.001
SBG	0.013	0.027	0.001	0.001	0.337	0.939	0.032	0.029	0.044
SBS	0.187	0.148	0.007	0.000	0.971	0.011	0.000	0.000	0.002
SCR	0.006	0.020	0.002	0.000	0.080	0.995	0.048	0.001	0.000
SCX	0.023	0.002	0.047	0.000	0.163	0.010	0.985	0.000	0.000
SIL	0.000	0.000	0.000	0.000	0.160	0.987	0.000	0.000	0.000
SJA	0.054	0.006	0.409	0.000	0.312	0.001	0.856	0.000	0.000
SKA	0.388	0.059	0.015	0.004	0.920	0.000	0.000	0.000	0.000
SKX	0.000	0.000	0.000	0.000	0.925	0.004	0.380	0.000	0.000
SLM	0.227	0.263	0.020	0.000	0.083	0.930	0.000	0.027	0.078
SOL	0.004	0.015	0.016	0.000	0.188	0.292	0.937	0.001	0.007
SOX	0.000	0.000	0.000	0.000	0.297	0.747	0.595	0.000	0.000
SPC	0.967	0.253	0.009	0.000	0.000	0.000	0.000	0.008	0.001
SPR	0.374	0.104	0.001	0.000	0.911	0.000	0.011	0.136	0.000
SQM	0.000	0.000	0.000	0.000	1.000	0.003	0.005	0.000	0.000
SQR	0.080	0.008	0.016	0.000	0.978	0.022	0.069	0.179	0.001
SQU	1.000	0.002	0.002	0.000	0.000	0.000	0.000	0.000	0.000
SSB	0.003	0.003	0.000	0.000	0.122	0.992	0.036	0.006	0.009
SVE	0.000	0.000	0.000	1.000	0.000	0.000	0.000	0.000	0.000
TGS	0.000	0.000	0.000	0.013	0.985	0.024	0.168	0.028	0.000
TRA	0.000	0.000	0.000	0.000	0.991	0.017	0.133	0.000	0.000
TUR	0.017	0.061	0.012	0.000	0.335	0.639	0.689	0.003	0.025
UUC	0.072	0.015	0.008	0.000	0.981	0.075	0.163	0.000	0.001
VEV	0.998	0.033	0.047	0.000	0.000	0.000	0.000	0.000	0.011
WEX	0.934	0.063	0.351	0.000	0.000	0.000	0.000	0.026	0.002
WHB	0.137	0.002	0.006	0.002	0.990	0.000	0.007	0.000	0.000
WHG	0.046	0.001	0.002	0.000	0.990	0.010	0.051	0.122	0.001

Supplementary Table 2. Input data for CMSY model, by species.

Stock	Year	Catch	Biomass index
Pecten jacobeus	1972	603.3	NA
Pecten jacobeus	1973	974.3	NA
Pecten jacobeus	1974	404.4	NA
Pecten jacobeus	1975	805	NA
Pecten jacobeus	1976	1014	NA
Pecten jacobeus	1977	1110	NA
Pecten jacobeus	1978	434	NA
Pecten jacobeus	1979	238	NA
Pecten jacobeus	1980	734	NA
Pecten jacobeus	1981	1328	NA
Pecten jacobeus	1982	1490	NA
Pecten jacobeus	1983	1386	NA
Pecten jacobeus	1984	1780	NA
Pecten jacobeus	1985	1161	NA
Pecten jacobeus	1986	1575	NA
Pecten jacobeus	1987	1837.4	NA
Pecten jacobeus	1988	700.7	NA
Pecten jacobeus	1989	190.2	NA
Pecten jacobeus	1990	278.9	NA
Pecten jacobeus	1991	744.1	NA
Pecten jacobeus	1992	1129.4	NA
Pecten jacobeus	1993	715.4	NA
Pecten jacobeus	1994	335.9	NA
Pecten jacobeus	1995	1149.6	NA
Pecten jacobeus	1996	1746.8	NA
Pecten jacobeus	1997	1270.3	NA
Pecten jacobeus	1998	720.1	NA
Pecten jacobeus	1999	299.4	NA
Pecten jacobeus	2000	271.5	NA
Pecten jacobeus	2001	192.3	NA
Pecten jacobeus	2002	113.8	NA
Pecten jacobeus	2003	140	NA
Pecten jacobeus	2004	194	NA
Pecten jacobeus	2005	103	2.3
Pecten jacobeus	2006	118.7	2.6
Pecten jacobeus	2007	77	2.5
Pecten jacobeus	2008	74.9	2.4
Pecten jacobeus	2009	163.6	1.8
Pecten jacobeus	2010	98.8	1.7
Pecten jacobeus	2011	81.9	1.9
Pecten jacobeus	2012	88.7	2.3
Pecten jacobeus	2013	113	3.4
Pecten jacobeus	2014	114.6	3.2
Pecten jacobeus	2015	130.4	4.1
Pecten jacobeus	2016	276	5.3

Pecten jacobeus	2017	199.3	5.6
Pecten jacobeus	2018	217.2	5.9
Aequopecten opercularis	2004	805.7	NA
Aequopecten opercularis	2005	754.4	NA
Aequopecten opercularis	2006	756.9	NA
Aequopecten opercularis	2007	640.3	NA
Aequopecten opercularis	2008	250	NA
Aequopecten opercularis	2009	336.1	NA
Aequopecten opercularis	2010	293.1	NA
Aequopecten opercularis	2011	247.4	NA
Aequopecten opercularis	2012	618.1	NA
Aequopecten opercularis	2013	281.5	NA
Aequopecten opercularis	2014	246.4	NA
Aequopecten opercularis	2015	217.4	NA
Aequopecten opercularis	2016	191.3	40.3
Aequopecten opercularis	2017	168.3	55.6
Aequopecten opercularis	2018	148.1	64.3
Scophthalmus rhombus	1972	201.5	NA
Scophthalmus rhombus	1973	256.7	NA
Scophthalmus rhombus	1974	311.9	NA
Scophthalmus rhombus	1975	344	NA
Scophthalmus rhombus	1976	450	NA
Scophthalmus rhombus	1977	728	NA
Scophthalmus rhombus	1978	540	NA
Scophthalmus rhombus	1979	270	NA
Scophthalmus rhombus	1980	130.3	NA
Scophthalmus rhombus	1981	335.5	NA
Scophthalmus rhombus	1982	450.4	NA
Scophthalmus rhombus	1983	473.1	NA
Scophthalmus rhombus	1984	444.7	NA
Scophthalmus rhombus	1985	354.6	NA
Scophthalmus rhombus	1986	331.5	NA
Scophthalmus rhombus	1987	390.3	NA
Scophthalmus rhombus	1988	408.3	NA
Scophthalmus rhombus	1989	243.2	NA
Scophthalmus rhombus	1990	225.4	NA
Scophthalmus rhombus	1991	274.3	NA
Scophthalmus rhombus	1992	344.9	NA
Scophthalmus rhombus	1993	357.5	NA
Scophthalmus rhombus	1994	354.4	NA
Scophthalmus rhombus	1995	221	NA
Scophthalmus rhombus	1996	168.2	NA
Scophthalmus rhombus	1997	156.5	NA
Scophthalmus rhombus	1998	128.8	NA
Scophthalmus rhombus	1999	119.6	NA
Scophthalmus rhombus	2000	117.3	NA
Scophthalmus rhombus	2001	24.6	NA

Scophthalmus rhombus	2002	25	NA
Scophthalmus rhombus	2003	38.6	NA
Scophthalmus rhombus	2004	52.1	NA
Scophthalmus rhombus	2005	44.2	3.4
Scophthalmus rhombus	2006	38.6	2.9
Scophthalmus rhombus	2007	40.7	2.5
Scophthalmus rhombus	2008	25	2.2
Scophthalmus rhombus	2009	34.6	2.1
Scophthalmus rhombus	2010	35.7	2.1
Scophthalmus rhombus	2011	49.7	2.4
Scophthalmus rhombus	2012	61	2.4
Scophthalmus rhombus	2013	49.5	2.5
Scophthalmus rhombus	2014	68.9	2.5
Scophthalmus rhombus	2015	65	2.3
Scophthalmus rhombus	2016	54.8	2.2
Scophthalmus rhombus	2017	35.9	2.3
Scophthalmus rhombus	2018	20	2
Bolinus brandaris	1972	308	NA
Bolinus brandaris	1973	238.1	NA
Bolinus brandaris	1974	168.2	NA
Bolinus brandaris	1975	216.3	NA
Bolinus brandaris	1976	191.8	NA
Bolinus brandaris	1977	210.7	NA
Bolinus brandaris	1978	180.3	NA
Bolinus brandaris	1979	314.6	NA
Bolinus brandaris	1980	609.6	NA
Bolinus brandaris	1981	683.2	NA
Bolinus brandaris	1982	506.4	NA
Bolinus brandaris	1983	485.6	NA
Bolinus brandaris	1984	455.3	NA
Bolinus brandaris	1985	557	NA
Bolinus brandaris	1986	732.6	NA
Bolinus brandaris	1987	769.4	NA
Bolinus brandaris	1988	790.4	NA
Bolinus brandaris	1989	736.1	NA
Bolinus brandaris	1990	678.2	NA
Bolinus brandaris	1991	1065.5	NA
Bolinus brandaris	1992	1022.7	NA
Bolinus brandaris	1993	938.8	NA
Bolinus brandaris	1994	782.6	NA
Bolinus brandaris	1995	828.4	NA
Bolinus brandaris	1996	864.5	NA
Bolinus brandaris	1997	747.2	NA
Bolinus brandaris	1998	551.8	NA
Bolinus brandaris	1999	638	NA
Bolinus brandaris	2000	680.8	NA
Bolinus brandaris	2001	881.2	NA

Bolinus brandaris	2002	486.2	NA
Bolinus brandaris	2003	989.9	NA
Bolinus brandaris	2004	1231	NA
Bolinus brandaris	2005	959.1	52.5
Bolinus brandaris	2006	482.7	39.8
Bolinus brandaris	2007	583.2	9.3
Bolinus brandaris	2008	546.5	51.3
Bolinus brandaris	2009	546.6	92.5
Bolinus brandaris	2010	971.8	66.9
Bolinus brandaris	2011	1460.9	66.4
Bolinus brandaris	2012	1106.1	66.7
Bolinus brandaris	2013	1319.2	34.6
Bolinus brandaris	2014	1198.8	107.3
Bolinus brandaris	2015	900.3	54.2
Bolinus brandaris	2016	1001.8	108
Bolinus brandaris	2017	1778.7	43.8
Bolinus brandaris	2018	1528.4	57.2
Solea solea	1972	1719	NA
Solea solea	1973	1769	NA
Solea solea	1974	1957	NA
Solea solea	1975	1826	NA
Solea solea	1976	2238	NA
Solea solea	1977	2538	NA
Solea solea	1978	2165	NA
Solea solea	1979	2890	NA
Solea solea	1980	2235	NA
Solea solea	1981	1123	NA
Solea solea	1982	1213	NA
Solea solea	1983	1652	NA
Solea solea	1984	1416	NA
Solea solea	1985	1547	NA
Solea solea	1986	1592	NA
Solea solea	1987	2653	NA
Solea solea	1988	1995	NA
Solea solea	1989	1890	NA
Solea solea	1990	1235	NA
Solea solea	1991	1177	NA
Solea solea	1992	1900	NA
Solea solea	1993	2013	NA
Solea solea	1994	2292	NA
Solea solea	1995	1971	NA
Solea solea	1996	1220	NA
Solea solea	1997	1250	NA
Solea solea	1998	1183	NA
Solea solea	1999	1278	NA
Solea solea	2000	1036	NA
Solea solea	2001	1104	NA

Solea solea	2002	1075	NA
Solea solea	2003	2107	NA
Solea solea	2004	1822	NA
Solea solea	2005	1994	26.2
Solea solea	2006	2022	32.5
Solea solea	2007	1588	36.4
Solea solea	2008	1370.3	29
Solea solea	2009	2018.3	22.4
Solea solea	2010	1670.9	26.6
Solea solea	2011	1628.7	28.9
Solea solea	2012	1914.6	42.5
Solea solea	2013	1283	50
Solea solea	2014	2133	82.7
Solea solea	2015	2158.1	60.7
Solea solea	2016	2093.8	65.7
Solea solea	2017	2290.2	56.9
Solea solea	2018	1923.3	79.7

Supplementary Table 2. The species list falling within the 99% of the cumulative distribution retained for the successive analysis.

3-Alpha code	Scientific_name	Cumulative percentage
SVE	*Chamelea gallina*	0.31
MUT	*Mullus barbatus*	0.38
CTC	*Sepia officinalis*	0.44
MTS	*Squilla mantis*	0.51
HKE	*Merluccius merluccius*	0.56
SOL	*Solea solea*	0.60
NSQ	*Nassarius mutabilis*	0.64
KLK	*Callista chione*	0.67
WHG	*Merlangius merlangus*	0.69
BOY	*Bolinus brandaris*	0.71
EDT	*Eledone moschata*	0.73
NEP	*Nephrops norvegicus*	0.75
MUL	*Mugilidae*	0.76
DPS	*Parapenaeus longirostris*	0.78
SQM	*Illex coindetii*	0.79
OCM	*Eledone spp*	0.80
SQR	*Loligo vulgaris*	0.81
TGS	*Penaeus kerathurus*	0.82
MGC	*Liza ramada*	0.83
SIL	*Atherinidae*	0.83
SBG	*Sparus aurata*	0.84
SCX	*Pectinidae*	0.85
OCC	*Octopus vulgaris*	0.86
OYF	*Ostrea edulis*	0.86

HOM	*Trachurus trachurus*	0.87
GUU	*Chelidonichthys lucerna*	0.87
GPA	*Gobiidae*	0.88
CRA	*Brachyura*	0.89
MSF	*Arnoglossus laterna*	0.89
POD	*Trisopterus minutus*	0.89
SQU	*Loliginidae, Ommastrephidae*	0.90
MON	*Lophius piscatorius*	0.90
MPT	*Mustelus punctulatus*	0.91
EOI	*Eledone cirrhosa*	0.91
GUG	*Eutrigla gurnardus*	0.91
WHB	*Micromesistius poutassou*	0.92
ANK	*Lophius budegassa*	0.92
SSB	*Lithognathus mormyrus*	0.92
SJA	*Pecten jacobaeus*	0.93
SCR	*Maja squinado*	0.93
PAC	*Pagellus erythrinus*	0.93
SPC	*Spicara smaris*	0.93
GRO	*Osteichthyes*	0.94
SKA	*Raja spp*	0.94
TUR	*Psetta maxima*	0.94
JAX	*Trachurus spp*	0.94
CTL	*Sepiidae, Sepiolidae*	0.95
MGA	*Liza aurata*	0.95
RJC	*Raja clavata*	0.95
CRU	*Crustacea*	0.95
VEV	*Venus verrucosa*	0.95
OUW	*Alloteuthis spp*	0.96
MNZ	*Lophius spp*	0.96
BSS	*Dicentrarchus labrax*	0.96
COE	*Conger conger*	0.96
GUX	*Triglidae*	0.96
CLV	*Veneridae*	0.96
CBC	*Cepola macrophthalma*	0.97
TRA	*Trachinidae*	0.97
RSE	*Scorpaena scrofa*	0.97
BOG	*Boops boops*	0.97
RAE	*Solen marginatus*	0.97
BLL	*Scophthalmus rhombus*	0.97
MSM	*Mytilus galloprovincialis*	0.97
SLM	*Sarpa salpa*	0.97
LEZ	*Lepidorhombus spp*	0.97
PRA	*Pandalus borealis*	0.98
JOD	*Zeus faber*	0.98
SKX	*Elasmobranchii*	0.98
FLE	*Platichthys flesus*	0.98

DGX	*Squalidae*	0.98
ANN	*Diplodus annularis*	0.98
HMM	*Trachurus mediterraneus*	0.98
CSH	*Crangon crangon*	0.98
UUC	*Uranoscopus scaber*	0.98
COB	*Umbrina cirrosa*	0.98
GAS	*Gastropoda*	0.98
WEX	*Trachinus spp*	0.98
CIL	*Citharus linguatula*	0.99
DGZ	*Squalus spp*	0.99
CTZ	*Chelidonichthys lastoviza*	0.99
SOX	*Soleidae*	0.99
SBS	*Oblada melanura*	0.99
MUR	*Mullus surmuletus*	0.99
BBS	*Scorpaena porcus*	0.99
FOR	*Phycis phycis*	0.99
SPR	*Sprattus sprattus*	0.99

3.7. References

AdriaMed (2011). Report of the Technical meeting on Solemon survey activities, May 2011. 21.

Amoroso, R. O., Pitcher, C. R., Rijnsdorp, A. D., McConnaughey, R. A., Parma, A. M., Suuronen, P., et al. (2018). Bottom trawl fishing footprints on the world's continental shelves. Proc. Natl. Acad. Sci. U. S. A. 115, E10275–E10282. doi:10.1073/pnas.1802379115.

Arbizu, M. (2017). Pairwiseadonis: Pairwise multilevel comparison using adonis. R Packag. Version 0.0. doi:10.1109/IROS.2007.4399402.

Berger, A., Harley, S., Pilling, G., Davies, N., and Hampton, J. (2012). Introduction to harvest control rules for WCPO tuna fisheries. Available at: http://citeseerx.ist.psu.edu/viewdoc/summary?doi=10.1.1.261.2622 [Accessed May 6, 2021].

Bion, R. (2021). ggradar: Create radar charts using ggplot2. Available at: https://github.com/ricardo-bion/ggradar.

Borcart, D., Gillet, F., and Legendre, P. (2018). Numerical Ecology with R. 2nd ed. Springer International Publishing AG, part of Springer Nature 2011, 2018.

Britten, G. L., Dowd, M., and Worm, B. (2016). Changing recruitment capacity in global fish stocks. Proc. Natl. Acad. Sci. 113, 134–139. doi:10.1073/pnas.1504709112.

Browman, H., Cury, P., Hilborn, R., … S. J.-M. E. P., and 2004, undefined Perspectives on ecosystem-based approaches to the management of marine resources. academia.edu. Available at: https://www.academia.edu/download/32633653/m274p269.pdf [Accessed January 22, 2020].

Cardinale, M., Osio, G. C., and Scarcella, G. (2017). Mediterranean Sea: A Failure of the European Fisheries Management System. Front. Mar. Sci. 4, 72. doi:10.3389/fmars.2017.00072.

Cognetti, G., Lardicci, C., Abbiati, M., and Castelli, A. (2000). The Adriatic Sea and the Tyrrhenian Sea. Seas Millenn. - an Environ. Eval. - Vol. 1, 267–284.

Colloca, F., Cardinale, M., Belluscio, A., and Ardizzone, G. (2003). Pattern of distribution and diversity of demersal assemblages in the central Mediterranean sea. Estuar. Coast. Shelf Sci. 56, 469–480. doi:10.1016/S0272-7714(02)00196-8.

Colloca, F., Cardinale, M., Maynou, F., Giannoulaki, M., Scarcella, G., Jenko, K., et al. (2013). Rebuilding Mediterranean fisheries: A new paradigm for ecological sustainability. Fish Fish. 14, 89–109. doi:10.1111/j.1467-2979.2011.00453.x.

Colloca, F., Scarcella, G., and Libralato, S. (2017a). Recent Trends and Impacts of Fisheries Exploitation on Mediterranean Stocks and Ecosystems. Front. Mar. Sci. 4. doi:10.3389/fmars.2017.00244.

Colloca, F., Scarcella, G., and Libralato, S. (2017b). Recent Trends and Impacts of Fisheries Exploitation on Mediterranean Stocks and Ecosystems. Front. Mar. Sci. 4, 244. doi:10.3389/fmars.2017.00244.

Demirel, N., Zengin, M., and Ulman, A. (2020). First Large-Scale Eastern Mediterranean and Black Sea Stock Assessment Reveals a Dramatic Decline. Front. Mar. Sci. 7, 1–13. doi:10.3389/fmars.2020.00103.

Eigaard, O. R., Bastardie, F., Hintzen, N. T., Buhl-Mortensen, L., Buhl-Mortensen, P., Catarino, R., et al. (2017). The footprint of bottom trawling in European waters: Distribution, intensity, and seabed integrity. ICES J. Mar. Sci. 74, 847–865. doi:10.1093/icesjms/fsw194.

European Parliament (2013). European Parliament and Council. regulation (EU) No. 1380/2013 of the European Parliament and of the Council of 11 December 2013 on the common fisheries policy, Off. J. Eur. Union L 354 (2013) 22–61.

Falsone, F., Scannella, D., Geraci, M. L., Gancitano, V., Vitale, S., and Fiorentino, F. (2021). How Fishery Collapses: The Case of *Lepidopus caudatus* (Pisces: Trichiuridae) in the Strait of Sicily (Central Mediterranean). Front. Mar. Sci. 7, 5–8. doi:10.3389/fmars.2020.584601.

FAO-GFCM (2019). Scientific Advisory Committee on Fisheries (SAC) Working Group on Stock Assessment of Demersal Species (WGSAD).

Ferrà, C., Tassetti, A. N., Grati, F., Pellini, G., Polidori, P., Scarcella, G., et al. (2018). Mapping change in bottom trawling activity in the Mediterranean Sea through AIS data. Mar. Policy 94, 275–281. doi:10.1016/j.marpol.2017.12.013.

Fortibuoni, T., Libralato, S., Arneri, E., Giovanardi, O., Solidoro, C., and Raicevich, S. (2018). Erratum: Fish and fishery historical data since the 19th century in the Adriatic Sea, Mediterranean. Sci. Data 5, 180144. doi:10.1038/sdata.2018.144.

Froese, R., Demirel, N., Coro, G., Kleisner, K. M., and Winker, H. (2017). Estimating fisheries reference points from catch and resilience. Fish Fish. 18, 506–526. doi:10.1111/faf.12190.

Froese, R., Winker, H., Coro, G., Demirel, N., Tsikliras, A. C., Dimarchopoulou, D., et al. (2018). Status and rebuilding of European fisheries. Mar. Policy 93, 159–170. doi:10.1016/j.marpol.2018.04.018.

Froese, R., Winker, H., Coro, G., Demirel, N., Tsikliras, A. C., Dimarchopoulou, D., et al. (2020). Estimating stock status from relative abundance and resilience. ICES J. Mar. Sci. 77, 527–538. doi:10.1093/icesjms/fsz230.

Froese, R., Winker, H., Coro, G., Palomares, M.-L. 'Deng,' Tsikliras, A. C., Dimarchopoulou, D., et al. (2021). Catch time series as the basis for fish stock assessments: the CMSY++ method and its worldwide applications. Submitt. to Fish Fish.

Froese, R., Winker, H., Gascuel, D., Sumaila, U. R., and Pauly, D. (2016). Minimizing the impact of fishing. Fish Fish. 17, 785–802. doi:10.1111/faf.12146.

Galdelli, A., Mancini, A., Tassetti, A. N., Ferrà Vega, C., Armelloni, E., Scarcella, G., et al. (2019). A Cloud Computing Architecture to Map Trawling Activities Using Positioning Data. Vol. 9 15th IEEE/ASME Int. Conf. Mechatron. Embed. Syst. Appl. doi:10.1115/DETC2019-97779.

Gamble, R. J., and Link, J. S. (2009). Analyzing the tradeoffs among ecological and fishing effects on an example fish community: A multispecies (fisheries) production model. Ecol. Modell. 220, 2570–2582. doi:10.1016/j.ecolmodel.2009.06.022.

GFCM (2018). Scientific Advisory Committee on Fisheries (SAC) Working Group on Stock Assessment of Demersal Species (WGSAD) GFCM and FAO headquarters , Rome , Italy , 13 – 18 November 2017 FINAL REPORT. 1, 13–18.

Giovanardi, O., Pranovi, F., and Franceschini, G. (1998). '"Rapido"' trawl-fishing in the Northern Adriatic: preliminary observations on effects on macrobenthic communities. Acta Adriat. 39, 37–52.

Grati, F., Aladzuz, A., Azzurro, E., Bolognini, L., Carbonara, P., Çobani, M., et al. (2018). Seasonal dynamics of small-scale fisheries in the Adriatic Sea. Mediterr. Mar. Sci. 19, 21. doi:10.12681/MMS.2153.

Grati, F., Scarcella, G., Polidori, P., Domenichetti, F., Bolognini, L., Gramolini, R., et al. (2013). Multi-annual investigation of the spatial distributions of juvenile and adult sole (*Solea solea* L.) in the Adriatic Sea (northern Mediterranean). J. Sea Res. 84, 122–132. doi:10.1016/j.seares.2013.05.001.

Hall-Spencer, J., Froglia, C., Atkinson, R. J. A., and Moore, P. G. (1999). The impact of Rapido trawling for scallops, *Pecten jacobaeus*(L.), on the benthos of the Gulf of Venice. ICES J. Mar. Sci. 56, 111–124. doi:10.1006/jmsc.1998.0424.

Hilborn, R. (2011). Future directions in ecosystem based fisheries management: A personal perspective. Fish. Res. 108, 235–239. doi:10.1016/j.fishres.2010.12.030.

Howell, D., and Subbey, S. (2019). Multispecies considerations in stock assessments: "yes we can". ICES C. 2013/E07.

ICES (2017). WGMIXFISH - Report of the Working Group on Mixed Fisheries Advice for the North Sea. 128.

Iles, T. C. (1994). A review of stock-recruitment relationships with reference to flatfish populations. Netherlands J. Sea Res. 32, 399–420. doi:10.1016/0077-7579(94)90017-5.

Kollmann, H., and Stachowitsch, M. (2001). Long-Term Changes in the Benthos of the Northern Adriatic Sea: A Phototransect Approach. Mar. Ecol. 22, 135–154. doi:10.1046/j.1439-0485.2001.01761.x.

Kritzer, J. P., and Liu, O. R. (2014). "Fishery Management Strategies for Addressing Complex Spatial Structure in Marine Fish Stocks," in Stock Identification Methods (Elsevier), 29–57. doi:10.1016/B978-0-12-397003-9.00003-5.

Legendre, P., and Gallagher, E. D. (2001). Ecologically meaningful transformations for ordination of species data. Oecologia 129, 271–280. doi:10.1007/s004420100716.

Link, J. S. (2010). Ecosystem-based fisheries management: Confronting tradeoffs. doi:10.1017/CBO9780511667091.

Maravelias, C. D., and Tsitsika, E. V. (2008). Economic efficiency analysis and fleet capacity assessment in Mediterranean fisheries. Fish. Res. 93, 85–91. doi:10.1016/j.fishres.2008.02.013.

Marini, M., Bombace, G., and Iacobone, G. (2017). Il mare Adriatico e le sue risorse. Carlo Saladino Editore, Palermo, Italy.

Mattei, N., and Pellizzato, M. (1996). A population study on three stocks of a commercial Adriatic pectinid (*Pecten jacobaeus*). Fish. Res. 26, 49–65. doi:10.1016/0165-7836(95)00413-0.

Maunder, M. N. (2012). Evaluating the stock-recruitment relationship and management reference points: Application to summer flounder (*Paralichthys dentatus*) in the U.S. mid-Atlantic. Fish. Res. 125–126, 20–26. doi:10.1016/j.fishres.2012.02.006.

Maunder, M. N., and Aires-da-silva, A. (2009). Evaluation of the Kobe plot and strategy matrix and their application to tuna in the EPO. Iattc, 191–211.

Maunder, M. N., and Punt, A. E. (2013). A review of integrated analysis in fisheries stock assessment. Fish. Res. 142, 61–74. doi:10.1016/j.fishres.2012.07.025.

Moffitt, E. A., Punt, A. E., Holsman, K., Aydin, K. Y., Ianelli, J. N., and Ortiz, I. (2016). Moving towards ecosystem-based fisheries management: Options for parameterizing multi-species biological reference points. Deep. Res. Part II Top. Stud. Oceanogr. 134, 350–359. doi:10.1016/j.dsr2.2015.08.002.

Oksanen, A. J., Blanchet, F. G., Friendly, M., Kindt, R., Legendre, P., Mcglinn, D., et al. (2016). Vegan: Community Ecology Package. https://github.com/vegandevs/vegan. doi:10.4135/9781412971874.n145.

Palomares, M., and Pauly, D. SeaLifeBase. Version (02/2018).

Petović, S., Marković, O., Ikica, Z., Đurović, M., and Joksimović, A. (2016). Effects of bottom trawling on the benthic assemblages in the south Adriatic Sea (Montenegro). Acta Adriat. 57, 81–92.

Pranovi, F., Raicevich, S., Franceschini, G., Farrace, M. G., and Giovanardi, O. (2000). Rapido trawling in the northern Adriatic Sea: effects on benthic communities in an experimental area. ICES J. Mar. Sci. 57, 517–524. doi:10.1006/jmsc.2000.0708.

Punt, A. E., Smith, A. D. M., and Cui, G. (2002). Marine Freshwater of technical interactions. Mar. Freshw. Res. 53, 615–629.

Riedel, B., Stachowitsch, M., and Zuschin, M. (2010). Low dissolved oxygen impacts in the northern Adriatic: critical thresholds for benthic assemblages. ICES Annu. Sci. Conf., 1–17.

Rogers, J. B., and Pikitch, E. K. (1992). Numerical Definition of Groundfish Assemblages Caught Off the Coasts of Oregon and Washington Using Commercial Fishing Strategies. Can. J. Fish. Aquat. Sci. 49, 2648–2656. doi:10.1139/f92-293.

Russo, E., Monti, M. A., Mangano, M. C., Raffaetà, A., Sarà, G., Silvestri, C., et al. (2020). Temporal and spatial patterns of trawl fishing activities in the Adriatic Sea (Central Mediterranean Sea, GSA17). Ocean Coast. Manag. 192, 105231. doi:10.1016/j.ocecoaman.2020.105231.

Santelli, A., Cvitković, I., Despalatović, M., Fabi, G., Grati, F., Marčeta, B., et al. (2017). Spatial persistence of megazoobenthic assemblages in the Adriatic Sea. Mar. Ecol. Prog. Ser. 566, 31–48. doi:10.3354/meps12002.

Scarcella, G., Fabi, G., and Grati, F. (2007). Rapido trawl fishery in the North-Central Adriatic Sea. Rapp. Comm. Int. Mer Mèditerr., 591.

Scarcella, G., Grati, F., Raicevich, S., Russo, T., Gramolini, R., Scott, R. D., et al. (2014). Common sole in the northern and central Adriatic Sea: Spatial management scenarios to rebuild the stock. J. Sea Res. 89, 12–22. doi:10.1016/J.SEARES.2014.02.002.

Schückel, S., Sell, A. F., Kihara, T. C., Koeppen, A., Kröncke, I., and Reiss, H. (2013). Meiofauna as food source for small-sized demersal fish in the southern North Sea. Helgol. Mar. Res. 67, 203–218. doi:10.1007/s10152-012-0316-1.

STEFC (2019). The 2019 Annual Economic Report on the EU Fishing Fleet (STECF 19-06), Carvalho, N., Keatinge, M. and Guillen Garcia, J. editor(s), EUR 28359 EN. Publications Office of the European Union, Luxembourg, 2019 doi:10.2760/911768.

Suzuki, R., and Shimodaira, H. (2015). Package ‘ pvclust .’ R Top. Doc.

Van der Hammen, T., Poos, J. J., Van Overzee, H. M. J., Heessen, H. J. L., Magnusson, A., and Rijnsdorp, A. D. (2013). Population ecology of turbot and brill: What can we learn from two rare flatfish species? J. Sea Res. 84, 96–108. doi:10.1016/j.seares.2013.07.001.

Ward, J. H. (1963). Hierarchical Grouping to Optimize an Objective Function. J. Am. Stat. Assoc. 58, 236–244. doi:10.1080/01621459.1963.10500845.

Welcomme, R. L. (1999). A review of a model for qualitative evaluation of exploitation levels in multi-species fisheries. Fish. Manag. Ecol. 6, 1–19. doi:10.1046/j.1365-2400.1999.00137.x.

Winker, H., Carvalho, F., and Kapur, M. (2018). JABBA: Just Another Bayesian Biomass Assessment. Fish. Res. 204, 275–288. doi:10.1016/J.FISHRES.2018.03.010.

Winker, H., and Sherley, R. B. (2019). JARA: 'Just Another Red-List Assessment.' bioRxiv, 1–27. doi:10.1101/672899.

4. Stock assessment of common sole in GSA17: an ensemble approach using data-rich model

From the FAO-GFCM report: ***Masnadi, F.**, Cardinale, M., Donato, F., Sabatini, L., Pellini, G., Scanu, M., et al. 2021. Stock Assessment Form Demersal species - Stock assessment of common sole in GSA 17.*

4.1. Abstract

In the Adriatic, common sole represents more than 20 million of euros in term of landing value. In 2020, 55% of the catches is provided by the Italian *rapido* trawl fleets (TBB), 23% from the Italian, Slovenian and Croatian set netters (GNS and GTR) operating mostly within 3 nautical miles from the coast, 19% from the Italian otter trawlers (OTB), and the remaining 3% from the Croatian *rampon* fishery (DCF ITA HRV). Furthermore, landings in 2020 are almost 25% less than in 2019. Ensemble modelling approaches using Stock Synthesis (SS3) was used to present final results based on alternative hypothesis of selectivity, natural mortality and steepness (18 runs). This is the first time an ensemble model was used in the Mediterranean to give management advice. All runs used in the final ensemble grid are size structure models based on historical landings data from 1958. Size are then converted to age inside the models using VBGP. Tuning data were collected during the SoleMon survey. Interconnected diagnostic tests were carried out on all ensemble candidate runs. Moreover, diagnostic scores were used as weighting factor during ensemble procedure. Considering the results of the analyses conducted, the common sole in GSA 17 is showing a positive recovering trend. Though fishing mortality is below to reference point (F/F40 = 0.81), spawning biomass is still low and around 70 % of the reference point. Probabilistic forecasts showed that an increased catch scenario should be avoided.

4.2. Fishery dependent information

4.2.1. Description of the fishery and official catch data

The common sole is a very important commercial species in the central and northern Adriatic Sea (Grati et al., 2013), where the stock is shared among Italy, Slovenia and Croatia, representing about 2000 tons and more than 20 million of euros in terms of landing value (FAO-GFCM, 2021). Despite the economic relevance of this species (included in the GFCM and Adriatic shared resources priority lists and in the EC action plan to reduce discards in the Mediterranean Sea), the sole has been included in the European Commission Data Collection Framework in the GSA 17 only since 2004 (DCF; EU Regulation 2017/1004). Common sole official landings data updated to 2020 from the framework of

Croatian, Italian and Slovenian Official Data Collection are showed in Figure 4.2.1.1 Catch from Slovenia are negligible, therefore Slovenian netters are not counted in the assessment. Italian *rapido* trawl fleets (TBB) has become dominant in the Italian catches since 2014, while Italian gill netters (GNS) has been decreasing total catches since the same period and Italian otter trawlers (OTB) catches are increasing slightly since 2015. Croatian total catches for trammel netters (GTR) are reported only since 2012 and are stable across years while *rampon* fishery (DRB) started as new fishery in recent years (~ 2012) and it is constantly increasing. In 2020, 55% of the catches is provided by Italian TBB, 23% from the Italian, Slovenian and Croatian netters (GNS and GTR) operating mostly within 3 nautical miles from the coast, 19% from the Italian OTB, and the remaining 3% from the Croatian DRB. Furthermore, in the beginning of the COVID-19 global pandemic has forced many governments to temporarily shut down large segments of their economies to promote social distancing and to reduce the infection rate, including businesses, restaurants and school .Depending on the typology of the fishery, it is possible to detect a sort of gradient in the effect of COVID-19, going from a fishing effort reduction that was almost negligible and did not affect the operators (Coro et al., 2022a) to a complete shutdown of some fisheries (Pita et al., 2021). In Italy, a lockdown period was imposed from March 11 to May 17. In almost the same period Croatia, Slovenia, Albania and Montenegro also adopted similar measures. During this period, restrictions in terms of social distancing affected the fishery sector, and a strong reduction in seafood requests caused a decrease in fishing activities and related, such as fish markets and harbours. Scarcella et al. (2022) showed that all fishing effort indicators agree on depicting TBB activity in 2020 at levels lower than 2019 for the entire year, in any case describing a more severe reduction than the management plan claim (-16% in GFCM/43/2019/5). As a consequence, there are evidence that the COVID-19 pandemic restriction effectively forced TBB activity to be far lower than expectations (see point 10 in Figure 4.2.2.1), leading to a drastic reduction of about 25% in the landings of this species compare to 2019.

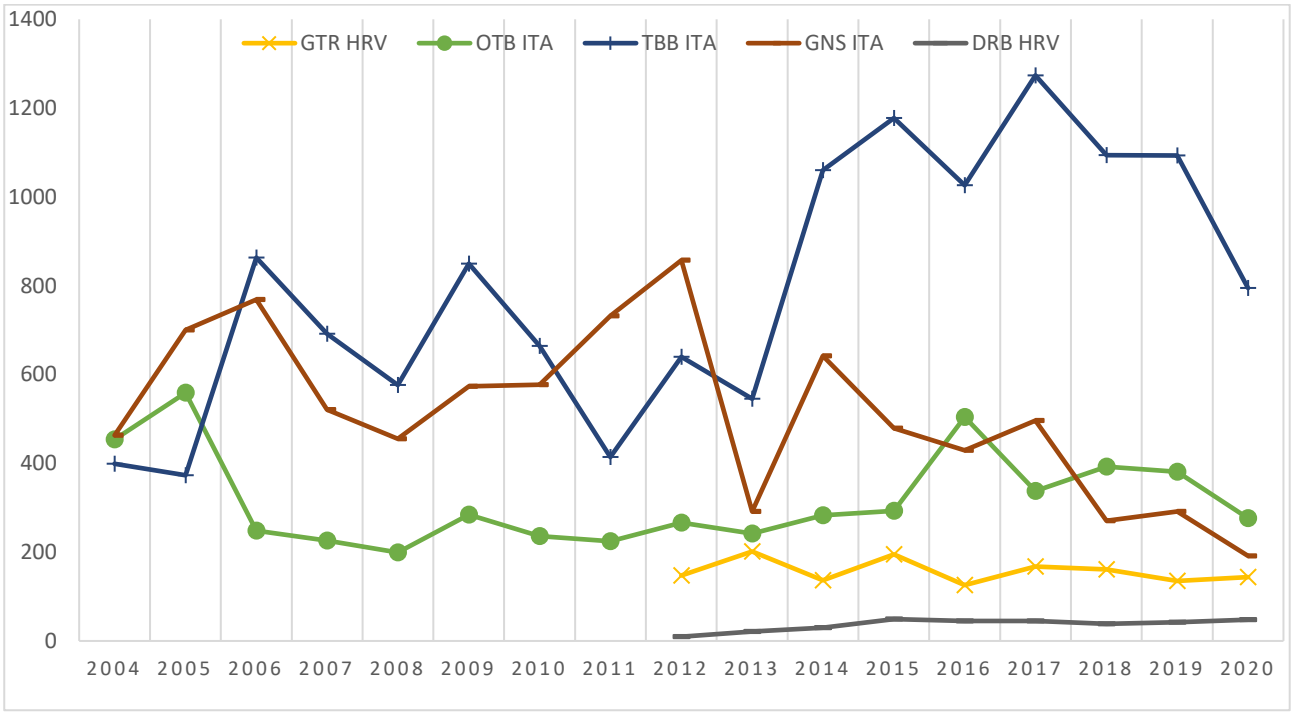

Figure 4.2.1.1. Time series of official DCF landings for common sole in GSA 17. OTB: bottom otter trawl, GNS: gillnets, GTR: trammel nets; TBB: modified beam trawl (rapido trawl); DRB: modified beam trawl for shellfish (rampon).

4.2.2. Timeline of landing data and management event

Historical evidence provides the context for present-day observations and allows studying long-term changes in marine populations and ecosystems. Moreover, the inclusion of historical information in stock assessments can revealed larger declines compared to those detected with short-term observations alone (Rosenberg et al., 2005; Fortibuoni et al., 2017). In the context of complex statistical age-structured models such as the ones used in FAO-GFCM and STECF context, historical data are fundamental in the calculation of reference points as they provide quantitative information used by the model to better estimate the initial exploitation condition of the stock (e.g. initial catch used to estimate initial fishing mortality). For this reason, the further historical data goes back in time to provide the general picture of what the conditions of the stock were like at the beginning of the evolution/expansion of fisheries in the study area, the more robust the assessment and the consequent scientific advice will be. However, historical data collection is time-consuming and difficult, being records reported in different languages, only accessible in small archives for which no electronic resources exist, or buried in documents created for a different purpose (McClenachan, Ferretti, & Baum 2012). In Italy, centralized reporting on landings of marine fisheries started in 1947 by the Italian National Institute of Statistics (ISTAT). However, it is only since 1953 that landings are reported at the species level (Fortibuoni et al., 2017).

Northern and Central Adriatic Sea historical landings data for common sole are presented in Figure 4.2.2.1 with the relative sources and time line of relevant management events for sole fishery. Relevant events are shown to provides the context to better understand the evolution of catches in conjunction with the evolution and implementation of the management regulations that led to the nowadays situation. Italian historical landings from 1953-1979 have been obtained from ISTAT revised by Fortibuoni et al., 2017. Data from 1980 to 2003 for both side of the basis (Italy and Croatia) are retrieved from FAO FishStatJ database (FAO, 2020), the public FAO's database of fisheries and aquaculture statistics that includes datasets on production, trade and consumption. More recent information, updated at 2020, came from DCF both for Italy and Croatia (as shown in the previous paragraph).

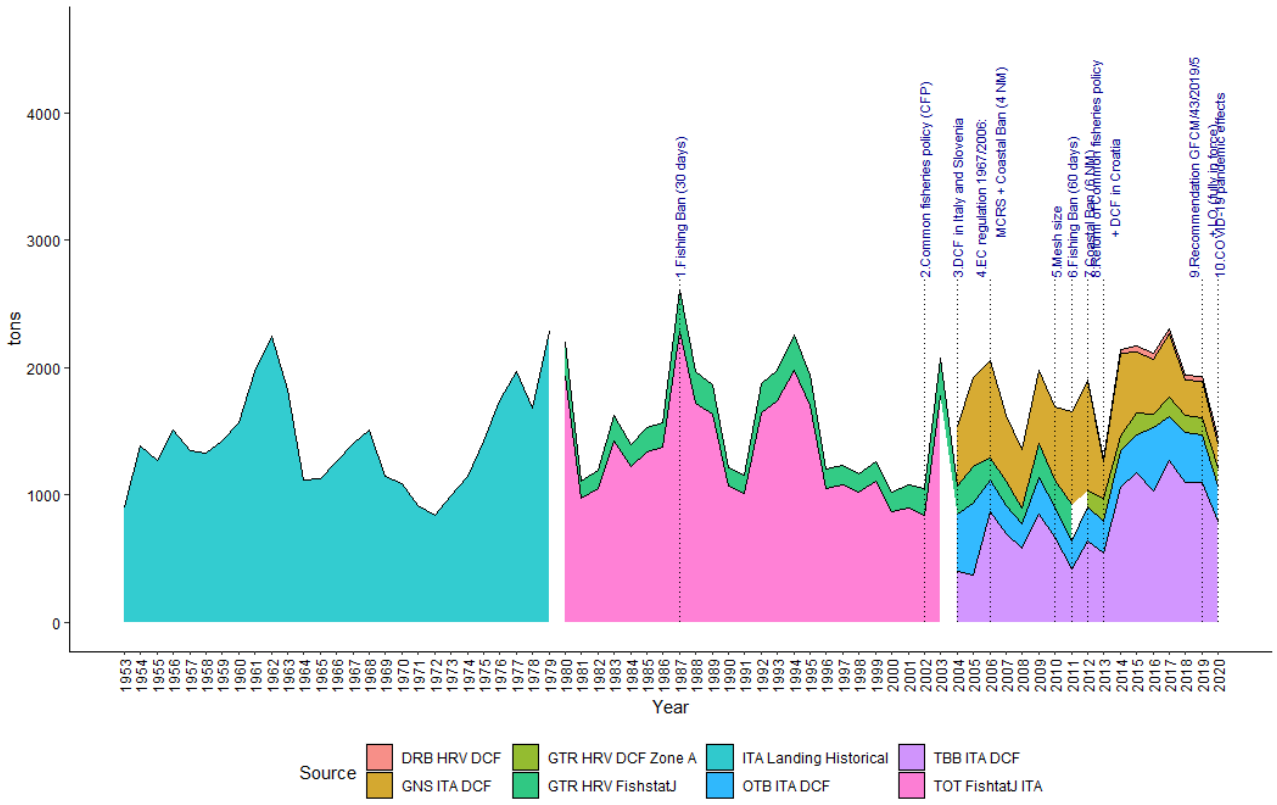

Figure 4.2.2.1. Time series of landings with relevant management events for common sole in GSA 17. OTB: bottom otter trawl, GNS: gillnets, GTR: trammel nets; TBB: modified beam trawl (rapido trawl); DRB: modified beam trawl for shellfish (rampon).

Below is a detailed description of the management event timeline shown in the plot:

1. 1987 - Fishing Ban (30 days): start of the summer fishing ban for trawlers, with a duration of 30 days;

2. 2002 - CFP + 8 weeks of technical measures: Council Regulation (EC) No 2371/2002 (4) established a Community system for the conservation and sustainable exploitation of fisheries resources under the Common Fisheries Policy (CFP). This law implies the introduction of technical measures such as reduction of fishing days during the first 8 weeks after the summer fishing ban;
3. 2004 - ITA_SVN_DCF start: Italian and Slovenian fishery dependent data collected according to the European schema, potentially affecting the coherence with the methodology in use prior to this year. European Commission Data Collection Framework (DCF; EU Regulation 2017/1004);
4. 2006 - MCRS + Coastal Ban (4 NM): (1) Minimum landing sizes (MCRS) adopted: Codend mesh size of trawl nets: 40 mm (stretched, diamond meshes) till 30/05/2010. From 1/6/2010 the existing nets have been replaced with a codend with 40 mm (stretched) square meshes or a codend with 50 mm (stretched) diamond meshes, in addition Set net minimum mesh size: 16 mm stretched andSet net maximum length x vessel x day: 5,000 m; (2) Coastal Ban (4NM): in the period following the fishing ban are adopted further technical measures, for a duration of ten weeks, indicating that trawlers may not fish within 4 nautical miles from the coast;
5. 2010 - Mesh size: enforcement of regulations (EC 1967/06) regarding the cod-end mesh size and the operative distance of fishing from the coasts;
6. 2011 - Fishing Ban (60 days): summer fishing ban for trawlers extended to 60 days. National regulations based on EC 2006;
7. 2012 - Coastal Ban (6 NM) + 10 weeks of technical measures + fishing ban reduced to 45 days: in the period following the fishing ban are adopted further technical measures, for a duration of ten weeks, indicating that trawlers may not fish within 6 nautical miles from the coast. National regulations based on EC 2006;
8. 2013 - Reform of CFP + HRV_DCF start: (1) The current CFP is adopted in December 2013, becoming applicable as of 1 January 2014. It focuses on the management of fisheries (whereas earlier CFP regulations focused only on stock conservation), and it includes aquaculture. Achieving maximum sustainable yield (MSY) by 2015 where possible, and at the latest by 2020, and having healthy fish stocks form the guiding principles of the 2013 CFP. Based on scientific advice, fishing must be adjusted to bring exploitation to the levels that maximise yields within the boundaries of sustainability; (2) Croatian fishery dependent data collected according to the European schema starts;
9. 2019 - GFCM/43/2019/5 + LO: (1) GFCM/43/2019/5: A five-year fishing effort regime shall be established for 2022–2026: each year, on the basis of SAC advice, the GFCM shall establish yearly effort quotas, thus contributing to reaching Fmsy and staying within safe

biological limits. In 2020 and 2021, a transitional fishing effort regime shall be established: at least 12% reduction for OTB and 16 % for TBB with respect to the annual effort exerted in 2015 or to the three-year average within the 2015–2018 period. The provisions shall not apply to national fleets operating with OTB and fishing for less than 1 000 days during the reference period; (2) Landing Obligation (LO). Enforcement of the EU law limiting the discards at sea of target species.

10. 2020 - COVID-19 pandemic effects (data from Scarcella et al., 2022): effort reduction imposed by pandemic-related restrictions added up to the effort regime by the GFCM/43/2019/5 management plan. *Rapido* trawlers was the most affected gear, showing reduced amount of activity over the entire year: hours at sea -23.5 %, fishing hours -18.7%, fishing days -25.4% compare to 2019.

4.2.3. Landing reconstruction

To derive the landings by gear in the past useful for stock assessment, Italian total landings from 1953 to 2003 (from Fortibuoni et al., 2017 and FAO-FishStatJ source) have been divided into fleet thanks to the proportion (average ratio along the years) observed in DCF data before COVID-19 pandemic effects (2004-2019). This was the procedure:

1. Starting data: ITA DCF official landings data (2004 – 2019)
2. OTB reconstruction: $\frac{OTB}{TOT\ ITA}$ calculated between 2004-2019 (~ 0.19) and applied backward
3. TBB reconstruction: $\frac{TBB}{TOT\ ITA}$ calculated between 2004-2019 (~ 0.47) and applied backward
4. GNS reconstruction: $\frac{GNS}{TOT\ ITA}$ calculated between 2004-2019 (~ 0.33) and applied backward

There is some evidence in Chioggia fish market database that *rapido* fishery started in the ’70s and not in the ‘50s. Nevertheless, before ’70s common sole was fished with a specific gear called *sfogliara*, considered by the experts of the area to be a very similar and comparable fishing method to modern *rapido* fishery.

In Croatia *S. solea* is usually caught only in some area, but in national statistics it is declared together with all other flat fishes. The main area of *S. solea* distribution is the Zone A (Northern Adriatic - western Istrian coast). In other parts of Adriatic there is some amount of the catch, but mostly it referes to other *Solea* species (*S. kleini* or *S. lascaris*). To solve this discrepancy also in historical data coming from FishtatJ, a ratio between Zone A catch and total DCF HRV catch has been used as follow:

1. Starting data: HRV DCF official landings data (2012 – 2019) + HRV Zone A landings data
2. Zone A reconstruction: $\frac{GTR\ Zone\ A}{TOT\ HRV\ Solea\ spp}$ calculated between 2012-2019 (~ 0.88) and applied backward to FistatJ HRV data

The information on total landings of *Solea* spp. are available through the FAO database since 1980. However, data prior to 1980 are lacking. During the benchmark session in 2021, a historical time series of Croatian catches reconstructed by Matić-Skoko et al. 2014 were considered, but these were not used due to probable overestimate and large discrepancy with official national statistics (78% higher). The group also debated on the use of a fixed landing amount for the period from 1953 to 1980 (150 tons), but this was also considered as inappropriate. In the end, assuming the proportionality between Italian and Croatian catches due to the exploitation of the same stock, it was agreed to use reconstructed landings by calculating a ratio between ITA and HRV in the first 10 years of FishtatJ data (~ 0.14) and applied backwards up to 1953. In conclusion, Figure 4.2.3.1 shows the final time series from 1953 to 2020 used in the assessments (landing by fleet for integrated model).

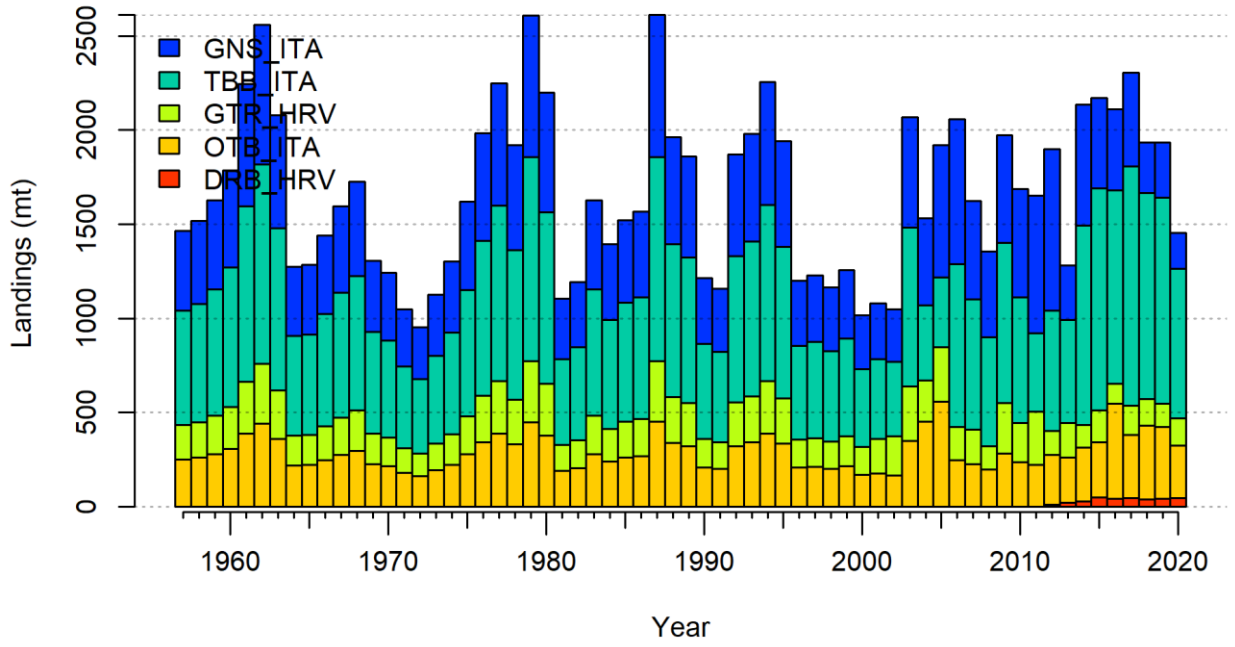

Figure 4.2.3.1 – Landings reconstruction by gear and country for common sole in GSA 17 used as input data in the assessment models.

4.2.4. Catch length frequency distributions (LFDs)

Italian catches are dominated by smaller individuals mainly caught by TBB and OTB, a smaller proportion of individuals is caught by GNS. On the contrary Croatian catches are dominated by bigger individuals caught by GTR (Figure 4.2.4.1). This agrees with the spatial distribution of common sole in the Adriatic Sea which is characterized by a migration of part of the adults from the west coast

(nursery areas) to the east coast (spawning areas) (Fabi et al., 2009; Scarcella et al., 2014).

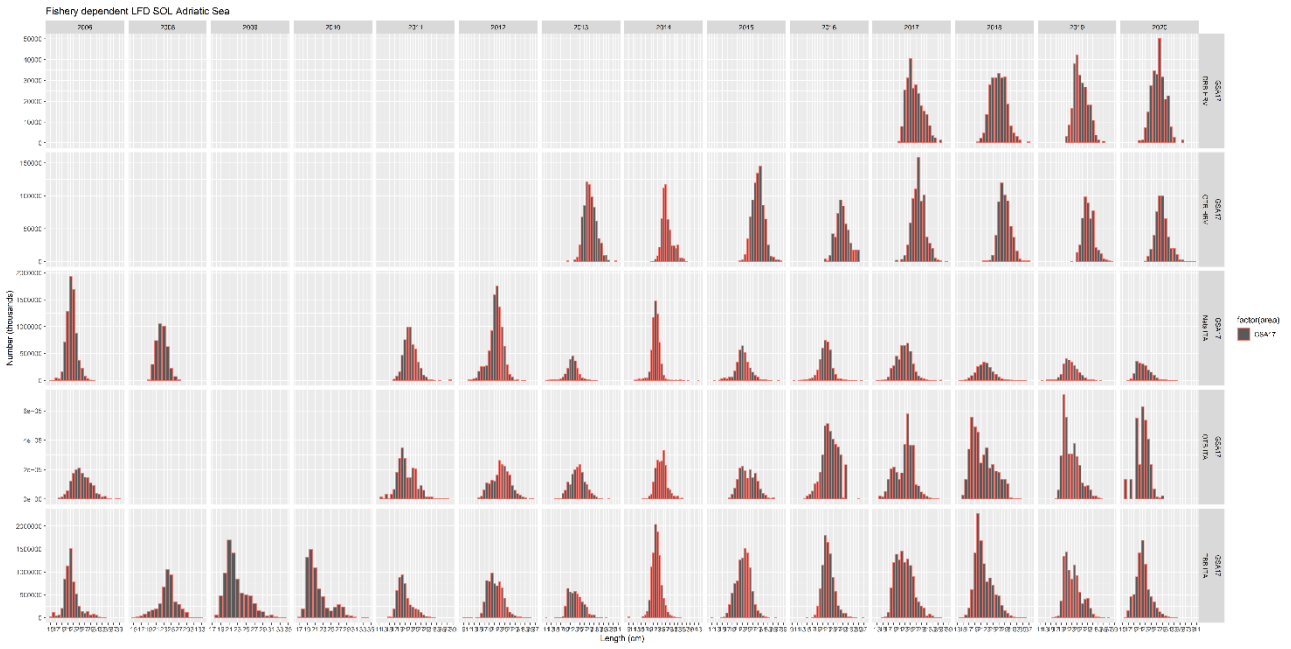

Figure 4.2.4.1. Length Frequency Distribution of catches from 2006 to 2020.

4.3. Fishery independent information

4.3.1. The SoleMon survey

The Adriatic scientific beam trawl survey started in 2005 in the framework of the SoleMon project, funded by the Italian Ministry of Agriculture (MIPAF). Initially, it involved two Italian Units, ISMAR – CNR of Ancona and the Istituto Centrale per la Ricerca scientifica e tecnologica Applicata al Mare (ICRAM), Chioggia and one Croatian Unit, IOF of Split.

The SoleMon surveys collect distribution, relative abundance and biological data on commercial marine species in GSA 17 for use in stock assessment and fishery management. The primary target species is common sole (*Solea solea*); further target species include spottail mantis squillid (*Squilla mantis*), common cuttlefish (*Sepia officinalis*), great Mediterranean scallop (*Pecten jacobaeus*), queen scallop (*Aequipecten opercularis*), turbot (*Scophthalmus maximus*), brill (*Scophthalmus rhombus*), European hake (*Merluccius merluccius*), red mullet (*Mullus barbatus*), skates (Rajdae) and the caramote prawn (*Penaeus kerathurus*). Since 2007, the SoleMon surveys have been moving towards an increasingly ecosystem integrated approach, and further tasks (e.g. seafloor litter and megazoobenthos monitoring) have been added to the original goals, which are still priority objectives. Although adding further tasks to an existing survey can only occasionally produce an 'ideal survey' of the full ecosystem or encompass all MSFD descriptors, a newly created survey can set accuracy constraints for some of the data collected, based on prioritization. Since 2009, the SoleMon surveys

have also been coordinated in the framework of the ICES WGBEAM and included in the WGBEAM Manual for Offshore Beam Trawl Surveys. The researchers involved in the SoleMon surveys participate in the ICES WGBEAM annual meeting, and common sole data have been uploaded in the DATRAS database since 2016 (https://ices.dk/marine-data/data-portals/Pages/DATRAS.aspx).

Up to now, annual *rapido* trawl fishing surveys were carried out in GSA 17 from 2005 to 2020: two systematic "pre-surveys" carried out with the chartered fishing vessels (years 2005 and 2006), followed by a sequence of fall surveys from 2007 to 2020 performed with CNR R/V Dallaporta. The surveys have a random stratified design with three depth strata (0-30 m, 30-50 m, 50-100m). Hauls were carried out during the day using 2-4 *rapido* trawls simultaneously (Figure 4.3.1.1; stretched codend mesh size = 40.2 ± 0.83). The following number of hauls was reported per depth stratum (Table 4.3.1.1).

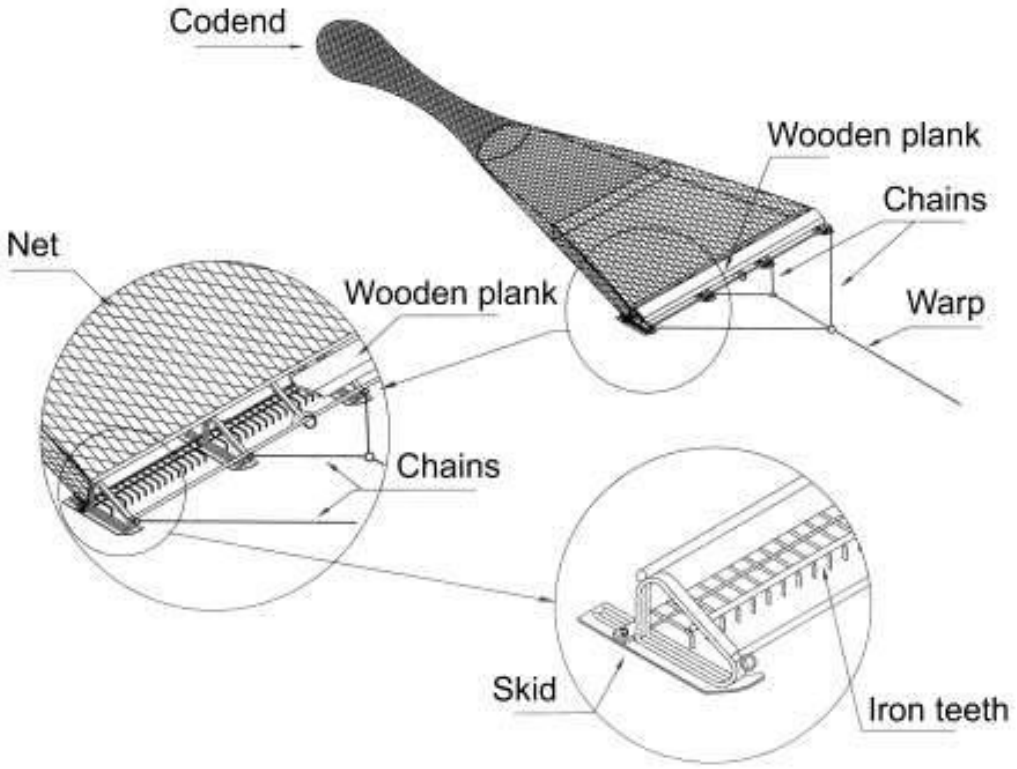

Figure 4.3.1.1. Graphical representation of rapido beam trawl gear used during SoleMon survey in GSA 17.

Table 4.3.1.1. Number of hauls per year and depth stratum in GSA 17, 2005-2020.

Depth strata	2005	2006	2007	2008	2009	2010	2011	2012	2013	2014	2015	2016	2017	2018	2019	2020
0-30	30	35	32	39	39	39	39	35	37	39	39	39	38	41	41	37
30-50	12	20	19	18	18	18	18	18	18	18	18	18	16	15	15	12
50-100	15	8	11	10	10	10	10	10	10	10	10	10	10	12	12	9
HRV	5	4	0	0	0	0	0	0	0	0	0	7	6	0	0	0
Total	62	67	62	67	67	67	67	63	65	67	67	74	70	68	68	58

Hauls inside Croatian national waters are present in 2005 and 2006 but have been fully implemented only in 2016 and were totally performed only in some year due to different issues (mainly time

coverage issue). For this reason, the 7 Croatian national waters hauls are not counted for the calculation of the abundance and biomass indices and LFDs to be used in the assessment models. In the future it is recommended to increase the coverage of survey sampling stations in the eastern part of GSA 17.

4.3.2. Calculation of abundance and biomass indexes

Abundance and biomass indexes from *rapido* trawl surveys were computed using TruST software (*https://www.kosmosambiente.it*). The abundance and biomass indices by GSA 17 were calculated through stratified means (Cochran et al., 1954; Saville, 1977). This implies weighting of the average values of the individual standardized catches and the variation of each stratum by the respective stratum area in the GSA 17:

$Yst = \Sigma (Yi*Ai) / A$

$V(Yst) = \Sigma (Ai^2 * si^2 / ni) / A^2$

Where:

A=total survey area

Ai=area of the i-th stratum

si=standard deviation of the i-th stratum

ni=number of valid hauls of the i-th stratum

n=number of hauls in the GSA

Yi=mean of the i-th stratum

Yst=stratified mean abundance

V(Yst)=variance of the stratified mean

The variation of the stratified mean is then expressed as the 95 % confidence interval:

Confidence interval = $Yst \pm t(student\ distribution) * V(Yst) / n$

It was noted that while this is a standard approach, the calculation may be biased due to the assumptions over zero catch stations, and hence assumptions over the distribution of data. A normal distribution is often assumed, whereas data may be better described by a delta-distribution, quasi-poisson. Indeed, data may be better modelled using the idea of conditionality and the negative binomial. Length distributions represented an aggregation (sum) of all standardized length frequencies over the stations of each stratum. Aggregated length frequencies were then raised to stratum abundance and finally aggregated (sum) over the strata to the GSA.

4.3.2.1. SoleMon 2020 reconstruction

The 2020 survey was carried out from 1/12-16/12/2020 with RV G. Dallaporta. Out of the 75 programmed hauls, only 58 (57 Italian + 1 Slovenian) were carried out during 2020 survey. All the hauls beyond the Adriatic midline (South West from Istria) and those in Croatian national waters had to be dropped due to overlap issues such as COVID-19 restriction (only 5 scientific members on board), bad weather conditions and limited ship-time (Figure 4.3.2.1.1).

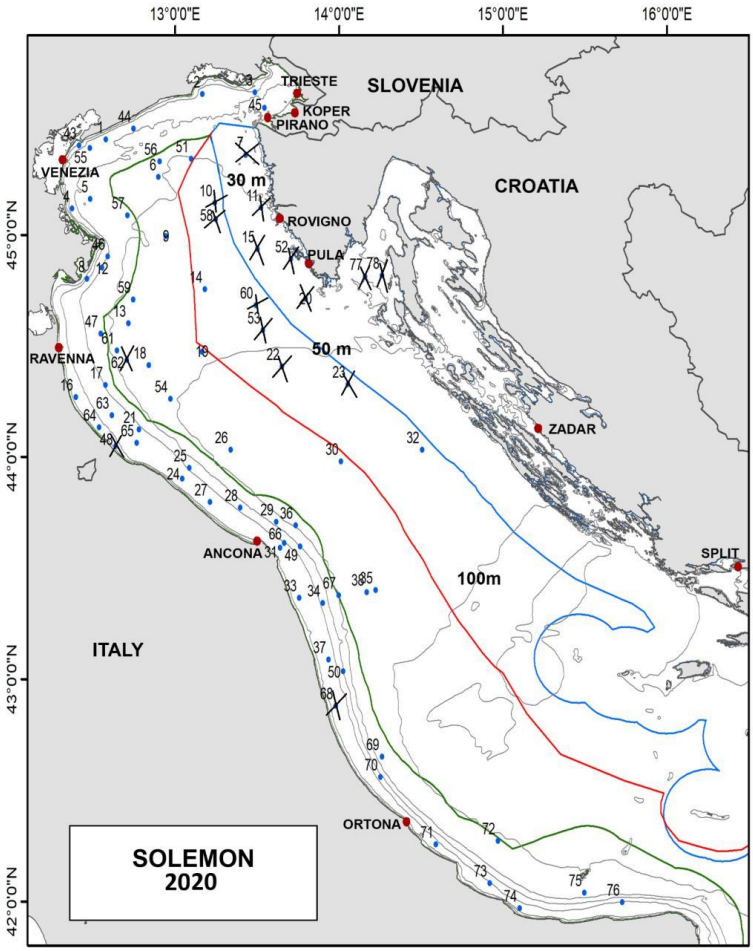

Figure 4.3.2.1.1. SoleMon map of hauls positions (2020 survey), the "X" means that the haul has not been performed.

Considering that adults concentrate in the missing hauls offshore area (deepest waters in at South West from Istria, Figure 4.3.2.1.1), spatial coverage effect on the survey indices have to be expected and explore. In the framework of EcoScope project (*https://ecoscopium.eu/*), researchers from ISTI and IRBIM CNR have developed a spatio-temporal ecological model to predict biomass in missing survey hauls (Coro et al., 2022b). This model has been applied to SoleMon survey to reconstruct biomass index for target species such as *Sepia officinalis*, *Squilla mantis*, *Pecten jacobeus* and *Solea solea* (Fig. 4.3.2.1.2). During simulation testing, accuracy on known hauls over the four species ranged between 80% and 100% and true total biomass index was always included in the confidence

intervals during 2019-year tests. Moreover, the model achieved higher performance than individual sub-component models (spatial, temporal, and ecological models *per se*) and a widely used equiproportional reconstruction (e.g. equiproportional; ICES, 2021a).

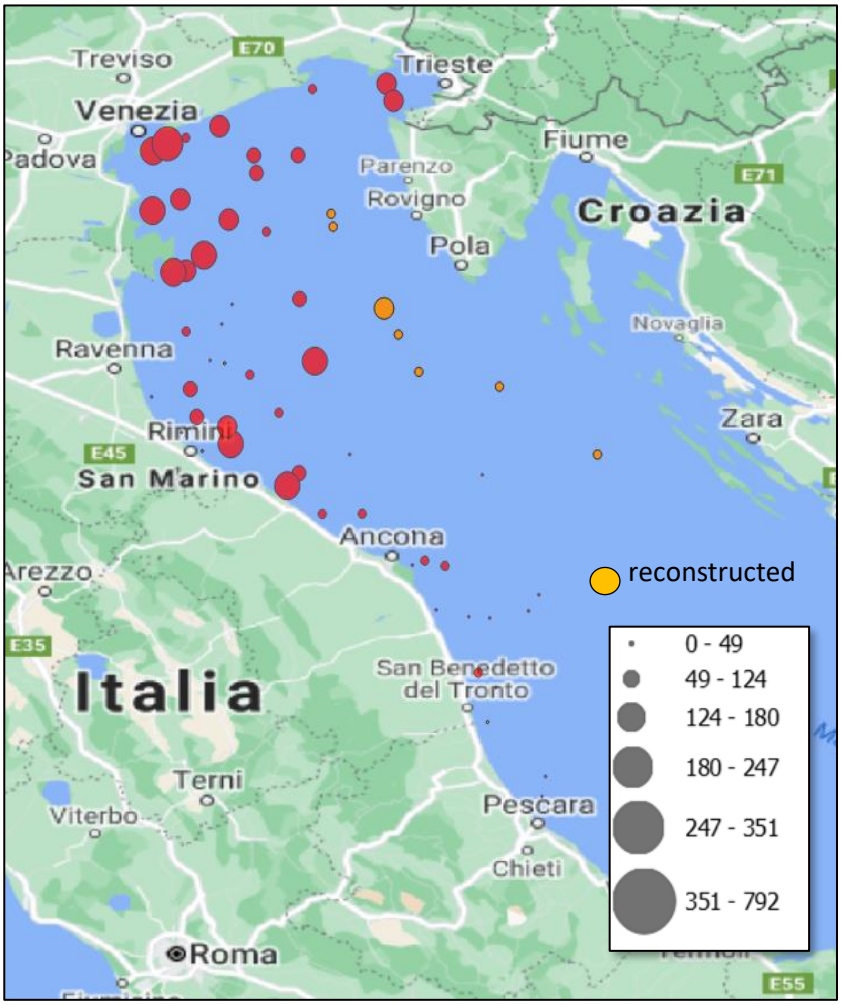

Figure 4.3.2.1.2. Common sole: Solemon 2020 biomass index with reconstructed hauls.

In particular, with the aim of obtaining an abundance index to be included in the following assessment model, the missing hauls biomass index has been converted to numbers assuming the same proportion of 2019 survey (point 1,2 of Figure 4.3.2.1.3). Then, 2020 overall abundance index were re-computed as usual through stratified means (Cochran et al., 1954; Saville, 1977) using TruST software with the inclusion of the missing hauls reconstructed values (point 3 of Figure 4.3.2.1.3).

Station N	BIOM prediction 2020	ABUN/BIOM 2019	ABUN 2020 in Missing hauls
10	79.09	8.41	664.92
22	123.63	4.90	605.41
23	108.76	5.31	577.70
32	73.85	5.25	387.98
48	33.35	14.39	479.79
53	103.02	5.63	580.40
58	88.99	7.03	625.77
60	234.78	5.81	1363.17
62	48.61	8.82	428.90
68	10.82	6.87	74.40

1. 2019: *Abb Index / Biom Index by missing hauls (10 hauls)*
2. 2020: *SOL_pred* * *Point1* → *Abb in* MISSING *hauls (by hauls)*
3. 2020: Abundance Index re-estimation using all hauls (*Real 2020* + *Point2*) = ***780 N/km2***

Figure 4.3.2.1.3. Solemon 2020 abundance index reconstruction process.

Figure 4.3.2.1.4 and Table 4.3.2.1.1 show the final abundance and biomass indices of sole obtained from 2005 to 2020; slightly increasing trends occurred till fall 2007, followed by a decrease in fall 2008-2009, and an increase in 2010-2020 with a maximum pick in 2014.

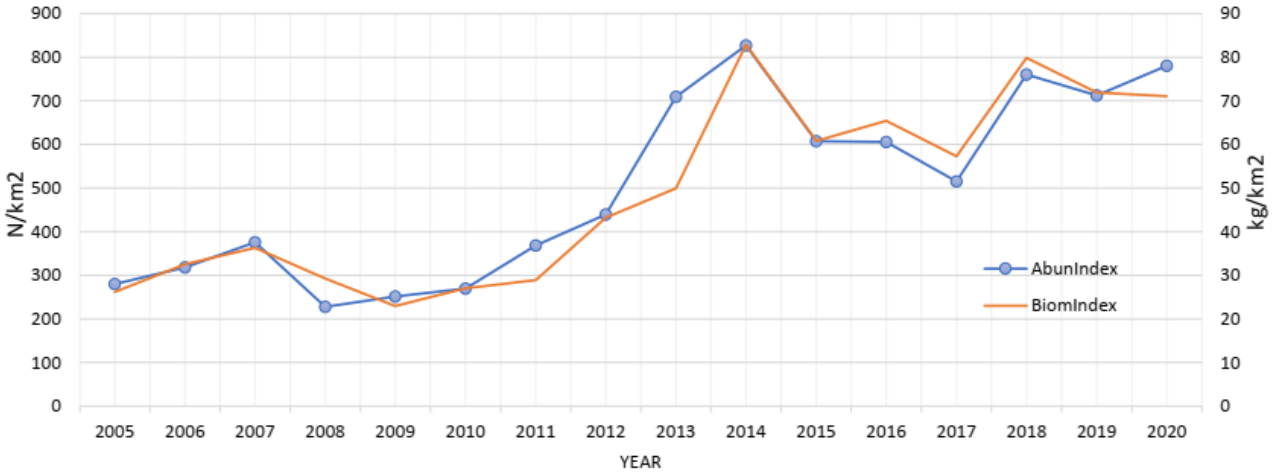

Figure 4.3.2.1.4. Abundance and biomass index of sole obtained from SoleMon surveys, 2005-2020.

Table 4.3.2.1.1. Solemon survey abundance and biomass results, 2005-2020.

Year	AbunIndex (N/km2)	AbunStDev	AbunCV	BiomIndex (kg/km2)	BiomStDev	BiomCV
2005	279.690	52.064	18.615	26.165	3.836	14.663
2006	318.273	70.138	22.037	32.544	5.506	16.919
2007	375.709	83.197	22.144	36.296	6.485	17.867
2008	227.629	41.155	18.080	29.229	5.208	17.819
2009	251.053	65.630	26.142	22.973	3.889	16.928
2010	269.536	49.490	18.361	27.027	4.027	14.899
2011	368.667	86.260	23.398	28.898	4.700	16.263
2012	439.591	73.752	16.778	43.195	5.322	12.321
2013	709.202	117.123	16.515	49.951	6.929	13.872
2014	827.245	188.386	22.773	82.874	12.717	15.345
2015	607.379	129.269	21.283	60.789	9.558	15.723
2016	605.569	70.380	11.622	65.399	6.486	9.917
2017	515.403	75.618	14.672	57.310	7.401	12.913
2018	760.500	117.654	15.471	79.661	10.506	13.188
2019	712.534	153.911	21.601	72.702	11.486	15.798
2020	780	-	-	71.09	-	-

Considering that adults concentrate in the missing hauls offshore area, also the LFD for the missing hauls has been reconstructed assuming the same proportion of 2019 survey LFD in that area (point 4,5 of Figure 4.3.2.1.5). Total LFD for the entire survey area (Figure 4.3.2.1.5 right panel) was obtain by adding the reconstructed LFDs of the missing hauls to the LFD of the hauls actually made in 2020 (point 6,7 of Figure 4.3.2.1.5). A bimodal distribution is detected. Figure 4.3.2.1.6 shows SoleMon LFD indices obtained in GSA 17 from 2006 to 2020.

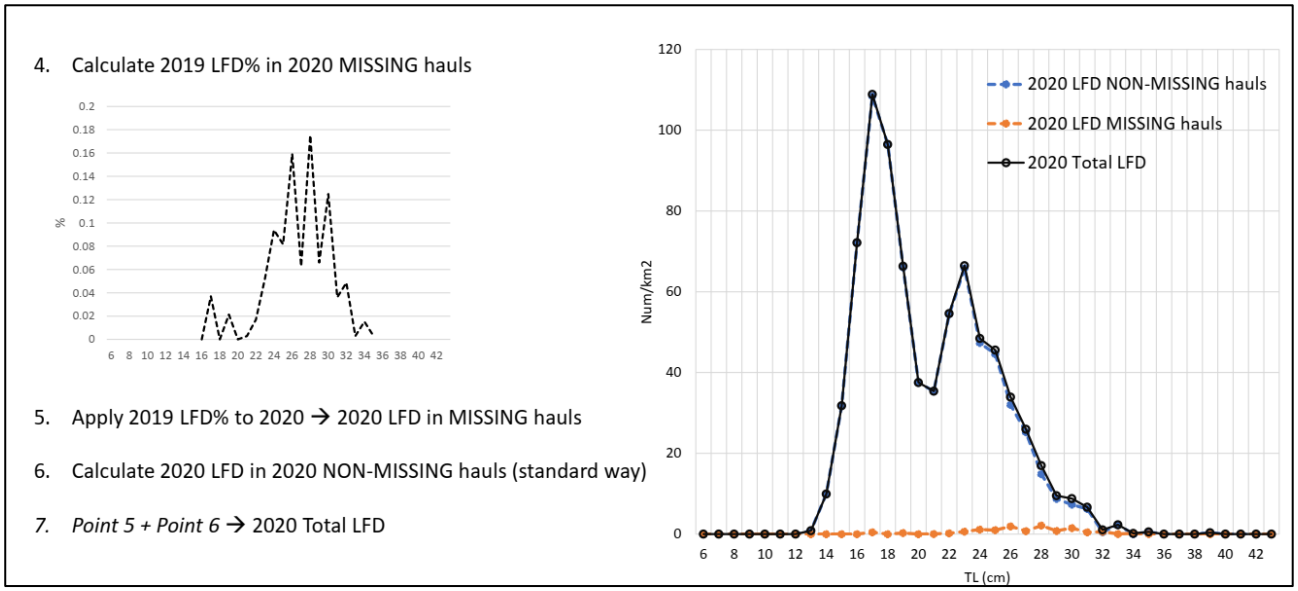

Figure 4.3.2.1.5. Solemon 2020 LFD reconstruction process.

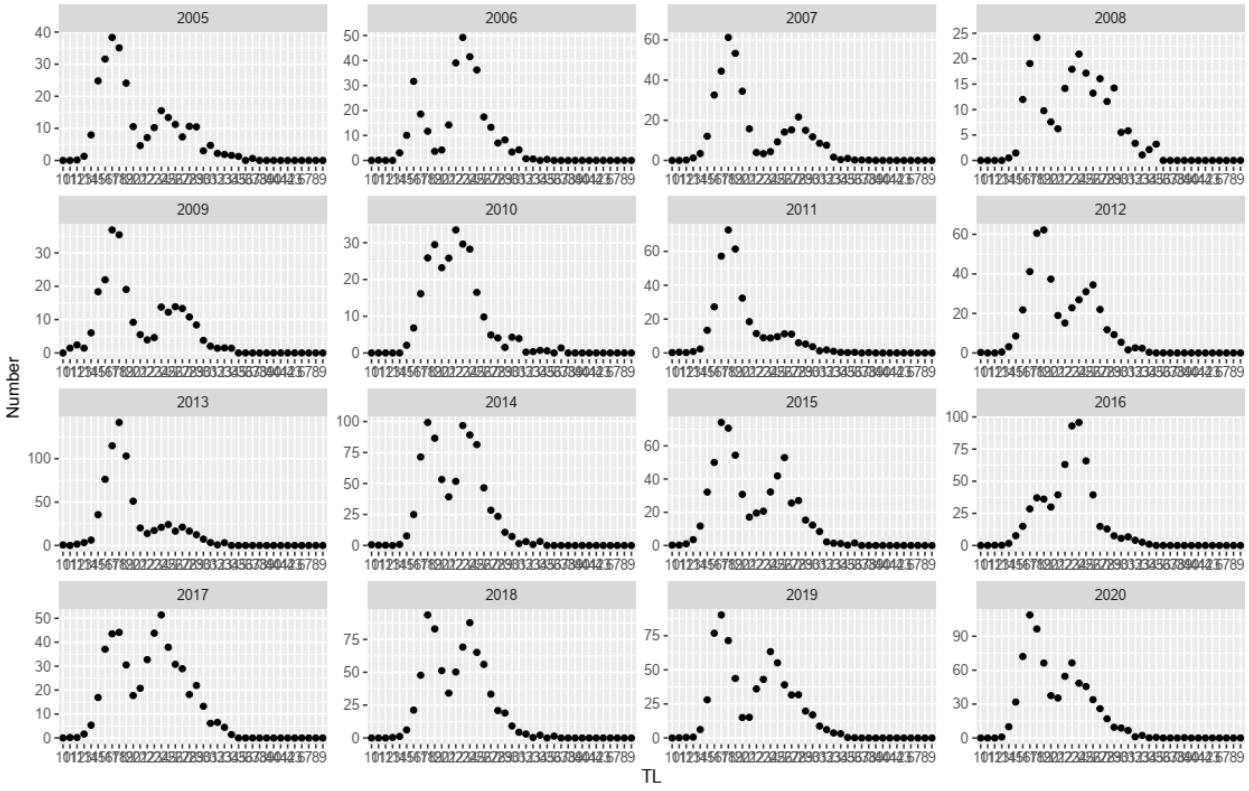

Figure 4.3.2.1.6. Solemon survey LFDs, 2005-2020.

4.4. Biology Data

4.4.1. Addressing aging issue: new analyses on otoliths and growth

In order to provide accurate estimates of von Bertalanffy growth parameters to be used in stock assessment, standardized methods for otolith preparation and validation of the rate of growth zone deposition (annuli) are essential (Gebremedhin et al., 2021). Moreover, different studies conducted in the Adriatic revealed a large variability in the growth rate of common sole: some specimens had grown 2 cm in one month, while others, of the same age group, needed a whole year (Piccinetti and Giovanardi, 1984). In this context, the FAO "*Handbook on fish age determination: a Mediterranean experience*" (Carbonara and Follesa, 2019) recommends, for bigger specimens of sole (greater than 28–30 cm TL) and for all samples for which the age determination is doubtful, a more suitable and precise otoliths reading method consisting in the transverse sectioning of the otolith (Arneri, Colella and Giannetti, 2001; Mahé et al., 2012). Within AdriaMed and FAO regional project, a study group on intercalibration of fish otolith reading (SG-OTH-SOLEA) was established. The SG-OTH-SOLEA began work in 2019 with an exchange of the margin reading (marginal analysis (MA) and marginal increment analysis (MIA)) on 439 otoliths from both sides (east and west coast) of GSA 17. The results obtained show that one transparent area and one opaque area are laid down per year in common sole in the Adriatic Sea. The transparent area is laid down between July and December, while the opaque is laid down between January and June. The MIA shows a significantly higher otolith growth in the winter and early-spring months and these results, in comparison with previous data (Froglia and Giannetti, 1986) for the Adriatic Sea, show an increase in the number months where transparent area deposition can occur (summer and early winter). This is probably due to the increase in temperature in the Adriatic in recent decades (Marasović et al., 1995; Giani et al., 2012). On the basis of these results, an ageing scheme was established. Following this, a full exchange on both sides of the Adriatic Sea was carried out on the 446 whole otoliths. The general results of the exchange are shown in Table 4.4.1.1 In terms of precision (agreement (PA) and coefficient of variation (CV)) by age group, a decreasing trend from age zero to nine is clear (Figure 4.4.1.1).

Table 4.4.1.1. General results of the exchange on whole otoliths in term of precision.

Species	Geographical area	Otoliths number	Length range (cm)	Age range (year)	Percentage of agreement	CV (%)	APE (%)
Solea solea	Adriatic west side	321	20–38	0/7	78%	34	20
	Adriatic east side	125	21.5–35	1/8	64%	29	19
	Adriatic Sea	446	20–38	0/8	74.22%	32.8	19.73

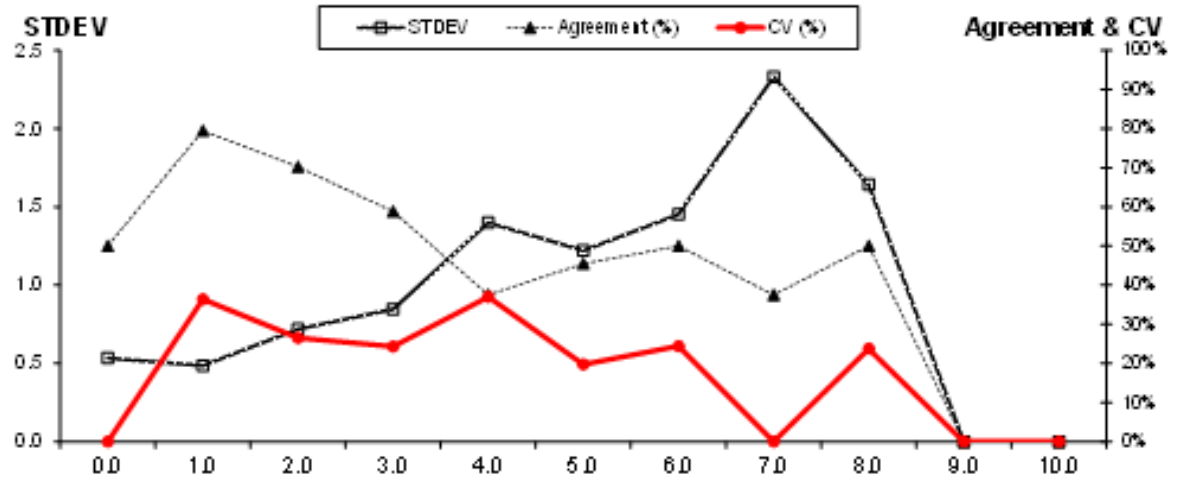

Figure 4.4.1.1. Coefficient of variation (CV), percent agreement, and standard deviation (STDEV) plotted against age group.

On basis of these results, it is clear that the overlapping of the ring in the oldest specimens may reduce the precision of the reading (Carbonara and Follesa, 2019). Therefore, an exchange was carried out to compare the precision with two otolith preparation methods: whole otolith and thin sectioned otolith. In total, 92 otoliths have been read whole and sectioned. The precision of the thin sectioned otolith is higher in terms of PA, CV and average percentage of error (APE), meaning that the section preparation method may provide age readings with higher precision (Table 4.4.1.2).

Table 4.4.1.2. General results of the exchange on whole otoliths in terms of precision.

Species	Preparations methods	Otoliths number	Length range (cm)	Modal age range (year)	Absolute age range (year)	% of agreement	CV (%)	APE (%)
Solea solea	Whole	92	20/38	0/8	0/12	64.08	30.7	20
	Thin section	92	20/38	0/9	0/12	70.55	25.93	20

However, the thin sectioned preparation method is time consuming and costly. To better understand in which length class the thin sectioned preparation method should be recommended, the difference in age assigned by length class was compared. The results showed that from 30 cm and greater in female specimens and from 26 cm and greater in male specimens, the difference in age estimations between the two preparation methods began to increase. Additionally, the percentage of samples without a difference in the age estimation between the two preparation methods began to decrease (Figure 4.4.1.2). Based on these results, the thin sectioned preparation method is recommended for the male specimens with a total length greater than 25 cm and for female specimens with a total length greater than 29 cm.

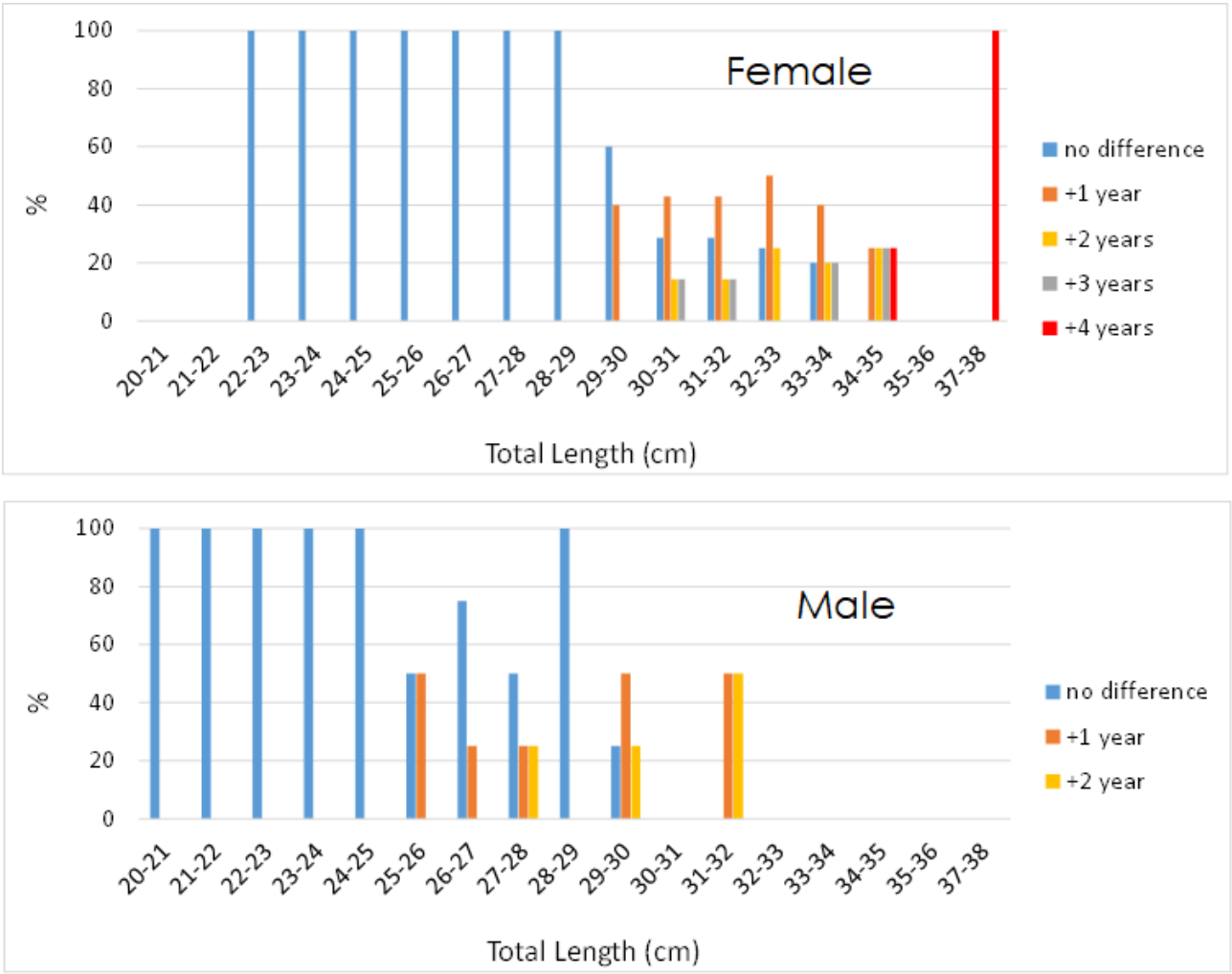

Figure 4.4.1.2. Comparison of modal age between the preparation methods (modal age for sectioned otolith vs modal age for whole otoliths).

To obtain a reading with a high rank in terms of PA, CV and APE from the sectioned otolith, the following measurements were taken: total length otolith (dorsal-ventral length) (AB), the dorsal length (OA) and the length of each ring (R1, R2… Rn) (Figure 4.4.1.3).

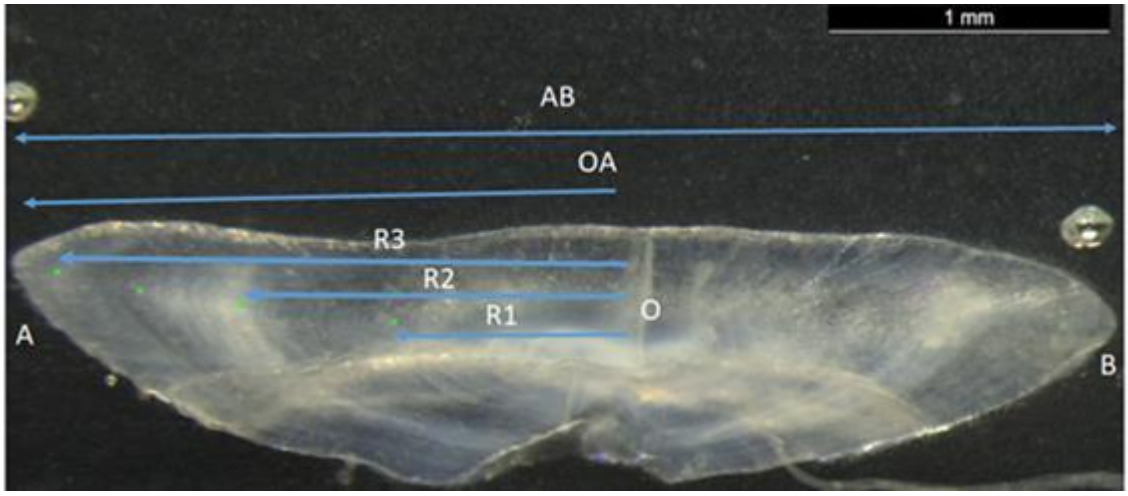

Figure 4.4.1.3. Scheme of the measurements taken on the thin section.

The relationship between AB and the total length of the fish; as well as the relationship between AB and AO are reported in Figure 4.4.1.4 and the results made it possible to apply the back calculation (Dahl-Lea model):

Eq. 1 $$L_i = \frac{R_i}{R_c} L_c$$

where *Li* is total length at *Ri*; *Lc* is length at capture; *Ri* is the dimension of the ring *i*; *Rc* is the dimension of the section (AB). In this way it was possible to obtain a new pair of data (age at length) corresponding to each annual growth increment (true ring).

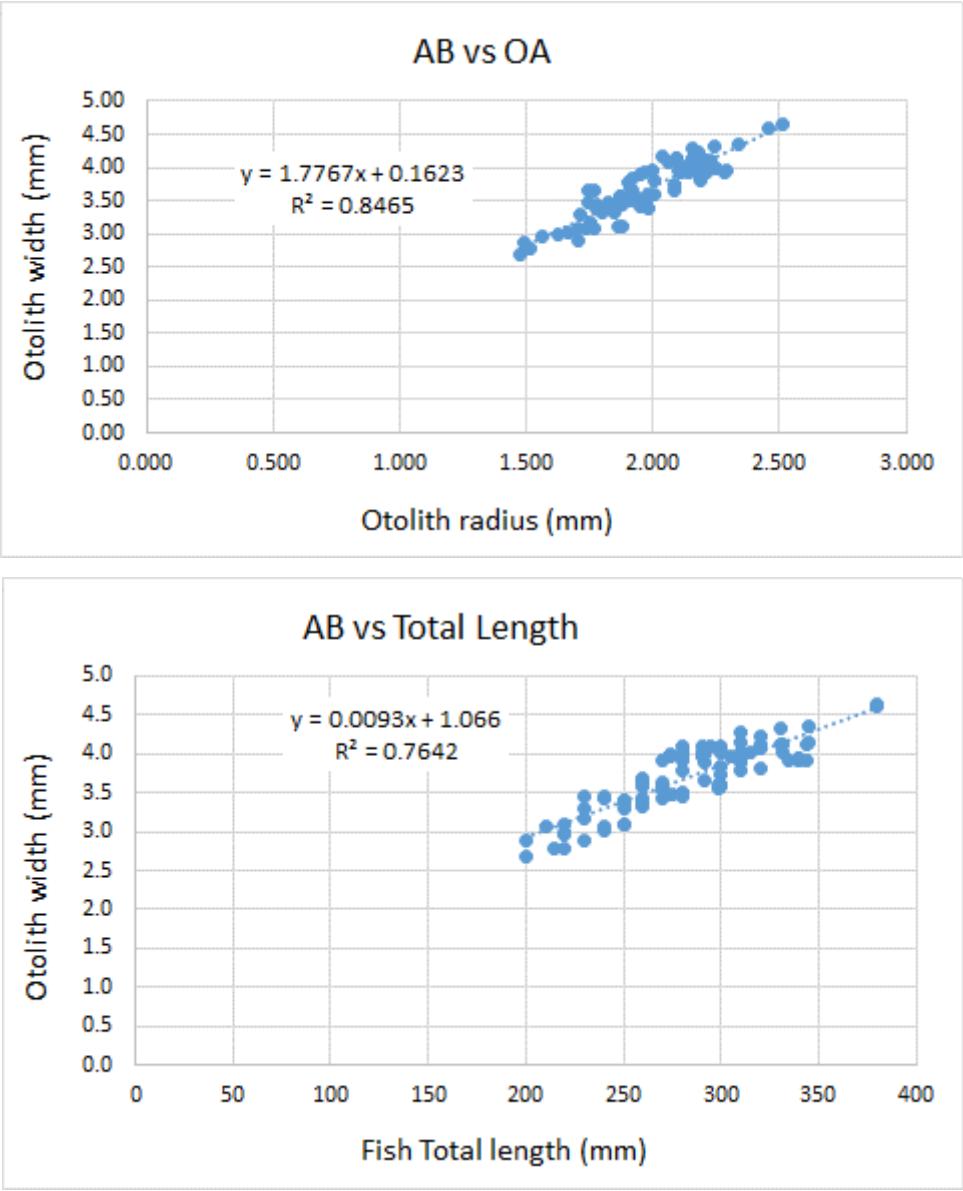

Figure 4.4.1.4. Linear relationship for otolith measurements. Upper panel: between dorsoventral otolith length and dorsal otolith length (OA); Bottom panel: dorsoventral otolith length (AB) and fish total length.

At the end of this process (whole otolith exchange, thin section exchange, back calculation exercise), modal age data for each otolith were available from both whole otoliths and thin sections. If the modal age of the same otolith was different for the two preparation methods, the thin section reading was used. Age group zero and data greater than age group four from the SoleMon survey (obtained with the same technique of the thin section exchange) was also added to the dataset. These aggregated data (Figure 4.4.1.5) were used to derive von Bertalanffy growth curve parameters for common sole in GSA 17 (Figure 4.4.1.6 and Table 4.4.1.3) by applying the non-linear least square algorithm.

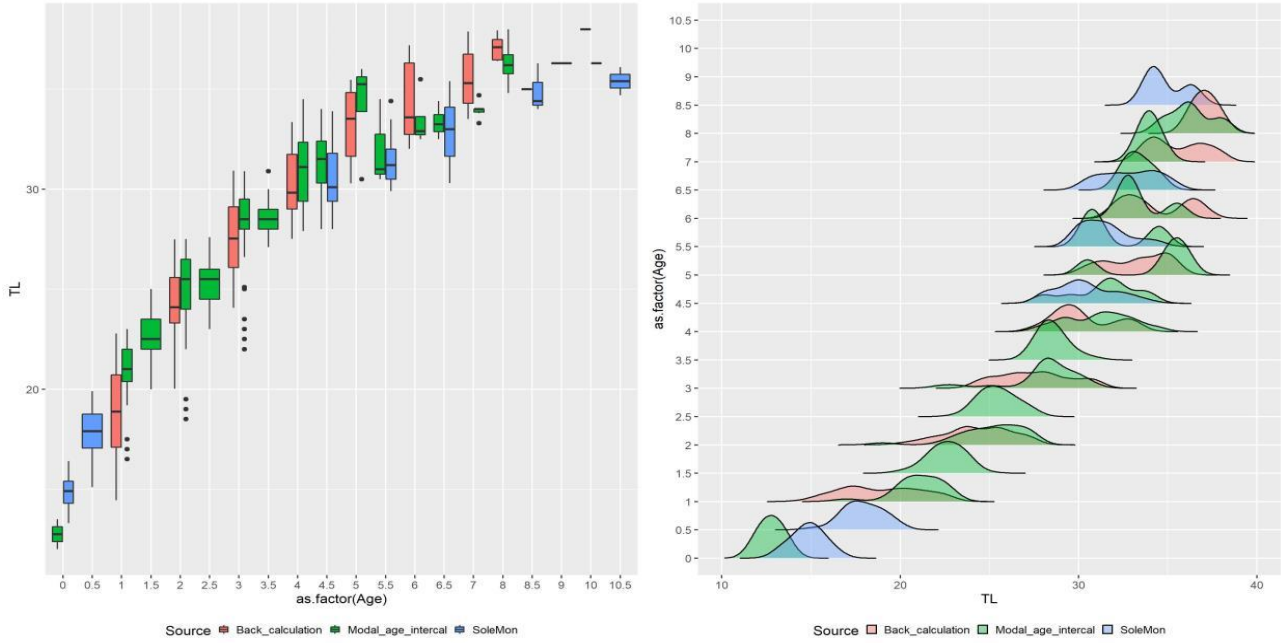

Figure 4.4.1.5. Otolith data source and distribution of age data by length.

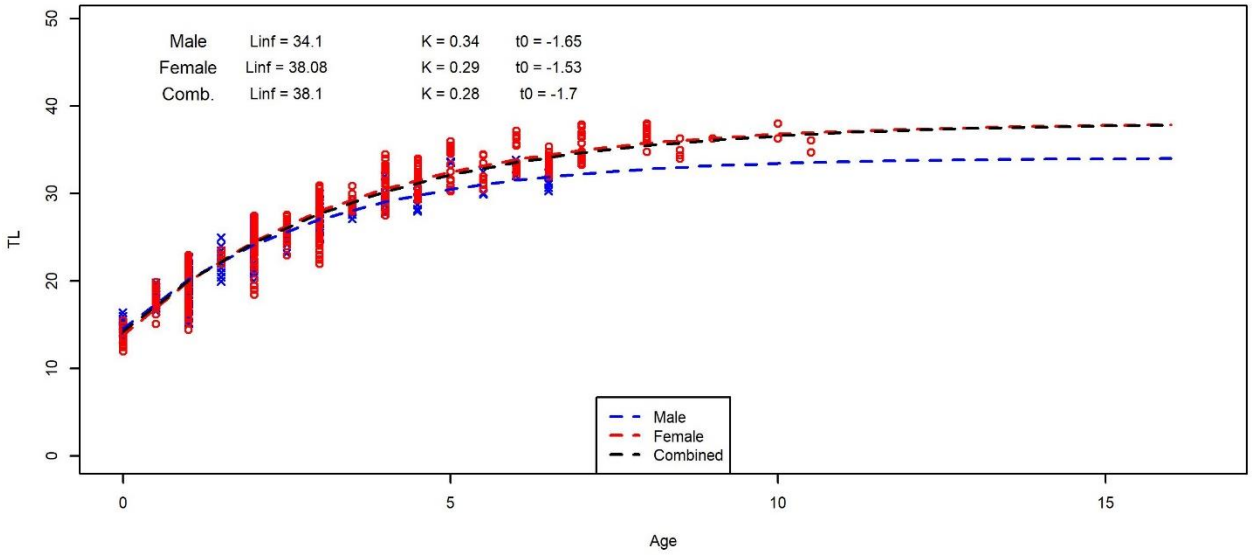

Figure 4.4.1.6. Von Bertalanffy growth curve (by sex and combined) coming from AdriaMed SG-OTH-SOLEA and related growth parameters.

Table 4.4.1.3. Growth parameters estimated from otolith readings in GSA 17.

	Males	**Females**	**Combine**
L_∞	34.1	38.08	38.1
k	0.34	0.29	0.28
t_0	-1.65	-1.53	-1.7

4.4.2. Length-weight relationship

Information on the length-weight relationship from 2007 onward are available from DCF samples and from 2005 onward from survey data (Table 4.4.2.1).

Table 4.4.2.1. Length-weight relationship parameters.

Source	Area	Time range	a	b	Sample size	Size range
DCF_ITA	GSA 17	2007–2019	0.0056	3.186	5 240	12–37 cm
DCF_HRV	GSA 17	2013–2019	0.002	3.307	-	-
SoleMon	GSA 17	2005–2020	0.0046	3.110	18 860	10–39 cm

4.4.3. Sex ratio

The male-female ratio is approximately 1:1 (Piccinetti and Giovanardi, 1984; Fabi et al., 2009).

4.4.4. Maturity

Length at first maturity (L50%) is 25.8 cm (MEDISEH, 2013); this value has been estimated using data from the SoleMon project. Females weighing 300 g have about 150 000 eggs, while those weighting 400 g have about 250 000 eggs (Piccinetti and Giovanardi, 1984).

4.4.5. Natural Mortality (M)

The natural mortality rate (M) of fish populations is one of the most important parameters for population dynamics and stock assessment models. Unfortunately, it is also one of the most difficult parameters to estimate. For this reason, a pool of methodologies has been considered. The Barefoot Ecologist's Toolbox (*http://barefootecologist.com.au/shiny_m*) has been used to derive different values of M (single M value or vector by age). This Toolbox, developed by Jason Cope, provides a straightforward method for obtaining the estimated value of M from a range of life-history based methods. In Table 4.4.5.1 and Figure 4.4.5.1 a summary of the input and output of all methods considered in the Toolbox divided by different input requirements (Input Categories). The VB parameter were taken from analyses above reported in section 4.4.1.

Table 4.4.5.1. Natural mortality from a range of life-history based methods for common sole in GSA 17

	Methods	Input Categories	Value	Reference
Vector by age	Gislason	Linf, k, length	see Figure 2.6.5.1.	*Gislason et al., 2010*
	Chen-Wat	Age, k, t0	see Figure 2.6.5.1.	*Chen and Watanabe, 1989*
Single M value	Then_nls	maximum age	0.41	*Then et al., 2015*
	Then_lm	maximum age	0.36	*Then et al., 2015*
	Hamel_Amax	maximum age	0.36	*Hamel (in press)*
	Then_VBGF	Linf, k	0.51	*Then et al., 2015*
	Jensen_VBGF 1	k	0.45	*Jensen, 1997*
	Jensen_VBGF 2	k	0.48	*Jensen, 1997*
	Roff	k, age at maturity	1.10	*Roff, 1984*
	Jensen_Amat	age at maturity	0.83	*Jensen, 1996*
	Ri_Ef_Amat	age at maturity	0.76	*Rikhter and Efanov, 1976*
	Lorenzen	wet weight	0.47	*Lorenzen, 1996*

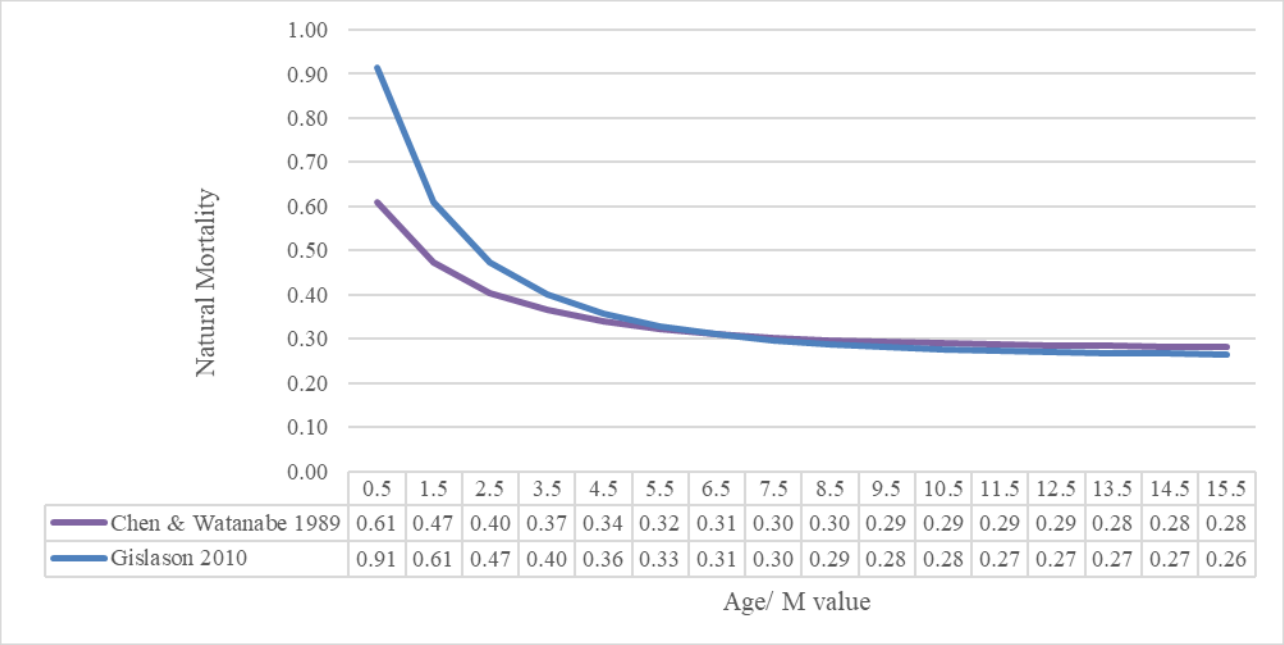

Figure 4.4.5.1. Natural mortality vectors by age for common sole in GSA 17.

4.5. Implementation of the stock assessment for common sole in GSA 17

In this chapter, the reference run and final assessment model for common sole in northern-central Adriatic Sea (GSA 17) are described. The ensemble approach is by far the biggest novelty used in this study, and its inclusion allows multiple plausible models (and parameter sets) to be tested within a single integrated framework. The model has been developed for the most part in the context of FAO-GFCM working groups of stock assessment of demersal species (WGSAD) during the

benchmark session of April 2021 (FAO-GFCM, 2021). The meeting was the first ever GFCM benchmark to use an ensemble model to provide management advice, so in that sense it was developing new approaches, methods and standards that have not been used elsewhere in GFCM to date. Moreover, the methodology, technique and the skills developed for common sole assessment, has been subsequently applied for conducting similar analysis for other stock in ICES context such as the *Pandalus borealis* in Skagerrak and Norwegian Deep area (ICES, 2022a) and *Coregonus albula* in Bothnian Gulf (Bergenius et al., 2022). Confirming the novelty and applicability of the methodology, ICES support the use of ensemble approach as a good practice to obtain more robust quantification of uncertainty when multiple solution are plausible (ICES, 2022a).

All scripts developed to support the methods described in this chapter, are available in the dedicated GitHub repository at https://github.com/framasnadi/SS3-ENSEMBLE-MODEL-scripts. Moreover, a shiny app has been developed for an easier interactive consultation of stock assessment process and results shown in the following sub-chapters (https://framasnadi.shinyapps.io/AppSOL).

4.5.1. Assessment model framework

The assessment of common sole in the Norther Adriatic Sea (GSA 17) was conducted using the Stock Synthesis (SS) model (Methot & Wetzel, 2013). Stock Synthesis is programmed in the ADMB C++ software and searches for the set of parameter values that maximizes the goodness-of-fit, then calculates the variance of these parameters using inverse Hessian and MCMC methods. Stock Synthesis 3.3 provides a statistical framework for the calibration of a population dynamics model using fishery and survey data. The model is designed to accommodate both population age and size structure data and multiple stock sub-areas can be analysed. It uses forward projection of population in the "statistical catch-at-age" (SCAA) approach. SCAA estimates initial abundance at age, recruitments, fishing mortality and selectivity. The total likelihood of SS model is composed of a number of components, including the fit to the survey and CPUE indices, tag recovery data (when tagging data are used), fishery length frequency data, age compositions and catch data. There are also contributions to the total likelihood from the recruitment deviates and priors on the individual model parameters (if any). SS model is configured to fit the catch almost exactly so the catch component of the likelihood is very small. In this assessment, fishing mortality was modelled using the hybrid method, which estimates the harvest rate using the Pope's approximation and then converts it to an approximation of the corresponding *F* (Methot & Wetzel, 2013). Option 5 was selected for the *F* report units. This option represents the last development of SS and corresponds to the fishing mortality requested by the ICES and GFCM framework (i.e. simple average of F of the age classes chosen to represent *Fbar*). Details of the formulation of the individual components of the likelihood are provided in Methot & Wetzel, 2013.

- *Why use an ensemble model?*

Stock assessment models require a number of highly influential, yet difficult to estimate parameters, many of which are commonly fixed in age-structured assessments. In reality, the actual value of these parameters is often uncertain. Therefore, assuming a specific fixed value results in making strong assumptions about stock's resilience, productivity and associated biological reference points (Maunder et al., 2021; Winker et al., 2020). This means that stock assessors are often faced with a range of model formulations which should be scrutinized before decisions are made (Mannini et al, 2021). In this context, when discussing which could be the best model used in assessing stocks, Hilborn and Walters (1992) recalled an adage that "*the truth often lies at the intersection of competing lies*". This uncertainty in 'what is the best model?' necessitates a comparison of a range of alternative models. Instead of comparing multiple model outputs and selecting a single final one, an ensemble modelling approach (Dietterich, 2000) was used to present results with a quantitative criterion for weighting several model predictions. An ensemble approach better encapsulates the variability and uncertainty of model predictions because instead of choosing a single set of fixed parameter values, can explore a contrasting but plausible range of values (Dietterich, 2000; Knutti, Tebaldi & Meehl, 2009). Ensemble models have been proven to be more accurate and less biased than the choice of an individual model, as they can effectively tease apart the conditions under which various model assumptions result in the most accurate predictions. This a promising approach when decisions have to be made despite the presence of multiple and potentially conflicting estimates of stock status (Anderson et al. 2017).

The objective when using an ensemble model is therefore to quantify the total uncertainty across all plausible models, where the structural uncertainty is likely to be much greater than the within model uncertainty. For example, ensembles are often helpful because modellers need not decide on dome versus asymptotic fisheries selectivity (e.g. Sampson & Scott, 2012), or whether to fix or estimate natural mortality (e.g. Johnson et al., 2015).

4.5.1.1. Parameters levels

Ensemble approach is capable of representing all the possible "states of nature" of the stock under analysis based on a number of sources of natural and fisheries uncertainty. In this study, major uncertainly was linked to alternative hypothesis of selectivity which has a large influence on the assessment. Other alternative hypothesis are based on different levels of natural mortality (M) and steepness (h). The final model grid for the ensemble included all combinations of alternative values for these three nested parameters, as listed in Table 4.5.1.1.1. A schematic graphical representation of the assessment workflow is provided in Figure 4.5.1.1.1. Its inclusion is designed to provide a

guideline via which the process of ensemble model grid construction can be followed as well as the steps taken prior to its implementation.

Table 4.5.1.1.1. Parameter and levels employed in the final ensemble grid for common sole in GSA 17 SS3 assessment.

Parameter	Levels	Progressive number of runs	Values
Selectivity (survey)	2	2	double normal (DN); cubic splines (CS)
Natural Mortality (*M*)	3	6	Average of Gislason & ChenWatanabe; Average of Then_nls,Then_lm,Hamel_Amax; Average of Then_VBGF, Jensen_VBGF 1, Jensen_VBGF 2
Steepness of the stock-recruitment relationship (*h*)	3	18	0.7; 0.8; 0.9

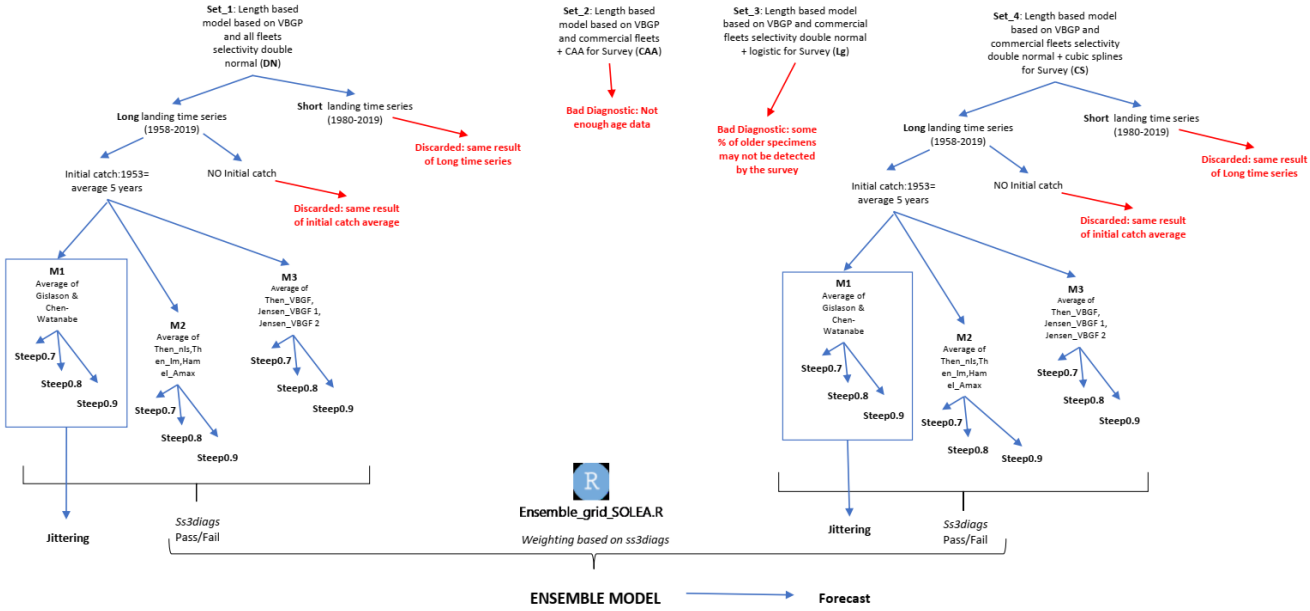

Figure 4.5.1.1.1. Schematic graphical representation of the assessment workflow for common sole assessment in GSA17.

The baseline configuration of all SS model runs is one-area yearly model where the population is comprised of 15+ age-classes with sexes combined (males and females are considered together). The final selected runs here presented are length-based models where the numbers at length in the fisheries and survey data are converted into ages using von Bertalanffy growth parameters presented in 4.4.1 section. The last age-class (i.e. 15+) represents a "plus group" in which mortality and other characteristics are assumed to be constant.

The following sections will be referring in general to all the runs present in the final grid. When necessary, the various aspects related to the different assumptions on the variables (selectivity, *M* and *h*) will be highlighted.

4.5.2. Input data and model setting

4.5.2.1. Fishery dependent and fishery independent input data

All models start in 1958 and the initial population age structure was assumed not to be in an unexploited equilibrium state, so that the initial fishing mortality was estimated for all fleets in the model. Initial catches were assumed as the average of the previous years (1953–1957; Fortibuoni e t al. 2017). The SS3 analyses has been carried out considering the following five fleets and (Figure 4.5.2.1.1):

1. Italian gill netters (GNS ITA);
2. Italian *rapido* trawler (TBB ITA);
3. Croatian set netters (GTR HRV).
4. Italian otter trawler (OTB ITA);
5. Croatian *rampon* fishery (DRB HRV)

All Stock Synthesis models used in the final grid are size structure data model based on the separate fleet LFD from 2006 to 2020. Size are then converted to age inside the model using von Bertalanffy growth equation. Tuning data were provided by SoleMon surveys, carried out in fall for the years 2005-2020. More details on fishery dependent and fishery independent data can be found in section 4.2 and 4.3.

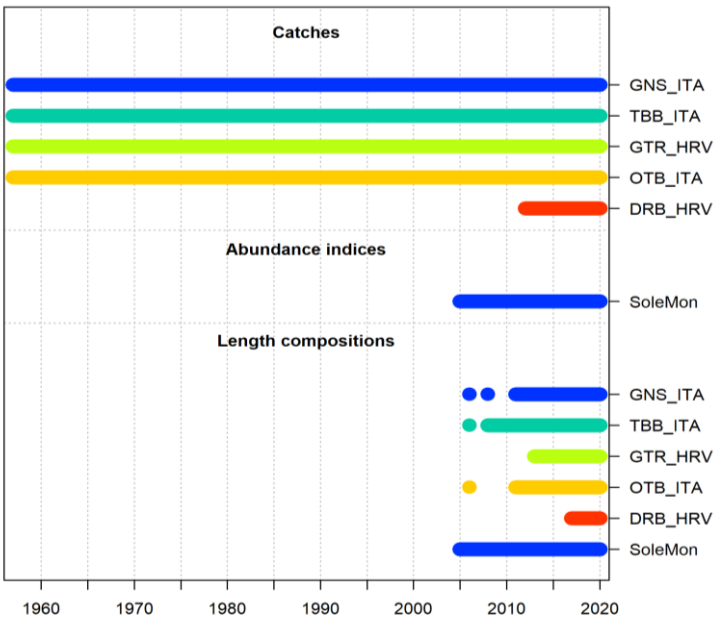

Figure 4.5.2.1.1. Data presence by year for each fleet and data type.

For the commercial fleets, the coefficient of variation (CV) of the catches was set to 0.1 for the historical part of the timeseries (until 1980), then 0.05. The CV of the initial catches of the commercial fleets was also set to 0.1. The choice for a higher CV for the historical part of the timeseries is due to the different sources of landings that may be affected by the underlying monitoring programs, and lead to higher catch-derived uncertainty in the past. The annual sample size associated with the LFD data is reported as the number of trips sampled for commercial catches (as reported from national sources) and the number of hauls for the surveys. CV in 2020 reconstructed survey index has been set by default to 0.15. No weighting of the LFDs was used in the model.

4.5.2.2. Growth and maturation

The von Bertalanffy growth parameters seen in section 4.4.1 has been used as input parameters in the SS3 model. The very fast growth in the first year of age does not allow to have a good estimate of *t0* using these data. True age 0 data are not available. Given the ecology of sole in the Adriatic, juveniles are widespread in coastal shallow water, lagoons or brackish waters, making impossible to capture these specimens both with commercial fishing gear or SoleMon survey. Even the smallest specimens captured during the survey are still to be considered at least 5-6 months old. This problem can be bypassed thank to the SS3 modeling platform because the SS growth model does not directly depend on *t0*. More precisely, when fish recruit at the real age of 0.0 at settlement, they have body size equal to the lower edge of the first population size bin. The fish then grow linearly until they reach a real age equal to the input value *growth-at-age for L1* and have a size equal to the parameter value for L1 (the minimum length parameter). As they age further, they grow according the selected growth equation. The SS3 deverived growth curve is showned in Figure 4.5.2.2.1. Reference length value for *growth-at-age for L1* equal to 0.5 (recruits at the half of the year) has been estimated by using a random walk for the period 2005-2020 around the average value of SoleMon age 0 data (17.5 cm).

The variance in length-at-age was fixed for older and younger individuals (Table 4.5.2.6.1) allowing the fitting for bigger specimens present in the commercial catches LFDs. Length-weight relationship and L50% values comes from survey data (Figure 4.5.2.2.1).

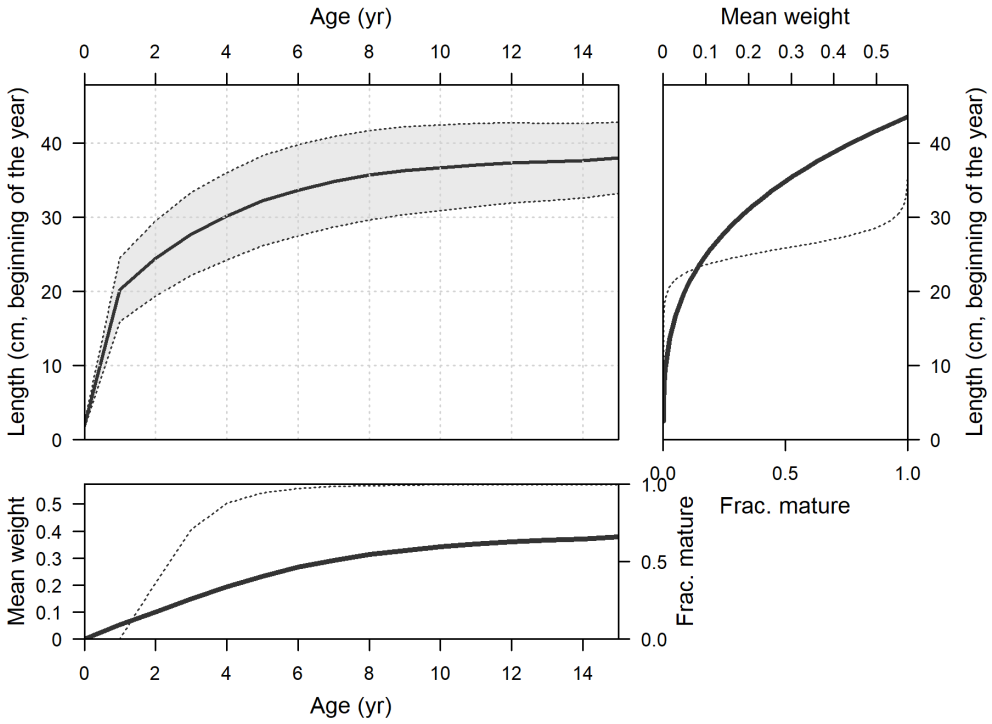

Figure 4.5.2.2.1. Growth and maturation for common sole in GSA17: length at age (top-left panel) with weight (thick line) and maturity (thin line) shown in the top-right panel and in the lower-left panel.

4.5.2.3. Selectivity patterns

In all the grid runs, fishery selectivity is assumed to be length-specific and time-invariant. Selectivity represents the probability that a fish of a particular length or age will be caught by the fishery. This is a combination of gear selection (e.g., the size of the hook or the width of mesh in a net) and availability (are fish of that age in the area being fished). In SS these components are not separate and instead modeled as a single probability. The selected proportions at age generally increase from young ages to older ages, but may also decline at the oldest ages. This is referred to as dome shaped selectivity and may occur because older fish move out of the fishing area and become less available to the fishery, older fish may be able to avoid or escape the fishing gear, etc. This type of selectivity can affect biomass estimation by producing a kind of cryptic biomass phenomenon.

Some evidences in the spatial distribution of the fishing fleet and of the species (Figure 4.5.2.3.1.), suggest a dome shape selectivity for all the fleets present in GSA17. In particular, the offshore area southward of Istria peninsula, an important spawning area for sole, is poorly exploited by trawlers (both otter and *rapido*) mainly due to the high concentrations of debris and benthic communities that are dominated by holothurians (Despalatović et al., 2009; Santelli et al., 2017). Moreover, survey age

data coming from otoliths sectioning show older specimen (already from age 4) gathering in this central area of the Adriatic Sea, with a greater chance of escaping fishing activities. Link to that, Adriatic sole stock shows higher resilience argued to be linked to high exploitation of juveniles but lower adult mortality because of these offshore spawning refuges (Scarcella et al. 2014). These considerations are important to justify the population selectivity curves used in the SS3 model but the scale of this phenomenon is not yet completely clear and it is difficult to understand how much it can affect the final selectivity shape.

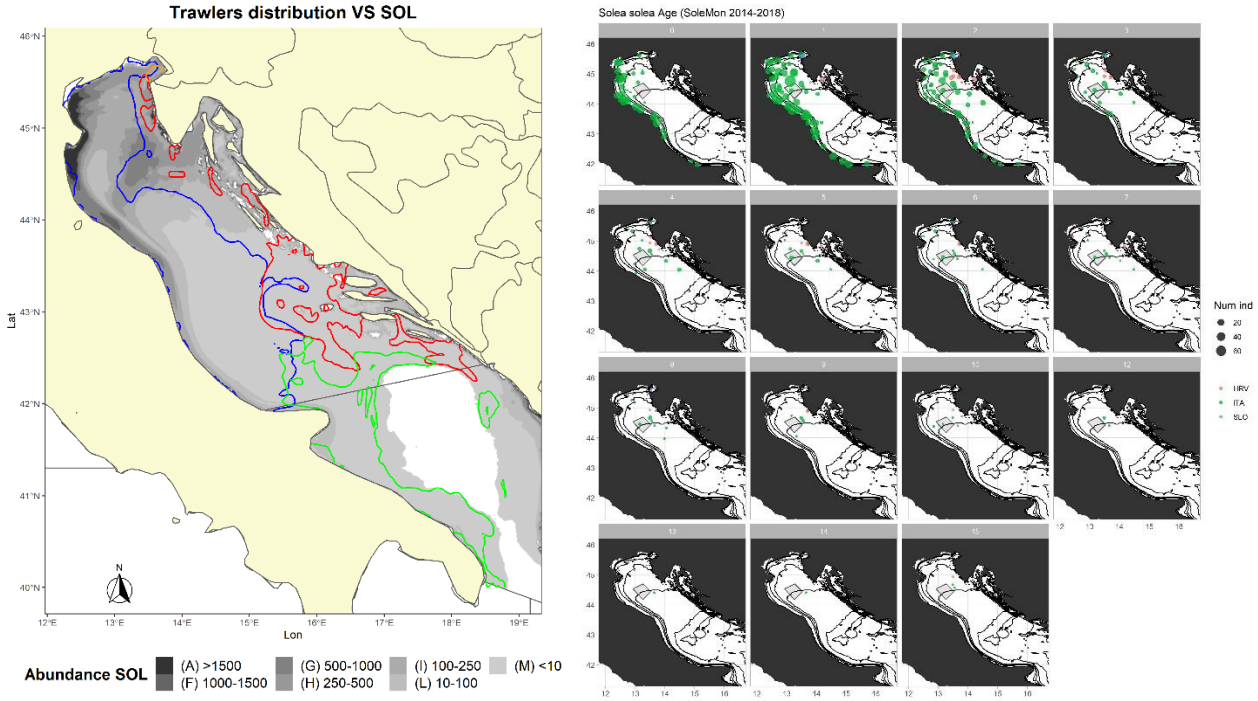

Figure 4.5.2.3.1. Spatial distribution of fishing fleet (transit of fishing boat, referred to the year 2017) on abundance (n individuals/km2) of Solea solea predicted with SoleMon data (2009-2017) (left side); Spatial distribution of common sole specimens by age from SoleMon data (2014-2018) (right side).

Several alternative assumptions for selectivity were discussed and examined, some alternative runs were tested but discarded after extensive diagnostics (e.g. red branches in figure 4.5.1.1.1). Finally, following a precautionary approach, ensemble modeling approaches were used to stitch two parallel configurations for selectivity that reflected two plausible scales of the phenomenon:

- DN) full double normal selectivity for all fleet (commercial and survey). For all the fleets, the selectivity was estimated by the model using a double normal function which estimates the peak, the ascending and the descending values of the selection curve. Figure 4.5.2.3.2.a represent length-based selectivity and derived age-based selectivity by the baseline DN model with steepness equal to 0.9 and M1, the parameters values of the other DN runs can be found in the summary Table 4.5.2.6.1;

- CS) cubic spline for survey selectivity. This specific selectivity pattern allows a better fitting to the bimodal distribution of survey LFDs (Figure 4.3.2.1.6; first mode juveniles, second mode adults). Figure 4.5.2.3.2.b represent length-based selectivity and derived age-based selectivity by the baseline CS model with steepness equal to 0.9 and M1, the parameters values of the other CS runs can be found in the summary Table 4.5.2.6.1. Note that changing the survey selectivity also has an effect on the shape of the other fleet normal double sel parameters which are left free to be estimated by the model.

Final derived age-based selectivities show that the biggest difference in the two selectivity patterns is the probability of fishing older specimens (approximately from age 4-5 onwards) for TBB ITA, GTR HRV and the survey.

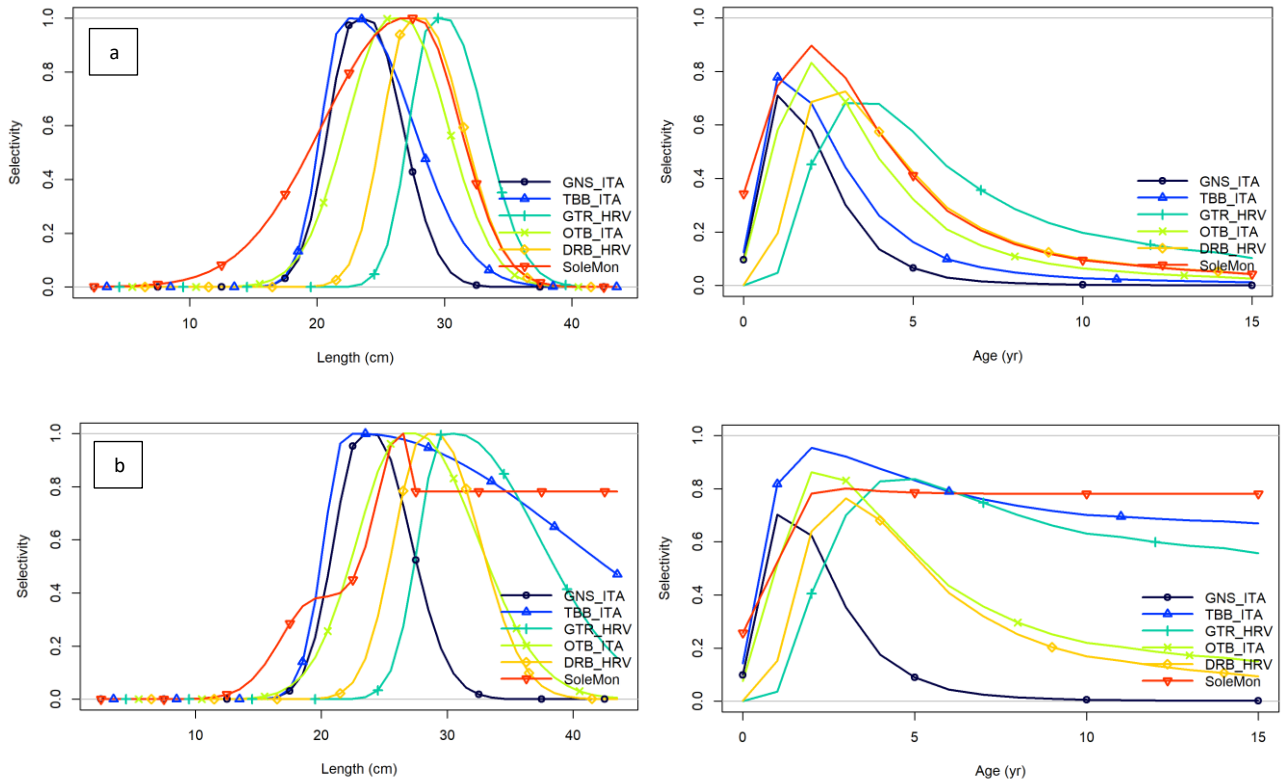

Figure 4.5.2.3.2. a) Baseline DN model: length-based selectivity by fleet estimated by the model (left side); age-based selectivity by fleet derived by the model (right side). b) Baseline CS model: length-based selectivity by fleet estimated by the model (left side); age-based selectivity by fleet derived by the model (right side).

4.5.2.4. Natural mortality

As previously mentioned, alternative hypotheses are reasonable given that M is considered one of the most difficult to estimate, yet most influential parameters in stock assessment (Mannini et al, 2021). Three final more plausible set of *M*'s has been selected from methods exposed in section 4.4.5 to represent structural uncertainty around natural mortality based on different life-history input requirement (Figure 4.5.2.4.1; Table 4.5.2.4.1):

- M1 configuration is based on average values of Gislason et al. (2010) & Chen-Watanabe (1989) vectors by age:
- M2 configuration is based on average values of Then_nls, Then_lm, Hamel_Amax (Then et al., 2015; Hamel, 2015);
- M3 configuration is based on average values of Then_VBGF, Jensen_VBGF 1, Jensen_VBGF 2 (Jensen, 1996; Jensen, 1997; Then et al., 2015).

M2 and M3 values are taken as value at maximum age (Age 15) and scaled by the body size-at-age of the fish with Lorenzen option within SS3.

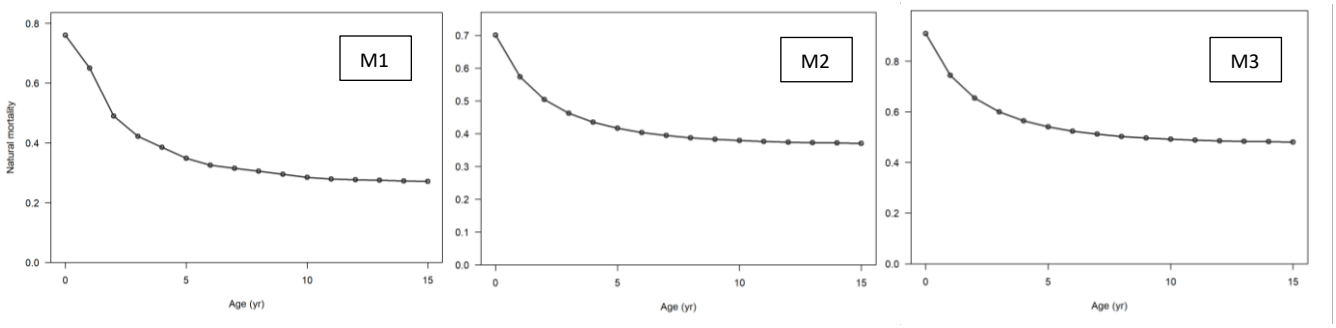

Figure 4.5.2.4.1. Age-specific natural mortality assumed for the three different model configurations: M1,M2,M3.

Table 4.5.2.4.1. Age-specific natural mortality value assumed for the three different model configurations: M1,M2, M3.

Age	0	1	2	3	4	5	6	7	8	9	10	11	12	13	14	15
M1	0.76	0.65	0.49	0.42	0.39	0.35	0.33	0.32	0.31	0.30	0.29	0.28	0.28	0.28	0.27	0.27
M2	0.70	0.57	0.50	0.46	0.44	0.42	0.40	0.39	0.39	0.38	0.38	0.38	0.37	0.37	0.37	0.37
M3	0.91	0.74	0.65	0.60	0.56	0.54	0.52	0.51	0.50	0.50	0.49	0.49	0.49	0.48	0.48	0.48

4.5.2.5. Recruitment

Recruitment (i.e. settlement) presents one peak in fall. It was assumed that recruitment event occurs at the beginning of the year. Spawning biomass was estimated at the beginning of the year. Recruitment was derived from a standard Beverton and Holt stock recruitment relationship (SRR) and the variation in recruitment was estimated as deviations from the SRR. Recruitment deviations were estimated for 2005 to 2020 (16 annual deviations). Recruitment deviations were assumed to have a standard deviation (σR) of 0.5.

Steepness (h) is a parameter noting the percentage of unfished equilibrium recruitment (R0) that occurs when the female spawning biomass is 20% of unfished equilibrium female spawning biomass. Steepness is typically fixed because accurate estimation requires long time series of data informative of recruitment at low biomass levels and variability in recruitment often reduces the information content. Initial reference model assumed a level of steepness (h) of 0.9. This value is in line with

literary knowledge, in particular flatfishes are suspected to demonstrate high steepness (h > 0.8 for Iles 1994, Myers et al. 1999; close to 1 for Maunder 2012). Likelihood profile analysis was appropriate to select *h* and σ*R* (Figure 4.5.2.5.1), however, more lower values comparable to the life history have been examined and added to the grid to explore different effect on production function. Final *h* values tested are: 0.7, 0.8 and 0.9 (Table 4.5.2.6.1).

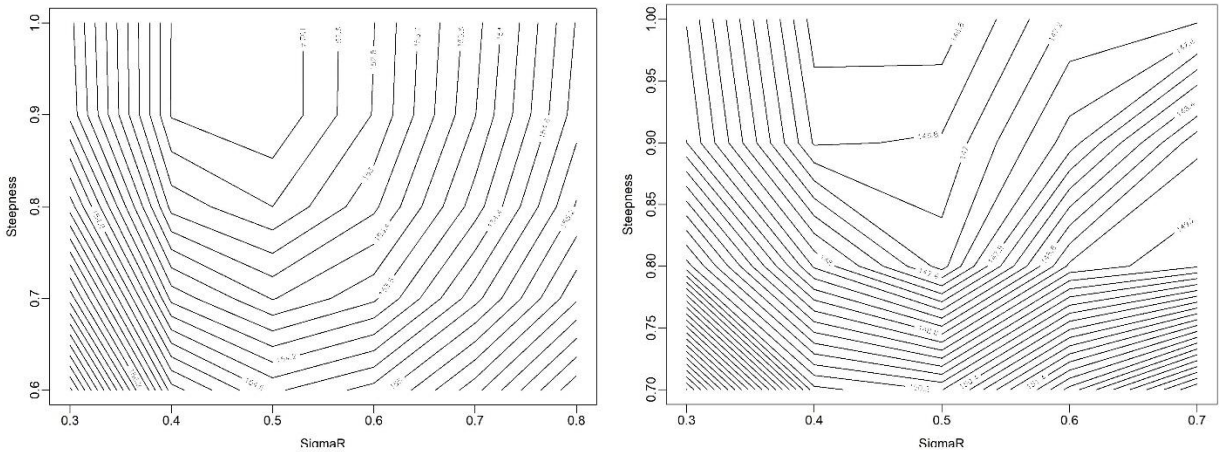

Figure 4.5.2.5.1. Two-dimensional likelihood profile for h and σR: e.g. run_DN_M3 (left side) and run_CS_M3 (right side).

4.5.2.6. Final configurations and settings

To summarise, in table 4.5.2.6.1 is reported the configuration of the models considering the different alternative hypothesis.

Table 4.5.2.6.1. Configurations and settings of SS3 models. The table columns show: initial value, the intervals allowed for the parameters and the estimation phase. Parameters in bold are set and not estimated by the models.

Parameter	Initial value	Bounds (low,high)	Phase
Natural mortality (age classes 0-15)	***M1*; *M2*; *M3***		
Stock and recruitment			
Ln(R0)	12.7	(3, 30)	1
Steepness (h)	**0.7; 0.8; 0.9**		
Recruitment variability (σR)	**0.5**		
Recruitment autocorrelation	**0**		
Growth			
Linf (cm)	**38.1**		
k	**0.28**		
L at minimum age t0	**17.5**		
CV of young individuals	**0.11**		

CV of old individuals	**0.065**		
Weight (kg) at length (cm)			
a	**0.0000046**		
b	**3.11**		
Maturity			
Length (cm) at 50% mature	**25.8**		
Slope of the length at maturity ogive	**-0.7**		
Initial fishing mortality			
ITA GNS	0.1	(0, 1.5)	1
ITA TBB	0.1	(0, 1.5)	1
HRV GTR	0.1	(0, 1.5)	1
ITA OTB	0.1	(0, 1.5)	1
Selectivity DN (double normal)			
ITA GNS			
Peak	21	(6, 41)	3
Asc-width	2.3	(-4, 12)	4
Desc-width	2.8	(-2, 6)	4
ITA TBB			
Peak	21	(6, 41)	3
Asc-width	1.3	(-10, 12)	4
Desc-width	2.8	(-2, 12)	4
HRV GTR			
Peak	29	(6, 41)	3
Asc-width	1.3	(-4, 12)	4
Desc-width	1.8	(-2, 6)	4
ITA OTB			
Peak	23.5	(6, 41)	3
Asc-width	3.3	(-10, 12)	4
Desc-width	2.8	(-2, 6)	4
HRV DRB			
Peak	21.5	(6, 41)	3
Asc-width	1.3	(-4, 12)	4
Desc-width	2.8	(-2, 6)	4
Solemon Survey			
Peak	21	(6, 41)	3
Asc-width	3.3	(-10, 12)	4
Desc-width	2.8	(-2, 6)	4
Selectivity CS (cubic splines)			
Solemon Survey			
Gradient at first node	**0.77**		
Gradient at last node	-0.78	(-1, 0.001)	3
Node 1	**13**		
Node 2	**18.5**		
Node 3	**22.5**		
Node 4	**26.5**		
Sel Node 1	**0.35**		
Sel Node 2	2.95	(-15, 7)	4
Sel Node 3	3.2	(-15, 7)	4
Sel Node 4	4	(-15, 7)	4

Catchability			
Solomen Survey			
Ln(Q) – catchability	**-2.81 (floated)**		

4.5.3. Model Diagnostics

Diagnostic tests are important in determining the robustness of estimates for management advice in integrated stock assessment models. There is little guidance and few objective criteria to determine how to best summarize the results of integrated assessment models, determine if the model fits the data adequately and if the model is well specified (Carvalho et al., 2017). Moreover, it is very difficult to easily evaluate convergence or identify problematic areas given the large number of estimable parameters in these assessments. However, selection of diagnostics (i.e., a diagnostic toolbox) is recommended to increase the ability to detect model misspecification while acknowledging that the use of multiple diagnostics may increase the probability that a diagnostic test results in a false positive. In this context, the recent "Cookbook" by Carvalho et al. 2021 provides a conceptual flow chart that lays out a generic process of model development and selection using model diagnostics. The cookbook, propose a series of interconnected diagnostic tests that should be carried out to establish a base model (Carvalho et al., 2017) or an ensemble of candidate models (Maunder et al., 2020). The procedure is based on the following four properties as objective criteria for evaluating the plausibility of a model: model convergence and stability (presented in section 4.5.3.1), fit to the data (presented in section 4.5.3.2), model consistency (presented in section 4.5.3.3), and prediction skill (presented in section 4.5.3.4). The R package *ss3diags* (github.com/JABBAmodel/ss3diags) has been used to produce all the diagnostic plots presented in this study.

In order to make the reading as effective as possible and since there are no big differences in the final outputs, the diagnostics plots presented and discussed in the following sections refer mostly to the baseline model based on the DN selectivity pattern.

4.5.3.1. Model convergence and stability

Model convergence should be assessed using several considerations. Convergence diagnostics include: checking for parameters estimated at a bound (can indicate problems with data or the assumed model structure); checking that the final gradient (must be relatively small); checking that the Hessian matrix (i.e., the matrix of second derivatives of the log-likelihood concerning the parameters, from which the asymptotic standard error of the parameter estimates is derived) is positive definite (must be relatively small).

The final gradient of all model runs was relatively small (e.g., < 1.00E-04), and the Hessian matrix for the parameter estimates was positive definite. Examination of parameter estimates indicated that no estimated parameters were near the bounds (Table 4.5.3.1.1).

Table 4.5.3.1.1. Convergence table showing the result for the 18 runs.

Name	Selectivity	Natural Mortality	Steepness	Final convergence	Par. near bound	Positive Hessian
run1	DN	M1	0.9	< 0.0001	No	Yes
run2	DN	M1	0.7	< 0.0001	No	Yes
run3	DN	M1	0.8	< 0.0001	No	Yes
run4	DN	M2	0.9	< 0.0001	No	Yes
run5	DN	M2	0.7	< 0.0001	No	Yes
run6	DN	M2	0.8	< 0.0001	No	Yes
run7	DN	M3	0.9	< 0.0001	No	Yes
run8	DN	M3	0.7	< 0.0001	No	Yes
run9	DN	M3	0.8	< 0.0001	No	Yes
run10	CS	M1	0.9	< 0.0001	No	Yes
run11	CS	M1	0.7	< 0.0001	No	Yes
run12	CS	M1	0.8	< 0.0001	No	Yes
run13	CS	M2	0.9	< 0.0001	No	Yes
run14	CS	M2	0.7	< 0.0001	No	Yes
run15	CS	M2	0.8	< 0.0001	No	Yes
run16	CS	M3	0.9	< 0.0001	No	Yes
run17	CS	M3	0.7	< 0.0001	No	Yes
run18	CS	M3	0.8	< 0.0001	No	Yes

The jitter procedure allows to verify the stability of the model examining the effect of varying the starting values of the model estimated parameters on model results. An accurate model should converge on a global solution across a reasonable range of starting values input parameters. In this

case, 200 runs were performed considering a 10 percent of jitter of the initial parameters, which means that a small random jitter is added to the initial parameter values. Starting values are jittered based on a normal distribution based on the pr(PMIN) = 0.1% and the pr(PMAX) = 99.9%.

Jittering analysis was applied only on the baseline model DN. In fact, it would not have made sense to apply jittering also to runs with different *M* and *h* in which these values are fixed. All of the 200 jitter iterations converged, with 136 model runs at the total negative likelihood estimate value of the base case model run ± one unit (161-162 likelihood units), and 64 model runs had larger total negative likelihood values (Figure 4.5.3.1.1). Given that all converged model runs implemented within the jitter test resulted in total likelihood values equal to or greater than the baseline models, the jitter test did not provide evidence to reject the hypothesis that model parameter optimization converged to the global solution.

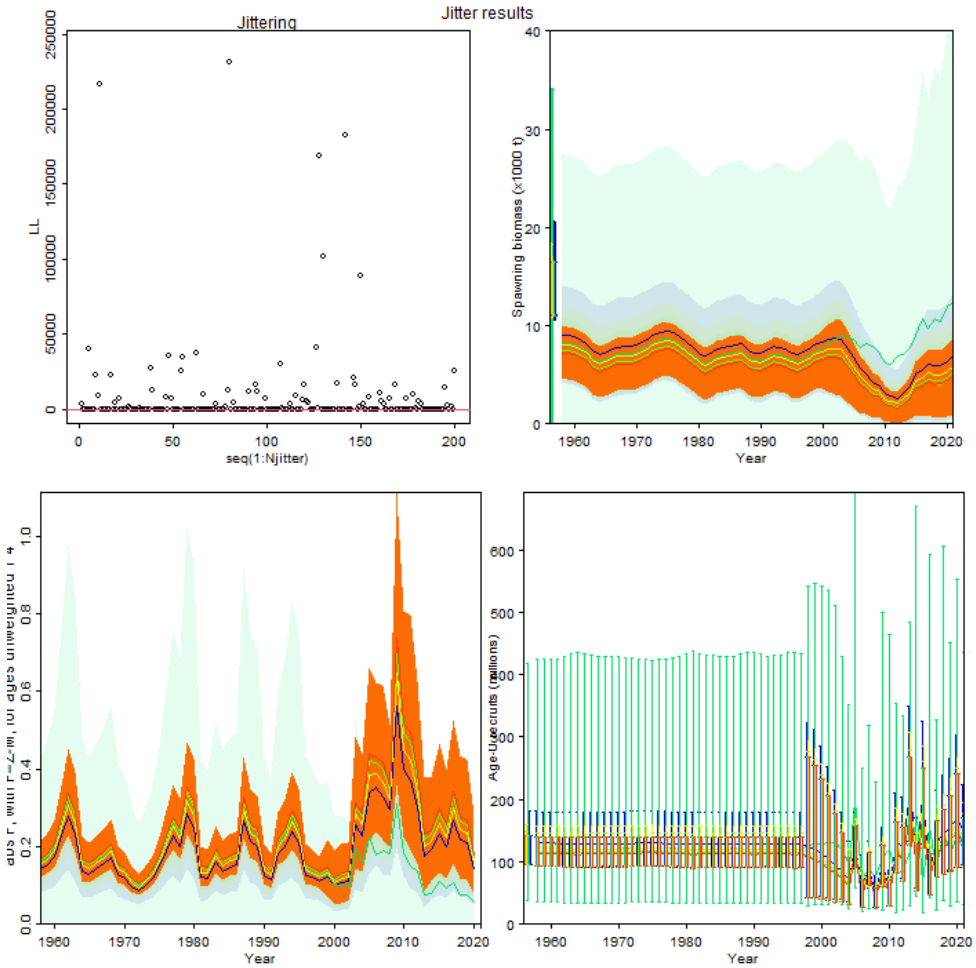

Figure 4.5.3.1.1. Results from jittering for DN baseline model using 200 iterations and an average jitter of 10%.

4.5.3.2. Goodness-of-fit

Systematic misfit to data should be considered a sign of model misspecification. Plotting residuals is a simple method to observe trends, patterns, and variations in data fit over time (e.g., bias, drift, skewness, heavy tails, correlation with states or driving inputs, and heteroscedasticity). The "Cookbook" (Carvalho et al., 2021) introduced joint residual plot that incorporates several features: lognormal residuals of abundance indices and mean-length color-coded by fleet with combined RMSE; boxplots indicating the median and quantiles of all residuals available for any given year, with the area of each box indicating the strength of the discrepancy between values (larger boxes indicate a higher degree of conflicting information); and a loess smoother through all residuals, which highlights systematically auto-correlated residual patterns. To evaluate the overall model fit of the relative abundance indices and composition data, the joint-index residual plot was applied to the residuals from the fits to indices and mean length (Figure 4.5.3.2.1). Overall, the joint-residual plot indicated a good fit to the data with the RMSE (root mean square error) less than 30 %.

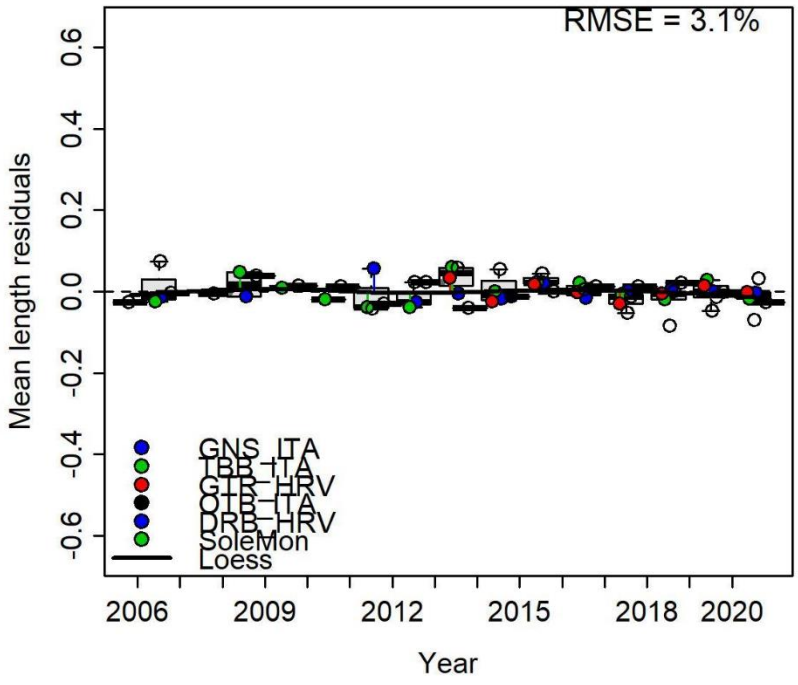

Figure 4.5.3.2.1. Joint-residual plots for the mean length for baseline run. RMSE value (in %) are printed at the top of the panels.

Runs tests in Figure 4.5.3.2.2 denote passing (green) and failing (red) residual as judged by the p-values computed for each series (Carvalho et al., 2017), applied to abundance index and mean-length residuals. Overall, there was no evidence ($p \geq 0.05$) to reject the hypothesis of randomly distributed residuals in the models.

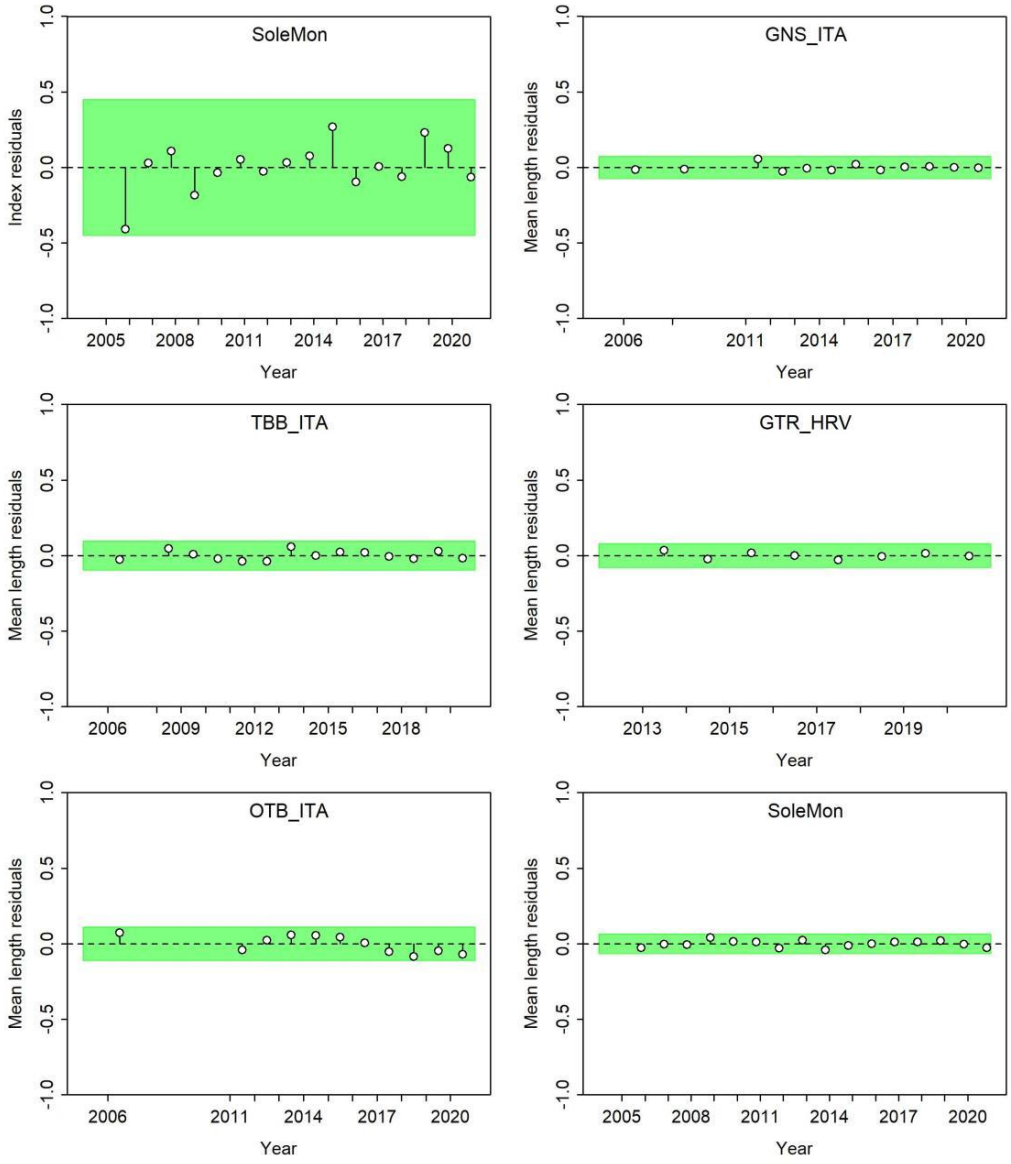

Figure 4.5.3.2.2. Runs tests results for the fit of the SoleMon survey index and length distributions for baseline run.

4.5.3.3. Model consistency

Retrospective analysis is commonly used to check the consistency of model estimates, i.e., the invariance in spawning stock biomass (*SSB*) and fishing mortality (*F*) as the model is updated with new data in retrospect. The retrospective analysis involves sequentially removing observations from the terminal year (i.e., peels), fitting the model to the truncated series, and then comparing the relative difference between model estimates from the full-time series with the truncated time-series. The most commonly used statistic for retrospective bias, rho (ρM), is obtained from Mohn, 1999. A "rule of thumb", proposed by Hurtado-Ferro et al., 2015, suggests values of ρM that fall outside (-0.15 to 0.20) for *SSB* for longer-lived species, or outside (-0.22 to 0.30) for shorter-lived species indicates an undesirable retrospective pattern. Moreover, extending the conventional retrospective analysis by retrospective forecasts can be a useful tool when verifying that the modeled quantities are not only historically stable (i.e., retrospective ρM) but at the same time consistent between forward projections and subsequent updates with newly available data (i.e., retro forecasts ρF). Both ρM and ρF are measures of an average bias across the years under evaluation.

The retrospective analysis was conducted for the last 5 years of the assessment time horizon to evaluate if there were any strong changes in model results. Retros were reasonably stable (Figure 4.5.3.3.1), the estimated Mohn´s indices (both ρM and ρF) were smaller than the threshold for *SSB* and *F*.

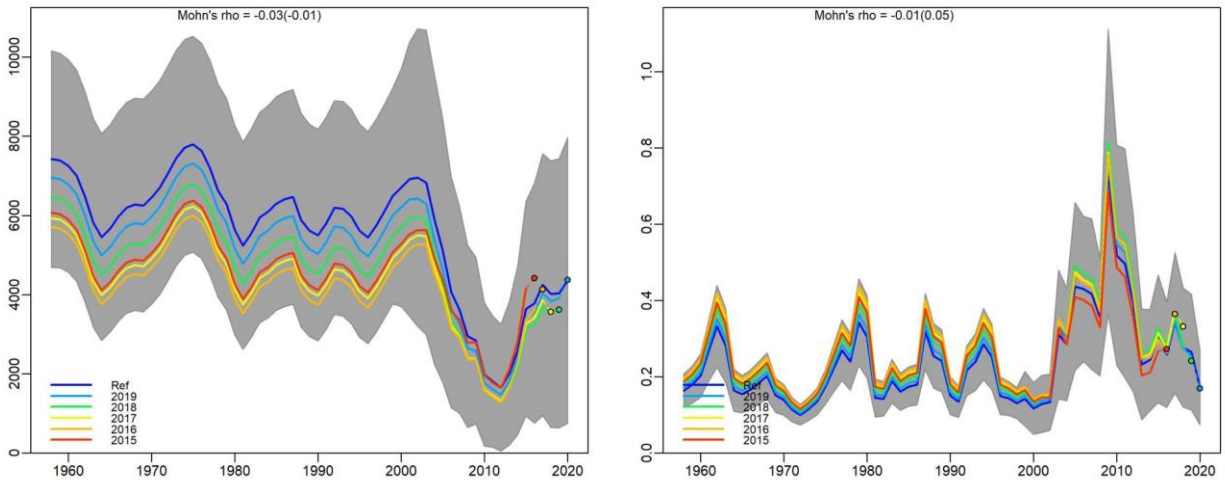

Figure 4.5.3.3.1. Retrospective analysis results for SBB and F for baseline run, ρM and ρF values (in brackets) are printed at the top of the panels.

4.5.3.4. Model prediction skills

The model diagnostics introduced thus far evaluate how well the model fits all available observations and how consistent the modeled quantities are in retrospect. However, providing fisheries management advice requires predicting a stock's response to management and checking that predictions are consistent with future reality (Kell et al., 2016). An intuitive approach to assess potential forecast bias is to extend the retrospective analysis to conduct model-based hindcasts by adding the additional step of projecting quantities, such as *SSB*, over the truncated years (Brooks and Legault, 2016). To address this, Kell et al. (2016) proposed the hindcasting cross-validation technique (HCXval) where observations are compared to their predicted future values. The key concept behind the HCXval approach is "prediction skill", which is defined as any measure of the accuracy of a forecasted value to the actual observed value that is not known by the model (Kell et al., 2021). The difference between the two values is hereafter referred to as the "prediction residual" (Michaelsen, 1987). The HCXval algorithm is similar to that used in the retrospective analysis. It requires the same procedure of peeling the observations and refitting the model to the truncated data series. Like retrospective forecasting, HCXval involves the additional steps of projecting forward (hindcasts). The difference is cross-validating the forecasts using the observations that were left out of the fit to the truncated time series in order to assess the model's prediction skill. A robust statistic for evaluating prediction skill is the mean absolute scaled error (MASE; Hyndman and Koehler, 2006). MASE builds on the principle of evaluating the prediction skill of a model relative to a naïve baseline prediction (MASE.base). MASE values greater than one indicate that in-sample one-step forecasts from the naïve baseline perform better than the forecast values under consideration. Moreover, adjusted MASE (MASE.adj) gets invoked in cases where the inter-annual variation in the observed values is very small (default MAE < 0.1 for naïve predictions), thus is more accurate when observations show extremely little variation. The reasoning is that prediction residuals must be already very accurate to fall below this threshold. The adjusted MASE essential keep the naive prediction MAE denominator of the MASE to a maximum. As for retrospective, hindcasting was conducted for the last 5 years of the assessment time horizon. The results indicated reasonably good prediction skill (MASE.adj < 1) for the survey index and for mean lengths of the five fisheries for the baseline runs (Figure 4.5.3.4.1).

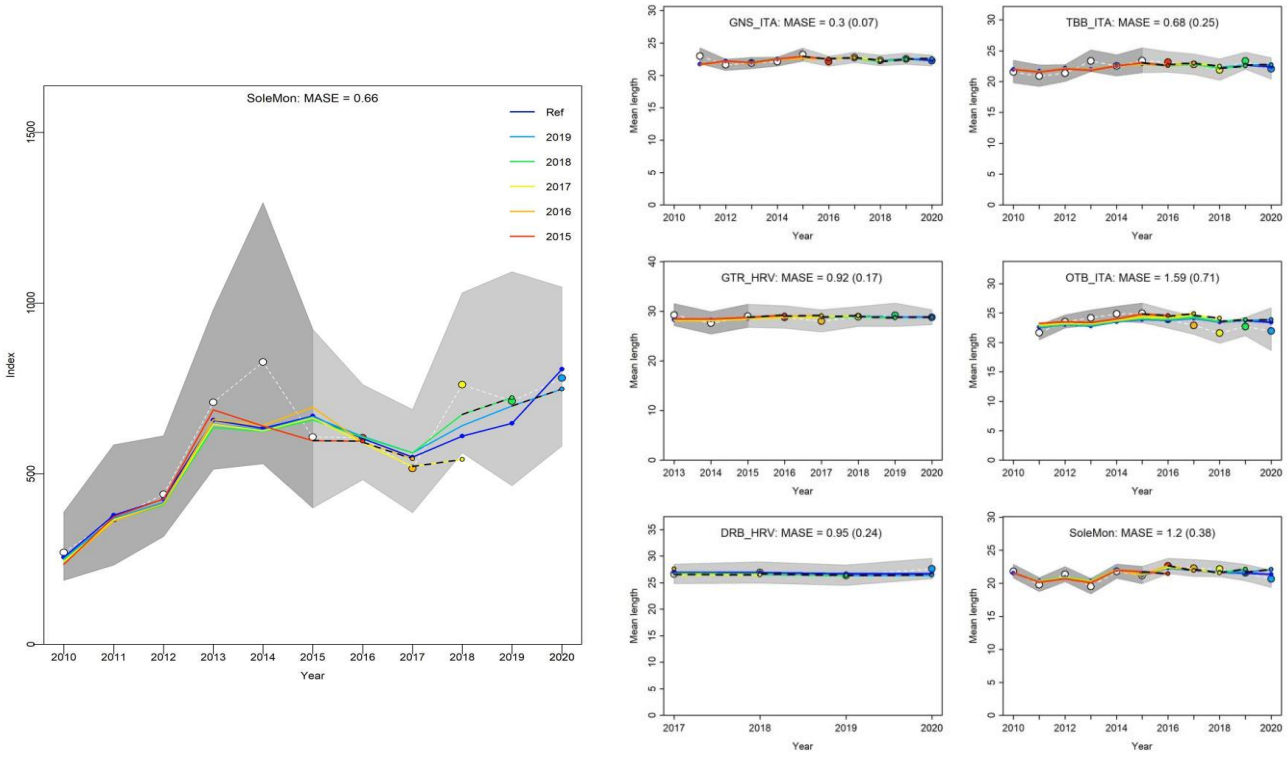

Figure 4.5.3.4.1. Hindcasting cross-validation (HCxval) results for survey index and length distributions for baseline run. MASE and adjusted MASE values (in brackets) are printed at the top of the panels.

4.5.4. Model weighting

The need to weight models based on information in the available data is recognized, but it is difficult to do so in a context in which the complexity of fisheries stocks assessment models prevents strict adherence with statistical rigor. In this context, the selected 18 grid runs represent the alternative states of nature of the stock and must be weighted in the final ensemble model. This is a necessary step because assigning the same weight (reliability) to all hypotheses could introduce biases into the management advice if some models are, in fact, highly unlikely or misspecified (model specification is the difference between the model and reality). To assign weights to the various models and hypotheses, it is preferable to establish a system of discrete weight categories. In this assessment we decided to use diagnostic scores (*W(Diagnostics)*) as weighting metrics (Maunder et al., 2020) to judge the plausibility of each candidate model based on each model's fit. In fact, when all diagnostic tests are considered together, the power to detect model misspecification improves without a substantial increase in the probability of incorrectly rejecting a correctly specified model (Carvalho et al., 2021).

In this context, the *W(Diagnostics)* component is calculated based on a series of interconnected diagnostic tests as discussed by Carvalho et al., 2021 and previously presented and explained for the reference run:

$$W(Diagnostics): \frac{W(\text{Diags 1}) + W(\text{Diags 2}) + W(\text{Diags 3}) \ldots + W(\text{Diags N})}{\text{Num of } W(\text{Diags})}$$

where to each *W* component a value of 1 is assigned when the run passed the diagnostic test and 0 when fail. A summary of all main diagnostics for the 18 model runs is provided is Table 4.5.4.1. Based on these results, different weights were used to stitch together the different runs in the final ensemble model.

The *W(Diagnostics)* values are used as a scaling factor for the number of simulations used by the ensemble estimator when estimating the posterior distributions of the derived quantities (i.e. 5000 simulations when the *W(Diagnostics)* value is 100% and less according to the assign weight such that a value of 50% would have 2500 simulations).

Table 4.5.4.1. Summary table of the diagnostics used in the weighting procedure. Green color refers to "Passed" score.

	Convergence and stability		Goodness of the fit								Consistency				Prediction skills			
	Positive	Jittering	Run test						Joint-residuals		Retrospective analysis				Hindcasting (MASE)			
Run name	Hessian		Index	lenGNS_ITA	lenTBB_ITA	lenGTR_HRV	lenOTB_ITA	lenSoleMon	Index	Length	Retro_SSB	Forecast_SSB	Retro_F	Forecast_F	Index	SurveyLen	COMfleet	*W(Diagnostics)*
Run1	Passed	Passed	Passed	Passed	Passed	Passed	Passed	Passed	15.2	3.1	-0.083	-0.070	0.021	0.035	0.726	0.399	0.320	**1.00**
Run2	Passed		Passed	Passed	Passed	Passed	Passed	Passed	14.7	3.1	-0.058	-0.054	0.026	0.052	0.863	0.363	0.312	**1.00**
Run3	Passed		Passed	Passed	Passed	Passed	Passed	Passed	14.9	3.1	-0.061	-0.053	0.016	0.036	0.766	0.382	0.316	**1.00**
Run4	Passed		Passed	Passed	Passed	Passed	Passed	Passed	15.4	3.1	-0.074	-0.059	0.018	0.029	0.714	0.407	0.319	**1.00**
Run5	Passed		Passed	Passed	Passed	Passed	Passed	Passed	14.7	3.1	-0.040	-0.036	0.014	0.040	0.842	0.370	0.312	**1.00**
Run6	Passed		Passed	Passed	Passed	Passed	Passed	Passed	14.9	3.1	-0.036	-0.030	0.008	0.026	0.743	0.334	0.316	**1.00**
Run7	Passed		Passed	Passed	Passed	Passed	Passed	Passed	15	3.1	-0.078	-0.064	0.034	0.047	0.744	0.410	0.317	**1.00**
Run8	Passed		Passed	Passed	Passed	Passed	Passed	Passed	14.4	3.1	-0.037	-0.033	0.017	0.042	0.825	0.377	0.312	**1.00**
Run9	Passed		Passed	Passed	Passed	Passed	Passed	Passed	14.7	3.1	-0.054	-0.044	0.021	0.040	0.750	0.396	0.315	**1.00**
Run10	Passed		Passed	Passed	Passed	Passed	Passed	Passed	21.2	3.3	0.126	0.157	-0.106	-0.072	0.967	0.455	0.375	**1.00**
Run11	Passed		Passed	Passed	Passed	Passed	Passed	Passed	20.1	3.6	0.013	0.003	-0.009	0.041	1.362	0.450	0.351	**0.93**
Run12	Passed		Passed	Passed	Passed	Passed	Passed	Passed	21.1	3.4	0.083	0.092	-0.067	-0.037	1.166	0.388	0.367	**0.93**
Run13	Passed		Passed	Passed	Passed	Passed	Passed	Passed	20.2	3.2	0.123	0.162	-0.113	-0.087	0.796	0.472	0.362	**1.00**
Run14	Passed		Passed	Passed	Passed	Passed	Passed	Passed	19.4	3.4	0.042	0.043	-0.040	-0.001	1.098	0.464	0.344	**0.93**
Run15	Passed		Passed	Passed	Passed	Passed	Passed	Passed	20.1	3.2	0.086	0.102	-0.078	-0.044	0.957	0.463	0.354	**1.00**
Run16	Passed		Passed	Passed	Passed	Passed	Passed	Passed	16.7	3.1	0.070	0.081	-0.067	-0.024	0.777	0.423	0.346	**1.00**
Run17	Passed		Passed	Passed	Passed	Passed	Passed	Passed	16.6	3.1	0.049	0.051	-0.045	0.001	0.887	0.421	0.340	**1.00**
Run18	Passed		Passed	Passed	Passed	Passed	Passed	Passed	16.7	3.1	0.062	0.070	-0.058	-0.014	0.810	0.423	0.344	**1.00**

4.5.5. Running the ensemble model

Once all plausible models have been run and have been assigned weights, a delta-Multivariate log-Normal estimator (delta-MVLN; Walter and Winker, 2019; Winker et al., 2019) was used to run the ensemble model. During this, the delta-MVLN generates and stitches together the joint posterior distributions of the target derived quantities (e.g. SSB/SSBtarget and F/Ftarget) coming from all the alternative runs of the ensemble grid. These quantities are derived by using the delta-method to calculate asymptotic variance estimates from the inverted Hessian matrix of the Stock Synthesis model (i.e. the quantities are calculated from each of the three model runs). The delta-MVLN is used to run the ensemble because it can infer within model uncertainty from maximum likelihood estimates (MLEs), standard errors (SEs) and the correlation of the untransformed quantities. Another commonly used approach to do so include the use of Markov Chain Monte Carlo methods (MCMC). However, in integrated age-structured stock assessment models such as SS3, this MCMC method is computationally intense and time consuming as it requires first inverting the Hessian matrix and then running sufficiently long MCMC chains (several hours to days; Magnusson et al., 2013; Maunder et al., 2006). This renders it as challenging task to complete during typically time-constrained stock assessment meetings. Therefore, the delta-MVLN estimator has been used here because is quite fast (take only few minutes to obtain final result from 18 runs grid) and has demonstrated the ability to mimic the MCMC and processes fairly closely both in general (Winker et al., 2019) and for the specific case study (Figure 4.5.5.1).

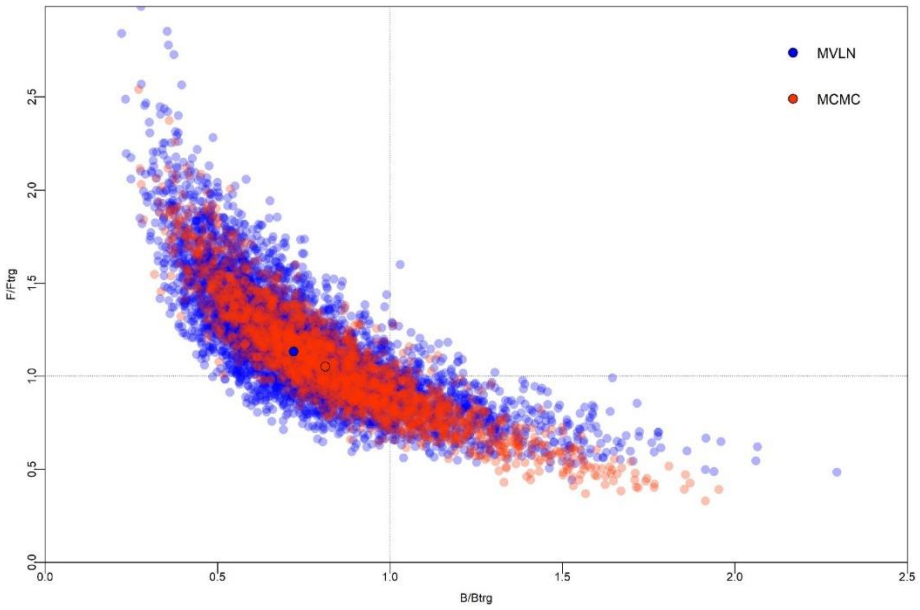

Figure 4.5.5.1. Comparison of the delta-MVLN approximation with MCMC method for baseline run for common sole in GSA 17.

4.5.6. Model final results

To recap, to capture structural uncertainties, a range of alternative models were selected through diagnostics (interconnected diagnostic tests) and were stitched together in an ensemble using the delta-Multivariate log-Normal estimator (delta-MVLN). The run specifications and final weighting factors used in the ensemble procedure are reported below. The final outputs from the ensemble model are based on the weighted-median value of the 18 runs.

Name	Selectivity	M	h	Weighting
run1	DN	M1	0.9	**1.00**
run2	DN	M1	0.7	**1.00**
run3	DN	M1	0.8	**1.00**
run4	DN	M2	0.9	**1.00**
run5	DN	M2	0.7	**1.00**
run6	DN	M2	0.8	**1.00**
run7	DN	M3	0.9	**1.00**
run8	DN	M3	0.7	**1.00**
run9	DN	M3	0.8	**1.00**
run10	CS	M1	0.9	**1.00**
run11	CS	M1	0.7	**0.93**
run12	CS	M1	0.8	**0.93**
run13	CS	M2	0.9	**1.00**
run14	CS	M2	0.7	**0.93**
run15	CS	M2	0.8	**1.00**
run16	CS	M3	0.9	**1.00**
run17	CS	M3	0.7	**1.00**
run18	CS	M3	0.8	**1.00**

Figures 4.5.6.1 presents the main outputs from the final ensemble model compared with the single runs:

- State of the adult biomass (*SBB*): Total spawning biomass of common sole follows a decreasing trend in the whole time series up to 2010. In the recent years, *SSB* followed an increasing trend. The last estimate of *SSB* in 2020 is 3037 tons (CI: 1524 - 7855). Confidence intervals associated

with the time-series of total spawning biomass are wide due the DN component of the ensemble grid.

- State of exploitation (*F*): Fishing mortality is defined as the average *F* of age classes 1 to 4. Fishing mortality rates are an approximation of the Baranov continuous *F* (Methot & Wetzel, 2013). Aggregated fishing mortality increased up to 2010 to follow then a continuous decreasing trend until 2020, reaching the value of 0.19 (CI: 0.10 – 0.34).

- State of the juveniles (*Recr*): Recruitment up to 2005 is quite constant as data informing recruits estimates are only available since 2005 (first year of SoleMon survey LFD). Since 2005, recruitment has shown an increasing trend; in the last year estimate recruits are 159254 (1000s) (CI: 87561 - 290927).

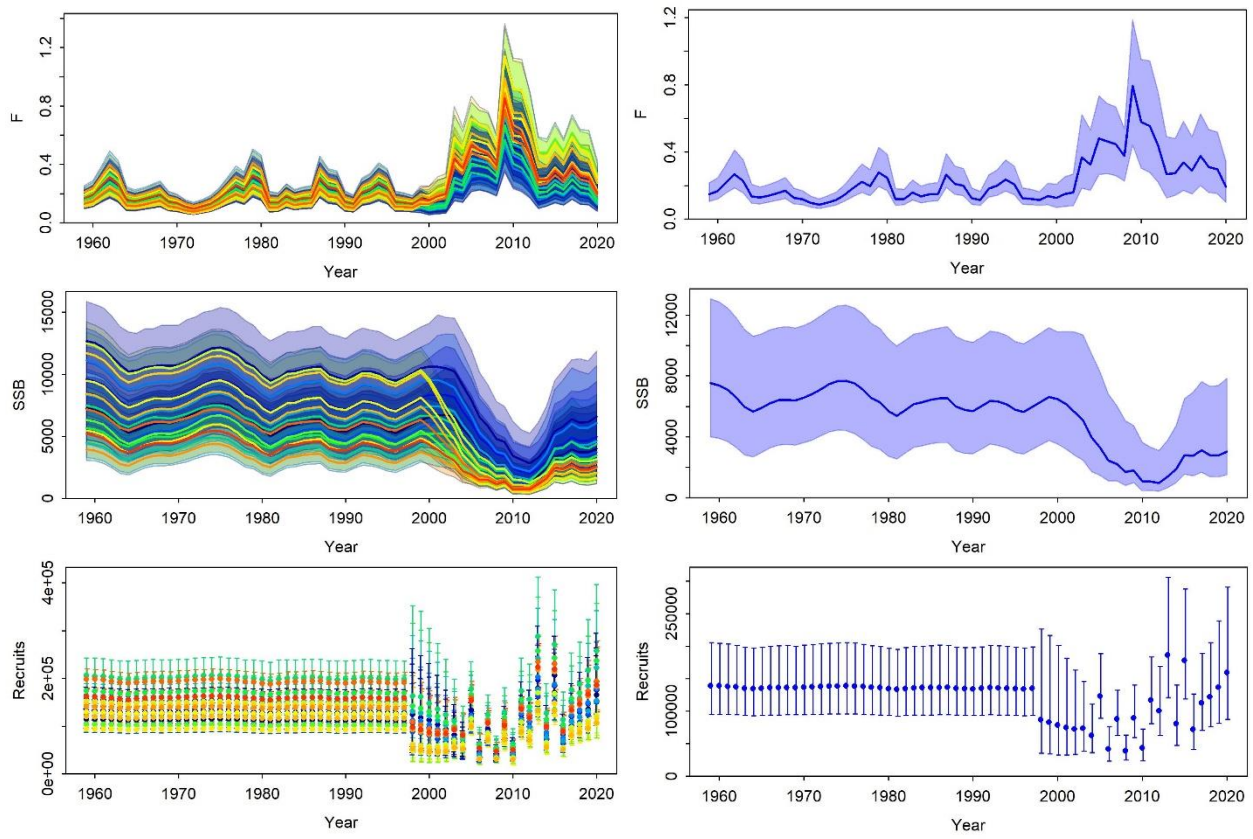

Figure 4.5.6.1. Comparison of stock assessment result between the 18 grid single runs (3 panels on the left) and the final ensemble model (3 panels on the right). Weighted-median value of SSB, F and Recr with 95% confidence intervals from delta-MVLN.

4.5.7. Reference points and current status of the stock

Reference points were estimated from Stock Synthesis ensemble model (Table 4.5.7.1); biomass reference points are considered as *SSB* and not total biomass. Deterministic MSY was discarded because the relative high steepness in all ensemble grid runs (0.7-0.9) appears to have a big effect on the skewness of the production function curve providing a very low SSB_{MSY} value for optimal fishing. On the other hand, Horbowy and Luzenzzyk (2012) and Punt et al. (2013) showed that fishing mortality corresponding to a biomass at 40% B_0 as a proxy for B_{MSY} leads to high yield and safe biomass levels irrespective of the steepness value of the stock recruitment function. Following this generic but more precautionary rule, SSB_{40} (biomass equal to 40% of unfished biomass) and F_{40} (fishing mortality level at SSB_{40}) has been chosen as proxies for MSY. Moreover, SSB_{lim}, defined as the level of spawning biomass below which recruitment is considered to be impaired, is set as 20% of unfished biomass B_0 (SSB_{20}) based on biological principles and international best practice (type 2; ICES, 2022b). However, further simulation analysis on the choice of best candidate reference points considering common sole stock-specific characteristic will be presented and discussed in chapter 6, following the "short-cut" MSE approach (ICES, 2020) developed and discussed during the ICES Workshops WKREF1 & 2 (ICES, 2022b,c).

Table 4.5.7.1. Common sole in GSA 17: estimated current value and relative reference points (with 95% confidence intervals from MVLN).

$F_{current}$ ($F_{bar\ 1\text{-}4}$ in 2020)	0.19 (0.10–0.34)
$F_{current}/F_{40\%}$	0.81 (0.43 - 1.57)
Current SSB (tonnes)	3037 (1524 - 7855)
$SSB_{current}/SSB_{40\%}$	0.73 (0.30 - 1.38)
$SSB_{current}/SSB_{20\%}$	1.46 (0.6 – 2.8)
Recruitment (1000s)	159254 (87561 - 290927)

Figure 4.5.7.1 shows the trajectory of the stock over the reference points, at present (2020) the stock is considered sustainable exploited ($F_{current}/F_{40}$= 0.81; CI: 0.43 - 1.57) with a low biomass ($SSB_{current}/SSB_{40}$= 0.73; CI: 0.30 - 1.38).

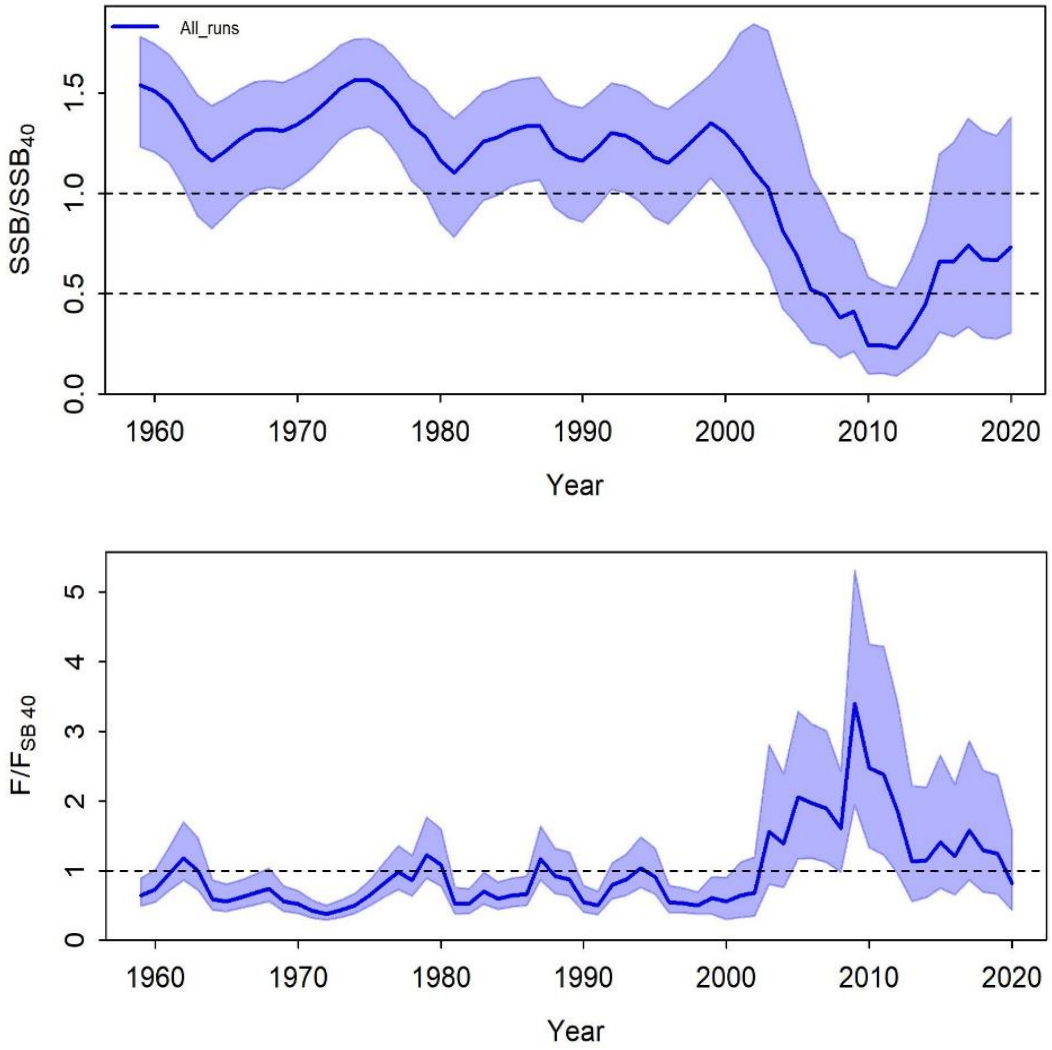

Figure 4.5.7.1. Stock status trajectories based on SS3 final ensemble model (weighted-median value of 18 runs). SSB/SSB_{40} (upper panel) and F/F_{40} (bottom panel) time series with 95% confidence intervals from delta-MVLN.

Figure 4.5.7.2 represent the Kobe plot for the ensemble model. Kobe plot represents the time series of pressure (F/F_{target}) on the Y-axis and of state of the Biomass (SSB/SSB_{target}) on the X-axis. The orange area indicates healthy stock sizes that are about to be depleted by overfishing. The red area indicates ongoing overfishing while the stock is too small to produce maximum sustainable yields. The yellow area indicates reduced fishing pressure on stocks recovering from still too small biomass. The green area is the target area for management, indicating sustainable fishing pressure and healthy stock size capable of producing high yields close to the reference point chosen (MSY or proxies).

For common sole the stock trajectory begun in 1958 in the green quadrant, when the biomass was quite higher than the SSB_{40}. Starting from 2000s, the *F* level registered an increasing trend that resulted in a progressive erosion of the stock size which led the stock trajectory towards the red quadrant. From 2010 onwards, the *F* has returned to decrease, falling under the reference point in the final year. In 2020 there is about 34% probability that the stock is in the red quadrant of the Kobe plot (i.e. SSB < SSB_{40} and F > F_{40}) with probabilities of about 44% to be in the yellow (i.e. SSB < SSB_{40} and F < F_{40}) and 22% to be in the green (SSB > SSB_{40} and F < F_{40}). In conclusion, the trajectory of the stock from 2010 onwards reflects its recovering status.

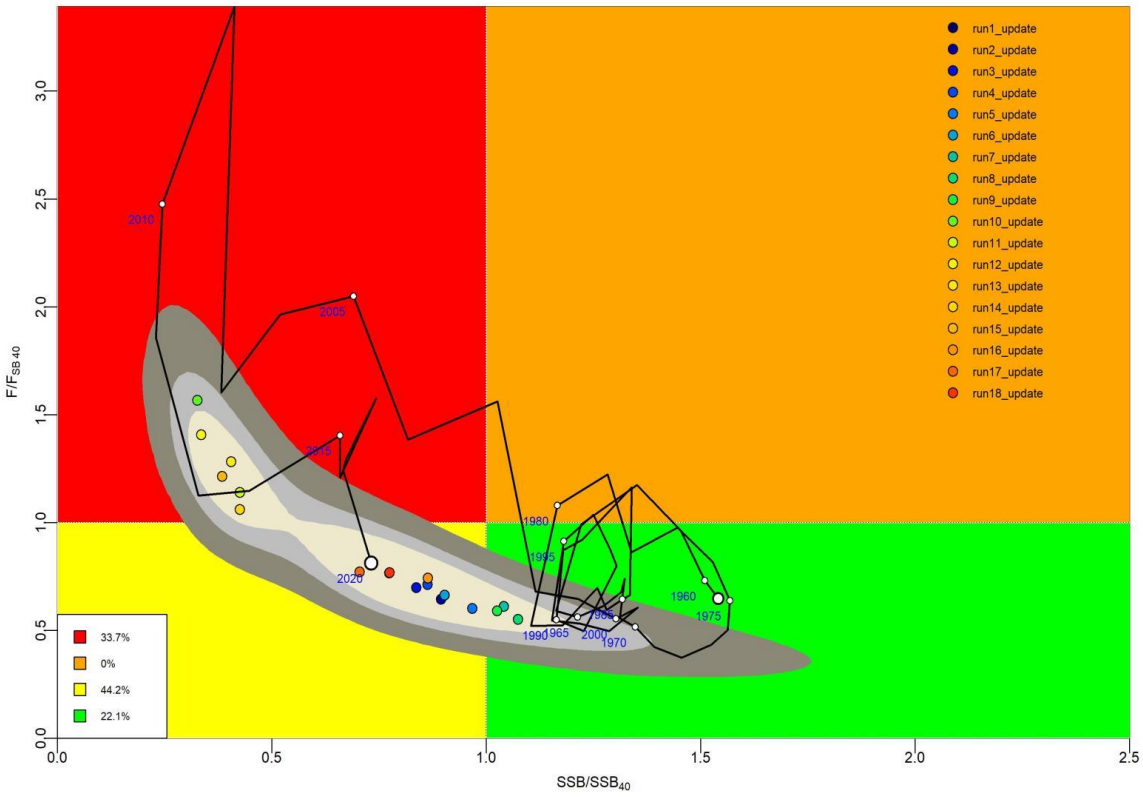

Figure 4.5.7.2. Kobe plot showing the trajectory of relative stock size (SSB/SSB40) over relative exploitation (F/F40) based on SS3 final ensemble model (white dot: weighted-median value of 18 runs). Gray shading indicates CI of 50%, 80% and 95% from delta-MVNL of the final assessment year (2020). The legend indicates the estimated probability of the stock status being in each of the Kobe quadrant.

Figure 4.5.7.3 shows the results of the ensemble model in the form of a kobe-plot by grouping the different runs by key parameters levels. The two alternative hypothesis of selectivity have a large influence on the assessment results by affecting the cryptic biomass levels (as discussed in section 4.5.2.4). As expected, dome shaped selectivity runs indicates a healthier stock status respect to cubic splines ones (Figure 4.5.7.3.a). Second for impact is the natural mortality (Figure 4.5.7.3.b); these results are reasonable given that *M* is considered one of the most influential parameters on the final result of a stock assessment (Mannini et al, 2021). The parameter that seems to have a minor influence on the results is the steepness used in stock recruitment relationship (Figure 4.5.7.3.c).

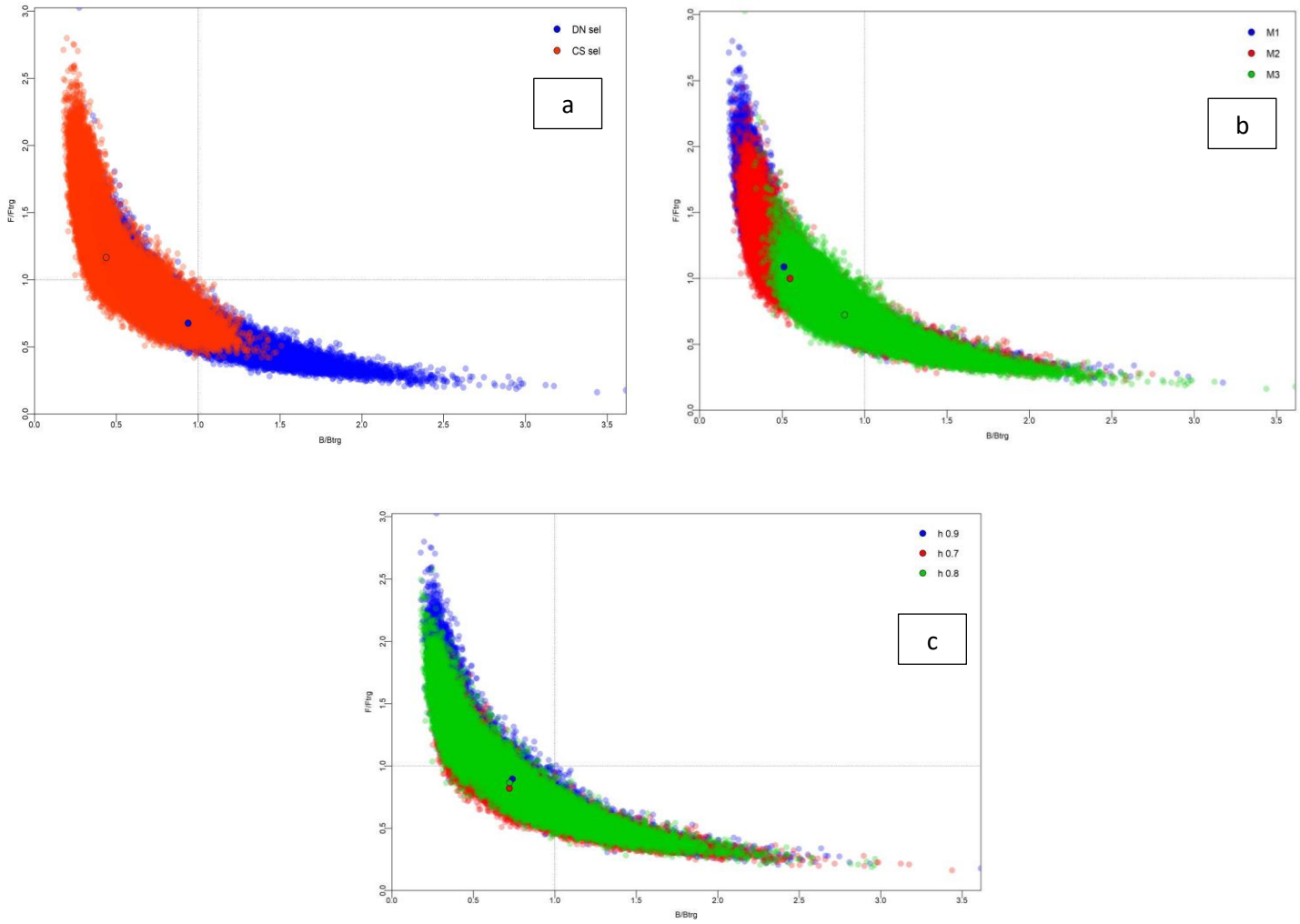

Figure 4.5.7.3. Kobe plots showing the relative stock size (SSB/SSBtarget) over relative exploitation (F/Ftarget) by grouping the different runs by key parameters levels (weighted-median values by level are showed). a) Selectivity pattern; b) Natural mortality; c) Steepnees (h).

In conclusion, the overall stock status slightly differs from the last benchmark assessment (FAO-GFCM, 2021). In fact, there is an increase in terms of biomass and fishing mortality is below the target level after many years of overfishing (Table 1.6.1). This is plausible if we consider the extra fishing activity reduction (almost 25% decrease in landings) that took place between 2019 and 2020 imposed by the COVID-19 pandemic restrictions (Scarcella et al., 2022). That said, a recovering trend status for these stocks had already been documented in assessment reports (FAO-GFCM, 2019; FAO-GFCM, 2021), probably due to the effective management actions put in place to protect the recruitment success in coastal areas, such as the coastal trawling ban (up to 4 nm) for eight weeks from 2006 and the temporary extension of this spatial restriction up to 6 nm for ten weeks since 2012 (EC, 2006). Therefore, the COVID-19 effect can be considered a positive accelerator of a recovery process already underway thanks to the management action and technical measures put in place to preserve the status of common sole stock in accordance with the objectives of the CFP (Scarcella et al. 2022).

4.5.8. Forecast: Short-term projection

The short-term projections are made with Stock Synthesis using the ensemble model. Recruitment in the forecast period was decided to be set to the average of the last 10 years for which recruitment deviations are estimated in the ensemble model. Probabilistic forecasts were also included. In this approach, catch and SSB levels corresponding to different TAC are calculated as in typical deterministic short term forecast but using delta-MVNL to also include the most correct associated probability of the *SSB* to be below biomass reference points, for each year of forecast. Therefore, an ensemble forecast was run for the different levels of assumed catches in the following 5 years (from 2021 to 2025), assuming catches equal to average landings of the last three years of data (2018, 2019, 2020). To simulate plausible reduction of 20%, 10% and the maintenance of catches at the *status quo* level, the following short-term TAC levels have been chosen: 80%, 90% and 100% of the last three years average catches respectively. To mimic a pre-pandemic condition, TAC 120% was also added to test possible effect of increased catches in the coming years. In fact, the drastic reduction in fishing effort recorded in 2020 in Adriatic Sea (-25% fishing days for *rapido* trawls compared to 2019) linked to the COVID-19 pandemic (Scarcella et al. 2022), it cannot be taken for granted for the next 5 years. On the contrary, despite the effort reductions that the current management plan claim (Recommendation GFCM/43/2019/5), it is reasonable to expect an increase in catches in the next years in response to the end of the state of emergency.

Figure 4.5.8.1 shows the stock trajectories of the forecast conducted applying the different fishing TAC levels. The graph only provides a zoom from 2010 to better see the forecasts for the last few years. Figure 4.5.8.2 shows the Kobe plot with forecast (final year 2025) divided by the 4 TAC scenarios. From these two graphs its evident how the reduction of catches it would improve the stock status (TAC80 & TAC90; blue and green lines and final points in figure 4.5.8.1 and figure 4.5.8.2 respectively). However, even the *status quo* condition (no reduction in caches) results in a sustainable exploitation of the stock (TAC100; yellow line and final point in figure 4.5.8.1 and figure 4.5.8.2 respectively). The only TAC level that would lead to an unsustainable exploitation ($F > F_{target}$) is the one mimic an increase in the catches (TAC120; red line and final point in figure 4.5.8.1 and figure 4.5.8.2 respectively). This means that a catch rate similar to the pre-pandemic level would slow down the current recovering of the stock. It should be noted that, even if still above the reference point in 2025, the trend of SSB in TAC120 is the only one in constant decrease during the forecast period (first two plots on the left in Figure 4.5.8.1).

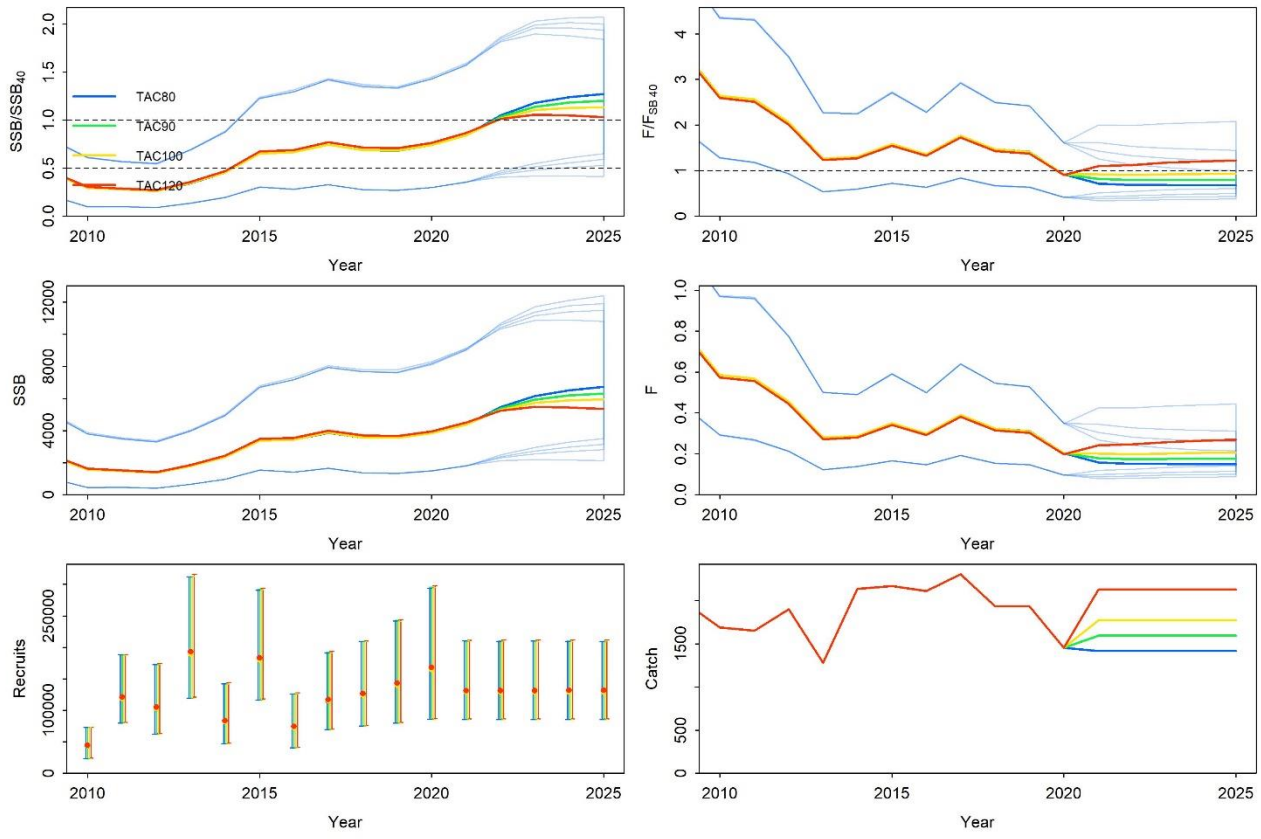

Figure 4.5.8.1. Stock status trajectories with forecast years (starting from 2010). The colors of the lines refer to the different TAC levels chosen: 80%, 90%, 100% and 120% of the catches in the last three years of data. Time series is provided with 95% confidence intervals from delta-MVLN.

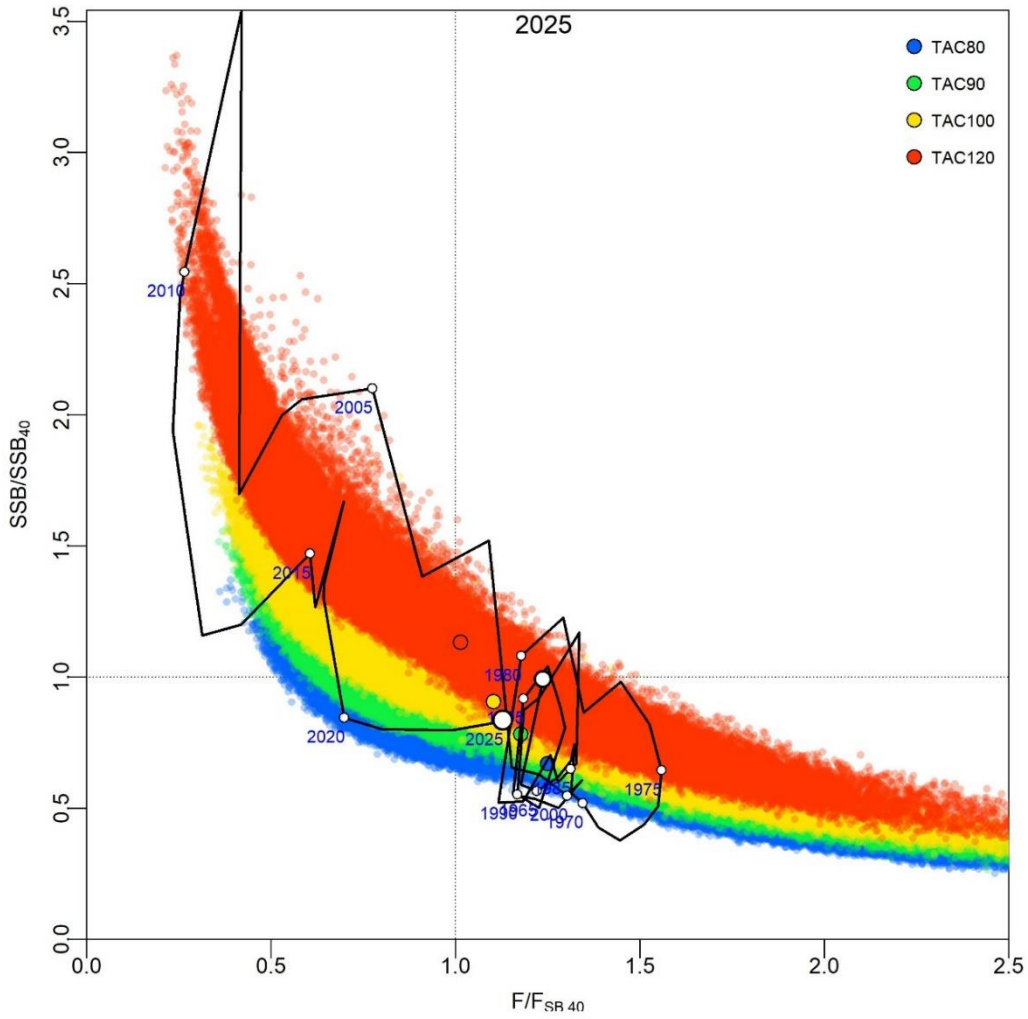

Figure 4.5.8.2. Kobe plot showing the trajectory with forecast years up to 2025 of relative stock size (B/B40) over relative exploitation (F/F40) using delta-MVLN. The colors of the points refer to the different TAC levels chosen: 80%, 90%, 100% and 120% of the catches in the last three years of data. The bigger white points refer to the median value of the stock considering all the TACs level together.

To confirm this, probabilistic forecasts show that the TAC120 is the only one that would fail to reach the *F* reference point with at least 50% probability by 2025 (40%; Table 4.5.8.1). Moreover, considering the biomass limit threshold (SSB_{20}), the probability of the SSB of falling below SSB_{lim} in TAC120 is more than 5% in any single year of the forecast period (13%; Table 4.5.8.3). This TAC scenario should be avoided because is not in line with the precautionary objectives of ICES advice framework (ICES, 2021b; ICES 2022b).

Table 4.5.8.1. Probabilistic Short-term forecasts: Probability of F to fall below target reference point (F_{40}) between 2021 and 2025 at different level of TAC.

Probability of being under Ftarget (F<Ftrgt)

TAC | Year	2022	2023	2024	2025
TAC80	87	91	93	95
TAC90	74	75	76	76
TAC100	63	61	59	58
TAC120	49	44	41	40

Table 4.5.8.2. Probabilistic Short-term forecasts: Probability of SSB to be above target reference point (SSB_{40}) between 2020 and 2025 at different level of TAC.

Probability of being above Btarget (SSB>SSBtrgt)

TAC | Year	2022	2023	2024	2025
TAC80	50	58	61	64
TAC90	49	55	58	59
TAC100	48	53	55	56
TAC120	49	53	52	51

Table 4.5.8.3. Probabilistic Short-term forecasts: Probability of SSB of falling below limit reference point (SSB_{20}) between 2020 and 2025 at different level of TAC.

Probability of falling below Blimit (SSB<SSBlim)

TAC | Year	2022	2023	2024	2025
TAC80	8	2	1	0
TAC90	10	4	2	1
TAC100	12	7	4	3
TAC120	15	13	13	13

4.6. References

Anderson S.C., Cooper A.B., Jensen O.P., Minto C., Thorson J.T., Walsh J.C., Afflerbach J., Dickey-Collas M., Kleisner K. M., Longo C., Osio G.C., Ovando D., Mosqueira I., Rosenberg A.A., Selig E.R, 2017. Improving estimates of population status and trend with superensemble models. Fish Fisheries,18: 732–741. Doi: https://doi.org/10.1111/faf.12200.

Arneri, E., Colella S. and Giannetti G. 2001. Age determination and growth of turbot and brill in the Adriatic Sea: reversal of the seasonal pattern of otolith zone formation. Journal of Applied Ichthyology, 17: 256– 261.

Artegiani, A., Bregant, D., Paschini, E., Pinardi, N., Raicich, F., Russo, A., 1997. The Adriatic Sea general circulation. Part II: baroclinic circulation structure. Journal of Physical Oceanography 27, 1515–1532.

Bergenius, M., Cardinale, M., Lundström, K., Kaljuste, O. 2022. Biologisk rådgivning för siklöja i Bottenviken. SLU.aqua.2021.5.5-272.

Brooks, E.N., Legault, C.M., 2016. Retrospective forecasting — evaluating performance of stock projections for New England groundfish stocks. Can. J. Fish. Aquat. Sci. 73, 935–950.

Carbonara, P., Follesa M.C., eds. 2019. Handbook on fish age determination: a Mediterranean experience. Studies and Reviews. No. 98. Rome, FAO. 2019. 180 pp.

Carvalho F, Winker H, Courtney D, Kapur M, Kell L, Cardinale M, Schirripa M, Kitakado T, Yemane D, Piner K.R, Maunder M.N., Taylor I, Wetzel C.R, Doering K, Johnson K.F, Methot R.D, 2021. A cookbook for using model diagnostics in integrated stock assessments, Fisheries Research, Volume 240, 2021, 105959, ISSN 0165-7836, https://doi.org/10.1016/j.fishres.2021.105959.

Carvalho Felipe, André E. Punt, Yi-Jay Chang, Mark N. Maunder, Kevin R. Piner, 2017. Can diagnostic tests help identify model misspecification in integrated stock assessments?, Fisheries Research, Volume 192, Pages 28-40, ISSN 0165-7836, https://doi.org/10.1016/j.fishres.2016.09.018

Chen, S. and S. Watanabe. 1989. Age Dependence of Natural Mortality Coefficient in Fish Population Dynamics. Nippn Suisan Gakkaishi 55(2): 205-208.

Cochran WG, Mosteller F, Tukey JW. 1954. Principles of Sampling. J Am Stat Assoc. doi: 10.1080/01621459.1954.10501212

Coro, G., Tassetti, A. N., Armelloni, E. N., Pulcinella, J., Ferrà, C., Sprovieri, M., et al. 2022a. COVID-19 lockdowns reveal the resilience of Adriatic Sea fisheries to forced fishing effort reduction. Sci. Rep. 12, 1052. doi: 10.1038/s41598-022-05142-w.

Coro G., Bove P., Armelloni E.N., Masnadi F., Scani M., Scarcella G. 2022b. Filling Gaps in Trawl Surveys at Sea through Spatiotemporal and Environmental Modelling. Front. Mar. Sci.

Despalatović, M., Grubelić, I., Piccinetti, C., Cvitković, I., Antolić, B., Žuljević, A., Nikolić, V., 2009. Distribution of echinoderms on continental shelf in open waters of the northern and middle Adriatic Sea. J. Mar. Biol. Assoc. U. K. 89, 585–591.

Dietterich, T.G. 2000. Ensemble methods in machine learning. In Multiple classifier systems (pp. 1–15). Berlin, Heidelberg: Springer.

Easey, M.W. & Millner, R.S. 2008. Improved methods for the preparation and staining of thin sections of fish otoliths for age determination. Science Series. Technical Report 143. Lowestoft, Suffolk, UK, Centre for Environment Fisheries and Aquaculture Science (Cefas). 12 pp.

Fabi, G., Grati, F., Raicevich, S., Santojanni, A., Scarcella, G., Giovanardi, O., 2009. Valutazione dello stock di Solea vulgaris del medio e alto Adriatico e dell'incidenza di diverse attività di pesca. Final Report. Ministero per le Politiche Agricole e Forestali. Direzione generale della pesca e dell'acquacoltura. VI Piano Triennale della pesca marittima e acquacoltura in acque marine e salmastre 1 (tematica c – c6). Programma di ricerca 6-a-74 (133 – XVII pp.).

FAO 2020. Fisheries Division, Statistics and Information Branch. FishStatJ: Universal software for fishery statistical time series. Copyright 2020.

FAO-GFCM. 2019. Report of the Working Group on Stock Assessment of Demersal Species (WGSAD), Scientific Advisory Committee on Fisheries (SAC). GFCM and FAO headquarters, Rome, Italy, 9-14 December 2019.

FAO-GFCM. 2021. Report of the Working Group on Stock Assessment of Demersal Species (WGSAD) – Benchmark session for the assessment of common sole in GSA 17, Scientific Advisory Committee on Fisheries (SAC). Online via Microsoft Teams, 12–16 April 2021.

Fisher, W., Schneider M., Bauchot M.L. 1987. Fishes FAO d'identification des espèces pour les besoins de la pêche. : Mediterranée et mer Noire, Vol. I – II. FAO, Rome, Italy, pp. 1–2.

Fortibuoni, T. et al. 2017. Fish and fishery historical data since the 19th century in the Adriatic Sea, Mediterranean. Sci. Data 4:170104 doi: 10.1038/sdata.2017.104.

Froglia, C. and G.F. Giannetti, 1986. Remarks on rings formation in otoliths of *Solea vulgaris* and other flatfishes from the Adriatic Sea. FAO Fisheries Report 345:121-122.

Gebremedhin, S., Bruneel, S., Getahun, A., Anteneh, W., Goethals, P. 2021. Scientific Methods to Understand Fish Population Dynamics and Support Sustainable Fisheries Management. Water 2021,13, 574 https://doi.org/10.3390/w13040574.

Giani, M., Djakovac, T., Degobbis, D., Cozzi, S., Solidoro, C., & Umani, S. F. 2012. Recent changes in the marine ecosystems of the northern Adriatic Sea. Estuarine, Coastal and Shelf Science, 115, 1-13.

Gislason, H., N. Daan, J. C. Rice, and J. G. Pope. 2010. Size, growth, temperature and the natural mortality of marine fish. Fish and Fisheries 11: 149-158.

Grati, F., Scarcella G., Polidori P., Domenichetti F., Bolognini L., Gramolini R., Vasapollo C., Giovanardi O., Raicevich S., Celić I., Vrgoč N., Isajlovic I., Jenič A., Marčeta B., Fabi G. 2013. Multi-annual investigation of the spatial distributions of juvenile and adult sole (*Solea solea*, L.) in the Adriatic Sea (Northern Mediterranean). J. Sea Res. http://dx.doi.org/10.1016/j.seares.2013.05.001 (2013).

Guarniero, I., Franzelletti S., Ungaro N., Tommasini S., Piccinetti C., Tinti F. 2002. Control region haplotype variation in the central 1 Mediterranean common sole indicates geographical isolation and population structuring in Italian stocks. J. Fish Biol. 60, 1459–1474.

Hamel, O.S., 2015. A method for calculating a meta-analytical prior for the natural mortality rate using multiple life history correlates. ICES Journal of Marine Science 72, 62-69. https://doi.org/10.1093/icesjms/fsu131.

Hilborn, R.W. and Walters C. 1992. Quantitative Fisheries Stock Assessment: Choice, Dynamics, and Uncertainty. New York: Chapman and Hall. 570 p.

Horbowy, J., and Luzeńczyk, A. 2012. The estimation and robustness of F MSY and alternative fishing mortality reference points associated with high long-term yield. Canadian Journal of Fisheries and Aquatic Sciences, 69: 1468–1480.

Hurtado-Ferro Felipe, Cody S. Szuwalski, Juan L. Valero, Sean C. Anderson, Curry J. Cunningham, Kelli F. Johnson, Roberto Licandeo, Carey R. McGilliard, Cole C. Monnahan, Melissa L. Muradian, Kotaro Ono, Katyana A. Vert-Pre, Athol R. Whitten, André E. Punt. 2015. Looking in the rear-view mirror: bias and retrospective patterns in integrated, age-structured stock assessment models, ICES Journal of Marine Science, Volume 72, Issue 1, January 2015, Pages 99–110, https://doi.org/10.1093/icesjms/fsu198.

Hyndman, R. J., & Koehler, A. B. 2006. Another look at measures of forecast accuracy. International journal of forecasting, 22(4), 679-688.

ICES. 2020. The third Workshop on Guidelines for Management Strategy Evaluations (WKGMSE3). ICES Scientific Reports. 2:116. 112 pp. http://doi.org/10.17895/ices.pub.7627.

ICES. 2021a. Joint NAFO\ICES Pandalus Assessment Working Group (NIPAG). ICES Scientific Reports. 3:22. 25 pp. https://doi.org/10.17895/ices.pub.7917.

ICES. 2021b. ICES fisheries management reference points for category 1 and 2 stocks; Technical Guidelines.

ICES. 2022a. Benchmark workshop on Pandalus stocks (WKPRAWN). ICES Scientific Reports. 4:20. 249 pp. http://doi.org/10.17895/ices.pub.19714204.

ICES. 2022b. Workshop on ICES reference points (WKREF1). ICES Scientific Reports. 4:2. 70 pp. http://doi.org/10.17895/ices.pub.9749.

ICES. 2022c. Workshop on ICES reference points (WKREF2). ICES Scientific Reports. 4:68. 96 pp. http://doi.org/10.17895/ices.pub.20557008.

Iles, T. 1994. A review of stock–recruitment relationships with reference to flatfish populations.Netherlands Journal of Sea Research 32:399– 420

Jardas, I., 1996. Jadranska ihtiofauna. Školska knjiga, Zagreb.

Jensen, A.L. 1996. Beverton and Holt life history invariants result from optimal trade-off of reproduction and survival. Can. J. Fish. Aquat. Sci. 53: 820-822.

Jensen, A.L. 1997. Origin of the relation between K and Linf and synthesis of relations among life history parameters. Can. J. Fish. Aquat. Sci. 54: 987-989.

Johnson, K. F., Monnahan, C. C., McGilliard, C. R., Vert-Pre, K. A., Anderson, S. C., Cunningham, C. J., ... & Punt, A. E. 2015. Time-varying natural mortality in fisheries stock assessment models: identifying a default approach. ICES Journal of Marine Science, 72(1), 137-150.

Kell, L.T., Kimoto, A., Kitakado, T., 2016. Evaluation of the prediction skill of stock assessment usingù hindcasting. Fish. Res. 183, 119–127. https://doi.org/10.1016/j.fishres.2016.05.017.

Kell, L.T., Sharma, R., Kitakado, T., Winker, H., Mosqueira, I., Cardinale, M., Fu, D., 2021. Validation of stock assessment methods: is it me or my model talking? in press ICES J. Mar. Sci.

Knutti, R., Furrer, R., Tebaldi, C., Cermak, J., & Meehl, G.A. 2009. Challenges in combining projections from multiple climate models. Journal of Climate,23,2739–2758.

Lorenzen, K. 1996. The relationship between body weight and natural mortality in juvenile and adult fish: a comparison of natural ecosystems and aquaculture. J. Fish. Biol. 49: 627-647.

Lorenzen, K. 2016. Toward a new paradigm for growth modeling in fisheries stock assessments: Embracing plasticity and its consequences. Fisheries Research, 180, 4–22. https://doi.org/10.1016/j.fishres.2016.01.006.

Magnusson, A., Punt, A.E., Hilborn, R., 2013. Measuring uncertainty in fisheries stock assessment: the delta method, bootstrap, and MCMC. Fish Fish. 14, no-no. doi:10.1111/j.1467-2979.2012.00473.x.

Magoulas, A., Tsimenides, N., Zouros, E., 1996. Mitochondrial DNA phylogeny and the reconstruction of the population history of a species: the case of the European anchovy (*Engraulis encrasicolus*). Mol. Biol. Evol. 13, 178–190.

Mahé, K., Moerman M., Maertens I., Holmes I., Boiron A. & Elleboode R. 2012. Report of the sole (*Solea solea*) in the Bay of Biscay otolith exchange scheme 2011. 14 pp.

Mannini A, Pinto C, Konrad C, Vasilakopoulos P and Winker H. 2021. "The Elephant in the Room": Exploring Natural Mortality Uncertainty in Statistical Catch at Age Models. Front. Mar. Sci. 7:585654. doi: 10.3389/fmars.2020.585654.

Marasović, I., Grbec, B., & Morović, M. 1995. Long-term production changes in the Adriatic. Netherlands journal of sea research, 34(4), 267-273.

Matić-Skoko S, Soldo A, Stagličić N, Blažević D, Šiljić J, Iritani D. 2014. Croatian marine fisheries (Adriatic Sea): 1950–2010. Fish Cent Work Pap. Vancouver, Canada.

Maunder, M. N. 2012. Evaluating the stock–recruitment relationship and management reference points: application to Summer Flounder (Paralichthys dentatus) in the U.S. Mid-Atlantic. Fisheries Research 125/ 126:20–26.

Maunder, M.N., Hamel, O., Ianelli, J., 2021. Natural Mortality: theory, estimation and application in fishery stock assessment models. Spec. Issue Fish. Res.

Maunder, M.N., Harley, S.J., Hampton, J., 2006. Including parameter uncertainty in forward projections of computationally intensive statistical population dynamic models. ICES J. Mar. Sci. 63, 969–979. doi:10.1016/j.icesjms.2006.03.016.

Maunder, M.N., Punt A.E. 2013. A review of integrated analysis in fisheries stock assessment. Fish Res 142: 61–74.

Maunder, M.N., Xu, H., Lennert-Cody, C.E., Valero, J.L., Aires-da-Silva, A., MinteVera, C., 2020. Implementing Reference Point-based Fishery Harvest Control Rules Within a Probabilistic Framework That Considers Multiple Hypotheses (No. SAC-11- INF-F). Scientific Advisory Commitee, Inter-American Tropical Tuna Commission, San Diego.

McClenachan, L., Ferretti, F. & Baum, J. K. 2012. From archives to conservation: Why historical data are needed to set baselines for marine animals and ecosystems. Conserv. Lett 5, 349–359.

Mediterranean Sensitive Habitats, 2013. Edited by Giannoulaki M., A. Belluscio, F. Colloca, S. Fraschetti, M. Scardi, C. Smith, P. Panayotidis, V. Valavanis M.T. Spedicato. DG MARE Specific Contract SI2.600741, Final Report, 557 p.

Methot, R. D., and Wetzel C. R. 2013. Stock synthesis: a biological and statistical framework for fish stock assessment and fishery management. Fisheries Research, 142: 86–99.

Michaelsen, J., 1987. Cross-validation in statistical climate forecast models. J. Clim. Appl. Meteorol. 26, 1589–1600. https://doi.org/10.1175/1520-0450(1987)026<1589:CVISCF>2.0.CO;2.

Mohn, R., 1999. The retrospective problem in sequential population analysis: An investigation using cod fishery and simulated data. ICES J. Mar. Sci. 56, 473–488. https://doi.org/10.1006/jmsc.1999.0481.

Myers, R. A., K. G. Bowen, and N. J. Barrowman. 1999. Maximum reproductive rate of fish at low population sizes. Canadian Journal of Fisheries and Aquatic Sciences 56:2404–2419.

Pagotto, G., Piccinetti, C., Specchi, M., 1979. Premières résultats des campagnes de marquage des soles en Adriatique: déplacements. Rapport de la Commission Internationale pour l'Exploration Scientifique de la mer Méditerranée 25/26 (10), 111–112.

Piccinetti, C., Giovanardi, O., 1984. Données biologique sur Solea vulgaris en Adriatique. FAO Fisheries Report 290, 117–118.

Pita, P., Ainsworth, G. B., Alba, B., Anderson, A. B., Antelo, M., Alós, J., et al. 2021. First assessment of the impacts of the COVID-19 pandemic on global marine recreational fisheries. Front. Mar. Sci. 8, 735741. doi: 10.3389/fmars.2021.735741.

Punt, A. E., Smith, A. D. M., Smith, D. C., Tuck, G. N., and Klaer, N. L. 2013. Selecting relative abundance proxies for BMSY and BMEY. ICES Journal of Marine Science, 71: 469–483. http://icesjms.oxfordjournals.org/content/71/3/469.short.

Rikhter, V.A., Efanov, V.N., 1976. On one of the approaches to estimation of natural mortality of fish populations. ICNAF Res. Doc. 79/VI/8, 12.

Roff, D. A. 1984. The evolution of life history parameters in teleosts. Can. J. Fish. Aquat. Sci. 41: 989-1000.

Rosenberg, A. A. et al. 2005. The history of ocean resources: modelling cod biomass using historical records. Front.Ecol.Environ. 3, 84–90.

Sampson, D.B., & Scott, R.D. 2012. An exploration of the shapes and stability of population–selection curves. Fish and Fisheries, 13, 89–104.

Santelli A, Cvitković I, Despalatović M, Fabi G and others (2017) Spatial persistence of megazoobenthic assemblages in the Adriatic Sea. Mar Ecol Prog Ser 566:31-48. https://doi.org/10.3354/meps12002.

Saville A (1977) Survey methods of appraising fishery resources. In: Fao Fisheries Technical Paper No 171.

Scarcella G, Angelini S, Armelloni EN, Costantini I, De Felice A, Guicciardi S, Leonori I, Masnadi F, Scanu M and Coro G (2022) The potential effects of COVID-19 lockdown and the following restrictions on the status of eight target stocks in the Adriatic Sea. Front. Mar. Sci. 9:920974.doi: 10.3389/fmars.2022.920974.

Scarcella, G., Grati F., Raicevich S., Russo T., Gramolini R., Scott R. D., Polidori P., Domenichetti F., Bolognini L., Giovanardi G., Celić I., Sabatini L., Vrgoč N., Isajlović I., Marčeta B., Fabi G., 2014. Common sole in the northern and central Adriatic Sea: Spatial management scenarios to rebuild the stock. J. Sea Res. http://dx.doi.org/10.1016/j.seares.2014.02.002.

STECF 2018. Scientific, Technical and Economic Committee for Fisheries (STECF) Stock Assessments - Part 2 (STECF-18-16). Publications Office of the European Union, Luxembourg, 2018, ISBN 978-92-79-79399-8, doi:10.2760/598716, JRC114787.

STECF 2020. Scientific, Technical and Economic Committee for Fisheries (STECF) Stock Assessments in the Mediterranean Sea – Adriatic, Ionian and Aegean Seas (STECF-20-15). EUR 28359 EN, Publications Office of the European Union, Luxembourg, 2020, ISBN 978-92-76-27168-0, doi:10.2760/877405, JRC122994.

Then, A.Y., J.M. Honeig, N.G. Hall, D.A. Hewitt, 2015. Evaluating the predictive performance of empirical estimators of natural mortality rate using information on over 200 fish species. ICES J. of Mar. Sci. 72(1); 82-92.

Tortonese, E. 1975. Osteichthyes - Fauna d'Italia vol. XI, Calderini, Bologna.

Walter, J., Winker, H., 2019. Projections to create Kobe 2 Strategy Matrices using the multivariate log normal approximation for Atlantic yellowfin tuna. ICCAT-SCRS/2019/145 1–12.

Winker, H., Carvalho, F., Thorson, J.T., Kell, L.T., Parker, D., Kapur, M., Sharma, R., Booth, A.J., Kerwath, S.E., 2020. JABBA-select: incorporating life history and fisheries' selectivity into surplus production models. Fish. Res. 222, 105355.

Winker, H., Walter, J., Cardinale, M., Fu, D., 2019. A multivariate lognormal Monte-Carlo approach for estimating structural uncertainty about the stock status and future projections for Indian Ocean Yellowfin tuna. IOTC-2019-WPM10-XX.

5. Biphasic versus monophasic growth curve equation, an application to common sole (*Solea solea*, L.) in the northern and central Adriatic Sea

From the paper: *Carbonara P. ‡, **Masnadi F.*‡,** Donato F., Sabatini L., Pellini G., Cardinale M., Scarcella G. 2023. " Biphasic versus monophasic growth curve equation, an application to common sole (Solea solea, L.) in the northern and central Adriatic Sea. Fisheries Research, 263, 106694. doi: 10.1016/j.fishres.2023.106694.*

‡These authors have contributed equally to this work.
*Corresponding author: Francesco Masnadi

5.1. Abstract

Traditionally, growth pattern is described as constant throughout life using von Bertalanffy's equation. However, a change in the growth due to a re-allocation of energy during individual lifespan is to be expected. Following this hypothesis, back-calculation measurements obtained from SoleMon survey data have been used to fit and compared monophasic and biphasic growth curves for common sole in the northern and central Adriatic Sea. Moreover, individual variability in growth has been considered through non-linear mixed effects models where the individual parameters were considered as a random effect. The analyses conducted in this study revealed systematic age-specific biases in the monophasic curve and demonstrated that the fitting of the biphasic curve was superior (Δ AIC: 329; Δ BIC: 310), confirming the theory that growth in size would decrease as a consequence of reproductive effort. Finally, since common sole is routinely assessed using models that relies on growth to derive assessment estimates and related management reference points, a stock assessment simulation was performed to compare the two growth alternatives. Results showed how the biphasic alternative was more adequate than the conventional one and that the use of the monophasic pattern would result in an overly optimistic view of stock status (+40% in SSB/SSB_{target} and -35% in F/F_{target} compared to biphasic pattern), thereby increasing leading the risk of overfishing.

5.2. Introduction

Fish growth is a consequence for the intake of energy and material resources from the environment, transformation into body mass, and allocation among maintenance, development, and reproduction (Carbonara et al., 2018; Meekan et al., 2006; Sibly et al., 2015). More specifically, growth depends on a complex interaction between energy allocation, foraging strategy, risk of predation, reproductive behaviour, short and long-term density dependence effects and the incidence of senescence (Carbonara

et al., 2022). It is convention in fisheries sciences to describe the growth pattern using monophasic function (such as conventional von Bertalanffy's equation) relying on the assumption of constant growth throughout life (Helser and Lai, 2004; Pardo, Cooper, & Dulvy, 2013). This type of curves tends to be straightforward to fit and the approach has been particularly common and used for decades as standard descriptors of fish growth (Ricker, 1975; Froese and Pauly, 2022). However, this approach often results in a simplification of reality and several criticisms have been encountered. For example, the limited inference on life-history and ecological information and the energetic justification for this model are problematic (Quince et al., 2008; Wilson et al., 2017). In particular, the conventional monophasic function has been proven to fails to account for energetic cost of maturation and reproduction (Day and Taylor, 1997) which, in female fish could exceeds 15% of somatic energy allocation (Shuter et al., 2005). An alternative approach suggested is to fit a biphasic model able to account for differential allocation of energy at different ages (Day and Taylor, 1997; Lester et al., 2004; Charnov, 2008; Alos et al., 2010; Wilson et al., 2017). Although fitting a biphasic model can be more challenging, they are proved to be statistically and biologically more valid than monophasic models (Lester et al., 2004; Alos et al., 2010; Moe, 2015). In bibliography, there is a considerable number of studies regarding the multi-stage or multi-phase growth theory according to which one or more changes in the growth parameter occur at some point during the life of an individual (Iles 1974; Hernandez-Llamas & Ratkowsky, 2004; Rogers-Bennett and Rogers 2016). In the review by Wilson et al. (2017), the authors summarize and analyze the factors that lead to different allocation of energetic costs between somatic growth and other bio-ecological processes. One of the key factors is the direct or indirect reproductive investment (Day and Taylor, 1997; Lester et al., 2004; Manabe et al., 2018) and it is based on the concept that sexual maturation should negatively influence growth (e.g. gonadal development, nesting, displaying, metabolic costs of storing gonads). Other factors can be related to the genetics and physiology of the species (Grønkjær, 2016), environmental drivers (Matthias et al., 2018), habitat change (Laslett, Eveson and Polacheck, 2002; Tracey and Lyle 2005), dietary changes (Paloheimo and Dickie, 1965; Soriano et al. 1992), or human exploitation (fishing pressure; Kraak et al., 2019, Carbonara et al., 2022). More likely many of these factors participate as contributing causes (Enberg et al., 2012). Conventional growth models assume that population growth can be described by average growth parameters but, considering natural variability, it is unrealistic to assume that individuals belonging to the same wild population follow exactly the same growth trajectory (Smith et al., 1997; Pilling et al., 2002; Pardo, Cooper, & Dulvy, 2013). In fact, individual growth is the result of an interaction between potential growth (at the genetic level of the species) and environmental conditions and can vary from individual to individual (Carbonara et al.,

2022). While traditional size-at-age observations are pulled together to fit an overall population growth curve (Haddon, 2011), individual growth trajectories can be back-calculated from the width of the annual increments recorded in the otoliths (Campana, 1990; Fossen et al., 1999; Wilson et al., 2009). Therefore, assuming each specimen to be randomly sampled from the same population of individuals, maximum likelihood or Bayesian methods can be used to explicitly treat individual growth variation as a component of variability in size-at-age (Lorenzen, 2016). Pooling data together through a shrinking process, combining population averages with individual data, has been proven to produce more reliable and generally less variable estimates of growth parameter (Pilling et al., 2002).

Provide reliable modeling of fish growth is an essential part of many fisheries stock status assessments (Reeves 2003; Gebremedhin et al., 2021). Growth parameters are key factors to describe fish population dynamics affecting biomass production, natural mortality and fishing mortality (Lorenzen, 2000; Francis, 2016; Sampson, 2014; Gebremedhin et al., 2021). They are crucial to the use of size composition data in stock assessment which, up today, remain more frequently available than age-frequency data (Lorenzen, 2016; Minte-Vera et al., 2016). In this context, the most accurate estimates of the growth pattern are essential to perform short-term projections of stock status (Punt et al., 2008; Eero et al., 2015; Hüssy et al., 2016) and guide decisions and management plans regarding future regulation of harvest (Hilborn and Walters, 1992, Lorenzen, 2016). On the contrary, biased estimates of stock status used for management advice can give rise to an overly optimistic or pessimistic view of stock status (Kuparinen et al., 2016; Stawitz et al., 2019), which in some extreme cases had led stocks to collapse (Beamish and McFarlane 1995, Liao et al. 2013). Most fish stock assessments treat growth with a firm focus on constant growth curves (Hilborn and Walters, 1992, Quinn and Deriso, 1999, Haddon, 2011). This is the case of common sole stock in Adriatic Sea where the stock assessment is routinely performed by the General Fisheries Commission for the Mediterranean, hereafter GFCM, using externally-fixed conventional von Bertalanffy growth curve to translate length composition data to age inside the model (FAO-GFCM, 2021). Nevertheless, in recent years there has been showed how sensitive management advice is to variation in growth patterns (Thorson et al., 2015) and the demand for comparative studies between conventional curve and alternative formulation has grown consequently (Minte-Vera et al., 2016). In this context, a more precise estimate of growth obtain by means of biphasic models could improve the use and interpretation of length-composition data in highly structured age-based stock assessments (Edwards et al., 2012; Methot and Wetzel, 2013). In agreement on this, GFCM specifically requested further analyses regarding the exploration and application of biphasic growth model for common sole in Adriatic

Sea (FAO-GFCM 2021). The study is therefore divided in two parts, a growth analysis and a stock assessment application for common sole in central and northern Adriatic Sea (GSA17). The aim of the first part was to detect possible differences in growth comparing monophasic and biphasic von Bertalanffy growth functions and discuss them in terms of best fit on the observed data using back-calculated length-at-age survey data. Moreover, individual growth variability was considered by means of mixed effect model. In the second part, an example of a practical application within common sole assessment models was present in order to investigate the impact of the two growth patterns on assessment main outcomes and scientific advice.

5.3. Material and methods

5.3.1. Species under analysis

The common sole (Solea solea; Linnaeus, 1758) is a demersal species, particularly abundant on relatively low depth sandy and muddy bottoms in the Mediterranean Sea and north-eastern Atlantic (Quéro et al., 1986). The species is commercially important in the northern and central Adriatic Sea (GSA17; FAO Geographical Sub-Area17) (Vallisneri et al., 2000; Grati et al., 2013), where the stock is shared among Italy, Slovenia and Croatia, representing about 2000 tons and more than 20 million of euros in terms of landing value (FAO-GFCM, 2021). Data on the spatial distribution reveals distribution is a function of age with a progressive spawners migration from coastal waters, which is a shallow water area characterized by a high concentration of nutrients, to deeper ones outside the western coast of Istria (Scarcella et al., 2014). In the Mediterranean Sea, the reproduction of common sole occurs from December to May (Fisher et al., 1987). Within the framework of SoleMon project, it has been observed that in the central and northern Adriatic Sea the reproduction takes place from November to March. Size at first sexual maturity in Mediterranean reported from literature is about 25 cm (Vallisneri et al., 2000) and more recent age-based maturity derived directly by data collected during the Adriatic Sea survey showed a shift in the proportion of mature fishes from 28% to 78% between age 1 and age 2 (FAO-GFCM, 2019).

5.3.2. Methods of sampling and age determination

All the sole samples used in this study were collected during the *rapido* trawl surveys (SoleMon) held in the northern and central Adriatic Sea by the National Research Council (CNR-IRBIM, Italy) in cooperation with the National Institute for Environmental Protection and Research (ISPRA, Italy), the

Institute of Oceanography and Fisheries (IOF, Croatia), and the Fisheries Research Institute of Slovenia (FRIS, Slovenia). The survey was selected as it was specifically designed to provide a representative sampling of the entire GSA17 stock. Common sole otolith sampling is stratified in three areas – stations south of Ancona; north of Ancona, and in international waters – to maximize the coverage of its spatial distribution and involves collecting 10 otoliths per cm class in each area. Sampling design and technical features can be found in detail in the reference papers or manuals (Grati et al. 2013; Anonymous 2019; ICES 2019). A dataset consisting of 563 individuals collected from 2014 to 2020 (TL: 72 - 380 mm) was available for this study. The preparation method for ageing was in line with Carbonara and Follesa, (2019) and following described. The right sagitta of each specimen was selected to be transversely sectioned down to the core. The otoliths were burned at 350° C for 10 minutes in a muffle furnace. Then, burned otoliths were included in resin (Crystalbond 509 Amber), ground on abrasive paper and polished with alumina powder. Burning technique was used to improve the quality of observations enhancing the growth rings contrast. The sections were immersed in fresh water and observed under stereomicroscope (Leica DM4000B) with reflected light against a black background (10x magnification). Images of sections were took using a charge-coupled device camera (Leica DFC 420) linked to a digitized computer video system (Leica Application Suite 4.3.0). To analyze the relationship between total fish length and otolith size, radius length (Rcpt) was measured in the whole dataset (Figure 5.3.2.1). The images from individuals with a total length (TL) $\geq$ 270 mm and who reached at least age 4 were analysed to measures opaque rings distance from the core (R1, R2, R3. etc.; Figure 5.3.2.1) relevant for the back-calculation aging process showed in the next paragraph. The *a priori* choice to focus on adult fish was made to obtain as much as possible a balanced sample size per annual ring and to avoid poor fitting due to a large number of fish for which fewer age observations than parameters were available (e.g. Alos et al. 2010). Moreover, focusing on adult fish, for whom interannual growth has begun to decrease, can provide a more reliable estimate of asymptotic body sizes (Kuparinen et al. 2016). Lastly, considering flatfishes sexual dimorphism and the lack of male specimens, the subset was restricted to include 38 females only (271-370 mm; age max 15 years). Figure 5.3.2.2 shows spatial-temporal distribution of this final dataset by sampling station and year. Soles in the Adriatic Sea are characterized by an opposite pattern of deposition as regard other fishes of temperate and cold waters: opaque ring during winter/spring and transparent ring in summer/autumn (Froglia and Giannetti, 1985). One opaque and one transparent ring are considered an annual growth (annulus) (Carbonara and Follesa, 2019). Considering the ring deposition pattern and the spawning period (autumn-winter), the age at each opaque growth increment was assigned as follows: 1st increment 0.5 years (age 0+), 2nd increment 1.5 years (age 1+), 3rd increment 2.5 years

(age 2+), and so on. Image processing and measurements during the aging process were performed using and following the workflow suggestions by the open-source R package RfishBC (Ogle, D.H. 2022. RFishBC. R package version 0.2.4.9000, https://derekogle.com/RFishBC/).

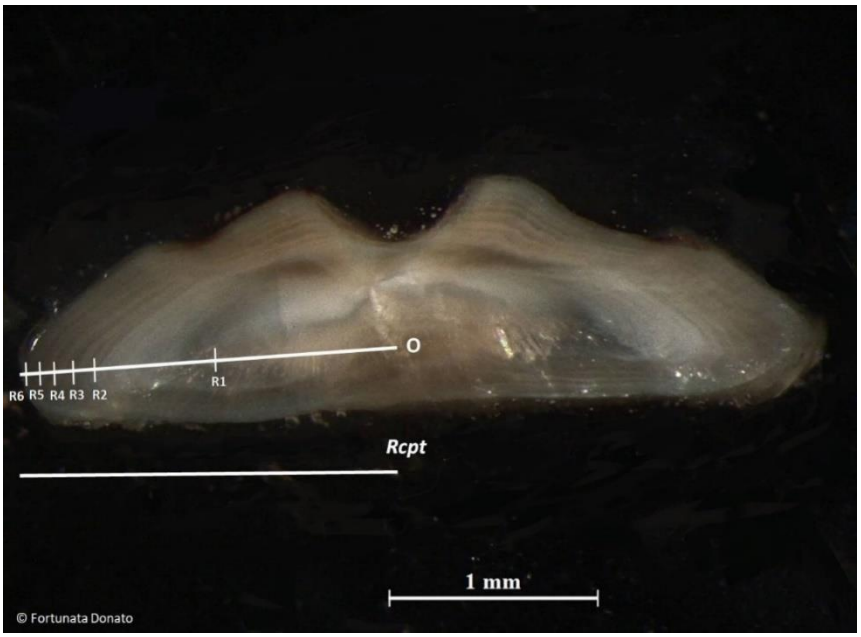

Figure 5.3.2.1. Sagittal otolith from 6-year-old common sole. Definition of the measurements taken during the aging process: radius length (Rcpt) and opaque rings distance from the core (R1, R2, R3. etc.).

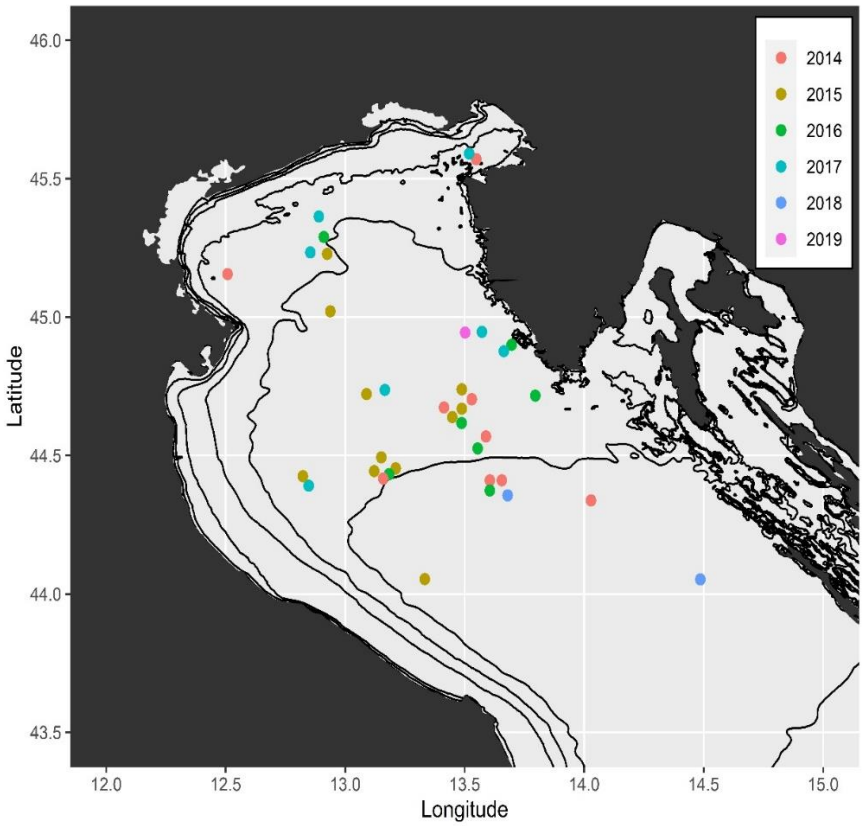

Figure 5.3.2.2. Spatial-temporal distribution of back-calculated individuals by year from SoleMon survey in northern-central Adriatic Sea. Colors correspond to different year.

5.3.3. Growth analyses

Back-calculation permits to infer the length of a fish at previous ages from the width of the annual increments recorded in the otoliths (Campana, 1990; Fossen et al., 1999). However, only when there is a strong relationship between otolith length and fish body length, it is possible to reconstruct individual growth trajectories through back-calculation techniques (Pilling et al., 2002).

Lengths at-age were back-calculated using the Fraser-Lee method (Fraser, 1916; Lee 1920). The underlying concept of the model is that growth increment of the calcified structure (ratio of Ri to Rcpt) is, on average, a constant proportion of the growth increment in length of the fish (ratio of Li to Lcpt).

Eq. 1 $$L_i = a + \left(L_{cpt} - a\right)\frac{R_i}{R_{cpt}}$$

where *Ri*, *Li* are the radius and length at age *i* , *Rcpt*, *Lcpt* are the radius and length at time when fish was captured and *a* is the intercept of the fitted "L-on-R" linear regression (Francis 1990). An alternative

non-linear relationship hypothesis was also tested but there was no evidence to reject the simpler model; models comparison and validation are shown in Supplementary materials (S.1.1).

To account for individual variability, the back-calculated length-at-age data were fitted to a non-linear mixed-effects model of longitudinal data (Pilling et al., 2002; Alos et al., 2010) using the modern and efficient stochastic approximation expectation maximization (SAEM) algorithm (Delyon, Lavielle, & Moulines 1999; Kuhn & Lavielle 2005). This algorithm is considered a state-of-the-art method for fitting non-linear models and is available as an open source R package available in CRAN (Comets et al. 2017). The use of mixed effects models allows to take into consideration both population parameters (fixed effect) and inter individual variability treating each parameters for each individual as a random effect. For the purpose of this study, growth trajectories were summarized through two different von Bertalanffy (VB) growth model: a monophasic form based on 3 parameters (equation 2; hereafter VB 3-par) and a biphasic implementation that allows for a change in the growth parameter at a specific moment of the lifespan (equation 3; hereafter VB 5-par).

Eq.2 $$L_{ij} = L_{\infty i}\,(1-exp(-k_i(t_{ij}-t_{0i}))) + \varepsilon_{ij}$$

where L_{ij} is the size of fish i at age j, $L_{\infty i}$ the asymptotic length of fish i, k_i the intrinsic growth rate of fish i, t_{ij} is the age j of the fish i, t_{0i} is the time when the fish i has zero size, and ε_{ij} a normally distributed error.

Eq.3 $$L_{ij} = L_{\infty i}\,(1-exp(-k_{0i}(t_{ij}-t_{0i}))) + \varepsilon_{ij} \quad \text{for } t_{ij} < t_{1i}$$

$$L_{ij} = L_{\infty i}\,(1-exp(-k_{0i}(t_{1i}-t_{0i})\,(-k_{1i}(t_{ij}-t_{1i}))) + \varepsilon_{ij} \quad \text{for } t_{ij} > t_{1i}$$

where k_{0i} and k_{1i} are the growth parameters before and after the moment of growth change (t_{1i}).

In the models the individual parameters were derived applying a transformation to the random parameters sampled from normal distributions (Comets et al. 2017). In this case we applied the logarithmic function for L_∞, k_0, k_1 and t_1 (log-normal distribution; to assure positive values) and the identity function for t_0 (normal distribution, allowing negative value). To optimize convergence, initial values for the population parameters (fixed effect) were provided considering plausibility of life histories of the species (Froese and Pauly, 2022) and information from previous analysis (i.e. FAO-GFCM 2021): 380 mm for L_∞, 0.3 years^{-1} for k_0, -0.5 years for t_0, 0.2 years^{-1} for k_1 and 1.8 years for t_1. Nevertheless, since non-linear optimization algorithms are known to be quite sensitive to starting values, a sensitivity analysis on initial values of the parameters was performed. Alterative values tested were: + 20% and -20% of initial values

used in Vallisneri et al. (2000) growth parameters for female (only available for *Linf*, *k0* and *t0*). Model validation and selection between the two growth alternative formulations were based on visual inspection of individual prediction residual plots, where predictions are computing using the conditional mode of the parameter's distribution (or Maximum A Posteriori; MAP), and Normalized Prediction Distribution Errors (NPDE), a simulated residuals specifically adapted to nonlinear mixed effect models (Brendel et al.2006; Comets et al. 2010). Moreover, models were compared through the Akaike criterion (AIC), and Schwarz's information criterion (BIC). The model that minimizes both estimators was retained as the best growth function. Individual estimates of parameters in common between models (L_∞, k_0, t_0) were compared using Student's two-sample t-test. Finally, a comparison with a model without random effect (fitted by nonlinear least-squares model) was performed on the biphasic formulation to test and verify the foreseen improvement in parameter estimation due to the intrinsic ability of the mixed effect model to explicitly consider and treat individual variation in growth. All the growth analyses have been implemented in R statistical software (R Core Team, 2022) using the "*saemix*" library. Full details of R Implementation of the SAEM Algorithm can be find in Comets et al. 2017.

5.3.4. Stock Assessment application

To compare and discuss the possible effects of the application of the two growth curves (3-par vs 5-par VB) on estimates of management quantities, the same assessment model of FAO-GFCM working group (Stock Synthesis, SS; Methot and Wetzel, 2013) was used. Stock Synthesis is programmed in the ADMB C++ software and searches for the set of parameter values that maximizes the goodness-of-fit, then calculates the variance of these parameters using inverse Hessian providing estimates for biomass, recruitments, fishing mortality and selectivity. For practical reasons, overall model structure has been kept the same as the reference model of the ensemble grid used during the last FAO-GFCM benchmark session in 2021 (FAO-GFCM, 2021). Models' configuration and setting are presented in detail together with a summary of input data and functional forms used in the dedicated section of Supplementary Materials (S.2.1). The SS models used were a one-area yearly model where the population consisted of 20+ age-classes (with age 20 representing a plus group) with sexes combined (males and females are considered together). The models relied on historical GSA17 landings data from 1958 divided by fleet and tuning data were provided from SoleMon survey (Table S.2.1.1 in Supplementary Materials). Numbers at length in the fisheries and survey data were converted into ages inside the model using a versatile version of the von Bertalanffy growth model (Schnute, 1981) that does not directly depend on t_0. According to the benchmark reference run configuration, time-invariant dome shape selectivity was

set for all fleets, natural mortality was based on average values of Gislason & ChenWatanabe vectors by age and the steepness in stock-recruitment relation was fixed at 0.9 (Table S.2.1.2 in Supplementary Materials). The only major changes made for the purpose of this study were the fixed growth parameters L_∞, k_0 and k_1 which, based on the growth pattern being analysed, have been replaced within each SS model with those resulting from the growth analyses conducted in this study (at the population level). Specifically, the change in growth in the biphasic model was managed through a specific SS option that allows the user to create age-specific *k* multipliers from a certain age onwards. Interconnected diagnostic test (Carvalho et al., 2021) were used to compare and select the best model. The procedure is based on the following four properties as objective criteria for evaluating the plausibility of a model: model convergence and likelihood, fit to the data (run-test and joint residuals), model consistency (retrospective analysis), and prediction skill (hindcasting). The results were discussed in terms of estimates of spawning-stock biomass (SSB) and fishing mortality and their ratio on reference points (estimated internally by SS model and calculated as 40% of the virgin biomass; FAO-GFCM, 2021). The R package "*ss3diags"* (github.com/JABBAmodel/ss3diags) has been used to produce all the diagnostic plots and table regarding the stock assessment application.

5.4. Results

5.4.1. Growth analyses

Analyses showed in section S.1.1. of the Supplementary Materials validated the existence of a linear relationship between total fish length (*Lcpt*) and otolith size at the time of capture (*Rcpt*) (r^2 = 0.91, *p-value* < 0.001). Since the *p-value* of the intercept is also significant the Fraser-Lee (FRALE) method was confirmed as the more appropriate and used to back-calculate lengths at-age data from otoliths. Back-calculated growth trajectories by individuals are shown in Figure 5.4.1.1. Moreover, data by year and year-class has been added in Supplementary Materials (Figure S.1.2.1). The colored points of the curves represent the intersection between each annulus measured on the otolith and the back-calculated fish length value at that time.

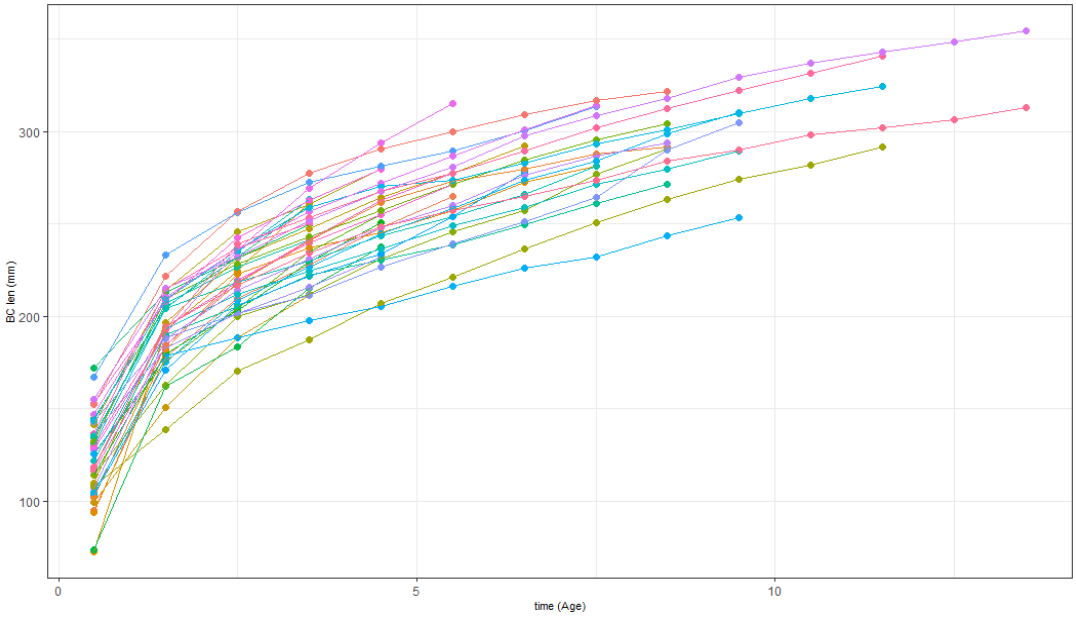

Figure 5.4.1.1. Individual common sole growth trajectories back-calculated from otoliths.

Table 5.4.1.1 revealed a huge fish length increment between age 0+ and age 1+ (67 mm) followed by a growth stabilization (12 mm on average from age 2+ onwards). This is in accordance with the hypothesis of a biphasic growth pattern in which young individuals grow faster in youth than in adulthood. Standard deviation shows more instability from age 10+ onwards due to a smaller number of data points.

Table 5.4.1.1. Mean back-calculated length for each growth increment for common sole analysed in the study. SD = standard deviation. MLI = mean length increment between subsequent annual rings (e.g. the back-calculated TL at the 2° annual ring minus the back-calculated TL at 1° annual ring, etc.).

N annuli	Reference age	N specimens	Mean length (mm)	SD	MLI (mm)
1	0+	38	124	22.9	-
2	1+	38	192	19.9	68
3	2+	38	219	19.7	27
4	3+	38	239	21.1	20
5	4+	32	252	22	13
6	5+	25	264	22.8	12
7	6+	21	274	21.8	10
8	7+	19	284	22.4	10
9	8+	15	291	20.8	7
10	9+	9	298	23.9	7
11	10+	5	313	23	15
12	11+	5	321	22.9	8
13	12+	2	328	29.7	7
14	13+	2	334	29.4	6

Despite both 3-par and 5-par VB curves were successfully fitted without major convergence issues in the models, fit to the data was appreciably superior in the biphasic formulation (e.g. ID 5479; Figure 5.4.1.2 and Figure S.1.11.1 in Supplementary Materials).

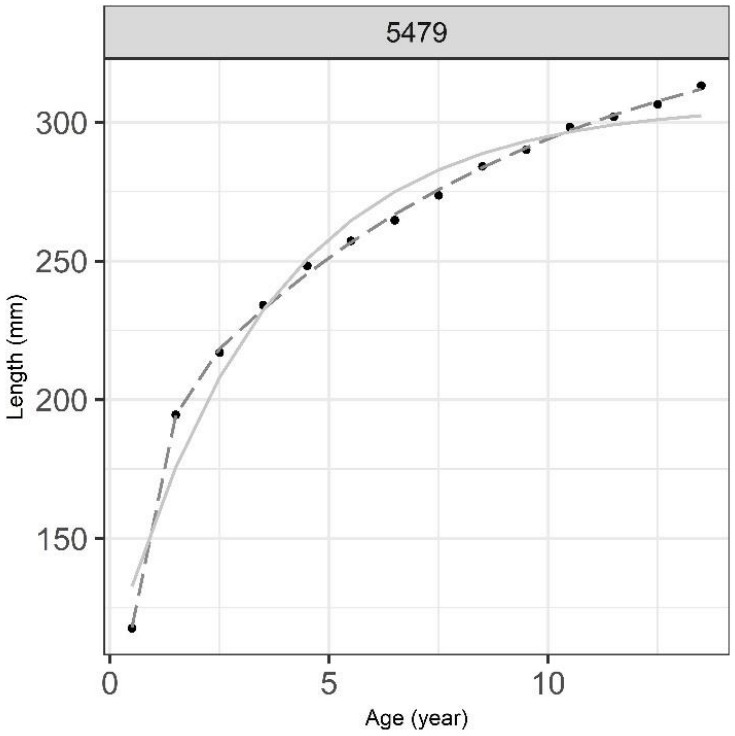

Figure 5.4.1.2. Individual predictions computed using Maximum A Posteriori (MAP) for a 13+ year old specimen (ID: 5479). The black points correspond to observed back-calculated lengths-at-age, the light grey line to the monophasic von Bertalanffy growth model (3-par VB), and the dark grey dashed one to the biphasic model (5-par VB).

All model's diagnostics performed revealed a systematic discrepancyin the 3-par VB (Figure S.1.10.1 and S.1.10.2 in Supplementary Materials) which is absent in the 5-par formulation (Figure S.1.5.1 and S.1.5.2 in Supplementary Materials). In particular, NPDE boxplot showed that the conventional 3-par model had a clear tendency to underestimate age 1+ and late ages while overestimate intermediate ages (Figure 5.4.1.3 left side). This error in predicting length-at-age data leads to an overestimation of t_0 (more negative value) and an underestimation of L_∞. On the other hand, the 5-par VB had no specific trends (Figure 5.4.1.3 right side). Moreover, model selection via statistical criteria selected the 5-par VB model as the best one (Δ AIC: 329; Δ BIC: 310, Table 5.4.1.2) confirming the systematic bias produced by the 3-par VB model. For each parameter effect estimated in the models, current value and relative coefficient of variation (CV%) are listed in Table 5.4.1.2. Sensitivity analysis performed on the 5-par VB parametrization reveals no drastic change in model estimates when alternative sets of initial values were used (Δ < 10% for all parameters when compared to the set adopted in the analysis; Table S.1.6.1 in Supplemntary Materials). All fixed parameters were well estimated, with coefficients of variation below

15%. while variation around the estimates of the random effects was quite high (CV > 30%) for both models. Moreover, AIC value and standard error of in common fixed effect were smaller in the 5-par VB mixed effect formulation rather than the nonlinear least-square alterative where no random effect is considered (section S.1.7 of Supplementary Materials).

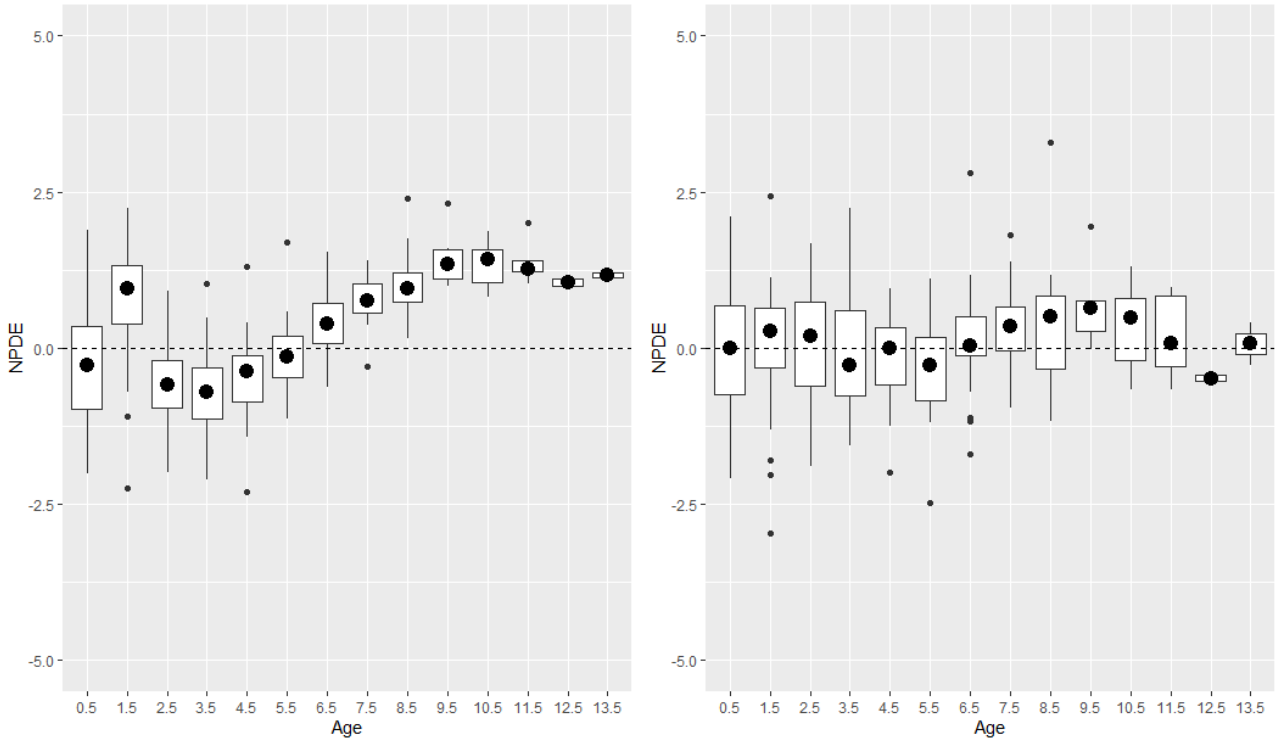

Figure 5.4.1.3. Normalized Prediction Distribution Errors (NPDE) based on 3-par VB (left side) or 5-par VB growth curves (right side). The dots are the median values, the boxes the 25 and 75% percentiles, the bars the minimum and maximum non-outlier values and the single black points are outlier values.

Table 5.4.1.2. Parameters estimates comparison between monophasic and biphasic von Bertalanffy growth curves. CV: coefficient of variation. AIC and BIC: statistical criteria used in model selection..

Model	Effect	L∞ (CV%)	k_0 (CV%)	t_0 (CV%)	k_1 (CV%)	t_1 (CV%)	AIC	BIC
3-par VB	fixed	302 (1.7)	0.35 (6.8)	-1.19 (9.74)	NA	NA	2298	2314
	random	0.01 (32.6)	0.12 (32.8)	0.38 (30.7)	NA	NA		
5-par VB	fixed	397 (3.6)	0.31 (7.4)	-0.76 (9.3)	0.11 (10.5)	1.5 (4.61)	1969	2004
	random	0.02 (46.7)	0.09 (44.1)	0.13 (31)	0.20 (42.5)	0.05 (33.6)		

The distributions of individual growth parameters are shown in Figure 5.4.1.4 Specifically, L_∞ was significantly smaller in the 3-par VB than in the 5-par VB (Figure 5.4.1.4a; 5-par VB: 307 – 462 mm, 3-par VB: 253 – 360 mm; *t*-test*: p-value* < 0.05). The parameter t_0 varied between -1.42 and 0.05 for the 5-par VB, and -2.58 and -0.21 for the 3-par VB (Figure 5.4.1.4b). In this case the value was significantly higher for the biphasic curve (*t*-test: *p-value* <0.05). The parameter t_1, responsible for the inflection point of the biphasic growth curve, varied from 0.85 to 2.11 years (Figure 5.4.1.4c). Finally, in terms of individual intrinsic growth rate, k_0 statistically differ between the two curves (Figure 5.4.1.4d; 5-par VB: 0.14 – 0.51 $year^{-1}$, 3-par VB: 0.15 – 0.71 $year^{-1}$; *t*-test*: p-value* <0.05), whereas for the 5-par VB k_1 ranged from 0.04 to 0.3 $year^{-1}$ (Figure 5.4.1.4e). Considering the biphasic growth pattern, after t_1 a general decrease in growth rate from k_0 to k_1 was expected.

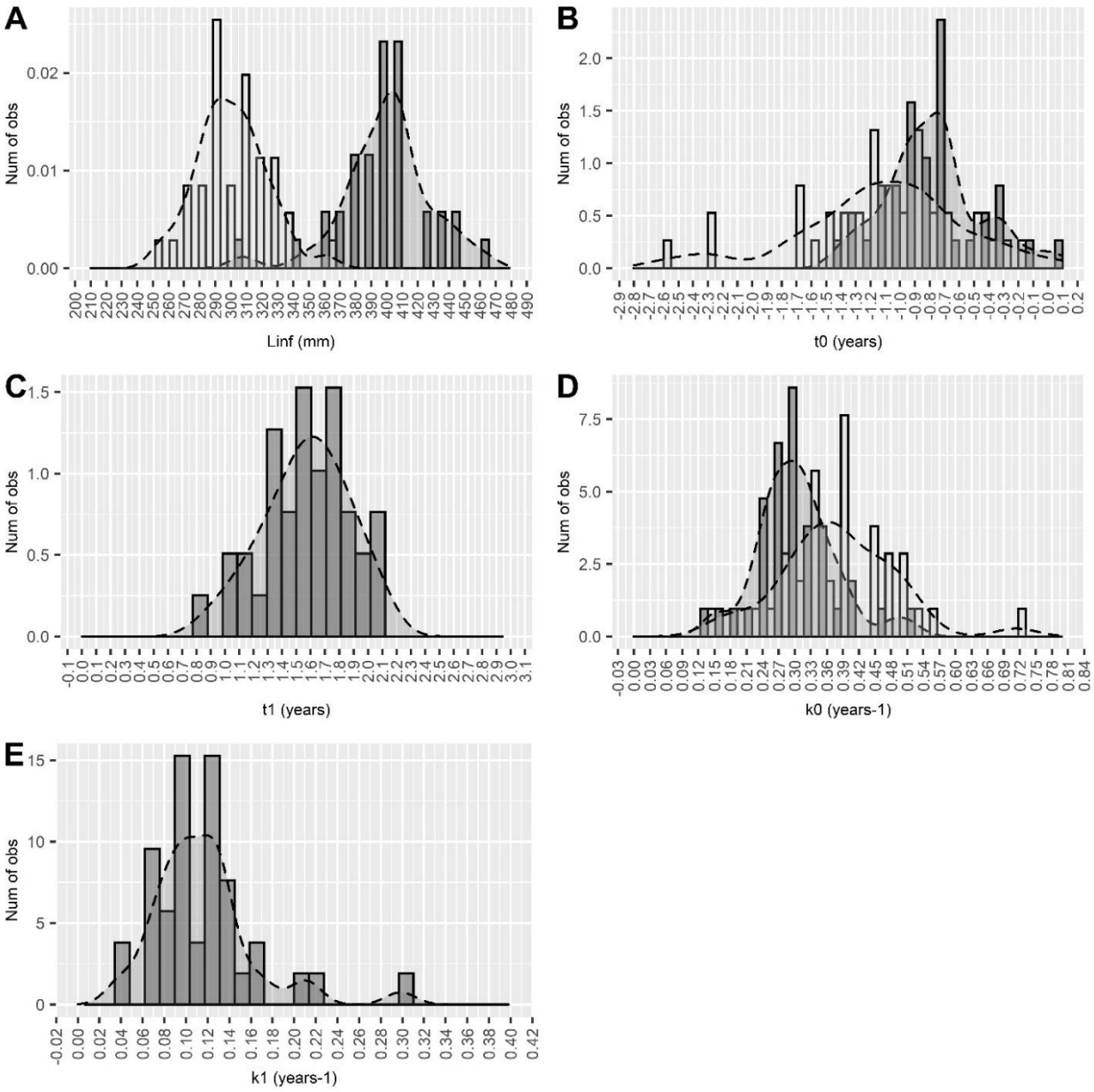

Figure 5.4.1.4. Frequency distribution of individual parameters from SAEMIX non-linear mixed effects model obtained using the conditional mode of the parameters distribution (or Maximum A Posteriori; MAP): a) L∞ estimated from 3-par and 5-par von Bertalanffy growth models; b) t0 estimated from 3-par and 5-par von Bertalanffy growth models; c) t1 estimated from 5-par von Bertalanffy growth model; d) k0 estimated from 3-par and 5-par von Bertalanffy growth models; e) k1 estimated from 5-par von Bertalanffy growth model.

Finally, correlation matrixes of random effect were reported in Supplementary Materials (Figure S.1.4.1 and S.1.9.1). The analysis showed an overall quite strong correlations among the individual parameters in both growth formulation alternatives. In term of relationship between L_∞ and intrinsic growth rate, both k_0 (r^2 = -0.75, *t*-test*: p-value* <0.001 in 5-par VB; r^2 = -0.47, *t*-test*: p-value* <0.01 in 3-par VB) and k_1 (r^2 = -0.53, *t*-test*: p-value* <0.001) were strongly negatively correlated. Also, L_∞ and t_0 were slightly negatively correlated (r^2 = -0.64, *t*-test*: p-value* <0.001 in 5-par VB; r^2 = -0.49, *t*-test*: p-value* <0.01 in 3-par VB). The parameters k_0 and t_0 showed a positive correlation in both alternatives (r^2 = 0.61, *t*-test*: p-value* <0.001 in 5-par VB; r^2 = 0.85, *t*-test*: p-value* <0.001 in 3-par VB). The two intrinsic growth rate parameter k_0 and k_1 showed a positive correlation (r^2 = 0.49, *t*-test*: p-value* <0.01). Interestingly, no significant correlation was found between the growth inflection point t_1 and other parameters.

5.4.2. Stock Assessment application

Within the 5-par VB SS assessment model tested, the age at which the change of growth occurs was approximated to age=2, since the software does not allow the use of intermediate ages (e.g. age 1.5). For both models (3-par VB & 5-par VB) convergence gradient was relatively small (<1.00E-04) and the Hessian matrix for the parameter estimates was positive definite (Table 5.4.2.1). The total likelihood of the 5-par VB model is lower than the 3-par (224.95 vs 166.97; Δ=57.98). More precisely, the difference between the two models is driven by the component of the fit to length data (245.06 vs 189.81; Δ=55.25) with the values relating to data from surveys and trawlers fleet appreciably lower in 5-par VB (Table 5.4.2.1). This is confirmed by the LFD plots where a slightly model improvement fit is detectable by passing from the three-parameter growth curve to the five parameter one (Figure S.2.2.1 in Supplementary Materials). The interconnected diagnostics showed a general improvement in scores when moving from the three to the five parametrizations. The most appreciable difference was in the model consistency where 3-par VB estimated Mohn´s indices for both retrospective (ρM) and forecast projections (ρF) were higher than the threshold indicating an undesirable retrospective pattern for both SSB and fishing mortality (Table 5.4.2.1). Despite no change in the trends of the time series is detected, the 3-par VB model showed a more optimistic status of the stock characterized by a higher amount of biomass and a lower F compared to the 5-par VB one. This is confirmed by looking at the estimates in relation to reference points, where the increment of 3-par VB value compared to 5-par VB one was approximately 40% for SSB (SSB/SSB_{target}: 1.39 for 3-par VB and 0.97 for 5-par VB in 2019; Figure 5.4.2.1a) and the decrement of F was around 35% (F/F_{target}: 0.57 for 3-par VB and 0.87 for 5-par VB in 2019; Figure 5.4.2.1b).

Table 5.4.2.1. Interconnected diagnostic table following the procedure proposed by Carvalho et al. (2021). Convergence and likelihood: final convergence gradient must be relatively small (e.g., < 1.00E-04) and the Hessian matrix for the parameter estimates must be positive definite; total likelihood of SS model is composed of a number of components, including the fit to the survey index, fishery length frequency data and catch data. Fit to the data: runs tests residual as judged by the p-values computed for each series; the joint-residual indicated a good fit to the data when RMSE (root mean square error) is less than 30 %. Consistency: Both ρM and ρF are measures of average bias across the years under evaluation. Following a "rule of thumb" by Hurtado-Ferro et al. (2015), values should fall within the range of -0.15 to 0.20 for the longest-lived species. Prediction skill: hindcasting cross-validation technique compare observations to their predicted future values. MASE values lower than one indicate that forecast values under consideration performed better than a naïve baseline. Colors denote the passing (green) or failure (red) of the test according to the above listed criteria.

		Diagnostic components	3-par VB	5-par VB
Convergence and likelihood	Convergence	Final convergence	2.80E-05	5.79E-05
		Positive Hessian matrix	Yes	Yes
	Likelihood components	Total	224.95	166.97
		Catch	9.90E-12	3.93E-11
		Equil_catch	1.47E-13	1.09E-11
		Survey	-20.1	-20.40
		Recruitment	-0.01	-2.45
		InitEQ_Regime	2.33E-31	2.23E-31
		Length_comp Total	245.06	189.81
		Len_GNS_ITA	38.41	48.91
		Len_TBB_ITA	18.14	17.90
		Len_GTR_HRV	7.21	3.10
		Len_OTB_ITA	41.82	36.56
		Len_DRB_HRV	0.94	0.83
		Len_SoleMon	138.53	82.51
Fit to the data	Run test	Survey Index	Passed	Passed
		Len_GNS_ITA	Passed	Passed
		Len_TBB_ITA	Passed	Passed
		Len_GTR_HRV	Passed	Passed
		Len_OTB_ITA	Passed	Passed
		Len_DRB_HRV	NA	NA
		Len_SoleMon	Passed	Passed
	Joint-residuals	Survey Index	16	15
		Length	3.6	3.2
Consistency	Retrospective analysis	Retro_SSB	0.30	-0.14
		Forecast_SSB	0.27	-0.14

		Retro_F	-0.18	0.11
		Forecast_F	-0.18	0.19
Prediction skill	Hindcasting (MASE)	MASE Index_Survey	0.84	0.76
		MASE GNS_ITA	0.13	0.13
		MASE TBB_ITA	0.27	0.26
		MASE GTR_HRV	0.13	0.16
		MASE OTB_ITA	0.58	0.58
		MASE DRB_HRV	NA	NA
		MASE Len_Survey	0.30	0.28

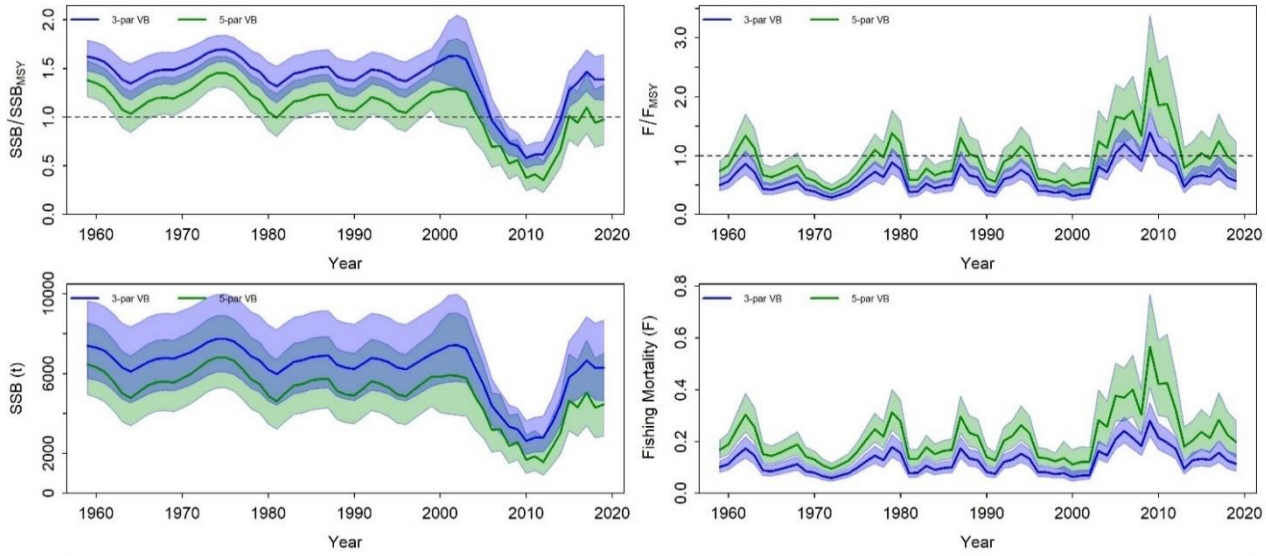

Figure 5.4.2.1. Comparison of stock status trajectories based on Stock Synthesis assessment models: a) Biomass outcomes in absolute value (SSB) and relative to the reference point (SSB/SSBtarget); b) Fishing mortality outcomes in absolute value (F) and relative to the reference point (F/Ftarget). The blue line represents the 3-par VB model result, while the green line represents the 5-par VB one. Shaded areas represent 95% confidence intervals.

5.5. Discussion

In this study we assessed and compare two different growth model formulation based on von Bertalanffy's equation for common sole in norther-central Adriatic Sea (GSA 17): the conventional three parameter formulation (3-par VB), which assume a constant growth throughout fish life, and the biphasic alternative (5-par VB), which instead separates the growth of individuals into two phases based on the assumption of re-allocation of energy during individual lifespan (Lester et al., 2004; Rogers-Bennett and

Rogers 2016). In agreement with the results presented for other species with similar growth patterns (Alos et. al. 2010; Minte-Vera et al., 2016), our analyses confirmed that a biphasic model displays a better fit to length-at-age data for both younger and older ages (Δ AIC: 329; Δ BIC: 310) to the conventional monophasic formulation. Using the 3-par VB model, diagnostic plots showed systematic age-specific biases at both the individual and population level that led to a severe underestimation of L_∞.This is driven by the assumption of a constant intrinsic growth parameters. Conversely, L_∞ from biphasic model were more biologically appropriate displaying a better fit to length-at-age data for older ages and effectively reflected real sampled values in northern and central Adriatic Sea (i.e. max TL: 39.3 cm in survey data, 43 cm in commercial data; Masnadi et al. 2021). The more reliable estimate of asymptotic length is due to the biphasic model's ability to accommodate a fast growth in early years (with the growth parameter k_0) and a sharp decrease in growth (with the growth parameter k_1) that occurs after the age of change (t_1), thus confirming that different growth parameter values were needed for juveniles and adults (Boukal et al., 2014). This change in growth, which occurs approximately in Adriatic sole in the middle of the second year of life (1.5 yr), also allows a better estimate of t_0 leading to a better fit to length-at-age data for younger ages. Following the theory that growth in size would decrease as a consequence of reproductive effort (Lester et al., 2004; Charnov 2005), the value of t_1 estimated by the biphasic model was in line with the spatial distribution studies conducted in the Adriatic that clearly showed a segregation between age groups 0–2, characterized mostly by sexually immature specimens who occupy coast shallow water, and the rest of the mature population who migrate towards deeper waters (Scarcella et al., 2014). In common parameter correlations from biphasic models are similar to the monophasic one, and in line with previous studies (Helser & Lai, 2004; Minte-Vera et al., 2016; Mollet, et al. , 2010). Interestingly, the two growth rate of the equation (k_0 and k_1) showed a positive correlation meaning that a fish displaying fast juveniles growth will have a high growth parameter also after maturation. However, no correlation has been found with the inflection time t_1 corroborating the hypothesis that sexual maturation seems to be a specific characteristic of the population more than a trait related to individual itself. This could be more linked to other factors such as the change of habitat and diet that occur during the ontogenetic coast-offshore migration of the species (MediSeH 2013). High estimates of among-individual variation in growth parameters should not be considered as a problem. In fact, studies conducted in the Adriatic have revealed great variability in the growth rate of common sole in general: some specimens grow by 2 cm in a month, while others, of the same age group, need an entire year (Piccinetti and Giovanardi, 1984). On the contrary, since individual variability in growth can strongly influence the reliability and accuracy of estimates of population parameters, the advantage of a

mixed effects models is that assume that the estimated growth parameters for each fish in the population represent a subsample of the growth parameters characteristic of the population itself (Pilling et al., 2002). In this sense, a mixed effect models applied to sole back-calculation data (multiple observations of the same subjects over lifespan) gives the possibility of explicitly taking into account individual variation in growth as a random effect in the model. As a result, the comparison with method where no random effect was considered showed an improvement in the precision of population parameters estimates when individual variability is considered, confirming once again the importance and benefits deriving from such an approach. Comparing growth data from previous studies on the species, mean lengths-at-age obtained from biphasic formulation fell within the general variability found in the Mediterranean area and in particular in GSA17 (Vallisneri et al., 2000; Fabi et al., 2009; FAO-GFCM 2021; see Table S.1.12 in Supplementary materials). However, an increase in the difference of mean length with age between the biphasic curve reported in this study and the others reported in literature was found. As for many other species, the interpretation of the growth band of the common sole can be prone to several error sources, such as the presence of false growth increments and the growth bands overlapping in older specimens (Carbonara et al., 2018; Etherton et al., 2019) The variability in age data could result from ecological, physiological, and genetic variability but it might also be the result of underrepresentation of small or large individuals in the sample (Neves et al. 2022), different age schemes (Carbonara and Follesa, 2019), otolith preparation methods (Smith et al., 1997), age criteria (Hüssy et al., 2016), and reader experience (Kimura and Lyons, 1991; Carbonara et al., 2019) or to a combination of all the aforementioned effects. For example, the use of only adult specimens leads to a greater risk of occurrence of the so-called "Rosa Lee effect" according to which in historically heavily exploited stocks (such as the one here) the removal of faster-growing individuals by selective fishing translates in a population dominated by slower-growing individuals (Lee, 1912). Ignoring this demographic effect most likely leads to an underestimation of the true average growth parameters of the population under analysis. In simulation framework, this phenomenon has been proven to introduce bias in the estimation of relevant quantities used for fisheries advice (Kraak et al., 2019). Another precondition that can reduce the reliability of the result was the assumption that the back-calculation procedure produced length-at-age measurement without error. In fact, even through the use of standardized and semi-automated reading procedures (i.e. use of the *RfishBC R* package) utilized by trained experts, the occurrence of observation error is very plausible. According to growth theory, the variability in length should be lower at younger ages and increase with older ages. On the contrary, the observed range of growth trajectories shown in this study remains quite constant and independent of the age. This is probably the result of a more

uncertain measures for annuli that are further away from the age of capture since back-calculation did not undergo any validation process. However, a full validation process by direct, semidirect and indirect methods (Campana, 2001) involve considerable effort and has to be properly designed to do that as a central aim (Vigliola and Meekan, 2009; Carbonara et al., 2018). Having a much larger data set and more readers could help in the exploration of the impact of propagation of error related to the back-calculation method. Moreover, in a situation of lacking data for very old individuals, such as most of the historically overfished stocks in the Mediterranean Sea, L_∞ is more subject to strong dependence on model structure and data on younger fish. This suggests that the true value of the asymptotic length may be different than that estimated using this constrained data set. In this context, it is even more important to promote the choice of a biphasic model structure that has proven to be statistically sound in comparison to the conventional one. Well aware of limitation presented, the results remain valid if contextualized in relation to the comparison between the monophasic and biphasic growth equations which remains unrelated to age validation *per se*. Indeed, since the two alternative models were fitted to the same dataset, the comparison is independent of possible sources of error in the procedure used to obtain the age backwards. As a final step of this study a simplified stock assessment comparison was performed on Adriatic sole size-composition based model to the quantify and discuss consequences of the two alternative growth models (monophasic vs biphasic) on the stock assessment outcomes. To our knowledge, this is one of the first attempt to analytically evaluate the effect of biphasic growth implementation in highly-structured stock assessment model such as Stock Synthesis. Clearly stating that the purpose of this study is not to provide management advice for the species under analysis, the result here presented confirmed that incorrect specification of growth within integrated models can have a significant impact on biomass and fishing mortality estimates. In age-based assessment models that rely on size-observation, where growth parameters are used to better fit the expected length composition to the observed length data and to translate them into population numbers-at-age, this change in growth pattern can directly affect biomass estimates (Maunder and Piner, 2015) and related management reference points such as spawning stock biomass at MSY (Lorenzen, 2016). In this particular case, a higher mean length of the oldest age in the 5-par VB (i.e. due to higher L_∞) caused the estimated relative abundance of the oldest age to reduce to fit the length composition of the largest fish. This phenomenon produced an increase in the estimated fishing mortality and a consequent lower estimate of SSB (Maunder and Piner, 2015). It must be remembered that this reduction is not always linked to a greater fishing mortality but can also be explained by the appearance of a cryptic biomass that can arise from the selectivity pattern used (Maunder and Piner, 2015). Despite this, the use of the same dome-shape selectivity for both models excluded that it had a

significant effect on the differences found here. Even if no drastic change has been notice comparing diagnostic for the two models, retrospective analyses clearly indicate a lack of predictive ability of the 3-par VB formulation. This, together with the improvement in the likelihood component, agrees and reinforces the results of the previously growth analyses which have already demonstrated how the biphasic curve is statistically and biologically more adequate than the conventional one. In relation to reference point the results showed that, the 3-par VB estimate would result in an appreciable overestimation of 40% in SSB/SSB_{target} and underestimation of 35% in F/F_{target} providing an overly optimistic view of stock status. This means that the use of monophasic growth pattern would lead to a critical underestimation of the risk of overfishing with respect to the biphasic one. These results are in line with studies showing that reference points are highly sensitive to biological parameters (Maunder, 2012) and in particular to asymptotic length (Aires-da-Silva et al., 2015). However, how the growth component affects results can vary differently based on data availability, assessment model choice and assumptions about process sub-models (Lorenzen, 2016). It is therefore important to contextualize these results specifically for the type of assessment model under discussion (model based on size-composition observation) while a generalization to purely aged-based model it is not recommended and sensible. Moreover, as reported in the description of the models, nothing has been changed apart from the growth pattern in the parameterization of the two models with respect to the reference run used during the FAO-GFCM benchmark assessment conducted in 2021 (Masnadi et al., 2021). In this regard, it has been shown how, the use of fixed steepness and natural mortality values, could introduce bias in the estimated derived quantities of interest (Mangel et al., 2013). In this sense, a simulation study from Thorson et al. (2015) highlighted that sensitivity of reference points to change in growth parameters was higher than those for recruitment parameters, but smaller than those for natural mortality. More in-depth studies conducted through the use of operating models in a proper simulation framework (e.g. *ss3sim R* package by Anderson et al., 2014), would be preferred and encouraged.

5.6. Conlusion

Although the results are quite regional (Adriatic Sea) and aware of the above reported caveats and limitation of the study, we believe that the comparison between the two sets of VB parameters presented is adequate to provide general information, indications and food for thought leading to a more careful selection of growth alternatives in building up specific case of stock assessment models. While representing a simplification, our analyses confirmed that, thanks to the greater flexibility of the biphasic model, a more precise estimate of the growth curve especially for older ages can have a substantial impact

on stock assessment results and scientific advice. This is especially true in management contexts where biomass estimates are used in the calculation of the fisheries total available catches (TACs) to be set for subsequent years (e.g. ICES advisory framework). As a final suggestion, stock assessment experts should consider more the use of biphasic growth curves in size-based assessment models when, on a case-by-case basis, they have proven to have superior fit than traditional ones.

5.7. References

Aires-da-Silva, A.M., Maunder, M.N., Schaefer, K.M., Fuller, D.W., 2015. Improved growth estimates from integrated analysis of direct aging and tag–recapture data: an illustration with bigeye tuna (*Thunnus obesus*) of the eastern Pacific Ocean with implications for management. Fish. Res. 163, 119-126.

Alós, J., Palmer, M., Balle, S., Grau, A. M., and Morales-Nin, B. 2010. Individual growth pattern and variability in Serranus scriba: A Bayesian analysis. ICES Journal of Marine Science, 67: 502–512.

Anderson, S.C., Monnahan, C.C., Johnson, K.F., Ono, K., Valero, J.L., 2014. ss3sim: an R package for fisheries stock assessment simulation with Stock Synthesis. PLoS One 9, e92725.

Anonymous. 2019. SoleMon Handbook.

Arneri, E., Colella, S. and Giannetti, G. 2001. Age determination and growth of turbot and brill in the Adriatic Sea: reversal of the seasonal pattern of otolith zone formation. Journal of Applied Ichthyology, 17: 256–261.

Beamish, R. J. & McFarlane, G. A. 1995. In “Recent developments in fish otolith research” (eds Secor, D. H., Dean, J. M. & Campana, S. E. 545–565; University of South Carolina Press, Columbia, 1995.

Boukal, D. S., Dieckmann, U., Enberg, K., Heino, M., & Jorgensen, C. 2014. Life-history implications of the allometric scaling of growth. Journal of Theoretical Biology, 359, 199–207. https://doi.org/10.1016/j.jtbi.2014.05.022.

Campana S.E. 2001. Accuracy, precision and quality control in age determination, including a review of the use and abuse of age validation methods. Journal of fish biology, 59: 197-242. https://doi.org/10.1006/jfbi.2001.1668.

Campana, S.E. 1990. How Reliable are Growth Back-Calculations Based on Otoliths? Canadian Journal of Fisheries and Aquatic Sciences, 47(11), 2219–2227. https://doi.org/10.1139/f90-246.

Carbonara, P., Ciccolella, A., De Franco, F., Palmisano, M., Bellodi, A., Lembo, G. et al. 2022. Does fish growth respond to fishing restrictions within Marine Protected Areas? A case study of the striped red mullet in the south-west Adriatic Sea (central Mediterranean). Aquatic Conservation: Marine and Freshwater Ecosystems, 1–13. https://doi.org/10.1002/aqc.3776.

Carbonara P., Zupa W., Anastasopoulou A., Bellodi A., Bitetto I., Charilaou C., Chatz- ispyrou A., Elleboode R., Esteban A., Follesa M.C., Isajlovic I., Jadaud A., García-Ruiz C., Giannakaki A., Guijarro B., Kiparissis S.E., Ligas A., Mahé K., Massaro A., Medvesek D., Mytilineou C., Ordines F., Pesci P., Porcu C., Peristeraki P., Thasitis I., Torres P., Spedicato M.T., Tursi A., Sion L. 2019. Explorative analysis on red mullet (Mullus barbatus) ageing data variability in the Mediterranean. Sci. Mar. 83S1: 271-279. https://doi.org/10.3989/scimar.04999.19A.

Carbonara, P., Intini, S., Kolitari, J., Joksimovic, A., Milone, N., Lembo, G., et al. 2018. A holistic approach to the age validation of Mullus barbatus L., 1758 in the Southern Adriatic Sea (Central Mediterranean). Sci. Rep. 8:13219. doi: https://10.1038/s41598-018-30872-1.

Carbonara, P., Follesa M.C., eds. 2019. Handbook on fish age determination: a Mediterranean experience. Studies and Reviews. No. 98. Rome, FAO. 2019. 180 pp.

Carvalho, F., H. Winker, D. Courtney, M. Kapur, L. Kell, M. Cardinale, M. Schirripa, T. Kitakado, D. Yemane, K.R. Piner, M.N. Maunder, I. Taylor, C.R. Wetzel, K. Doering, K.F. Johnson, R.D. Methot. 2021. A cookbook for using model diagnostics in integrated stock assessments Fish. Res., 240 (2021), Article 105959, https://doi.org/10.1016/j.fishres.2021.105959.

Charnov, E. L. 2005. Reproductive effort is inversely proportional to average adult lifespan. Evolutionary Ecology Research, 7:1221–1222.

Comets, Emmanuelle, Audrey Lavenu, and Marc Lavielle. 2017. Parameter Estimation in Nonlinear Mixed Effect Models Using Saemix, an R Implementation of the Saem Algorithm. Journal of Statistical Software, Articles 80 (3): 1–41. doi:10.18637/jss.v080.i03.

Day, T., and Taylor, P. D. 1997. von Bertalanffy's growth equation should not be used to model age and size at maturity. American Naturalist, 149: 381–393.

Delyon B, Lavielle M, Moulines E. 1999. Convergence of a Stochastic Approximation Version of the EM Algorithm. The Annals of Statistics, 27(1), 94–128.

Edwards, C.T.T., Hillary, R.M., Levontin, P., Blanchard, J., Lorenzen, K., 2012. Fisheries assessment and management: a synthesis of common approaches with special reference to deep water and data poor stocks. Rev. Fish. Sci. 20,126–153.

Eero, M., Hjelm, J., Behrens, J., Buchmann, K., Cardinale, M., Casini, M., Gasyukov, P., Holmgren, N., Horbowy, J., Hussy, K., Kirkegaard, E., Kornilovs, G., Krumme, U., Koster, F. W., Oeberst, R., Plikshs, M., Radtke, K., Raid, T., Schmidt, J., Tomczak, M. T., Vinther, M., Zimmermann, C., & Storr-Paulsen, M. 2015. Eastern Baltic cod in distress: biological changes and challenges for stock assessment. ICES Journal of Marine Science, 72: 2180–2186.

Enberg, K., Jørgensen, C., Dunlop, E.S., Varpe, Ø., Boukal, D.S., Baulier, L. et al. 2012. Fishing-induced evolution of growth: Concepts, mechanisms and the empirical evidence. Marine Ecology, 33(1), 1–25. https://doi.org/10.1111/j.1439-0485.2011.00460.x.

Etherton M., Songer S., Smith J., Bland B. 2019. Chapter 3: Flatfish. In: Vitale F., Worsøe Clausen, L., and Ní Chonchúir, G. (Eds.). Handbook of fish age estimation protocols and validation methods. ICES Cooperative Research Report No. 346, 36-58 pp. doi: 10.17895/ices.pub.5221.

EU Regulation 2017/1004 of the European Parliament and of the Council of 17 May 2017 on the establishment of a Union framework for the collection, management and use of data in the fisheries sector and support for scientific advice regarding the common fisheries policy and repealing Council Regulation (EC) No 199/2008. https://eur-lex.europa.eu/legal-content/EN/TXT/?uri=CELEX%3A32017R1004.

Fabi, G., Grati, F., Raicevich, S., Santojanni, A., Scarcella, G. & Giovanardi, O. 2009. Valutazione dello stock di Solea vulgaris del medio e alto Adriatico e dell'incidenza di diverse attività di pesca. Final Report. VI Piano Triennale della pesca marittima e acquacoltura in acque marine e salmastre 1 (tematica c – c6). Programma di ricerca 6-a-74 (133 – XVII pp.). Rome, Ministero per le Politiche Agricole e Forestali, direzione generale della pesca e dell'acquacoltura.

FAO-GFCM. 2021. Report of the Working Group on Stock Assessment of Demersal Species (WGSAD) – Benchmark session for the assessment of common sole in GSA 17, Scientific Advisory Committee on Fisheries (SAC). Online via Microsoft Teams, 12–16 April 2021.

FAO-GFCM. 2019. Report of the Working Group on Stock Assessment of Demersal Species (WGSAD), Scientific Advisory Committee on Fisheries (SAC). GFCM and FAO headquarters, Rome, Italy, 9-14 December 2019.

Fisher, W., Schneider M., Bauchot M.L. 1987. Fishes FAO d'identification des espèces pour les besoins de la pêche. Mediterranée et mer Noire, Vol. I – II. FAO, Rome, Italy, pp. 1–2.

Fossen, I., Albert, O.T., and Nilssen, E.M. 1999. Back-calculated individual growth of long rough dab (Hippoglossoides platessoides) in the Barents Sea. ICES J. Mar. Sci. 56: 689–696.

Francis, R.I.C.C., 2016. Growth in age-structured stock assessment models. Fish.Res. 180, 77–86. https://doi.org/10.1016/j.fishres.2015.02.018.

Fraser, CMcL. 1916. Growth of the spring salmon. Trans Pacif Fish Soc 1915:29–39.

Froese, R. and D. Pauly. Editors. 2022. FishBase. World Wide Web electronic publication. www.fishbase.org. Version 02/2022.

Froglia, C., & Giannetti, G. 1985. Growth of common sole Solea vulgaris (Quensel 1806) in the Adriatic Sea (Osteichthyes, Soleidae). Rapports et procés-verbaux des réunions Commission internationale pour l'exploration scientifique de la Mer Méditerranée, 29(8), 91-93.

Gebremedhin, S., Bruneel, S., Getahun, A., Anteneh, W., Goethals, P. 2021. Scientific Methods to Understand Fish Population Dynamics and Support Sustainable Fisheries Management. Water 2021,13, 574 https://doi.org/10.3390/w13040574.

Grati, F., Scarcella G., Polidori P., Domenichetti F., Bolognini L., Gramolini R., Vasapollo C., Giovanardi O., Raicevich S., Celić I., Vrgoč N., Isajlovic I., Jenič A., Marčeta B., Fabi G. 2013. Multi-annual investigation of the spatial distributions of juvenile and adult sole (Solea solea, L.) in the Adriatic Sea (Northern Mediterranean). J. Sea Res. http://dx.doi.org/10.1016/j.seares.2013.05.001.

Grønkjær, P. 2016. Otoliths as individual indicators: A reappraisal of the link between fish physiology and otolith characteristics. Marine and Freshwater Research, 67(79), 881–888. https://doi.org/10.1071/MF15155.

Haddon, M. 2011. Modelling and Quantitative Methods in Fisheries, 2nd ed. CRCPress, Boca Raton.

Helser, T. E., and Lai, H. L. 2004. A Bayesian hierarchical meta-analysis of fish growth: with an example for North American largemouth bass, Micropterus salmoides. Ecological Modelling, 178: 399–416.

Hernandez-Llamas, A. and Ratkowsky, D. 2004. Growth of Fishes, Crustaceans and Mollusks: Estimation of the von Bertalanffy, Logistic, Gompertz and Richards Curves and a New Growth Model. Marine Ecology Progress Series, 282, 237-244. http://dx.doi.org/10.3354/meps282237.

Hilborn, R. & Walters, C.J. 1992. Quantitative fisheries stock assessment: choice, dynamics and uncertainty. London: Chapman & Hall.

Hurtado-Ferro, F., Szuwalski, C. S., Valero, J. L., Anderson, S. C., Cunningham, C. J., Johnson, K. F., Licandeo, R., McGilliard, C. R., Monnahan, C. C., Muradian, M. L., Ono, K., Vert-Pre, K. A., Whitten, A. R., & Punt, A. E. 2015. Looking in the rear-view mirror: Bias and retrospective patterns in integrated, age-structured stock assessment models. ICES Journal of Marine Science, 72(1), 99 110. https://doi.org/10.1093/icesjms/fsu198.

Hüssy, K., Radtke, K., Plikshs, M., Oeberst, R., Baranova, T., Krumme, U., Sjo¨berg, R., Walther, Y., and Mosegaard, H. 2016. Challenging ICES age estimation protocols: lessons learned from the eastern Baltic cod stock. – ICES Journal of Marine Science, 73: 2138–2149. https://doi.org/10.1093/icesjms/fsw107.

ICES. 2019. Manual for the Offshore Beam Trawl Surveys, Version 3.4, April 2019, Working Group on Beam Trawl Surveys. 54pp. http://doi.org/10.17895/ices.pub.5353.

Iles, T.D., 1974. The tactics and strategy of growth in fishes. In: Jones, F.R.H. (Ed.), Sea Fisheries Research. Paul Elek, London, pp. 331–346.

Jardas, I., 1996. Jadranska ihtiofauna. Školska knjiga, Zagreb.

Kimura D.K., Lyons J.J. 1991. Between-Reader Bias and Variabil-ity in the Age-Determination Process. Fish. Bull. 89: 53-60.

Kraak, S.B.M., Haase, S., Minto, C. & Santos, J. 2019. The Rosa Lee phenomenon and its consequences for fisheries advice on changes in fishing mortality or gear selectivity. ICES Journal of Marine Science, 76(7), 2179–2192. https://doi.org/10.1093/icesjms/fsz107.

Kuhn E, Lavielle M. 2005. Maximum Likelihood Estimation in Nonlinear Mixed Effects Models. Computational Statistics & Data Analysis, 49(4), 1020–1038. doi:10.1016/j. csda.2004.07.002

Kuparinen, A., Roney, N. E., Oomen, R. A., Hutchings, J. A., and Olsen, Esben M. 2016. Small-scale life history variability suggests potential for spatial mismatches in Atlantic cod management units. – ICES Journal of Marine Science, 73: 286–292.

Laslett, G. M., Eveson, J. P., & Polacheck, T. 2002. A flexible maximum likelihood approach for fitting growth curves to tag-recapture data. Canadian Journal of Fisheries and Aquatic Sciences, 59, 976–986. https://doi.org/10.1139/f02-069.

Lea, E. 1910. On the methods used in the herring investigations. Publ Circ Cons Perm Int Explor Mer 53:7–25.

Lee, R.M. 1920. A review of the methods of age and growth determination in fishes by means of scales. Fish Invest Lond Ser 24(2):1–32.

Lee, R. M. 1912. An investigation into the methods of growth determination in fishes. Conseil Permanent International pour l'Exploration de la Mer, Publications de Circonstance, 63. 35 pp.

Lester, N. P., Shuter, B. J., and Abrams, P. A. 2004. Interpreting the von Bertalanffy model of somatic growth in fishes: the cost of reproduction. Proceedings of the Royal Society of London, Series B: Biological Sciences, 271: 1625–1631.

Liao, H., Sharov, A. F., Jones, C. M. & Nelson, G. A. 2013. Quantifying the Effects of Aging Bias in Atlantic Striped Bass Stock Assessment. Trans. Am. Fish. Soc. 142, 193–207.

Lorenzen, K. 2016. Toward a new paradigm for growth modeling in fisheries stock assessments: Embracing plasticity and its consequences. Fisheries Research, 180, 4–22. https://doi.org/10.1016/j.fishres.2016.01.006.

Lorenzen, K., 2000. Allometry of natural mortality as a basis for assessing optimalrelease size in fish stocking programmes. Can. J. Fish. Aquat. Sci. 57, 2374–2381.

Mahé, K., Moerman M., Maertens I., Holmes I., Boiron A. & Elleboode R. 2012. Report of the sole (Solea solea) in the Bay of Biscay otolith exchange scheme 2011. 14 pp.

Manabe, A., Yamakawa, T., Ohnishi. S., Akamine, T., Narimatsu, Y., Tanaka, H., et al. 2018. A novel growth function incorporating the effects of reproductive energy allocation. PLoS ONE 13(6): e0199346. https://doi.org/10.1371/journal.pone.0199346.

Mangel, M., MacCall, A.D., Brodziak, J., Dick, E.J., Forrest, R.E., Pourzand, R., Ralston, S., 2013. A perspective on steepness, reference points, and stock assessment. Can. J. Fish. Aquat. Sci. 70 (6), 930–940.

Masnadi, F., Cardinale, M., Donato, F., Sabatini, L., Pellini, G., Scanu, M., et al. 2021. Stock Assessment Form Demersal species - Stock assessment of common sole in GSA 17. https://gfcmsitestorage.blob.core.windows.net/website/5.Data/SAFs/DemersalSpecies/2019/SOL_GSA_17_2019_HRV_ITA_SVN.pdf.

Matthias, B.G., Ahrens, R.M.N., Allen, M.S., Tuten, T., Siders, Z.A. & Wilson, K.L. 2018. Understanding the effects of density and environmental variability on the process of fish growth. Fisheries Research, 198, 209–219. https://doi.org/10.1016/j.fishres.2017.08.018.

Maunder, M. N. 2012. Evaluating the stock-recruitment relationship and management reference points: application to summer flounder (Paralichthys dentatus) in the U.S. mid-Atlantic. Fisheries Research, 125–126: 20–26.

Maunder, M. N., and Piner, K. R. 2015. Contemporary fisheries stock assessment: many issues still remain. – ICES Journal of Marine Science, 72: 7–18. doi:10.1093/icesjms/fsu015.

Maunder M. N., and Punt A. E. 2013. A review of integrated analysis in fisheries stock assessment. Fisheries Research, 142: 61–74.

MediSeH - Mediterranean Sensitive Habitats. 2013. Edited by Giannoulaki M., A. Belluscio, F. Colloca, S. Fraschetti, M. Scardi, C. Smith, P. Panayotidis, V. Valavanis M.T. Spedicato. DG MARE Specific Contract SI2.600741, Final Report, 557 p.

Meekan, M.G., Vigliola, L., Hansen, A., Doherty, P.J., Halford, A., Carleton, J.H., 2006. Bigger is better: size-selective mortality throughout the life history of a fast-growing clupeid, Spratelloides gracilis. Mar. Ecol. Prog. Ser. 317, 237–244. doi:10.3354/meps317237.

Methot R. D., and Wetzel C. R. 2013. Stock synthesis: a biological and statistical framework for fish stock assessment and fishery management. Fisheries Research, 142: 86–99.

Minte-Vera, C. V., Maunder, M. N., Casselman, J. M., & Campana, S. E. 2016. Growth functions that incorporate the cost of reproduction. Fisheries Research, 180, 31–44. https://doi.org/10.1016/j.fishres.2015.10.023.

Moe, B. J. 2015. Estimating growth and mortality in elasmobranchs: are we doing it correctly? Nova Southeastern University. Retrieved from http://nsuworks.nova.edu/occ_stuetd/42.

Mollet, F. M., Ernande, B., Brunel, T., & Rijnsdorp, A. D. 2010. Multiple growth-correlated life history traits estimated simultaneously in individuals. Oikos, 119, 10–26. https://doi.org/10.1111/oik.2010.119.

Neves, A., Vieira, A.R., Sequeira, V., Silva, E., Silva, F., Duarte, A.M., Mendes, S., Ganhão, R., Assis, C., Rebelo, R., et al. 2022. Modelling Fish Growth with Imperfect Data: The Case of Trachurus picturatus. Fishes , 7, 52. https://doi.org/10.3390/fishes7010052.

Paloheimo, J. E., & Dickie, L. M. 1965. Food and growth of fishes. I. A growth curve derived from experimental data. Journal of the Fisheries Research Board of Canada, 22, 521–542. https://doi.org/10.1139/f65-048.

Pardo, S.A., Cooper,A. B., and Dulvy, N. K. 2013.Avoiding fishy growth curves. Methods in Ecology and Evolution, 4: 353–360. https://doi.org/10.1111/mee3.2013.4.issue-4.

Piccinetti, C., Giovanardi, O., 1984. Données biologique sur Solea vulgaris en Adriatique. FAO Fisheries Report 290, 117–118.

Pilling, G. M., Kirkwood, G. P., and Walker, S. G. 2002. An improved method for estimating individual growth variability in fish, and the correlation between von Bertalanffy growth parameters. Canadian Journal of Fisheries and Aquatic Sciences, 59: 424–432.

Punt, A. E., Smith, D. C., KrusicGolub, K., and Robertson, S. 2008. Quantifying age-reading error for use in fisheries stock assessment, with application to species in Australia's southern and eastern scalefish and shark fishery. Canadian Journal of Fisheries and Aquatic Sciences, 65: 1991–2005.

Quéro, J.-C., M. Desoutter and F. Lagardère, 1986. Soleidae. p. 1308-1324. In P.J.P. Whitehead, M.-L. Bauchot, J.-C. Hureau, J. Nielsen and E. Tortonese (eds.) Fishes of the North-eastern Atlantic and the Mediterranean. UNESCO, Paris. Vol. 3.

Quince, C., Abrams, P. A., Shuter, B. J., and Lester, N. P. 2008a. Biphasic growth in fish. 1. Theoretical foundations. Journal of Theoretical Biology, 254: 197–206.

Quince, C., Shuter, B. J., Abrams, P. A., and Lester, N. P. 2008b. Biphasic growth in fish. 2. Empirical assessment. Journal of Theoretical Biology, 254: 207–214.

Quinn, T.J., Deriso, R.B. 1999. Quantitative Fish Dynamics. Oxford University Press.

R Core Team. 2022. R: A language and environment for statistical computing. Version 4.1.3. R Foundation for Statistical Computing, Vienna, Austria.

Reeves, S. A. 2003. A simulation study of the implications of age-reading errors for stock assessment and management advice. ICES Journal of Marine Science, 60: 314–328.

Rogers-Bennett, L. and Rogers, D.W. 2016. A Two-Step Growth Curve: Approach to the von Bertalanffy and Gompertz Equations. Advances in Pure Mathematics, 6, 321-330. http://dx.doi.org/10.4236/apm.2016.65023.

Sainsbury, K. J. 1980. Effect of individual variability on the von Bertalanffy growth equation. Canadian Journal of Fisheries and Aquatic Sciences, 37: 241–247.

Sampson, D.B., 2014. Fishery selection and its relevance to stock assessment andfishery management. Fish. Res. 158, 5–14.

Scarcella, G., Grati F., Raicevich S., Russo T., Gramolini R., Scott R. D., Polidori P., Domenichetti F., Bolognini L., Giovanardi G., Celić I., Sabatini L., Vrgoč N., Isajlović I., Marčeta B., Fabi G., 2014. Common sole in the northern and central Adriatic Sea: Spatial management scenarios to rebuild the stock. J. Sea Res. http://dx.doi.org/10.1016/j.seares.2014.02.002.

Schnute, J., 1981. A versatile growth model with statistically stable parameters. Can. J. Fish. Aquat. Sci. 38, 1128–1140.

Shuter, B. J., Lester, N. P., LaRose, J., Purchase, C. F., Vascotto, K., Morgan, G., … Abrams, P. A. 2005. Optimal life histories and food web position: Linkages among somatic growth, reproductive investment, and mortality. Canadian Journal of Fisheries and Aquatic Sciences, 62, 738–746. https://doi.org/10.1139/f05-070.

Sibly, R.M., Baker, J., Grady, J.M., Luna, S.M., Kodric-Brown, A., Venditti, C., Brown, J.H. 2015 Fundamental insights into ontogenetic growth from theory and fish. Proc Natl Acad Sci U S A ;112(45):13934-9. doi: 10.1073/pnas.1518823112. Epub 2015 Oct 27. PMID: 26508641; PMCID: PMC4653220.

Smith, E. B., Williams, F. M., and Fisher, C. R. 1997. Effects of intrapopulation variability on von Bertalanffy growth parameter estimates from equal mark-recapture intervals. Canadian Journal of Fisheries and Aquatic Sciences, 54: 2025–2032.

Soriano, M., Moreau, J., Hoenig, J. M., & Pauly, D. 1992. New functions for the analysis of two-phase growth of juvenile and adult fishes, with application to Nile perch. Transactions of the American Fisheries Society, 121, 486–493. https://doi.org/10.1577/1548-8659(1992)121<0486:NFFTAO>2.3.CO;2.

Stawitz, C.C., Haltuch, M.A. & Johnson, K.F. 2019. How does growth misspecification affect management advice derived from an integrated fisheries stock assessment model? Fisheries Research, 213,12–21.

Thorson, J.T., Monnahan, C.C., Cope, J.M., 2015. The potential impact oftime-variation in vital rates on fisheries management targets for marine fishes.Fish. Res. 169, 8–17.

Tortonese, E. 1975. Osteichthyes - Fauna d'Italia vol. XI, Calderini, Bologna.

Tracey, S. R., & Lyle, J. M. 2005. Age validation, growth modeling, and mortality estimates for striped trumpeter (Latris lineata) from southeastern Australia: Making the most of patchy data. Fishery Bulletin, 103, 169–182. Retrieved from http://aquaticcommons.org/id/eprint/9650.

Vallisneri, M., Piccinetti, C., Stagni, A.M., Colombari, A., Tinti, F., 2000. Dinamica di popolazione, accrescimento, riproduzione di Solea vulgaris (Quensel 1806) nell'alto Adriatico. Biologia Marina Mediterranea 7 (1), 65–70.

Vigliola, L., Meekan, M.G. 2009. The Back-Calculation of Fish Growth From Otoliths. In: Green, B.S., Mapstone, B.D., Carlos, G., Begg, G.A. (eds) Tropical Fish Otoliths: Information for Assessment, Management and Ecology. Reviews: Methods and Technologies in Fish Biology and Fisheries, vol 11. Springer, Dordrecht. https://doi.org/10.1007/978-1-4020-5775-5_6.

von Bertalanffy, L. 1938. A quantitative theory of organic growth (inquiries on growth laws II). Human Biology, 10: 181–213.

Wagemans, F. and Vandewalle, P. 2001. Development of the bony skull in common sole: brief survey of morpho-functional aspects of ossification sequence. Journal of Fish Biology, 59: 1350 1369. https://doi.org/10.1111/j.1095-8649.2001.tb00197.x.

Wilson KL, Honsey AE, Moe B, Venturelli P. 2017. Growing the biphasic framework: Techniques and recommendations for fitting emerging growth models. Methods Ecol Evol. 2018;9:822–833. https://doi.org/10.1111/2041-210X.12931.

5.8. Supplementary materials

S1- Growth section:

S.1.1. Back calculation methods selection process

Linear regression -> apply Dahl-Lea or Fraser-Lee* (BCM1 and BCM2 in Vigliola & Meekan, 2009)

Non-Linear regression -> apply Fry Scale Proportional Hypothesis (BCM 16 in Vigliola & Meekan, 2009)

*apply only if intercept is significant

```
Linear regression:
formula = radcap ~ TL

Coefficients:
             Estimate Std. Error t value Pr(>|t|)
(Intercept) 5.024e-01  1.741e-02   28.86   <2e-16 ***
TL          5.204e-03  6.855e-05   75.91   <2e-16 ***
---

Multiple R-squared:  0.9113, Adjusted R-squared:  0.9111
F-statistic:  5762 on 1 and 561 DF,  p-value: < 2.2e-16

Non-Linear regression:
Formula: radcap ~ ((TL - A)/B)^(1/C)

Parameters:
   Estimate Std. Error t value Pr(>|t|)
A -149.0166    49.5444  -3.008  0.00275 **
B  241.5220    46.6944   5.172 3.22e-07 ***
C    0.8554     0.1151   7.433 4.01e-13 ***
---
```

```
AIC(Linear regression): -891.3026

AIC(Non-Linear regression): -890.8115
```

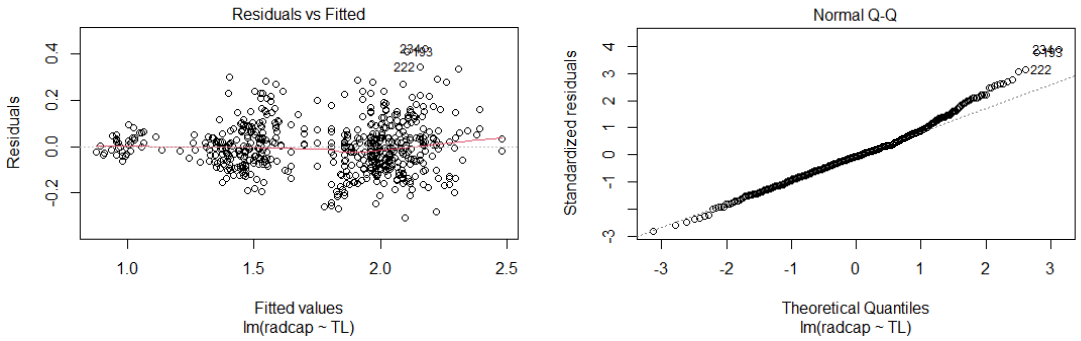

Figure S.1.1.1. Residual plot for linear regression: residual versus fitted values and Q-Q plot.

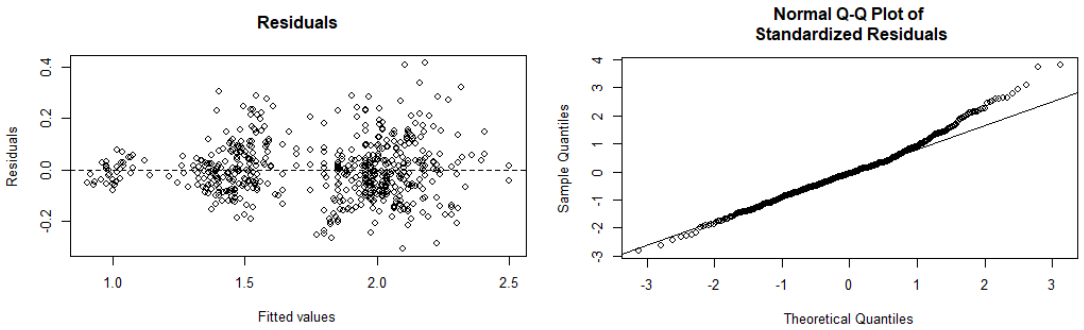

Figure S.1.1.2. Residual plot for non-linear regression: residual versus fitted values and Q-Q plot.

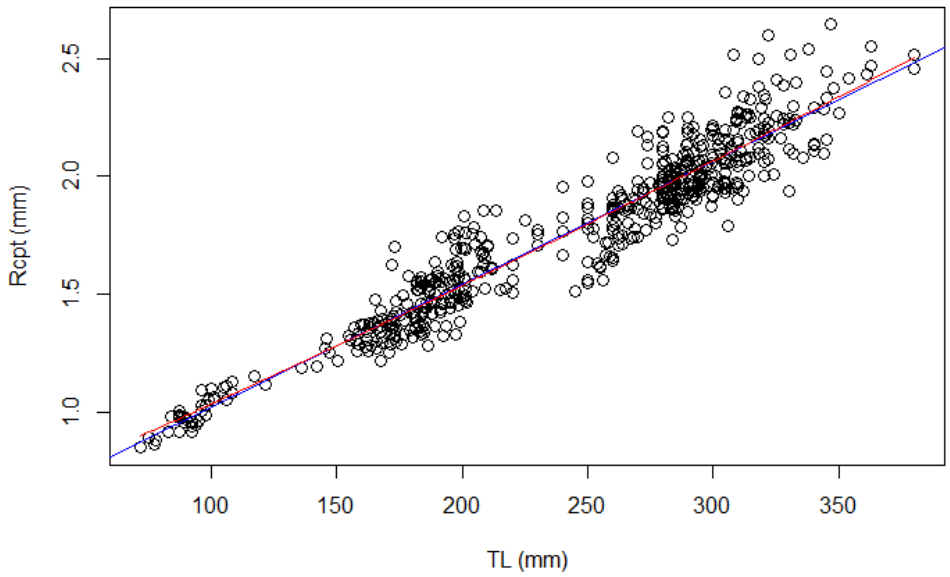

Figure S.1.1.3. Relationship between total fish length (TL) and otolith size at the time of capture (Rcpt). Blue and red lines represent respectively the linear and non-linear regressions previously fitted.

S.1.2. Data plotting

Plotting back-calculated length-at-age obtain with Fraser-Lee method

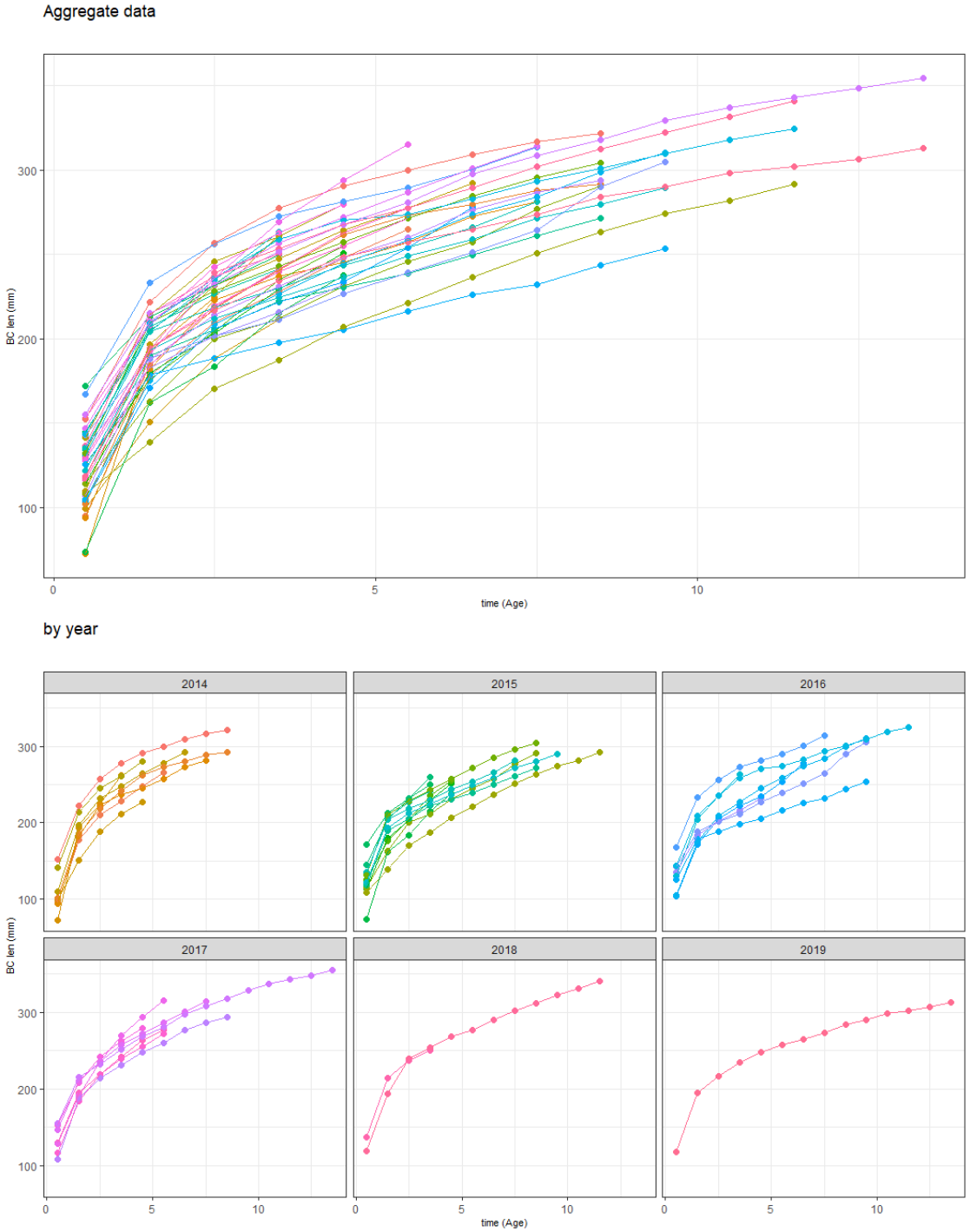

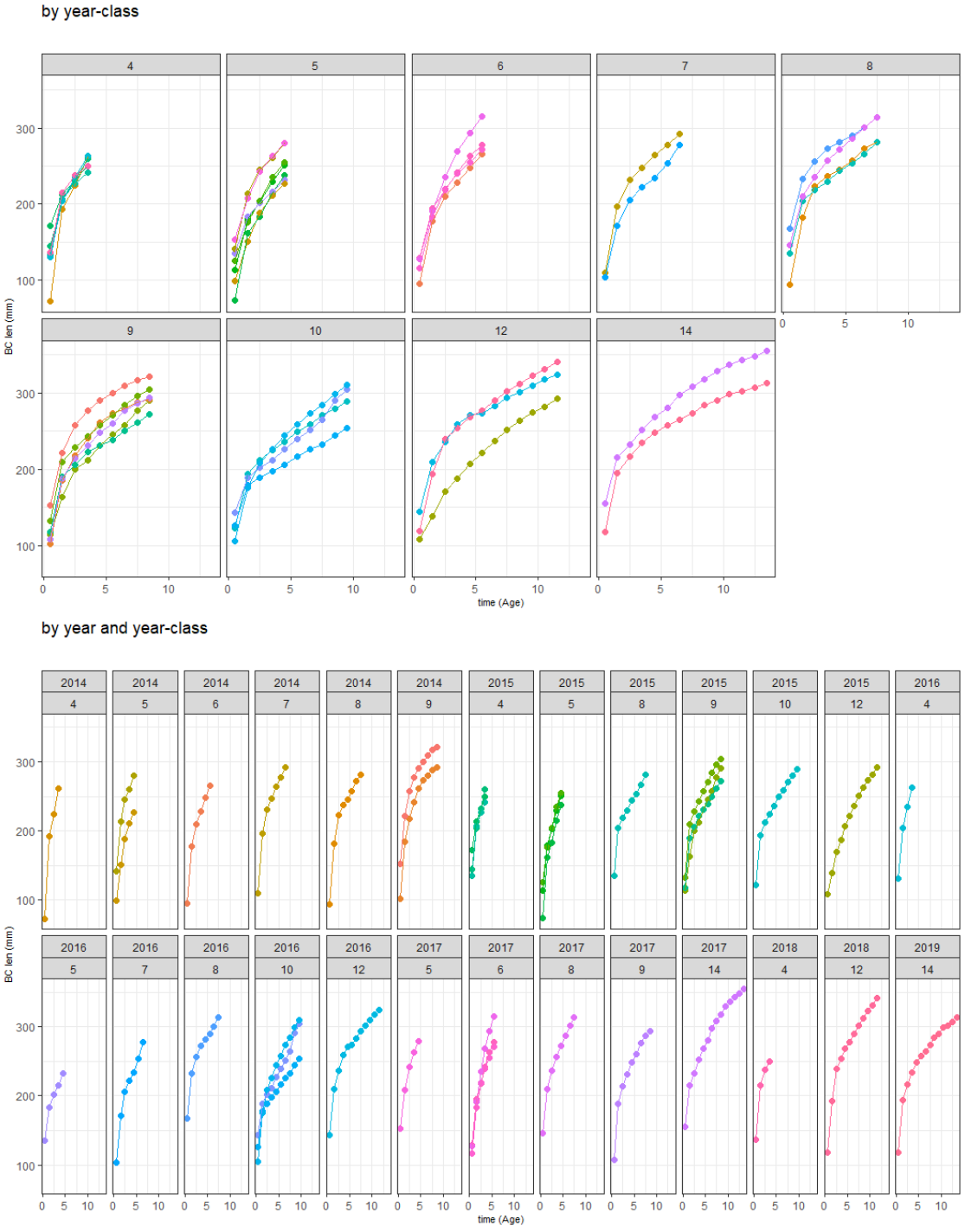

Figure S.1.2.1. Individual common sole growth trajectories back-calculated from otoliths.

S.1.3. Model estimates (5-par VB)

Fit a Biphasic von Bertalanffy growth model:

$$L_{ij} = L_{\infty i}\,(1-\exp(-k_{0i}(t_{ij}-t_{0i}))) + \varepsilon_{ij} \quad \text{for } t_{ij} < t_{1i}$$

$$L_{ij} = L_{\infty i}\,(1-\exp(-k_{0i}(t_{1i}-t_{0i})\,(-k_{1i}(t_{ij}-t_{1i}))) + \varepsilon_{ij} \quad \text{for } t_{ij} > t_{1i}$$

For each parameter estimated in the model, estimates of the standard error are reported, as an absolute value (SE) and relative to the estimate, as a coefficient of variation (% CV).

```
-----------------------------------------------------
-----------------  Fixed effects  -------------------
-----------------------------------------------------
  Parameter Estimate  SE     CV(%)
      Linf   397.30  14.508  3.65
        k0     0.31  0.023   7.36
        t0    -0.76  0.071   9.30
        k1     0.11  0.012   10.51
        t1     1.50  0.069   4.61
        a.     2.88  0.173   6.01
-----------------------------------------------------
-----------  Variance of random effects  -----------
-----------------------------------------------------
       Parameter  Estimate  SE   CV(%)
Linf omega2.Linf    0.020 0.0091 46.75
k0     omega2.k0    0.095 0.0419 44.11
t0     omega2.t0    0.133 0.0412 30.99
k1     omega2.k1    0.200 0.0850 42.48
t1     omega2.t1    0.052 0.0174 33.58
-----------------------------------------------------
---------------  Statistical criteria  -------------
-----------------------------------------------------
Likelihood computed by linearisation
      -2LL= 1927.725
      AIC = 1969.725
      BIC = 2004.115
-----------------------------------------------------
```

S.1.4. Correlations plots (5-par VB)

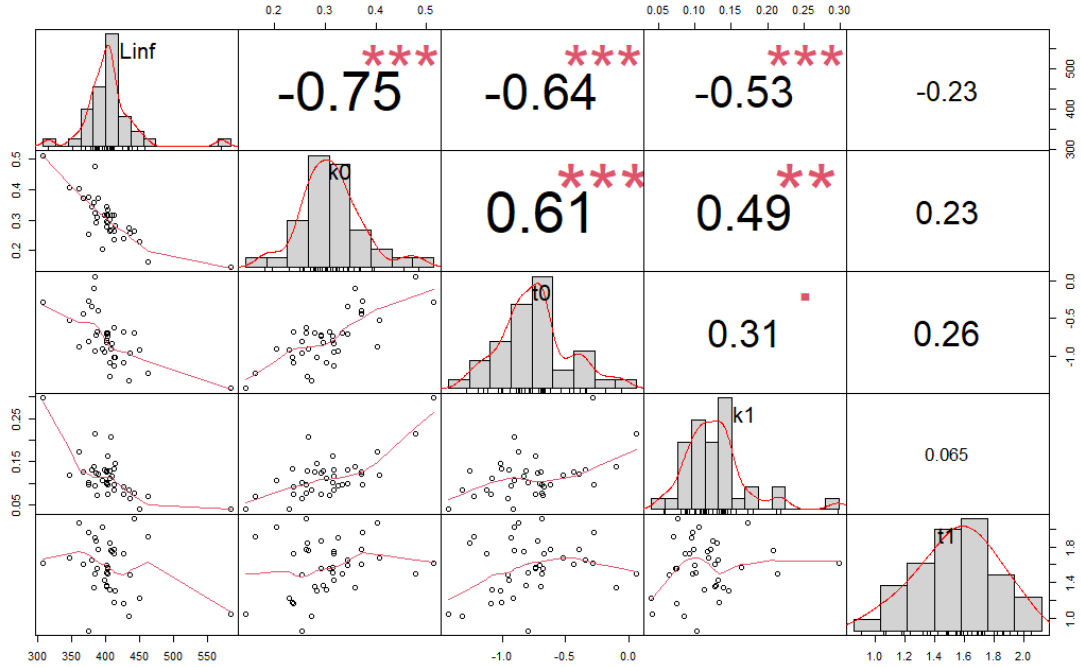

Figure S.1.4.1. Matrix plot showing the correlation between random effects in the 5-par VB model. The distribution of each variable is shown on the diagonal. On the bottom of the diagonal the bivariate scatter plots with a fitted line are displayed. On the top of the diagonal the correlation coefficients measure the strength of that relationship plus the significance level as stars. Each significance level is associated to a symbol: p-values (0.001, 0.01, 0.05, 0.1, 1) <=> symbols("***", "**", "*", ".", " ")

S.1.5. Diagnostic plots (5-par VB)

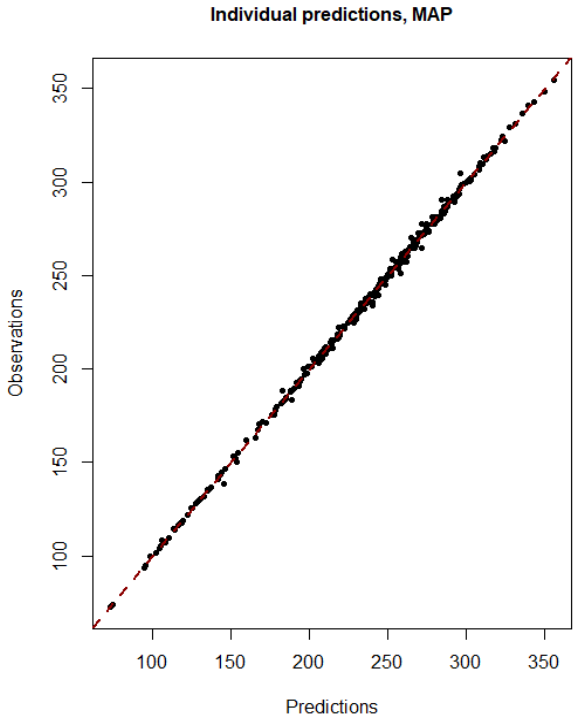

Figure S.1.5.1. Plot of the individual predictions versus the observations for the 5-par VB model. Predictions are computing using the conditional mode of the parameter's distribution (or Maximum A Posteriori; MAP).

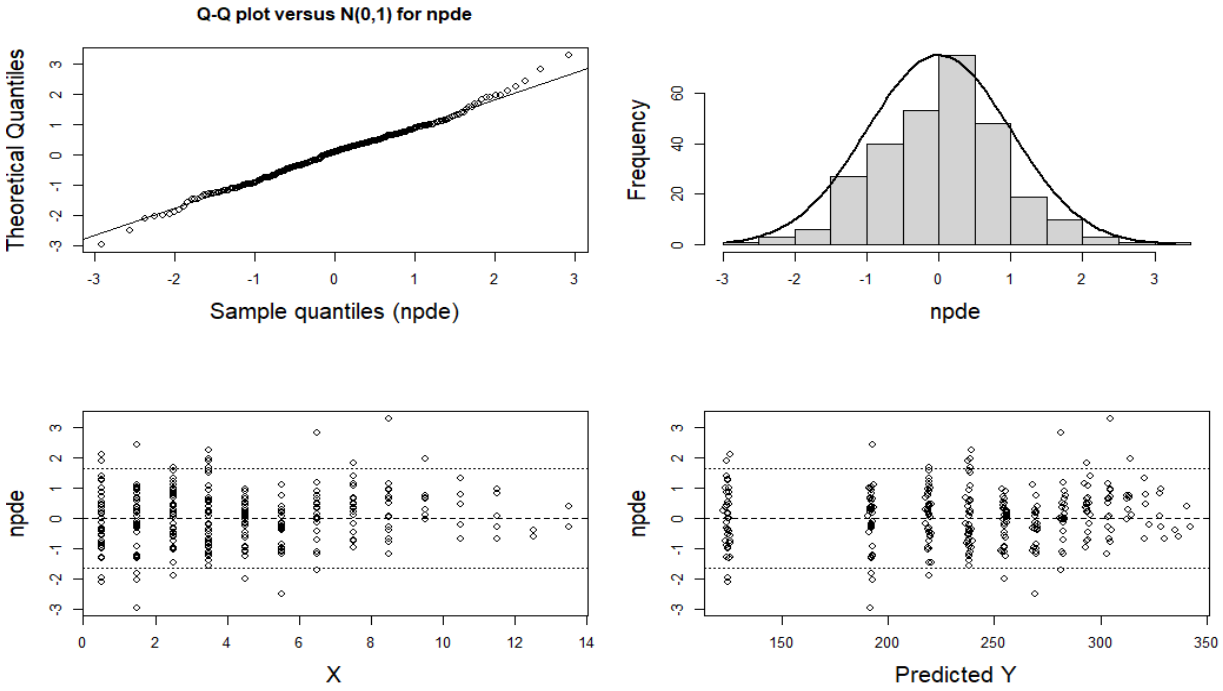

Figure S.1.5.2. Upper plots: Q-Q plot and histogram of NPDE* for the 5-par VB model. Bottom plots: NPDE versus back calculated fish-length and versus age for the 5-par VB model.

*NPDE (Normalised Prediction Distribution Errors) are simulated residual adapted to nonlinear mixed effect models (Brendel et al.2006; Comets et al. 2010). Simulated datasets used for NPDE:1000.

S.1.6. Sensitivity analysis on initial values (5-par VB)

Table S.1.6.1. Summary table of sensitivity analysis on initial values provided to the nonlinear optimization algorithms. Initial values: Set 1 includes the parameters used in the final analysis. Alterative values tested are: + 20% and -20% of Set 1 (Set 2 & 3); Vallisneri et al. (2000) VB parameters for female (only available for *Linf*, *k0* and *t0*; Set 4). Model estimates: estimated parameters considering the different initial values sets provided to the model.

	Initial values				Model estimates						
Parameter	Set 1	Set 2	Set 3	Set 4	Set 1	Set 2	Set 3	Set 4	Δ*Set 1-2	Δ*Set 1-3	Δ*Set 1-4
Linf	380	456	304	457.3	397.3	394.98	392.6	397.5	-0.6%	-1.2%	+0.1%
k0	0.30	0.36	0.24	0.21	0.31	0.33	0.32	0.30	+6.5%	+3.2%	-3.2%
t0	-0.50	-0.60	-0.40	-1.28	-0.76	-0.73	-0.79	-0.79	-3.9%	+3.9%	+3.9%
k1	0.20	0.24	0.16	0.20	0.11	0.12	0.12	0.11	+9.1%	+9.1%	0.0%
t1	1.80	2.16	1.44	1.80	1.50	1.47	1.59	1.55	-2.0%	+6.0%	+3.3%

*Percentual difference in the estimated parameter value between Set 1 and the alternatives.

S.1.7. Comparison with model without random effects (5-par VB)

Fitting a nonlinear least-squares model for the biphasic formulation.

```
Formula: TL ~ (Age <= t1) * (Linf * (1 - exp(-k0 * (Age - t0)))) + (Age >
    t1) * (Linf * (1 - exp(-k0 * (t1 - t0) - k1 * (Age - t1))))

Parameters:
      Estimate Std. Error t value Pr(>|t|)
Linf 383.21707   43.26359   8.858  < 2e-16 ***
k0     0.30328    0.06333   4.788 2.72e-06 ***
t0    -0.79286    0.14698  -5.394 1.46e-07 ***
k1     0.09943    0.03807   2.612  0.00949 **
t1     1.83126    0.16336  11.210  < 2e-16 ***
---
Signif. codes:  0 '***' 0.001 '**' 0.01 '*' 0.05 '.' 0.1 ' ' 1

Residual standard error: 21.34 on 282 degrees of freedom

Algorithm "port", convergence message: relative convergence (4)
```

Table S.1.7.1. Comparison table (standard error and AIC value) for in common fixed effect.

		NLS	Saemix
Standard Error of fixed effect	*Linf*	43.26359	14.508
	k0	0.06333	0.023
	t0	0.14698	0.071
	k1	0.03807	0.012
	t1	0.16336	0.069
AIC		2576.42	1969.725

S.1.8. Model estimates (3-par VB)

Fit a Monophasic von Bertalanffy growth model:

$$L_{ij} = L_{\infty i}\,(1-\exp(-k_i(t_{ij}-t_{0i}))) + \varepsilon_{ij}$$

For each parameter estimated in the model, estimates of the standard error are reported, as an absolute value (SE) and relative to the estimate, as a coefficient of variation (% CV).

```
-----------------------------------------------------
-----------------  Fixed effects  ------------------
-----------------------------------------------------
  Parameter Estimate  SE   CV(%)
```

```
      Linf   302.09 5.225  1.73
         k     0.35 0.024  6.80
        t0    -1.19 0.116  9.74
        a.     8.57 0.445  5.19
-----------------------------------------------------
-----------  Variance of random effects  -----------
-----------------------------------------------------
       Parameter Estimate   SE   CV(%)
Linf omega2.Linf   0.0075 0.0024 32.61
k       omega2.k   0.1196 0.0392 32.80
t0     omega2.t0   0.3793 0.1166 30.76
-----------------------------------------------------
--------------  Statistical criteria  -------------
-----------------------------------------------------
Likelihood computed by linearisation
      -2LL= 2278.604
      AIC = 2298.604
      BIC = 2314.98
-----------------------------------------------------
```

S.1.9. Correlations plots (3-par VB)

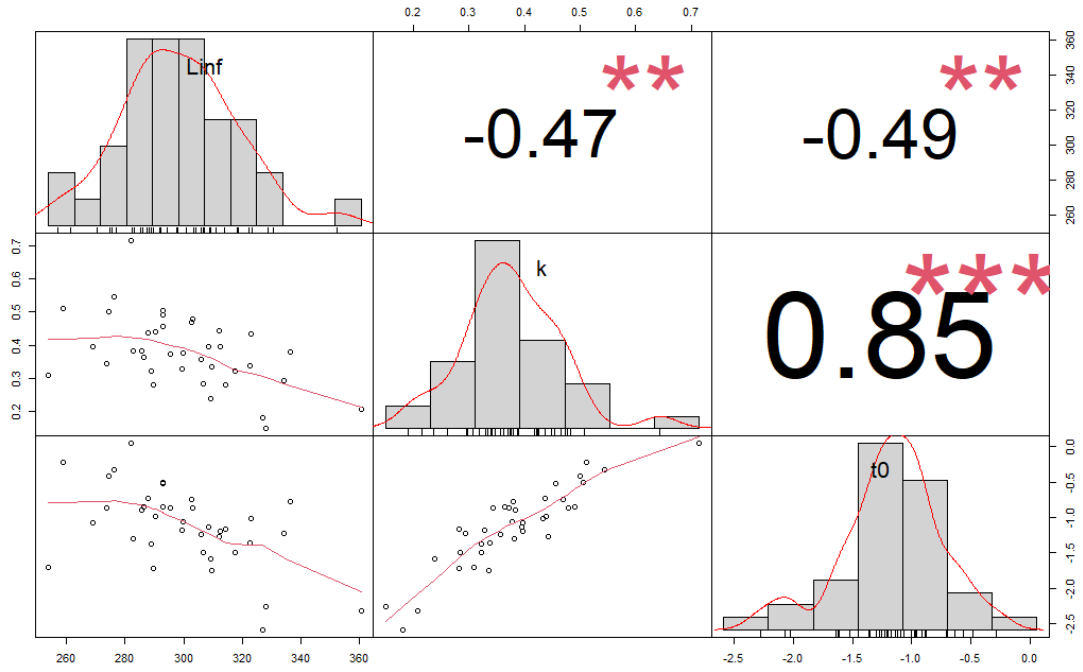

Figure S.1.9.1. Matrix plot showing the correlation between random effects in the 3-par VB model. The distribution of each variable is shown on the diagonal. On the bottom of the diagonal the bivariate scatter

plots with a fitted line are displayed. On the top of the diagonal the correlation coefficients measure the strength of that relationship plus the significance level as stars. Each significance level is associated to a symbol: p-values(0, 0.001, 0.01, 0.05, 0.1, 1) <=> symbols("***", "**", "*", ".", " ")

S.1.10. Diagnostic plots (3-par VB)

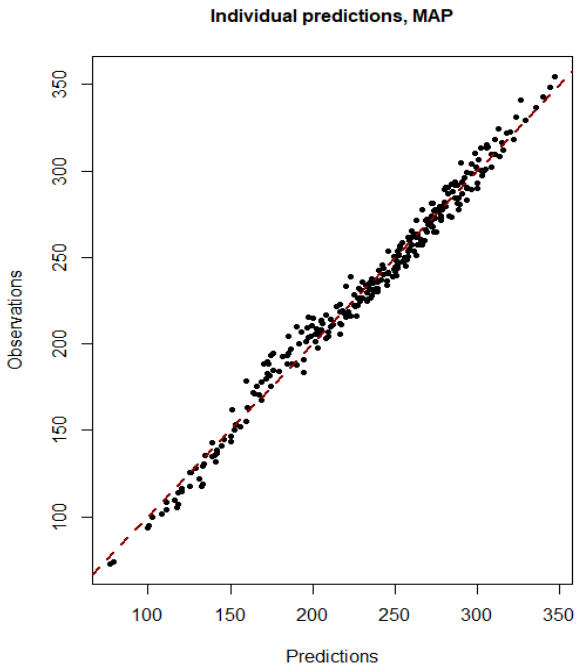

Figure S.1.10.1. Plot of the individual predictions versus the observations for the 3-par VB model. Predictions are computing using the conditional mode of the parameter's distribution (or Maximum A Posteriori; MAP).

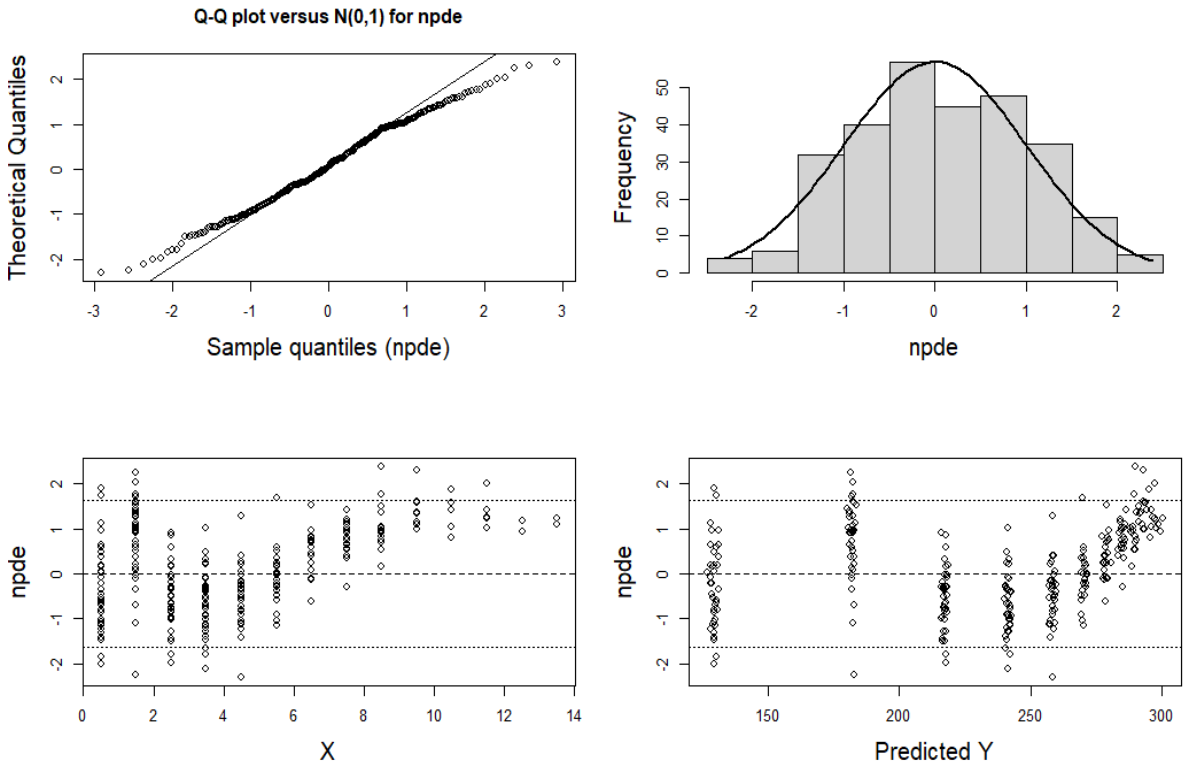

Figure S.1.10.2. Upper plots: Q-Q plot and histogram of NPDE* for the 3-par VB model. Bottom plots: NPDE versus age and versus back-calculated fish length for the 3-par VB model.

*NPDE (Normalised Prediction Distribution Errors) are simulated residual adapted to nonlinear mixed effect models (Brendel et al.2006; Comets et al. 2010). Simulated datasets used for NPDE:1000.

S.1.11. Individual fits (5-par VB versus 3-par VB)

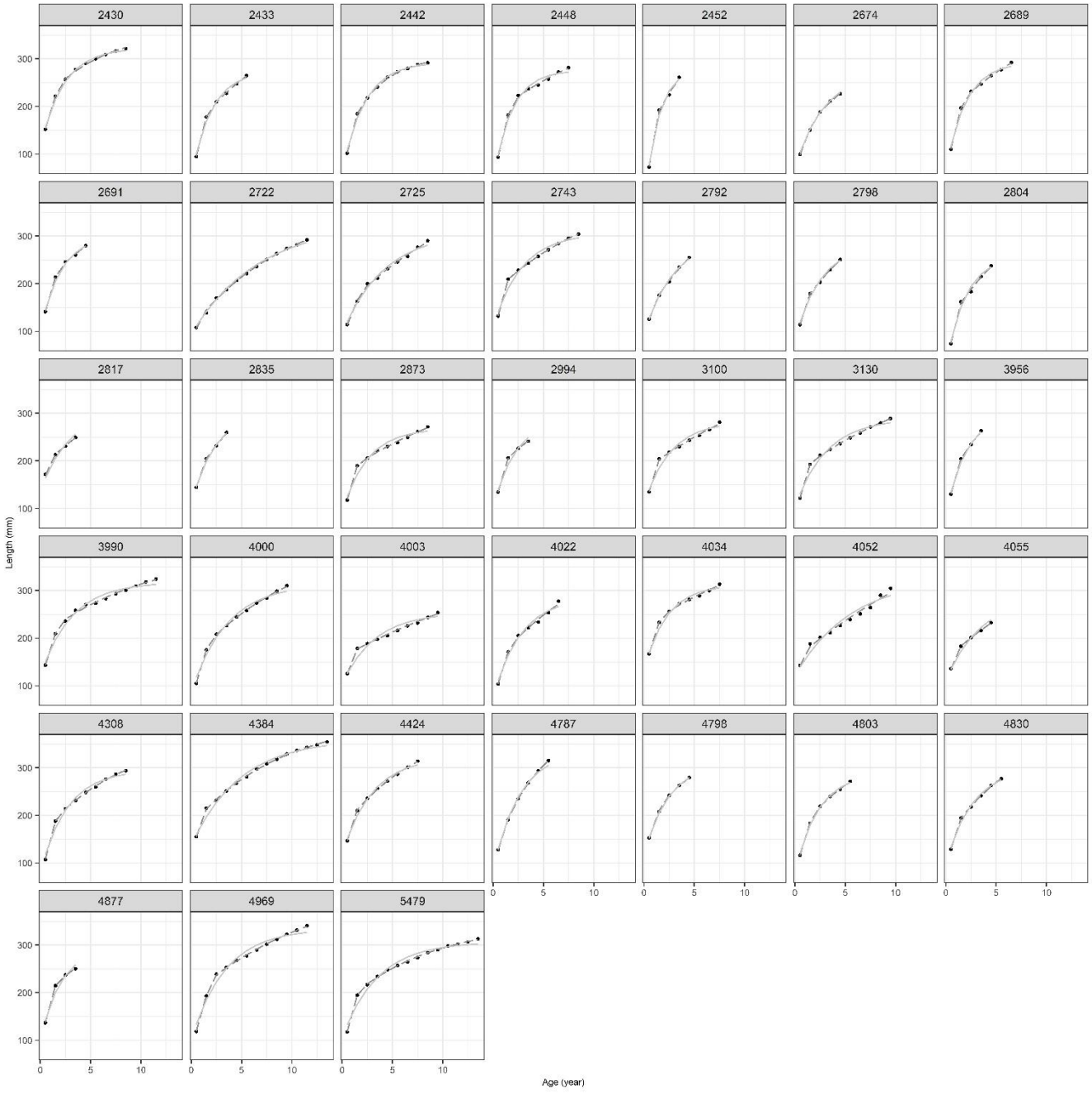

Figure S.1.11.1. Individual predictions computed at each time-point using the mode of the individual distribution for each subject (Maximum A Posteriori; MAP). The black points correspond to observed back-calculated lengths-at-age, the light grey line to the monophasic von Bertalanffy growth model (3-par VB), and the dark grey dashed one to the biphasic model (5-par VB).

S.1.12. Previous growth studies on common sole in Mediterranean sub-region

Table S.1.12.1. Common sole (*Solea solea*) von Bertalanffy Growth Parameters by reference studies on the species, estimated length (mm) at age (from 0 to 15) by sex, Mediterranean sub-region and age estimation method. Geographical area is also indicated. Sex: F= female; M= male; U= unsexed; LFD: length frequency distribution analysis; otolith BC: back calculation.

References	Sex	von Bertalanffy Growth Parameters					Area	Method	GSA	Length (mm) at Age (year) calculated by growth parameters																
		L_∞	k0	t_0	k1	t1				0	1	2	3	4	5	6	7	8	9	10	11	12	13	14	15
Vallisneri et al. 2000	F	457.3	0.208	-1.28	NA	NA	Northern and central Adriatic	otolith	17	107.40	173.11	226.48	269.83	305.03	333.63	356.85	375.72	391.04	403.48	413.59	421.80	428.46	433.88	438.28	441.85
	M	419.2	0.194	-2.1	NA	NA				140.22	189.42	229.94	263.31	290.80	313.44	332.09	347.45	360.11	370.53	379.11	386.18	392.00	396.80	400.75	404.00
Papaconstantinou et al., 1990	U	349	0.38	-0.41	NA	NA	Gulf of Amvrakikos	otolith	22	50.35	144.76	209.33	253.49	283.68	304.33	318.45	328.11	334.71	339.23	342.32	344.43	345.88	346.86	347.54	348.00
Turkmen 2003	F	299.5	0.1811	-1.55	NA	NA	Iskenderun Bay	otolith	24	73.27	110.72	141.98	168.06	189.82	207.98	223.13	235.78	246.33	255.13	262.48	268.61	273.72	277.99	281.55	284.52
	M	260.3	0.2211	-1.55	NA	NA				75.50	112.14	141.52	165.07	183.95	199.09	211.23	220.96	228.76	235.01	240.03	244.05	247.27	249.85	251.92	253.59
Ramos 1982	U	464	0.22	-0.75	NA	NA	Castellon	otolith	6	70.58	148.27	210.62	260.66	300.81	333.04	358.90	379.66	396.31	409.68	420.41	429.02	435.92	441.47	445.92	449.49
Vianet et al., 1989	U	488.3	0.24	-0.77	NA	NA	Gulf of Lion	otolith	7	82.39	169.00	237.13	290.72	332.88	366.04	392.13	412.65	428.79	441.49	451.48	459.33	465.51	470.38	474.20	477.21

	M	263.8	1.03	-0.07	NA	NA				18.35	176.17	232.52	252.63	259.81	262.38	263.29	263.62	263.74	263.78	263.79	263.80	263.80	263.80	263.80	263.80
	F	515.6	0.27	-0.41	NA	NA				54.03	163.25	246.62	310.27	358.85	395.94	424.26	445.87	462.37	474.96	484.58	491.92	497.52	501.80	505.07	507.56
Hossucu et al., 1999	M	311	0.33	-1.04	NA	NA	Izmir Bay	otolith	22	90.35	152.37	196.96	229.01	252.06	268.62	280.53	289.10	295.25	299.68	302.86	305.15	306.79	307.98	308.83	309.44
	F	425	0.17	-0.17	NA	NA				12.11	76.66	131.11	177.06	215.82	248.52	276.11	299.39	319.03	335.59	349.57	361.36	371.31	379.71	386.79	392.76
Fabi et al., 2009	U	396	0.44	-0.46	NA	NA	North Adriatic	LFD	17	72.56	187.69	261.84	309.60	340.35	360.16	372.92	381.13	386.43	389.83	392.03	393.44	394.35	394.94	395.32	395.56
FAO-GFCM 2021	M	341	0.34	-1.65	NA	NA	Northern and central Adriatic	otolith	17	146.41	202.50	242.42	270.83	291.06	305.45	315.70	322.99	328.18	331.88	334.51	336.38	337.71	338.66	339.33	339.81
	F	380.8	0.29	-1.53	NA	NA				136.46	197.97	243.99	278.43	304.20	323.48	337.91	348.71	356.79	362.83	367.36	370.74	373.27	375.17	376.59	377.65
	U	381	0.28	-1.7	NA	NA				144.30	202.10	245.79	278.81	303.77	322.63	336.89	347.66	355.80	361.96	366.61	370.12	372.78	374.79	376.30	377.45
5-par VB (present study)	U	397	0.31	-0.76	0.11	1.5	Northern and central Adriatic	otolith BC	17	83.33	166.94	210.51	229.46	247.50	262.20	276.70	289.10	300.51	310.03	319.73	327.70	334.01	341.72	347.89	352.56

S2- Stock assessment section:

S.2.1. Input data and model setting

Table S.2.1.1. Input data and functional forms used in the Stock Synthesis models. ITA GNS: Italian gillnets; ITA TBB: Italian modified beam trawl (*rapido trawl*); ITA OTB: bottom otter trawl, HRV GTR: Croatian trammel nets; HRV DRB: Croatian modified beam trawl for shellfish (*rampon*).

TYPE	NAME	YEAR	MAIN SOURCES
Landing	Landing in tonnes for each fleet and year	ITA GNS: 1958- 2019 *,**,^,° ITA TBB: 1958- 2019 *,**,^,° ITA OTB: 1958- 2019 *,**,^,° HRV GTR: 1958- 2019 ***,^^,°° HRV DRB: 2012- 2019 ***,^^	FAO-GFCM, 202; Fortibuoni e t al. 2017; FAO, 2020
Length compositions	Catch in numbers (thousand) per lenght class	ITA GNS: 2006- 2019 ITA TBB: 2006- 2019 ITA OTB: 2006- 2019 HRV GTR: 2012- 2019 HRV DRB: 2017- 2019	FAO-GFCM, 2021
Surveys indices	Abundance index from SoleMon Survey	2005- 2019	FAO-GFCM, 2021
Maturity ogives	Age at 50% maturity ($A_{50\%}$) of the females (see values in table S.2.1.2)	Assumed to be constant for the entire time series	FAO-GFCM, 2019
Length-weight relationship	Coefficients (*a, b*) to convert length in cm to weight in kg (see values in table S.2.1.2)	Assumed to be constant for the entire time series	FAO-GFCM, 2021
Growth	Von Bertalanffy growth curve (sex combined) fixed for the entire time series (see values in table S.2.1.2)	Assumed to be constant for the entire time series	This paper
S-R relationship	Spawner-recruitment relationship accordind to standard Beverton-Holt (see values of ln(R0) and steepness in table S.2.1.2)	Assumed to be constant for the entire time series	FAO-GFCM, 2021
Natural mortality	Average values of Gislason & Chen-Watanabe vectors by age (see values in table S.2.1.2)	Assumed to be constant for the entire time series	FAO-GFCM, 2021
Selectivity	Double normal for all fleets (see values in table S.2.1.2)	Assumed to be constant for the entire time series	FAO-GFCM, 2021

Initial catch	The initial equilibrium catches were assumed as the average of the first 5 years of historical data.	1953–1957	FAO-GFCM, 2021 & Fortibuoni e t al. 2017
Fishing mortality (F) method	Fishing mortality rates are an approximation of the Baranov continuous F		Methot & Wetzel, 2013

*Values from 1953-1979 are catches obtained from ISTAT-IREPA revised by Fortibuoni et al., 2017. **Values from 1980-2003 are catches from FishStatJ (FAO, 2020). ***Values from 1980-2011 are catches from FishStatJ (FAO, 2020). ^Values in 2004-2021 are official catches from ITA DCF (EU Regulation 2017/1004). ^^Values in 2012-2021 are official catches in Zone A from HRV DCF (EU Regulation 2017/1004). ° Partition by fleet from 1953 to 2003 applying to the proportion (average ratio along the years) observed in DCF data (2004-2019). °° Reconstruction from 1953 to 1980 applying a ratio between ITA and HRV in the first 10 years of FishStatJ data.

Table S.2.1.2. Configurations and settings of SS3 models. The table columns show: initial value, the intervals allowed for the parameters and the estimation phase. Parameters in bold are set and not estimated by the models.

Parameter	Initial value	Bounds (low,high)	Phase
Natural mortality	Age 0.5: **0.76** Age 1.5: **0.54** Age 2.5: **0.44** Age 5.5: **0.33** Age 10.5: **0.28** Age 15.5: **0.27** Age 20.5: **0.27**		
Stock and recruitment			
Ln(R0)	12.7	(3, 30)	1
Steepness (h)	**0.9**		
Recruitment variability (σR)	**0.5**		
Growth			
Linf (cm)	5-par VB: **39.7** 3-par VB: **30.2**		
k0	5-par VB: **0.31** 3-par VB: **0.35**		
k multiplier (k1= k0* k multiplier)	5-par VB: **0.35**		
Age for k multiplier (t1)	5-par VB: **2**		
CV of young individuals	**0.11**		
CV of old individuals	**0.065**		
Weight (kg) at length (cm)			
a	**0.0000046**		

b	**3.11**		
Maturity			
Age (cm) at 50% mature	**2**		
Initial fishing mortality			
ITA GNS	0.1	(0, 1.5)	1
ITA TBB	0.1	(0, 1.5)	1
HRV GTR	0.1	(0, 1.5)	1
ITA OTB	0.1	(0, 1.5)	1
Selectivity DN (double normal)			
ITA GNS			
Peak	21	(6, 41)	3
Asc-width	2.3	(-4, 12)	4
Desc-width	2.8	(-2, 6)	4
ITA TBB			
Peak	21	(6, 41)	3
Asc-width	1.3	(-10, 12)	4
Desc-width	2.8	(-2, 12)	4
HRV GTR			
Peak	29	(6, 41)	3
Asc-width	1.3	(-4, 12)	4
Desc-width	1.8	(-2, 6)	4
ITA OTB			
Peak	23.5	(6, 41)	3
Asc-width	3.3	(-10, 12)	4
Desc-width	2.8	(-2, 6)	4
HRV DRB			
Peak	21.5	(6, 41)	3
Asc-width	1.3	(-4, 12)	4
Desc-width	2.8	(-2, 6)	4
SoleMon Survey			
Peak	21	(6, 41)	3
Asc-width	3.3	(-10, 12)	4
Desc-width	2.8	(-2, 6)	4
Catchability			
SoeMon Survey			
Ln(Q) – catchability	**-2.81 (floated)**		

S.2.2. Stock assessment results (5-par VB versus 3-par VB)

Diagnostic: fit to the data

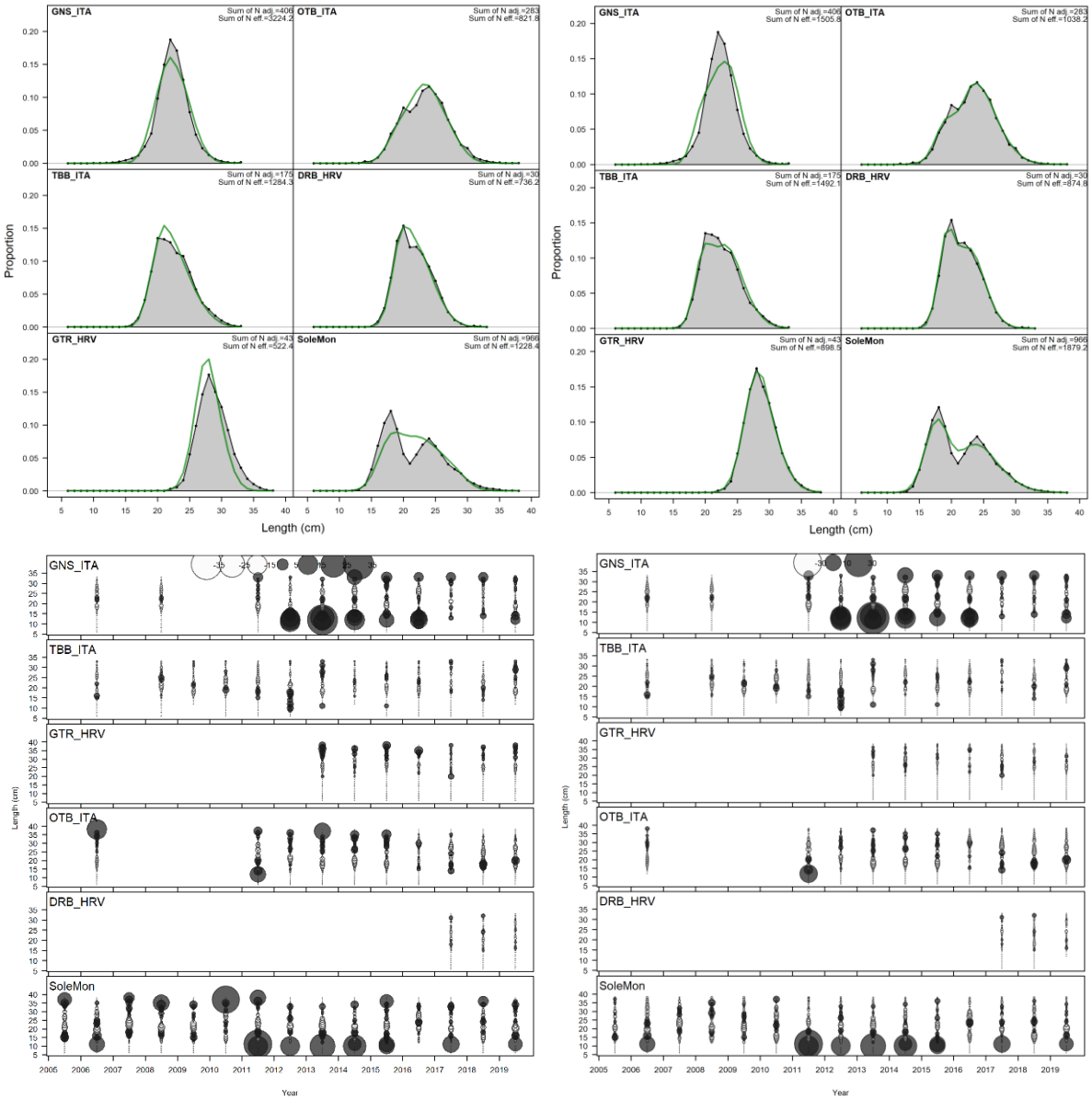

Figure S.2.2.1. Fit of the expected length composition to the observed length data and residual bubble plots by fleet and year for 3-par VB (left side) and 5-par VB (right side).

S3 - References

EU Regulation 2017/1004 of the European Parliament and of the Council of 17 May 2017 on the establishment of a Union framework for the collection, management and use of data in the fisheries sector and support for scientific advice regarding the common fisheries policy and repealing Council Regulation (EC) No 199/2008. https://eur-lex.europa.eu/legal-content/EN/TXT/?uri=CELEX%3A32017R1004.

Fabi, G., Grati, F., Raicevich, S., Santojanni, A., Scarcella, G. & Giovanardi, O. 2009. Valutazione dello stock di *Solea vulgaris* del medio e alto Adriatico e dell'incidenza di diverse attività di pesca. Final Report. VI Piano Triennale della pesca marittima e acquacoltura in acque marine e salmastre 1 (tematica c – c6). Programma di ricerca 6-a-74 (133 – XVII pp.). Rome, Ministero per le Politiche Agricole e Forestali, direzione generale della pesca e dell'acquacoltura.

FAO, 2020. Fisheries Division, Statistics and Information Branch. FishStatJ: Universal software for fishery statistical time series. Copyright 2020.

FAO-GFCM. 2021. Report of the Working Group on Stock Assessment of Demersal Species (WGSAD) – Benchmark session for the assessment of common sole in GSA 17, Scientific Advisory Committee on Fisheries (SAC). Online via Microsoft Teams, 12–16 April 2021.

Fortibuoni, T. et al. 2017. Fish and fishery historical data since the 19th century in the Adriatic Sea, Mediterranean. Sci. Data 4:170104 doi: 10.1038/sdata.2017.104.

Hossucu, B., M. Kaya and E. Taskavak, 1999. An investigation of growth parameters and otolith-total length relationship of *Solea solea* (L., 1758)(Pisces:Soleidae) in Izmir Bay. Israel Journal of Zoology 45:277-287.

Methot R. D., and Wetzel C. R. 2013. Stock synthesis: a biological and statistical framework for fish stock assessment and fishery management. Fisheries Research, 142: 86–99.

Papaconstantinou, C., G. Petrakis and E. Caragitsou, 1990. Natural history of sole (*Solea vulgaris* L. 1758) in the Amvrakikos Gulf (Greece). Rapports et Procès-Verbaux des Réunions Commission Internationale pour l'Exploration Scientifique de la Mer Méditerranée 32:266.

Ramos, J., 1982. Estudio de la edad y crecimiento del lenguado, *Solea solea* (Linneo, 1758) (Pisces, Soleidae). Inv. Pesq. 46(1):15-28.

Türkmen, M., 2003. Investigation of some population parameters of common sole, (*Solea solea* (L,. 1758)) from Iskenderun Bay. Turk. J. Vet. Anim. Sci. 27:317-323.

Vallisneri M., Piccinetti C., Stagni A.M., Colombari A., Tinti F., 2000. Dinamica di popolazione, accrescimento, riproduzione di *Solea vulgaris* (Quensel 1806) nell'Alto Adriatico. Biol. Mar. Medit. 7(1): 101-106.

Vianet, R., J.-P. Quignard and J.-A. Tomasini, 1989. Age et croissance de quatre poissons Pleuronectiformes (flet, turbot, barbue, sole) du golfe du Lion. Cybium 13(3):247-258.

Vigliola, L., Meekan, M.G., 2009. The Back-Calculation of Fish Growth From Otoliths. In: Green, B.S., Mapstone, B.D., Carlos, G., Begg, G.A. (eds) Tropical Fish Otoliths: Information for Assessment, Management and Ecology. Reviews: Methods and Technologies in Fish Biology and Fisheries, vol 11. Springer, Dordrecht. https://doi.org/10.1007/978-1-4020-5775-5_6.

6. Common sole in GSA 17: searching for best combination of reference points using shortcut-MSE approach

Application of the methodology developed during Workshops on ICES reference points (WKREF1&2) to common sole in GSA 17 case study.

6.1. Introduction

Reference points are used in fisheries advice to classify and communicate current resource status with the aim to prevent overfishing. Growth and recruitment overfishing are generally associated with limit reference points (LRPs; e.g. B_{lim}), while overfishing may be expressed in terms of either targets (TRPs; e.g. B_{trg} and F_{trg}) or limits. The difference between targets and limits is that indicators may fluctuate around targets, but in general limits should not be crossed. Target overfishing occurs when a target is overshot, although variations around a target are not necessarily considered of serious concern unless a consistent bias becomes apparent. In contrast, even a single violation of the LRP may indicate the need for immediate action in order to be consistent with the Precautionary Approach (PA). On the other hand, trigger biomass point ($B_{trigger}$) is intended to implement action before limits are reached (such operationalized trigger points in harvest control rules), while threshold biomass point (B_{thresh}) is used only to classify the stock status. However, despite common commitments to maintain or restore stocks at levels capable of producing maximum sustainable yield (MSY) and the PA to fisheries (UN 1995; FAO 1995), international advice standards vary widely in how this challenge is addressed in particular regarding specifying and estimating the corresponding target and limit reference points. In data-rich assessments, MSY based reference points can be either estimated in the model, i.e. when the SR is fitted internally in the assessment model, or derived post-hoc from the model results, using yield and spawner per recruit assumption combined with a stock-recruitments relationship (S-R). These reference points typically assume equilibrium, or an alternative approach is to run long-term stochastic projections. Benefits of the latter approach are that reference points can account for structural uncertainties and estimation errors (e.g. required for ensembles). A problem, however, is that as reference points estimation procedures become more complicated and computationally demanding, they become less transparent and difficult to verify and validate; where verification is the provision of objective evidence that a given procedure meets the specified requirements, and validation is ensuring that management objectives are actually met. This is complicated by the fact that the quantities used to compute reference points are model-based estimated latent quantities, such as numbers-at-age, spawning stock biomass (SSB) and fishing selectivity, which can therefore not be validated by observations (Kell et al. 2021). Thus, verification and validation of reference point systems need to be based on simulation-testing. Simulation-testing

allows verifying consistency of a reference point system in meeting the quantifiable management objectives (e.g. thresholds of B_{trg} and B_{lim}) and validating the system's robustness of achieving the underlying goals (e.g. biomass levels at MSY). The consistency of a reference point system relies on the setting TRPs, LRPs and trigger points so that target thresholds are exceeded and the limit thresholds are not breached. By contrast, a reference point system would be internally inconsistent if, for example, the rules for setting the target fishing mortality (F_{trg}) would fail systematically to exceed the corresponding target biomass. Evaluating consistency does not need knowledge of the "true" quantities and can therefore be simulation-tested using "self-tests". The term self-test is used because the assumptions for simulating the stock dynamics are the same as the assumptions for computing biological reference point proxies. Thus, the reference point estimator is correctly specified with respect to the operating model (OM) simulator (Deroba et al., 2015). In contrast to consistency, the term robustness refers in statistics to a model that provides correct inference despite its assumptions being violated; whereas robustness in engineering means that a system functions correctly in presence of uncertainty (Kell et al., 2016). In the context of fisheries advice both meanings are interrelated and highly relevant. Evaluating the robustness of a reference point system therefore requires testing if it can also produce desired outcomes in situations where the reality (OM) differs in assumptions from the reference point estimator (Deroba et al., 2015). Using simulations for robustness testing provides an additional scope beyond a self-test because it can be used to validate that if by meeting management objectives, the desired yet latent state of the stock (e.g. biomass at or above the "true" deterministic B_{MSY}) is achieved with high probability despite imperfect knowledge of the true population dynamics. Recently, a series of ICES Workshops on ICES reference points (ICES, 2022a, b) explored the consistency and robustness of candidate reference point systems as a basis to re-evaluate the process for estimating, updating and communicating reference points in accordance with the precautionary objectives of CFP and ICES advice framework. Following the guidelines provided during the workshops, the aim of the study was to test and evaluate sets of candidate reference points considering stock-specific characteristic and to rank them on the basis of performance evaluation criteria. We have to keep in mind that, ensemble model does require a shift in the concept of reference points as the competing models must be treated in a relative sense. In this particular application the different assumptions of selectivity, steepness and natural mortality result in substantially different absolute levels of productivity but comparison can be made in relative terms to the virgin or unexploited biomass (i.e. see Dynamic B_0 concept) in each scenario. To this aim, the determination of reference points was established using a shortcut management strategy evaluations approach (MSE; Punt et al. 2015), testing a range of fishing mortalities and biomass levels in relation to virgin stock size (B_0). Fishing mortalities that resulted in biomasses target (B_{target}) of 20%, 25%, 30%, 35%

and 40% of B_0 were explored, this range being well established in global fisheries (ICES, 2022c). A range of multipliers (100% or "target as trigger", 80% and 60%) on B_{target} was explored as candidates for $B_{trigger}$. With the aim to unify the MSY and Precautionary approach within a single reference point system, the best candidates were presented using the Advices rules plot (source `FLRef` function plotAR(); https://github.com/henning-winker/FLRef). Namely, the Advices rules plot integrates the four-colour classification system of the Kobe MSY framework used in tuna RFMOs (de Bruyn et al., 2013) with key elements for the PA frameworks drawn from ICES (ICES, 2020), the New Zealand Harvest Standard (New Zealand Ministry of Fisheries, 2008) and the Canadian Harvest Strategy (DFO, 2009).

6.2. Simulation-test framework

To develop the short-cut MSE model, the simulation-testing framework available in the Fisheries Library for R (FLR; Kell et al., 2007; https://flr-project.org/) was used. To best simulate all possible state of nature in the OMs implementation, the 18 SS3 models included in the ensemble grid presented in chapter 4 were converted to FLR single sex and single fleet models with an annual time step (Figure 6.2.1). The simulation framework was implemented in the FLR library `mse` (https://github.com/flr/mse) with `FLasher` (https://github.com/flr/FLasher) being used to carry out the forward projections. Reference points at equilibrium were calculated with `FLBRP` (https://github.com/flr/FLSRTMB). To facilitate customized reference point estimation and visualization of F_{MSY} proxy (hereafter defined as F_{brp}, which in this case was expressed as the F that brings the stock at a given fraction of B_0, i.e. FB%), B_{lim}, B_{trg}, F_{trg}, the FLR package `FLRef` was used (https://github.com/henning-winker/FLRef).

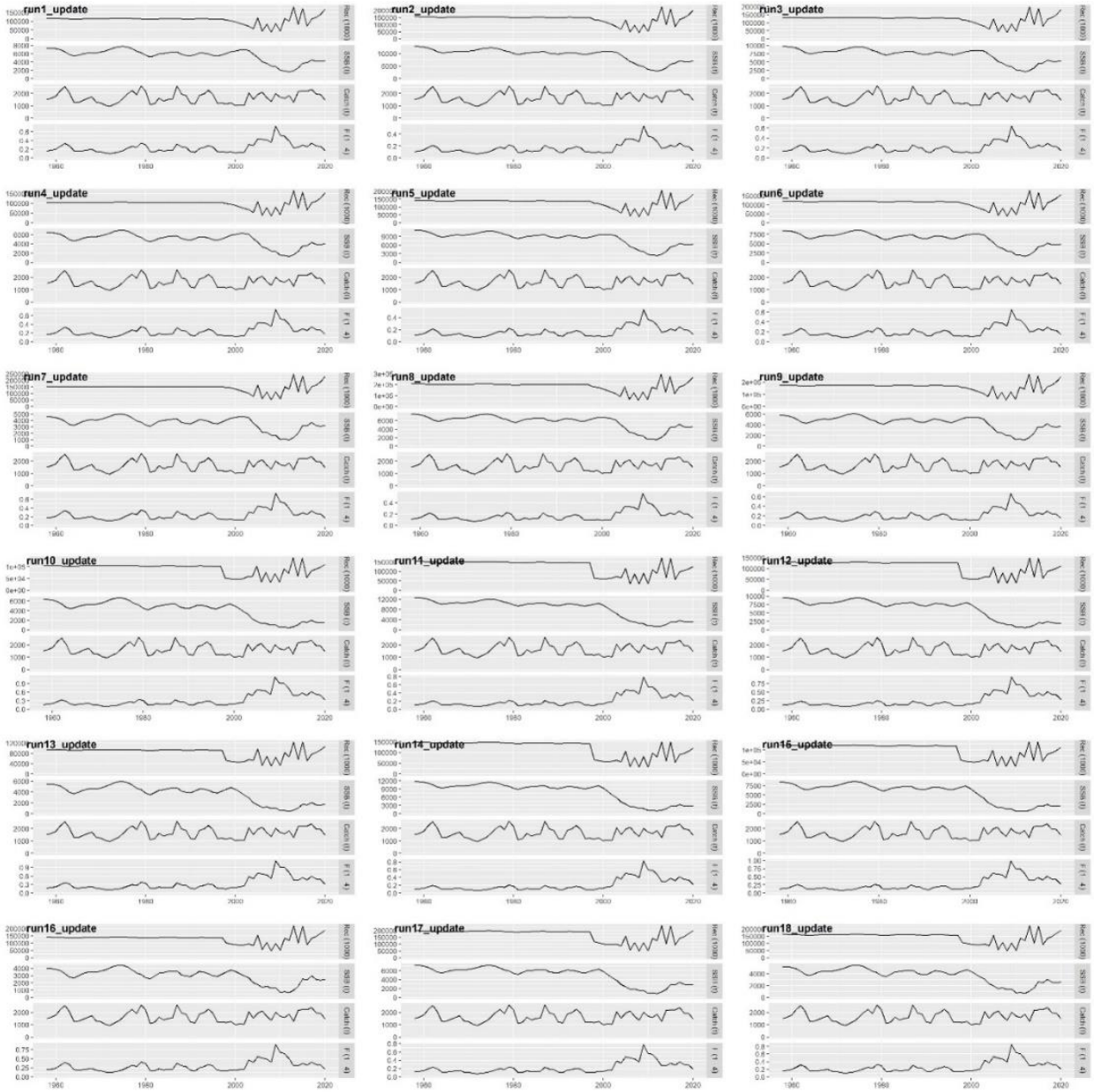

Figure 6.2.1. Graphical representation of the 18 FLR single sex and single fleet models used for shortcut MSE simulation.

Future projections were run for 60 years (i.e. 2021-2080) with 250 iterations, and were based on the 3-year average of the most recent data (i.e. 2017-2020) for weight-at-age, maturity-at-age, natural mortality-at-age and the F pattern determining the selectivity-at-age. This choice was made to account for non-stationary processes in these quantities. The performance evaluations were based on the last 10 years of the 60-year projection horizon (i.e. 2071-2080). For the simulation testing, stock and recruitment, steepness, sigma R were all set at the same values previously derived for each model of the ensemble (chapter 4). The recruitment deviation is assumed to be associated with a first-order autocorrelation (AR1) process and a function of recruitment standard deviation (sigma R) and the AR1 coefficient ρ (Johnson et al., 2016). Recruitment autocorrelation coefficient ρ is taken from a

MVN Monte-Carlo tool used to condition stock specific life-history traits, by sampling of predictive distributions from FishLife2.0 (Thorson 2020). The different sets of reference points were simulated by variations in the parameters F_{trg} and $B_{trigger}$ using a generic harvest control rule (HCR), in the same form of the conventional ICES Advice Rule (ICES, 2021), where the advice decreases from F_{trg} to zero and from $B_{trigger}$ to zero SSB (Figure 6.2.2).

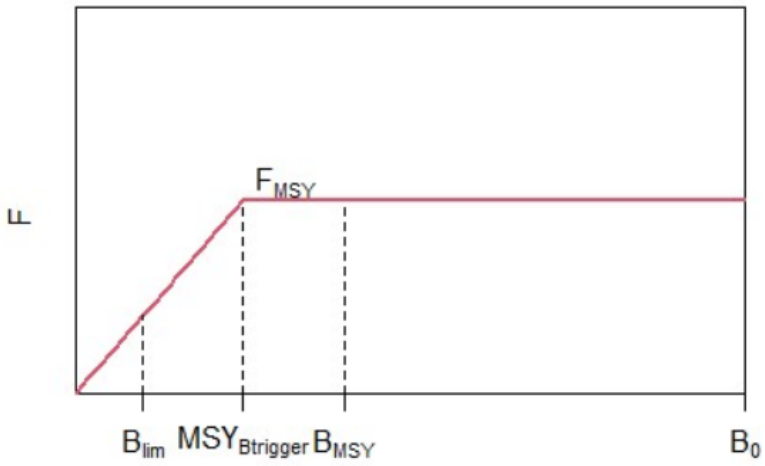

Figure 6.2.2. Graphical illustration of the generalized ICES Harvest Control Rule applied in the simulation.

The HCRs were implemented using a simulated feedback control loop between the implementation system and the operating model, where the implementation system translates the assessment outcome via the HRC into the Total Allowable Catch (TAC) advice (Figure 6.2.3). The loop accounts for the lag between the last year of data used in the assessment and the implementation year of TAC advice. The implementation system of HCR assumes that advice is given for year y+1 based on an assessment completed in year y, which is typically fitted to data up until year y-1 (ICES, 2020). Therefore, implementation of the TAC derived through HCR requires projection of the stock dynamics by way of a short-term forecast (Mildenberger et al., 2021). In contrast to a full MSE simulation design, a short-cut approach omits the step of annually updating the estimation model (assessment) in the feedback control. Instead, it passes the 'true' age-structured dynamics from the operating model to the HCR implementation. The merits of a short-cut MSE approach include the incorporation of the lag effect between data, assessment, and management implementation. The limitations of the MSE short-cut approach are that it cannot fully account for uncertainties resulting from imperfect sampling of the full age-structure (e.g. poorly sampled recruits), observation error and model estimation error. Therefore, robustness testing is limited here to the structural uncertainty about the externally fitted SRR, which determines the stock's recruitment relationship and the absolute scale of R_0, with direct impacts on reference points such as F_{MSY}, B_{MSY}, MSY, B_0, B_{trg} or $B_{trigger}$.

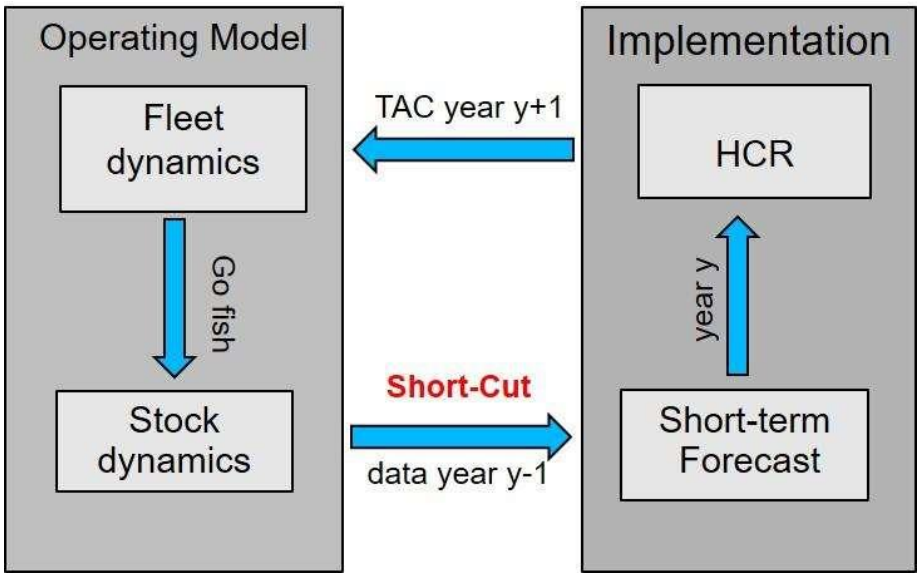

Figure 6.2.3. Schematic illustrating the key processes of the short-cut approach to MSE, showing the Operating Model that simulates the fishery and stock dynamics on the left and Implementation System including the short-term forecast on the right. The short-cut denotes the omission of the estimation (stock assessment) model which updates with new observations (with estimation error) in a conventional MSE implementation with a full feedback control loop. Source: ICE, 2022b.

6.3. Performance Evaluation Criteria

The consistency tests were designed to identify the generic rules for specifying F_{brp}, B_{trg} and $B_{trigger}$ according to the stock-specific productivity that provides the optimal trade-off among the following three main objectives: (1) to not exceed a 5% probability of SSB falling below B_{lim} in any single year (2) to achieve high long-term yields that correspond whenever possible, to at least 95% of the median long-term yield attained by fishing at the deterministic MSY, (3) to attain at least 50% probability that SSB is above the 80% of B_{trg} (B_{thresh}). These three objectives are interpreted hierarchically whereby (1) is the overriding criteria of maintaining stock size above B_{lim} with at least 95% probability to be compliant with the ICES Precautionary Approach (PA). Conditional on objective (1), objective (2) is based on the ICES definition for using plausible values around F_{MSY} in the advice rule, which are derived so that they lead to no more than a 5% reduction of MSY obtained by fishing at F_{MSY} in the long term. The B_{tresh} in objective (3) is adopted by FAO (e.g. Sharma et al., 2021) and Canada (DFO, 2019) for classifying stock status as "sustainably fished" and within "Healthy Zone (Green)", respectively. To set B_{lim} for objective (1), plausible fractions of B_0 based on biological principles and life history of the stock are used (B_{lim} type 2; ICES, 2022a). When expressed as a fraction of B_0, B_{lim} typically ranges from 0.1 to 0.2 of B_0 while, as shown by simulations, setting B_{lim} well under 10% of B_0 renders the reference point system ineffective for most ICES stocks with or

without the use of $B_{trigger}$ (ICES, 2022a). Moreover, the presence of the Allee effect (i.e. depensation) in exploited fish was identified to occur when the stock is below 15-25% of B_0 (Perälä and Kuparinen, 2017; Perälä et al., 2022). For this study simulation, two fractions of B_0 have been tested as limit reference point: 0.15 and 0.2. The stock-recruitment relationship for the 18 different models of the ensemble is shown in Figure 6.3.1 with the addition of two overall B_{lim} calculated as the median value of 0.15 and 0.20 B_0 of all the runs explored.

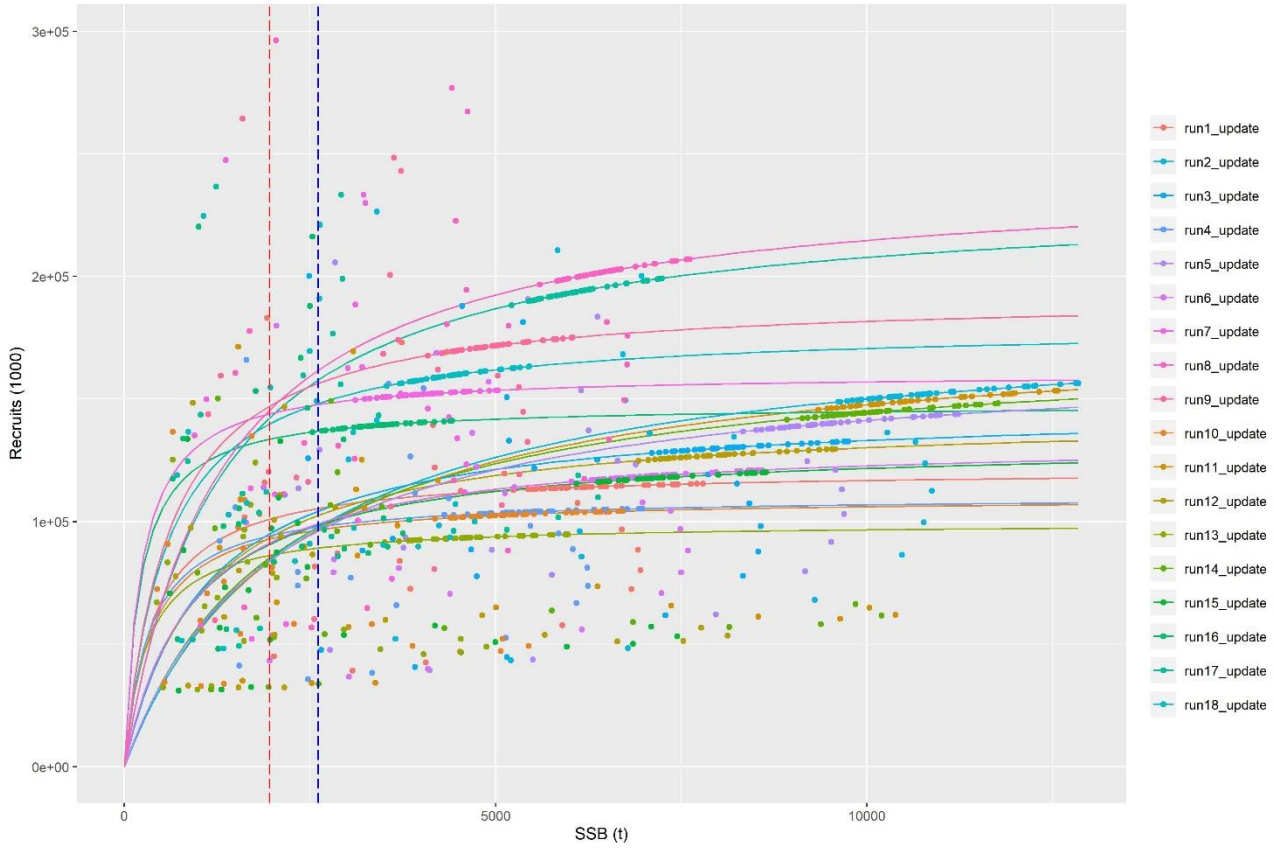

Figure 6.3.1. Stock-Recruitment relationship for the 18 models of the ensemble. Red and blue and black line are median 15%B_0 and 20%B_0 respectively.

6.4. Results

Sixteen scenarios (i.e. 5 x B_0 fraction x 3 x $B_{trigger}$) and the deterministic F_{MSY} were run in the short-cut MSE. The whole process was done twice, once for each level of B_{lim} tested (B_{lim} = 0.2 B_0 or 0.15 B_0). As an example of the simulations output, trends in SSB, F, landings, and Recruitment for the different combinations of F_{target} and $B_{trigger}$ as compared to the deterministic F_{MSY} are shown for Run1 in Figure 6.4.1 (with B_{lim} = 15%B_0). The *a priori* adopted reference point based on general considerations (Horbowy, J., and Luzeńczyk, A. 2012) used for giving official advice in the FAO-GFCM Benchmark (FAO-GFCM, 2021) and shown in chapter 4, is represented by the combination of B_{target} = 40%B_0, B_{lim} = 20%B_0 without a specific trigger value ("target as trigger").

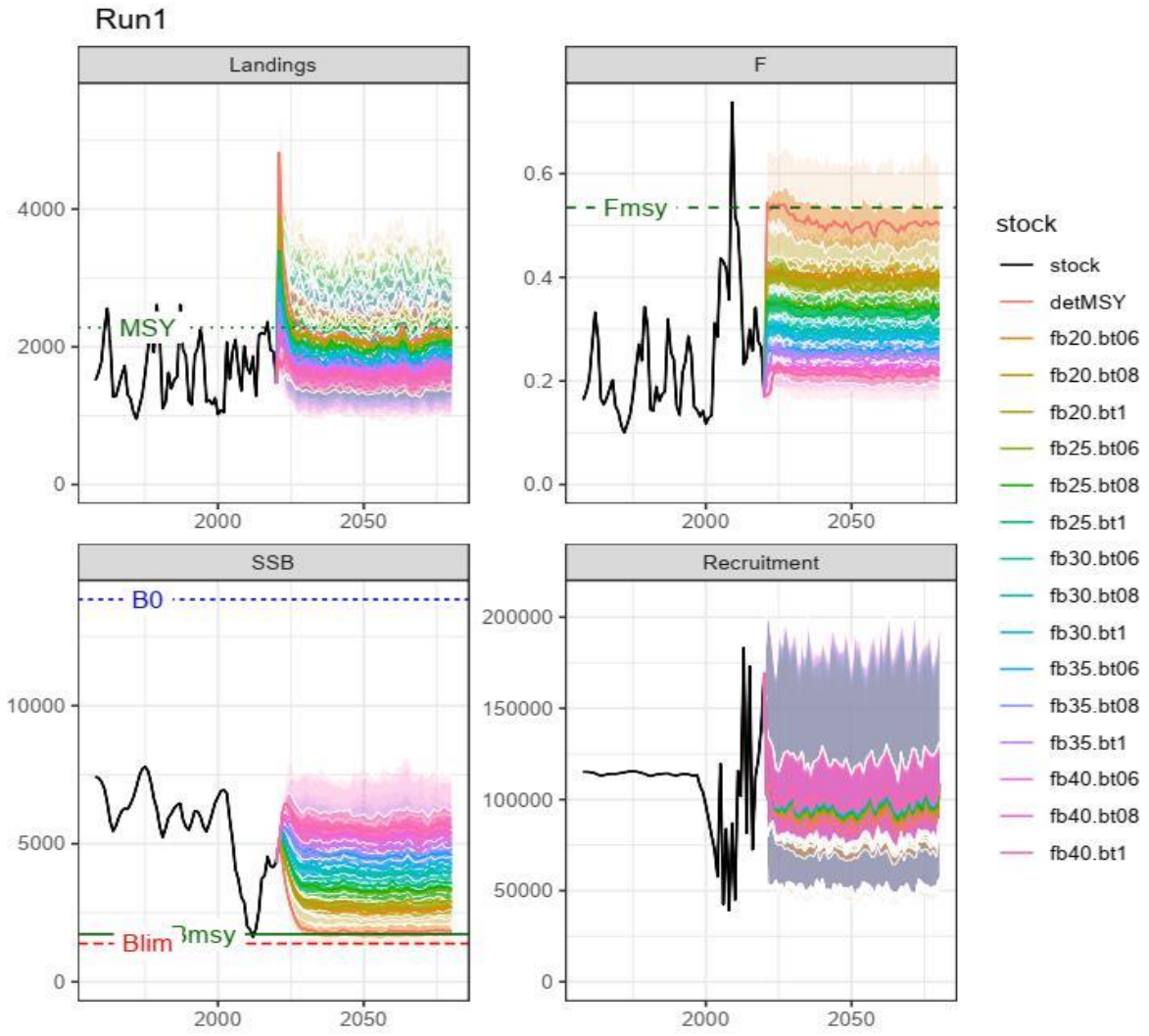

Figure 6.4.1. Long-term simulations for Run1. Trends in SSB, F, landings, and R for different combinations of F_{target} and $B_{trigger}$ and compared to the deterministic F_{MSY}.

The simulation showed that fishing at deterministic F_{MSY} implies a probability of SSB falling below B_{lim} that is larger than 20% for $B_{lim}0.15$ (with extreme values up to 70%) and larger than 60% for $B_{lim}0.2$ (with extreme values up to 90%) (Figure 6.4.2.d,e; Table 6.4.1). Considering $B_{lim}0.15$, the first set of reference points to reach the objective (1) of not exceeding a 5% median probability of SSB falling below B_{lim} is the $FB_{25\%}$ with $B_{trigger}$ equal to B_{target} (fb25.bt1; Figure 6.4.2.d; Table 6.4.1). This combination also achieves objective (2) since the difference in long term yield between fb25.bt1 and fishing at the determinist F_{MSY} is less than 4% with no probability of SSB falling under B_{thresh} (objective 3), indeed biomass is about 50% larger than the deterministic target (B_{MSY}) with an F still reaching 75% of the deterministic value (Figure 6.4.2.a,b,c; Table 6.4.1). However, it is important to note that this combination implies a right tail of probabilities of SSB to be below B_{lim} above 5% (upper whisker in the boxplot of Figure 6.4.2.d, data.95% in Table 6.4.1). On the other hand, the first combination with B_{lim} equal to 15% B_0 and with no values over the 5% threshold is the $FB_{30\%}$ with

$B_{trigger}$ set at 60% of B_{target} (fb30.bt06; Figure 6.4.2.d; Table 6.4.1). On the other hand, considering B_{lim}0.2, the first set of reference points to reach the objective (1) is the $FB_{35\%}$ with $B_{trigger}$ set at 80% of B_{target} (fb35.bt08; Figure 6.4.2.e; Table 6.4.1). This combination fails to achieve goal (2) since the difference in long term yield between fb35.bt08 and fishing at the determinist F_{MSY} is around 11%. However, objective (3) is easily achieved by also allowing to nearly double the biomass at sea (SSB is 95% larger than B_{MSY}) while giving up only 11% of potential catches at MSY with an F reaching 60% of the deterministic value (Figure 6.4.2.a,b,c; Table 6.4.1). Also for this combination, there is a right tail of probability of SSB to be below B_{lim} above 5% (upper whisker in the boxplot of Figure 6.4.2.e, data.95% in Table 6.4.1). On the other hand, the first combination with B_{lim} equal to 20% B_0 and with no values over the 5% threshold is the $FB_{35\%}$ with $B_{trigger}$ equal to B_{target} (fb35.bt1; Figure 6.4.2.e; Table 6.4.1). The a-priori adopted Benchmark reference point simulated in the fb40.bt1 set is the best in reaching objective (1) and (3) with nearly 0 possibility to fall below B_{lim} and resulting in more than double of biomass and half the F level (Figure 6.4.2.a,b,e; Table 6.4.1). On the other hand, is the combination with the major loss of catches in the long-term yield, around 20% (Figure 6.4.2.c; Table 6.4.1).

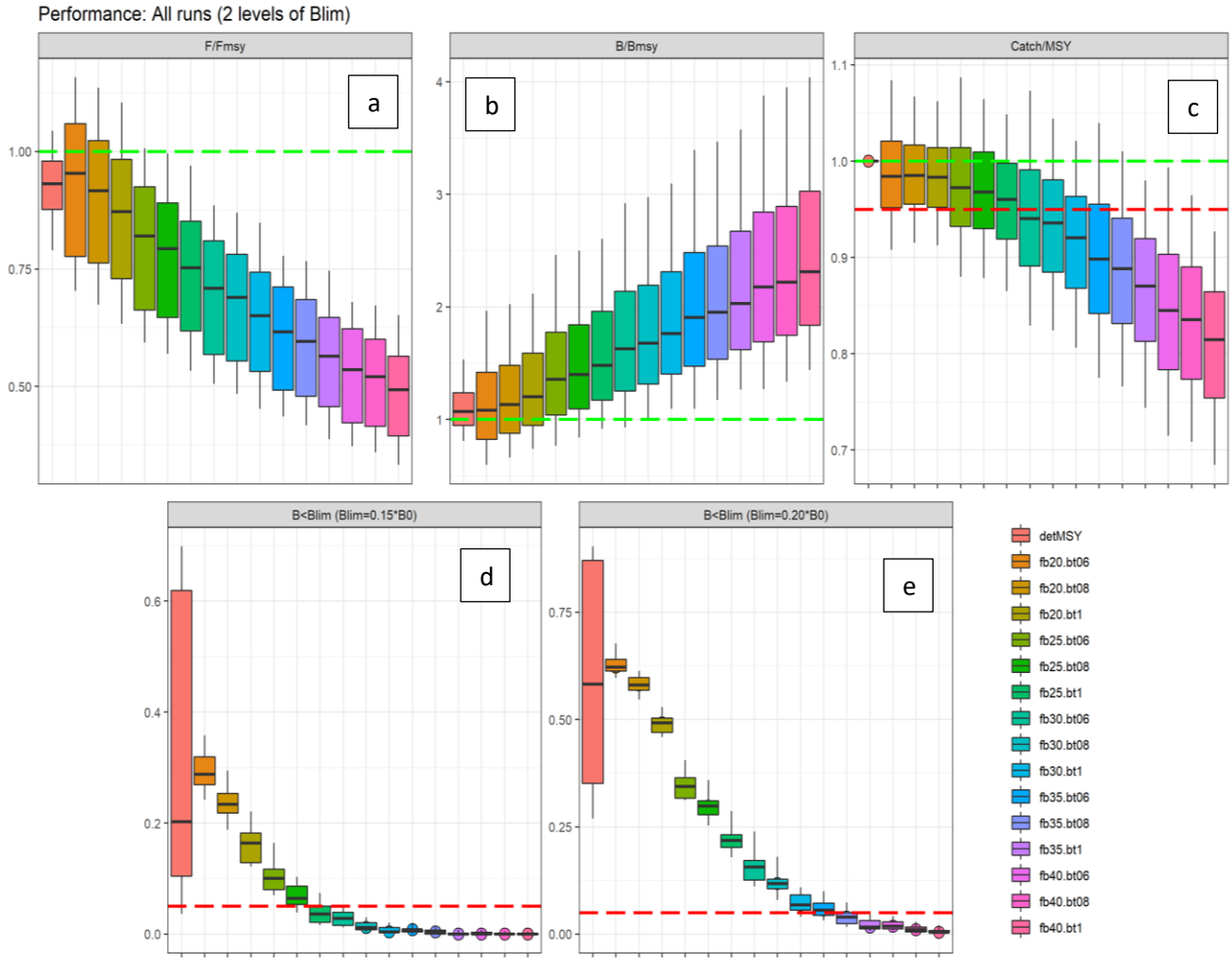

Figure 6.4.2. Graphical results of the shortcut MSE used to evaluate reference point systems: (a,b) median long-term F and SSB relative to the deterministic F_{MSY} and B_{MSY} , (c) median long-term yield relative the median long term obtained at fixed deterministic F_{MSY} , (d,e) the probability of SSB falling below B_{lim} using B_{lim}= 0.15 and 0.20 B_0 respectively. Green and red dashed lines denoting the target and limit probability thresholds, respectively. Candidates based on different combinations of F_{target} and $B_{trigger}$ and compared to the deterministic $F_{MSY.}$

Indicator	Value	detMSY	fb20.bt06	fb20.bt08	fb20.bt1	fb25.bt06	fb25.bt08	fb25.bt1	fb30.bt06	fb30.bt08	fb30.bt1	fb35.bt06	fb35.bt08	fb35.bt1	fb40.bt06	fb40.bt08	fb40.bt1
B/B_{MSY}	data.50%	1.07	1.08	1.13	1.20	1.36	1.40	1.48	1.63	1.68	1.76	1.90	1.95	2.03	2.18	2.22	2.31
	data.5%	0.81	0.60	0.66	0.74	0.76	0.84	0.92	0.93	1.00	1.10	1.10	1.17	1.26	1.27	1.34	1.44
	data.95%	1.53	1.97	2.02	2.11	2.46	2.50	2.60	2.92	2.97	3.09	3.39	3.46	3.57	3.88	3.95	4.03
$B<B_{lim}$ ($B_{lim}=0.15*B_0$)	data.50%	0.20	0.29	0.23	0.16	0.10	0.06	0.04	0.03	0.01	0.00	0.01	0.00	0.00	0.00	0.00	0.00
	data.5%	0.04	0.24	0.19	0.12	0.07	0.04	0.02	0.01	0.00	0.00	0.00	0.00	0.00	0.00	0.00	0.00
	data.95%	0.70	0.36	0.29	0.22	0.16	0.10	0.07	0.05	0.03	0.02	0.02	0.01	0.01	0.01	0.00	0.00
$B< B_{lim}$ ($B_{lim}=0.20*B_0$)	data.50%	0.58	0.62	0.58	0.49	0.34	0.30	0.22	0.16	0.12	0.07	0.06	0.04	0.02	0.02	0.01	0.00
	data.5%	0.27	0.60	0.55	0.46	0.31	0.25	0.18	0.11	0.08	0.04	0.03	0.02	0.01	0.01	0.00	0.00
	data.95%	0.90	0.68	0.61	0.53	0.40	0.36	0.29	0.24	0.18	0.11	0.10	0.07	0.05	0.04	0.03	0.02
Catch/MSY	data.50%	1.00	0.98	0.99	0.98	0.97	0.97	0.96	0.94	0.94	0.92	0.90	0.89	0.87	0.84	0.84	0.81
	data.5%	1.00	0.91	0.91	0.91	0.88	0.88	0.86	0.83	0.82	0.81	0.77	0.77	0.74	0.71	0.71	0.68
	data.95%	1.00	1.08	1.07	1.06	1.09	1.06	1.05	1.07	1.04	1.02	1.04	1.01	0.98	0.99	0.96	0.93
F/F_{MSY}	data.50%	0.93	0.95	0.92	0.87	0.82	0.79	0.75	0.71	0.69	0.65	0.62	0.60	0.56	0.54	0.52	0.49
	data.5%	0.79	0.70	0.67	0.63	0.59	0.57	0.53	0.50	0.48	0.45	0.43	0.42	0.39	0.37	0.36	0.33
	data.95%	1.04	1.16	1.14	1.10	1.01	1.00	0.97	0.88	0.87	0.85	0.78	0.77	0.75	0.68	0.67	0.65

Table 6.4.1. Results of the shortcut MSE used to evaluate reference point systems. B/B_{MSY}: median long-term of SSB relative to the deterministic B_{MSY} ; F/F_{MSY}: median long-term of F relative to the deterministic F_{MSY}; Catch/MSY: median long-term yield relative the median long term obtained at fixed deterministic F_{MSY} ; $B<B_{lim}$ ($B_{lim}=0.15*B_0$): the probabilities of SSB falling below B_{lim} using B_{lim}= 15% of B_0; $B<B_{lim}$ ($B_{lim}=0.20*B_0$): the probabilities of SSB falling below B_{lim} using B_{lim}= 20% of B_0. Coloured columns highlight the scenarios of interest described in the text.

As an example of how the selection process of possible candidate reference points could be done, Figure 6.4.3 shows the Advices rules plots for the scenarios of interest applied to the reference run of the ensemble shown in chapter 4 (Run 1 of the ensemble grid). The scenarios are presented from left to right from the least to most precautionary one given B_{lim} values adopted in the simulation and the consideration or not of the asymmetric risk. The system includes five stock status zones delineated for stock size by B_{lim} and B_{thresh} (80% of target in objective 3), and for fishing pressure by F_{trg}. The trigger has only an operational value so is not considered for stock status classification. The stock status zone below F_{trg} and above B_{thresh} is the "Sustainable" zone illustrated in green ($B > B_{thresh}$ and $F < F_{trg}$). The orange "Overfishing" zone demarcates sustainable biomass levels above B_{thresh}, but unsustainable fishing pressure ($B > B_{thresh}$ and $F > F_{trg}$). The stock is classified to be in the yellow rebuilding zone if biomass is below B_{thresh} but fishing pressure is below F_{trg} so that biomass is predicted to increase ($B > B_{tresh}$ and $F > F_{trg}$). According to this new classification system, the stock status of the reference run would be classified as "Sustainable" for all scenarios. However, considering the combinations based on B_{lim}=20%B_0 the biomass level would still be below the target (blue line in the Advice rule plot).

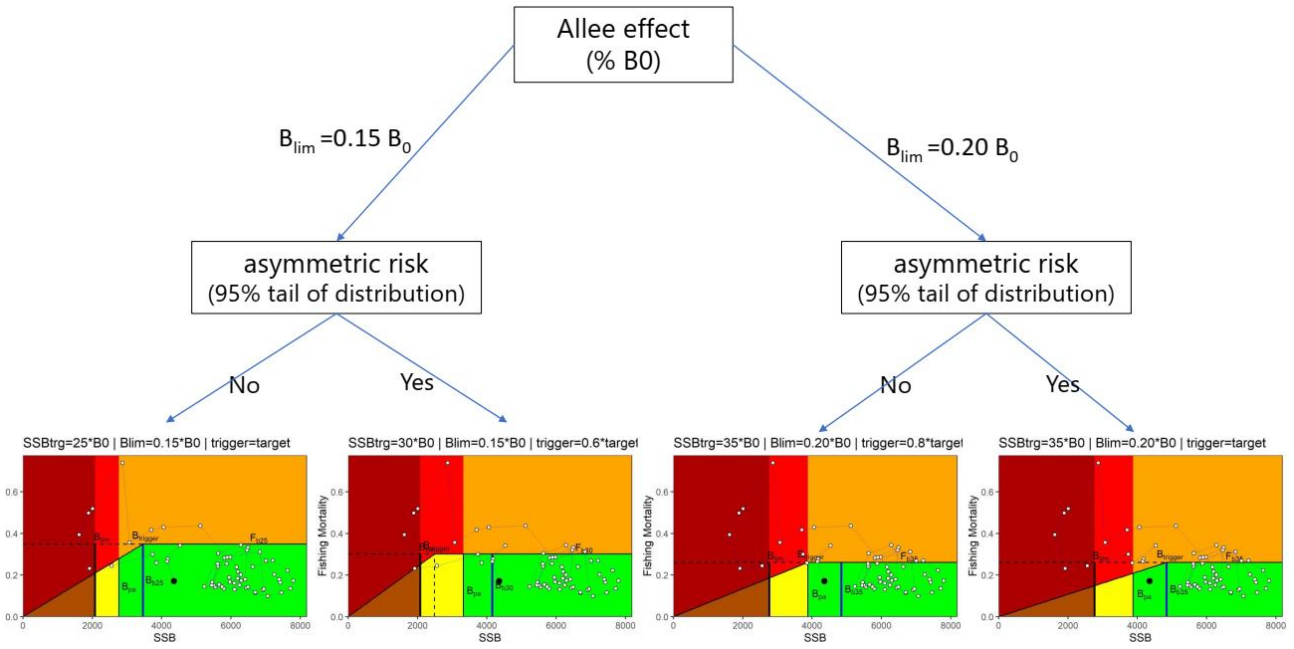

Figure 6.4.3. Selection process workflow for common sole candidate reference points in GSA17. "Advice Rule" plots show modelled quantities against corresponding reference point with integrated Harvest Control Rule applied to the reference run (Run 1 of the ensemble grid).

6.5. Discussion

The analyses proposed in this chapter is aiming to deeply explore specific stock-related reference point for common sole in GSA17. The generic rule applied in the official assessment - mortality corresponding to a biomass at 40% B_0 as a proxy for B_{MSY}- is to be considered quite robust to generate safe biomass levels irrespective of the steepness value of the stock recruitment function (Punt et al., 2013). Nevertheless, the discussion generated during the first ICES Workshop on reference points meetings (ICES 2022a) has led to a request for greater transparency in the calculation of reference points while offering tools and technologies that are publicly accessible and easily replicable for experts in the sector. Among them, the shortcut MSE approach offers wider flexibility and represents an optimal tool to test and evaluate the consistency and robustness of alternative set of reference point in accordance with the overarching principles and precautionary objectives of CFP and international best practices. The large-scale simulation testing experiment for 64 ICES stocks conducted in preparation of the meeting delineated some guidelines for setting reference points according to productivity category. For medium productive species like flatfishes, the mortalities that resulted in biomasses target of 35% of virgin biomass and a trigger value of 0.8 of the target (B_{trg} = 35%B_0 and $B_{trigger}$ set at 0.8 B_{trg}) has been recommended as candidates reference point. However, concerns were raised regarding the need to condition the simulation for the specificities of individual stocks (e.g. stock specific S-R functions) rather than using a generic approach (ICES, 2022b). Practical examples come from *Pandalus borealis* in divisions 3.a and 4.a East (ICES 2022c) and *Coregonus albula* in Bothnian Gulf (Bergenius et al., 2022), where the shortcut MSE approach has already been used for setting *ad-hoc* reference points during official ICES and national benchmark processes.

The choice of B_{lim} is generally difficult. B_{lim} should only be specified empirically in cases where there is sufficient contrast in the S-R data to estimate a well-defined break-point (ICES, 2021a). Accurate estimation requires long time series of data informative of recruitment. This is not the case for common sole in Adriatic where recruitment data coming from the survey started only in 2005 (long after commercial fishing for common sole has started). The uncertainty on the S-R relation is also underlined by the inclusion of the steepness parameter (*h*) among the variability considered during the implementation of the ensemble model in chapter 4. The alternative approach used in this study is to use some fraction of B_0 as a limit, since this quantity is estimated from the top of the recruitment function and does not rely on being able to estimate the break point of that recruitment function. Moreover, the inclusion of historical data in the assessment provides a reasonable estimate of B_0. Finding the proper fraction can be challenging given the variability between stocks, but, in accordance with international best practice, B_{lim} should be set at levels of SSB that avoid possible Allee effect.

Allee effects describe the association between population size (e.g., SSB) per capita population growth rate (realized or simply r), a metric of the average individual fitness in a population. The SSB at which r begins to decline (relative to the negatively density dependent pattern exhibited at larger SSB) is termed the Allee-effect threshold (Hutchings, 2015; Perälä et al., 2022). That is, Allee-effect thresholds identify the SSB below which negative density-dependence weakens and below which stock recovery is increasingly impaired and uncertain. Albeit without empirical confirmation in this study, the two levels tested in this simulation are in line with the updated scientific knowledge (15-25% of B_0; Hutchings, 2014; Hutchings, 2015; Perälä and Kuparinen, 2017; Perälä et al., 2022).

In the case study conducted for this thesis and here presented, the simulation confirmed that fishing at MSY is not precautionary for common sole in Adriatic Sea. In fact, even fishing at F_{MSY} under HCR can still be associated with high risk of a collapse below B_{lim} (despite the B_{lim} level chosen). Subsequent rebuilding requires fishing mortalities lower than F_{MSY} which may come at high costs of reduced catches and long recovery time. This scenario is to be avoided and confirms that fishing at MSY level is too risky for the stock in the long term, breaching the sustainability principles of the EU Common Fisheries Policy (Reg EU No. 1380/2013). Conversely, fishing mortality that produces the MSY should be considered as a fishing mortality limit rather than a management target (guidelines for applying a PA in UN Fish Stocks Agreement, UN 1995). Following the principle of the "pretty good yield" (Hilborn, 2010) fishing somewhat below F_{MSY} is proved to be more robust to asymmetric risk associated with fishing below or above the 'true' unknown F_{MSY}, where asymmetric risk describes the phenomenon that one direction of bias for an estimate lead to disproportionately higher risk than if the bias would occur in the other direction (Hordyk et al., 2019).

The official reference point adopted in chapter 4 (fb40.bt1) show in the simulation a sharply reduction of long-term catches strongly below the potential MSY (-20%). On the other hand, deciding to remain as precautionary as possible (avoid possible Allee-effect and asymmetric risk), mortality that results in SSB of 35% of virgin biomass (fb35.bt1) should be indicated as a good alternative to the reference point set officially adopted since it is more compatible with the fundamental principles of CFP (Reg EU No. 1380/2013) providing the theoretical best compromise between long-term environmental and economical sustainability. However, aware of the presence of an asymmetric risk on the achievement of the objective (1), the trigger in the HCR could be shifted up to 80% of the target (fb35.bt08 scenario). As further confirmation, this set is in concordance with ICES guideline for deriving ref points for medium productive species like flatfishes (ICES, 2022b). On the other hand, considering a lower level of B_{lim} but still in the limit given by the current scientific knowledge, fb30.bt06 scenario would allow a major high long-term yield. Ultimately, although linked to a less precautionary B_{lim}

level and more prone to the asymmetric risk, it must be acknowledged that fb25.bt1 is the only case in which there are more possibility to achieve the goal of high long-term yields (95% of deterministic MSY). In fact, fishing at 75% of deterministic F_{MSY}, would still yield on average 96% of MSY; this result is in agreement with what is described by Mace 1994 and Restrepo et al. 1998. To conclude, instead of adopting an a priori reference point system, the methods shown in this chapter allow the expert to be able to show, discuss and guide the manager among different possible candidates towards the best choice considering initial managerial objectives (e.g. trade-offs between environmental and socio-economic sustainability). Awareness of the benefits and risks associated with each choice would add greater transparency in the calculation process of reference points during benchmark sessions.

6.6. References

Bergenius, M., Cardinale, M., Lundström, K., Kaljuste, O. 2022. Biologisk rådgivning för siklöja i Bottenviken. SLU.aqua.2021.5.5-272.

de Bruyn, P., Murua, H., Aranda, M., 2013. The precautionary approach to fisheries management: how this is taken into account by Tuna regional fisheries management organisations (RFMOs). Mar. Policy 38, 397–406. http://dx.doi.org/10.1016/j.marpol.2012.06.019.

Deroba, J. J., Butterworth, D. S., Methot Jr, R. D., De Oliveira, J. A. A., Fernandez, C., Nielsen, A., Cadrin, S. X., et al. 2015. Simulation testing the robustness of stock assessment models to error: some results from the ICES strategic initiative on stock assessment methods. ICES Journal of Marine Science, 72: 19–30. https://doi.org/10.1093/icesjms/fst237.

DFO. 2009. A fishery decision-making framework incorporating the precautionary approach. https://www.dfo-mpo.gc.ca/reports-rapports/regs/sff-cpd/precaution-eng.htm.

European Parliament (2013). European Parliament and Council. regulation (EU) No. 1380/2013 of the European Parliament and of the Council of 11 December 2013 on the common fisheries policy, Off. J. Eur. Union L 354 (2013) 22–61.

FAO. 1995. Code of Conduct for Responsible Fisheries. FAO Technical Guidelines for Responsible Fisheries, 4 (Suppl.: 1–112. Rome.

FAO-GFCM. 2021. Report of the Working Group on Stock Assessment of Demersal Species (WGSAD) – Benchmark session for the assessment of common sole in GSA 17, Scientific Advisory Committee on Fisheries (SAC). Online via Microsoft Teams, 12–16 April 2021.

Hilborn, R. 2010. Pretty good yield and exploited fishes. Marine Policy, 34: 193–196.

Horbowy, J., and Luzeńczyk, A. 2012. The estimation and robustness of F MSY and alternative fishing mortality reference points associated with high long-term yield. Canadian Journal of Fisheries and Aquatic Sciences, 69: 1468–1480.

Hordyk, A. R., Huynh, Q. C., and Carruthers, T. R. 2019. Misspecification in stock assessments: Common uncertainties and asymmetric risks. Fish and Fisheries, 20: 888–902.

Hutchings JA. 2014 Renaissance of a caveat: Allee effects in marine fishes. ICES Journal of Marine Science 71, 2152-2157.

Hutchings JA. 2015 Thresholds for impaired species recovery. Proceedings of the Royal Socie-ty B 282, 20150654.

ICES. 2020. The third Workshop on Guidelines for Management Strategy Evaluations (WKGMSE3). ICES Scientific Reports, 2: 1–112.

ICES. 2021. ICES fisheries management reference points for category 1 and 2 stocks; Technical Guidelines. In Report of the ICES Advisory Committee, 2021. ICES Advice 2021, Section 16.4.3.1. https://doi.org/10.17895/ices.advice.7891.

ICES. 2022a. Workshop on ICES reference points (WKREF1). ICES Scientific Reports. 4:2. 70 pp. http://doi.org/10.17895/ices.pub.9749.

ICES. 2022b. Workshop on ICES reference points (WKREF2). ICES Scientific Reports. 4:68. 96 pp. http://doi.org/10.17895/ices.pub.20557008.

ICES. 2022c. Benchmark workshop on Pandalus stocks (WKPRAWN). ICES Scientific Reports. 4:20. 249 pp. http://doi.org/10.17895/ices.pub.19714204.

Johnson, K.F., Councill, E., Thorson, J.T., Brooks, E., Methot, R.D., Punt, A.E., 2016. Can autocorrelated recruitment be estimated using integrated assessment models and how does it affect population forecasts? Fish. Res. 183, 222–232.

Keith DM, Hutchings JA. 2012 Population dynamics of marine fishes at low abundance. Ca-nadian Journal of Fisheries and Aquatic Sciences 69, 1150-1163.

Kell, L. T., Nash, R. D. M., Dickey-Collas, M., Mosqueira, I., and Szuwalski, C. 2016. Is spawning stock biomass a robust proxy for reproductive potential? Fish and Fisheries, 17: 596–616.

Kell, L. T., Sharma, R., Kitakado, T., Winker, H., Mosqueira, I., Cardinale, M., and Fu, D. 2021. Validation of stock assessment methods: is it me or my model talking? ICES Journal of Marine Science, 78: 2244–2255.

Kell, L.T., Mosqueira, I., Grosjean, P., Fromentin, J-M., Garcia, D., Hillary, R., Jardim, E., Mardle, S., Pastoors, M.A., Poos, J.J., Scott, F., Scott, R.D. 2007. FLR: an open-source framework for the evaluation and development of management strategies. ICES Journal of Marine Science, 64: 640-646.

Mace, P. M. 1994. Relationships between common biological reference points used as thresholds and targets of fisheries management strategies. Canadian Journal of Fisheries and Aquatic Sciences, 51: 110–122.

Mildenberger, T. K., Berg, C. W., Kokkalis, A., Hordyk, A. R., Wetzel, C., Jacobsen, N. S., Punt, A. E., et al. 2021. Implementing the precautionary approach into fisheries management: Biomass reference points and uncertainty buffers. Fish and Fisheries: 1–20.

New Zealand Ministry of Fisheries. 2008. Harvest Strategy Standard for New Zealand Fisheries. https://fs.fish.govt.nz/Page.aspx?pk=113&dk=16543.

Perälä T, Kuparinen A. 2017. Detection of Allee effects in marine fishes: analytical biases generated by data availability and model selection. doi/full/10.1098/rspb.2017.1284.

Perälä T, Kuparinen A., Jeffrey Huthchings 2022. Allee Effects and the Allee-effect Zone in Atlantic Cod. Biology Letter. http://doi.org/10.1098/rsbl.2021.0439.

Punt, A. E., Butterworth, D. S., de Moor, C. L., De Oliveira, J. A. A., and Haddon, M. 2015. Management strategy evaluation: best practices. Fish and Fisheries, 17: 303–334. http://doi.wiley.com/10.1111/faf.12104.

Punt, A. E., Smith, A. D. M., Smith, D. C., Tuck, G. N., and Klaer, N. L. 2013. Selecting relative abundance proxies for BMSY and BMEY. ICES Journal of Marine Science, 71: 469–483. http://icesjms.oxfordjournals.org/content/71/3/469.

Restrepo, V. R., Thompson, G. G., Mace, P. M., Gabriel, W. L., Low, L. L., MacCall, A. D., Methot, R. D., et al. 1998. Technical Guidance On the Use of Precautionary Approaches to Implementing

National Standard 1 of the Magnuson-Stevens Fishery Conservation and Management Act. 56 pp. http://www.st.nmfs.noaa.gov/StockAssessment/documents/Tech-Guidelines.pdf.

Sharma, R., Winker, H., Levontin, P., Kell, L., Ovando, D., Palomares, M. L. D., Pinto, C., et al. 2021. Assessing the potential of catch-only models to inform on the state of global fisheries and the UN's SDGs. Sustainability (Switzerland), 13.

Thorson, J. T. 2020. Predicting recruitment density dependence and intrinsic growth rate for all fishes worldwide using a data-integrated life-history model. Fish and Fisheries, 21: 237–251. John Wiley & Sons, Ltd. https://doi.org/10.1111/faf.12427.

UN. 1995. United Nations Conference on Straddling Fish Stocks and Highly Migratory Fish Stocks. New York.

7. General discussion and conclusions

7.1. Summary of stock status and forecast scenarios (data-poor and data-rich approaches)

The partial isolation of the common sole stock in the northern and central Adriatic (GSA17) in conjunction with the high quantity and temporal extension of the data collected over time, makes this specific stock an ideal candidate for an in-depth study on the population dynamics and fishery. A peculiarity of common sole stock in GSA17 is the fact that the majority of catches come from the Italian *rapido* trawl fishery (55% according to data updated to 2020); a unique reality in the Mediterranean panorama, usually characterized by a highly multi-specific fishery (Colloca et al., 2003). In the context of this thesis an in-depth study was carried out aimed at characterizing and analyzing the *rapido* trawl catch assemblage. In this regard, the work presented in chapter 3 appears to be the first extensive assessment-based meta-analysis of the main target and accessories species of *rapido* trawl fishery in the Adriatic Sea. Based on cluster analysis, the catch assemblage of this fishery was identified and assessed using CMSY model. Despite the use of a data-poor approach does not allow the estimates to be taken as the best simulation of reality, they were sufficient to produce an overall sound snapshot of the performance of different future inter-correlated fisheries scenarios, which would have required many years of data preparation and data gap-filling if data-rich approaches had been used. In this regard, the common sole case study offers a precious opportunity to compare the results of the two different approaches (given the due differences in assumptions between the models presented): data-poor (chapter 3) and data-rich (chapter 4). Indeed, although the Adriatic Sea is one of the most intensively trawled area of the Mediterranean Sea (Ferrà et al., 2018) and in the entire world (Amoroso et al., 2018), common sole showed a recovery status at the end of the analysis time-scale in both methodologies (evident in the CMSY Kobe plot trajectory in figure 3.4.2d and SS3 final ensemble model Kobe plot in figure 4.5.7.2). The recovering trend status for this stock is probably due to the effective management actions underway in the area, such as the coastal trawling ban (up to 4 nm) for eight weeks from 2006 and the temporary extension of this spatial restriction up to 6 nm for ten weeks since 2012 (EC, 2006; Scarcella et al., 2022), rather than the moderate effort reduction according to the actual management plan (Recommendation GFCM/43/2019/5). These ad-hoc technical measures might have had relevant consequences for recruitment success in coastal areas (Scarcella et al., 2014) leading to a general improvement in the overall status of common sole stock. Also interesting is to see the effect on stock status of a completely exceptional event such as the COVID-19 pandemic which can be considered a sort of substantial non-programmed effort reduction put in place in 2020 (-25% fishing days for *rapido* trawls compared to 2019). More precisely, the results presented in this thesis are in agreement with

independent analyses results by Scarcella et al. (2022), confirming that the COVID-19 effect can be considered a positive accelerator of a recovery process already underway. In fact, excluding this occasional and extreme effect of Covid-19, it has already been seen how the moderate limitation of fishing days is a measure capable of being circumvented by increasing the duration of fishing trips and/or by increasing fishing efficiency (Palomares and Pauly, 2019). On the other hand, a more severe long-term limitations to effort cannot be considered an optimal management strategy since is likely to create conflicts between the fishery sector and the management system. Moreover, while common sole seems to have benefited from the management measures put in place, the data-poor analysis reveals that reduction in fishing pressure seems to have had a limited effect on those stocks in poor biomass status such as scallops and brill. This confirms that effort reduction by itself does not imply a concomitant overall reduction of the fishing mortality (see "hyperstability" problem in Cardinale et al., 2017) and that the reduction enforced by the current effort-based system must be accompanied by other management measures such as spatial-temporal closures. Alternative option could be to move towards a management regime based on output control system such as quotas (e.g. TAC); this type of management has been proven to be successful for North East Atlantic stocks. If the reduction of effort does not always have a direct effect on fishing mortality, acting on the catches is a more direct and efficient method to reduce F. Although conducting projections from a stock assessment is not the same as applying a simulation-based model (e.g. full-MSE analysis), the probabilistic short-term forecasts presented in chapter 4 can be considered a first attempt, even if simplified, to apply TACs to the case of common sole in the Adriatic. Specifically, the analyses show how, maintaining an overall catch level close to current values (*status quo* condition in 2020), Adriatic stock would remain at a sustainable exploitation level. On the contrary, a return to pre-pandemic values would cause an increase in F, also breaching the precautionary objectives of the CFP. A disadvantage of this exercise is that the quotas were set equal for all the gears involved (TBB, OTB, DRB and Nets) without taking into account the actual differences and complexity of the Mediterranean fisheries panorama, characterized by a large number of small vessels operating on a small spatial scale and which could hardly sustain such reductions. In fact, if not adequately controlled, a TAC-based system can create incentives for discarding, black landings and misreporting of catches. This is likely considering that Mediterranean system has returned from a past of continuous non-adherence to the scientific advice and low level of compliance and enforcement compared to the North East Atlantic (Vasilakopoulos et al., 2014; Cardinale et al., 2017). Moreover, despite fisheries science has long pushed for probabilistic advice (Röckmann et al., 2012), further consideration is needed on how to include technical advances of the approach within the Mediterranean management system which is generally still ‘looking for a single number’.

7.2. The novelty of ensemble approach

Since the TAC-based system strongly depend on the recent stock estimates, a good reliability of the assessment procedure is required. In this sense, the novelty of ensemble approach developed in chapter 4 used in combination with conventional stock assessment software, provides a more robust quantification of model uncertainty and more reliable predictions of stock status compared to past advice. Usually, in stock assessment standard procedure, best available information are used to fix key population parameters in a so called "base case" configuration. Indeed, this necessarily implies strong assumptions regarding stock's productivity, reference points and associated management implications (Merino et al. 2022). Conversely, the use of a more modern ensemble approach makes it possible to provide advice based on the combination of the outcomes of several alternative hypotheses to be tested within a single integrated framework (Merino et al. 2022). In the common sole specific case, this allows to capture a greater structural uncertainty related to alternative assumptions about functional relationships (selectivity) and fixed parameter values (natural mortality and steepness). Another element of innovation is the use of an interconnected diagnostic system to evaluate and validate the individual models of the grid. In fact, Carvalho et al. (2021) have shown how difficult and sometimes counterproductive could be to use a single criterion for discarding or selecting models. Although it is common to evaluate diagnostics for a reference case (Fu et al., 2021), or in a subset of models (Minte-Vera et al., 2020; Xu et al., 2020), only a few cases where diagnostics were used to weigh all models of the ensemble grid have been reported to date (e.g. South Pacific Albacore tuna - Castillo et al., 2021). Only recently, in fact, the development and use of new techniques such as the delta-Multivariate log-Normal estimator (delta-MVLN; Walter and Winker, 2019; Winker et al., 2019) has made possible to significantly reduce the time compared to conventional techniques more computationally intensive and time consuming, such as MCMC. This makes the ensemble approach described in this thesis ideal for typically time-constrained stock assessment meetings. As proof, the application of the time-step procedure to the Common sole in GSA 17, take only a few minutes to process final result from the final 18 runs grid. Furthermore, the development of highly automated, easily reproducible and public procedures and scripts in R language (https://github.com/framasnadi/SS3-ENSEMBLE-MODEL-scripts) allow the methodology to be highly transferable and enforceable for other stocks. Practical examples of the application of the work done for this thesis in the ICES framework are the stock assessment of *Pandalus borealis* in divisions 3.a and 4.a East (ICES 2022a) and *Coregonus albula* in Bothnian Gulf (Bergenius et al., 2022). Confirming the novelty and applicability of the methodology, ICES support the use of ensemble approach as a good practice to obtain more robust quantification of uncertainty when multiple solution are plausible (ICES, 2022b). Finally, the use of a stand-alone app (developed

through R in a shiny environment) to enable faster consultation of assessment results is once again a significant step forward in typically time and space-limited stock assessment meetings, especially when it comes to ensemble with more than 1000 models per grid (e.g. tuna-like species stock assessment). Having all the results easily available for consultation at any time allows the experts at the meeting to examine outcomes more calmly and therefore more in depth than usually occurs during the 10-15 minutes granted in power point presentations. Nevertheless, the more and more frequent use of the ensemble approach has raised discussions on how to assign weights to models according to the associated plausibility of each hypotheses/parameters (Maunder et al., 2020; Merino et al., 2022). Although it is straightforward that the models which perform better in diagnostics should be given higher weights, Maunder et al. (2020) shows that problems remain when expert's opinions have to be translated into quantitative weighting. Many questions are still open and experts are debating about which are the best diagnostics to select a model and which one are best suited to weighing them (Merino et al. 2022). Main topics focus on whether or not it is right to look for "superior" diagnostics (to which give a greater significance on the final weight of the ensemble) or whether it is better to give the same importance to each diagnostic, others on how to combine the various weights into a final score. To conclude, the approach taken to weight the individual runs within the ensemble described in this thesis should be considered further as the science and experience around ensemble modeling develops in international community (e.g. dedicated CAPAM workshop; Center for the Advancement of Population Assessment Methodology).

7.3. Growth effect on stock assessment and advice

Another way to increase reliability of stock assessment, is to reduce incorrect specification of growth within statistical age-structured models such as the ones used and presented in this thesis. Indeed, it has been shown that misspecification of stock's population dynamics in assessment models has a huge impact on biomass and fishing mortality; two of the most important estimates used in scientific advice and fisheries management system (Carvalho et al., 2021). In this contest, due to the aging problems highlighted in the introduction, 2018 official stock assessment of common sole in GSA 17 was not performed. Hence, the priority of this thesis was to revise the biological information for common sole in GSA17. Specifically, growth curve to be use for assessment presented in chapter 4 have been recalibrated based on new available data provided by AdriaMed-FAO SGOTHSOLEA expert in 2020 following the methodology described by Carbonara and Follesa (2019). Nevertheless, experts from the FAO-GFCM benchmark session 2021 suggested further analyses regarding the exploration and application of a two-stages growth model for Adriatic sole since biphasic models are proved to be statistically and biologically more valid than monophasic one (Lester et al., 2004; Moe,

2015). To explore this new approach, in the second-last chapter of the thesis, back-calculation measurements obtained from SoleMon survey data have been used to fit and compared monophasic and biphasic growth curves. The analyses revealed systematic age-specific biases in the monophasic curve and demonstrated that the fitting of the biphasic curve was superior both at population and individual level, confirming the theory that growth in size would decrease as a consequence of reproductive effort (Lester et al., 2004). To test the implication on scientific advice a simplified stock assessment simulation showed how the use of the monophasic pattern would result in a critical overestimation of biomass providing an overly optimistic view of stock status and a greater risk of overfishing condition. While representing a simplification, the analyses suggested that stock assessment experts should consider more the use of biphasic growth curves in assessment models when, on a case-by-case basis, they have proven to have superior fit than traditional ones. This sounds critical to move towards a management context in which biomass estimates are used in the calculation of quotas such as that of North Europe (TACs in ICES advisory framework).

7.4. Testing ad-hoc reference points

To conclude, a recent meta-analysis conducted for ICES stocks highlight that, for medium productive species like flatfishes, the mortalities that resulted in biomasses target of 35% of virgin biomass and a trigger value of 0.8 of the target (Btrg = 35%B0 and Btrigger set at 0.8 Btrg) has been recommended as candidates reference point. However, concerns were raised regarding the need to condition the simulation for the specificities of individual stocks (e.g. stock specific S-R functions) rather than using a generic approach. Practical examples come from *Pandalus borealis* in divisions 3.a and 4.a East (ICES, 2022a) and *Coregonus albula* in Bothnian Gulf (Bergenius et al., 2022), where the shortcut MSE approach has already been used for setting ad-hoc reference points during official ICES benchmark processes. For the specific case of common sole in GSA 17, mortality that results in SSB of 35% of virgin biomass and a trigger value equal to the target should be indicated as a good alternative to the reference point set officially adopted since it is more sustainable and compatible with the fundamental principles of CFP, which are to match sustainable exploitation of the fish stocks within socio-economic sustainability. Overall, the simulation clearly highlights how stock's biological and productivity characteristics have a huge impact on setting reference points and need to be account as much as possible case by case in the view of sustainable management purpose, both from ecological and economical point of view. Another added value of this process is the possibilities to create a more direct link between fisheries science and governance processes promoting increased stakeholder involvement in fisheries management through a participatory modelling process during benchmark sessions (e.g. manager and practitioners in natural resource governance; Röckmann et al.,

2012). Instead of adopting an a priori reference point system, the experts shold be able to show, discuss and guide the manager among different possible candidates towards the best choice considering initial managerial objectives (e.g. trade-offs between environmental and socio-economic sustainability). Awareness of the benefits and risks associated with each choice would add greater transparency in the calculation process of reference points enhancing the credibility and legitimacy of scientific advice.

7.5. References

Amoroso, R. O., Pitcher, C. R., Rijnsdorp, A. D., McConnaughey, R. A., Parma, A. M., Suuronen, P., et al. (2018). Bottom trawl fishing footprints on the world's continental shelves. Proc. Natl. Acad. Sci. U. S. A. 115, E10275–E10282. doi:10.1073/pnas.1802379115.

Bergenius, M., Cardinale, M., Lundström, K., Kaljuste, O. 2022. Biologisk rådgivning för siklöja i Bottenviken. SLU.aqua.2021.5.5-272.

Carbonara, P., Follesa M.C., eds. 2019. Handbook on fish age determination: a Mediterranean experience. Studies and Reviews. No. 98. Rome, FAO. 2019. 180 pp.

Cardinale, M., Osio, G. C., and Scarcella, G. (2017). Mediterranean Sea: A Failure of the European Fisheries Management System. Front. Mar. Sci. 4, 72. doi:10.3389/fmars.2017.00072.

Carvalho F, Winker H, Courtney D, Kapur M, Kell L, Cardinale M, Schirripa M, Kitakado T, Yemane D, Piner K.R, Maunder M.N., Taylor I, Wetzel C.R, Doering K, Johnson K.F, Methot R.D, 2021. A cookbook for using model diagnostics in integrated stock assessments, Fisheries Research, Volume 240, 2021, 105959, ISSN 0165-7836, https://doi.org/10.1016/j.fishres.2021.105959.

Castillo, C., Hampton, J., Ducharme-Barth, N., Xu, H., Vidal, T., Williams, P., Scott, F., Pilling, G., Hamer, P., 2021. Stock assessment of South Pacific albacore tuna. WCPFC-SC17–2021/SA-WP-02.

Colloca, F., Cardinale, M., Belluscio, A., and Ardizzone, G. (2003). Pattern of distribution and diversity of demersal assemblages in the central Mediterranean sea. Estuar. Coast. Shelf Sci. 56, 469–480. doi:10.1016/S0272-7714(02)00196-8

Ferrà, C., Tassetti, A. N., Grati, F., Pellini, G., Polidori, P., Scarcella, G., et al. (2018). Mapping change in bottom trawling activity in the Mediterranean Sea through AIS data. Mar. Policy 94, 275–281. doi:10.1016/j.marpol.2017.12.013.

ICES. 2022a. Benchmark workshop on Pandalus stocks (WKPRAWN). ICES Scientific Reports. 4:20. 249 pp. http://doi.org/10.17895/ices.pub.19714204.

ICES. 2022b. Workshop on ICES reference points (WKREF1). ICES Scientific Reports. 4:2. 70 pp. http://doi.org/10.17895/ices.pub.9749.

Lester, N. P., Shuter, B. J., and Abrams, P. A. 2004. Interpreting the von Bertalanffy model of somatic growth in fishes: the cost of reproduction. Proceedings of the Royal Society of London, Series B: Biological Sciences, 271: 1625–1631.

Maunder, M.N., Xu, H., Lennert-Cody, C.E., Valero, J.L., Aires-da-Silva, A., MinteVera, C., 2020. Implementing Reference Point-based Fishery Harvest Control Rules Within a Probabilistic Framework That Considers Multiple Hypotheses (No. SAC-11- INF-F). Scientific Advisory Commitee, Inter-American Tropical Tuna Commission, San Diego.

Merino, G., Urtizberea, A., Fu, D., Winker, H., Cardinale, M., Lauretta, M. V., ... & Santiago, J. 2022. Investigating trends in process error as a diagnostic for integrated fisheries stock assessments. Fisheries Research, 256, 106478.

Minte-Vera, C.V., Maunder, M.N., Xu, H., Valero, J.L. Lennert-Cody, C.E., Aires-da-Silva, A., 2020. Yellowfin tuna in the eastern Pacific Ocean, 2019: benchmark assessment. 11th meeting of the Scientific Advisory Committee. Document SAC-11–07

Moe, B. J. 2015. Estimating growth and mortality in elasmobranchs: are we doing it correctly? Nova Southeastern University. Retrieved from http://nsuworks.nova.edu/occ_stuetd/42.

Palomares, M. L. D., and D. Pauly. 2019. On the creeping increase of vessels' fishing power. Ecology and Society 24(3):31. https://doi.org/10.5751/ES-11136-240331.

Röckmann, C., Ulrich, C., Dreyer, M., Bell, E., Borodzicz, E., Haapasaari, P., ... & Pastoors, M. 2012. The added value of participatory modelling in fisheries management–what has been learnt?. Marine Policy, 36(5), 1072-1085.

Scarcella G, Angelini S, Armelloni EN, Costantini I, De Felice A, Guicciardi S, Leonori I, Masnadi F, Scanu M and Coro G (2022) The potential effects of COVID-19 lockdown and the following restrictions on the status of eight target stocks in the Adriatic Sea. Front. Mar. Sci. 9:920974.doi: 10.3389/fmars.2022.920974.

Scarcella, G., Grati F., Raicevich S., Russo T., Gramolini R., Scott R. D., Polidori P., Domenichetti F., Bolognini L., Giovanardi G., Celić I., Sabatini L., Vrgoč N., Isajlović I., Marčeta B., Fabi G.,

2014. Common sole in the northern and central Adriatic Sea: Spatial management scenarios to rebuild the stock. J. Sea Res. http://dx.doi.org/10.1016/j.seares.2014.02.002.

Vasilakopoulos, P., Maravelias C.D., Tserpes G. 2014. The alarming decline of Mediterranean fish stocks. Curr. Biol. 24, 1643–1648. doi: 10.1016/j.cub.2014.05.070.

Walter, J., Winker, H., 2019. Projections to create Kobe 2 Strategy Matrices using the multivariate log normal approximation for Atlantic yellowfin tuna. ICCAT-SCRS/2019/145 1–12.

Winker, H., Walter, J., Cardinale, M., Fu, D., 2019. A multivariate lognormal Monte-Carlo approach for estimating structural uncertainty about the stock status and future projections for Indian Ocean Yellowfin tuna. IOTC-2019-WPM10-XX.

Xu, H., Maunder,M.N., Minte-Vera, C., Valero, J.L., Lennert-Cody, C., Aires-da-Silva, A., 2020. Bigeye tuna in the eastern Pacific Ocean, 2019: benchmark assessment. InterAmerican Tropical Tuna Commission. 11th meeting of the Scientific Advisory Committee. Document SAC-11–06.

8. Acknowledgment

This journey would not have been possible without the full support of my tutor and co-tutors. I would like to thank them for the invaluable knowledge share with me, the feedbacks and the guidance through the challenging research career. Thank you for fully believing in me.

Moreover, I am deeply indebted to all those who have helped me grow professionally during these three years, such as colleagues and experts from Adriamed, FAO-WGSAD and WGBEAM.

Many thanks to the colleagues and friends at CNR for all the tangible and intangible supports. Among them, a special thanks to the *Solemon soldiers* and the crew of the N/O Dallaporta with whom I shared several adventures across the seven seas (but with a fixed stop in Ravenna). Thanks should also go to the *CNR juveniles*, may the force be with you! Nonetheless, I would like to thank FishMed PhD colleagues.

I would be remiss in not mentioning the *AMAREMED gang* with whom I shared moments of intense coding, leisure activities and finest songwriting in the sultry Venetian, Croatian and Cypriot summers. Noi siamo quelli di Amaremed ma diversi da loro!

I would like to express my deepest gratitude to the collegues and friends of the Havsfiskelaboratorietin of Lysekil, for welcomed and hosted me in the longest swedish fjord and for innebandy's knee peeler workouts. Thanks also to the friends of the BioCentrum in Uppsala for clandestinely support me with a desk and Wi-Fi connection in the last months of this adventure. Tack så mycket!

Words cannot express my gratitude to all the members of *I tre porcellini*, *Sfigati anconetani, Bird Box Fans, 2ndBreakfastClub, CUINTA EFFE* and *Best adventure tribe*. Without the support of true friends, I would never have made it! Thanks again for all the adventures lived together.

A huge thank to my family. My parents, my nonna, my uncles and aunts, cousins, brothers and sister-in-law. Their belief in me has kept my spirits and motivation high. Tusen takk til min nye norske familie også.

Last but not least, a kjærlig takk to my Stella Polare for guiding me through the dark arctic nights (but also quite sunny summer days!). Keep showing me the way.

"So long, and thanks for all the fish!"